Finite Element Analysis

Thermomechanics of Solids

David W. Nicholson

CRC PRESS

Boca Raton London New York Washington, D.C.

Library of Congress Cataloging-in-Publication Data

Nicholson, D.W.
Finite element analysis : thermomechanics of solids / David W. Nicholson.
p. cm.
Includes bibliographical references and index.
ISBN 0-8493-0749-X (alk. paper)
1. Thermal stresses—Mathematical models. 2. Finite element method. I. Title.

TA418.58.N53 2003
620.1′121—dc21 2002041419

No claim to original U.S. Government works
International Standard Book Number 0-8493-0749-X
Library of Congress Card Number 2002041419
Printed in the United States of America 1 2 3 4 5 6 7 8 9 0
Printed on acid-free paper

© 2003 by CRC CRC Press LLC

Dedication

To Linda and Mike, with profound love

Preface

Thousands of engineers use finite-element codes, such as ANSYS, for thermomechanical and nonlinear applications. Most academic departments offering advanced degrees in mechanical engineering, civil engineering, and aerospace engineering offer a *first-level course* in the finite-element method, and by now, almost all undergraduates of such programs have some exposure to the finite-element method. A number of departments offer a second-level course. It is hoped that this text will appeal to instructors of such courses. Of course, it hopefully will also be helpful to engineers engaged in self-study on nonlinear and thermomechanical finite-element analysis.

The principles of the finite-element method are presented for application to the mechanical, thermal, and thermomechanical response, both static and dynamic, of linear and nonlinear solids. It provides an integrated treatment of:

- Basic principles, material models, and contact models (for example, linear elasticity, hyperelasticity, and thermohyperelasticity).
- Computational, numerical, and software-design aspects (such as finite-element data structures).
- Modeling principles and strategies (including mesh design).

The text is designed *for a second-level course, as a reference work, or for self study.* Familiarity is assumed with the finite-element method at the level of a first-level graduate or advanced undergraduate course.

A first-level course in the finite-element method, for which many excellent books are available, barely succeeds in covering static linear elasticity and linear heat transfer. There is virtually no exposure to nonlinear methods, which are topics for a second-level course. Nor is there much emphasis on *coupled* thermomechanical problems. However, many engineers could benefit from a text covering nonlinear problems and the associated continuum thermomechanics. Such a text could be used in a formal class or for self-study. Many important applications have significant nonlinearity, making nonlinear finite-element modeling necessary. As a few examples, we mention polymer processing; metal forming; rubber components, such as tires and seals; biomechanics; and crashworthiness. Many applications combine thermal and mechanical response, such as rubber seals in hot engines. Engineers coping with such applications have access to powerful finite-element codes and computers. However, they often lack and urgently need an in-depth but compact exposition of the finite-element method, which provides a foundation for addressing future problems. It is hoped this text also fills this need.

Of necessity, a selection of topics has been made, and topics are given coverage proportional to the author's sense of their importance to the reader's understanding. Topics have been selected with the intent of giving a unified and complete, but still compact and tractable, presentation. Several other excellent texts and monographs

have appeared over the years, from which the author has benefited. Four texts to which the author is indebted are:

1. Zienkiewicz, O.C. and Taylor R.L., *The Finite Element Method*, Vols. 1 and 2, McGraw Hill, London, 1989.
2. Kleiber, M., *Incremental Finite Element Modeling in Nonlinear Solid Mechanics*, Chichester, Ellis Horwood, Ltd., 1989.
3. Bonet, J. and Wood, R.D., *Nonlinear Continuum Mechanics for Finite Element Analysis*, Cambridge, Cambridge University Press, 1997.
4. Belytschko, T., Lui, W.K, and Moran, B., *Nonlinear Finite Elements for Continua and Structures*, New York, John Wiley and Sons, 2000.

This text has the following characteristics:

1. Emphasis on the use of Kronecker Product notation instead of tensor, tensor-indicial, Voigt, or traditional finite-element, matrix-vector notation.
2. Emphasis on integrated and coupled thermal and mechanical effects.
3. Inclusion of elasticity, hyperelasticity, plasticity, and viscoelasticity *with thermal effects.*
4. Inclusion of nonlinear boundary conditions, including contact, in an integrated *incremental variational* formulation.

Kronecker Product algebra (KPA) has been widely used in control theory for many years (Graham, 1982). It is highly compact and satisfies simple rules: for example, the inverse of a Kronecker Product of two nonsingular matrices is the Kronecker Product of the inverses. Recently, a number of extensions of KPA have been introduced and shown to permit compact expressions for otherwise elaborate quantities in continuum and computational mechanics. Examples include:

1. Compact expressions for the tangent-modulus tensors in hyperelasticity (invariant-based and stretch-based; compressible, incompressible, and near-incompressible), thermohyperelasticity, and finite-strain plasticity.
2. A general, compact expression for the tangent stiffness matrix in nonlinear FEA, including nonlinear boundary conditions, such as contact.

KPA with recent extensions can completely replace other notations in most cases of interest here. In the author's experience, students experience little difficulty in gaining a command of it.

The first three chapters concern mathematical foundations, and Kronecker Product notation for tensors is introduced. The next four chapters cover relevant linear and nonlinear continuum thermomechanics to enable a unified account of the finite-element method. Chapters 8 through 15 represent a compact presentation of the finite-element method in linear elastic, thermal, and thermomechanical media, including solution methods. The final five chapters address nonlinear problems based on a unified set of incremental variational principles. Material nonlinearity is treated also, as is geometric nonlinearity and nonlinearity due to boundary conditions. Several numerical issues in nonlinear analysis are discussed, such as iterative triangularization of stiffness matrices.

Acknowledgment

Finite Element Analysis: Thermomechanics of Solids is the culmination of many years of teaching and research, made possible through the love and patience of my wife Linda and son Michael, to whom this is dedicated. To my profound love, I cheerfully add my immense gratitude. Much of my understanding of the advanced topics addressed in this book arose through the highly successful research of my then-doctoral student, Dr. Baojiu Lin. He continued his invaluable support by providing comments and corrections on the manuscript. Also deserving of acknowledgment is Ashok Balasubranamian, whose careful attention to the manuscript has greatly helped to make it achieve my objectives. Thanks are due to hundreds of graduate students in my courses in continuum mechanics and finite elements over the years. I tested and refined the materials through the courses and benefited immensely from their strenuous efforts to gain command of the course materials. Finally, I would like to thank CRC Press for taking a chance on me and especially for Cindy Renee Carelli for patience and many good suggestions.

About the Author

David W. Nicholson, Ph.D. is a professor in the Department of Mechanical, Materials, and Aerospace Engineering at the University of Central Florida, Orlando, Florida, where he has served as the Chair (1990–1995) and Interim Chair (2000–2002). He earned an S.B. degree at MIT in 1966 and a doctorate at Yale in 1971. He has 31 years of experience since the doctorate, including research in industry (Goodyear, 7 years) and government (the Naval Surface Weapons Center, 6 years), and faculty positions at Stevens Institute of Technology and UCF. He has authored over 140 articles on the finite-element method, continuum mechanics, fracture mechanics, and dynamics. He has served as a technical editor for *Applied Mechanics Review*, as an associate editor of *Tire Science and Technology*, and as a member of scientific advisory committees for a number of international conferences. He has been the instructor in over 20 short courses and workshops. Recently, he served as Executive Chair of the XXIst Southeastern Conference on Theoretical and Applied Mechanics and as co-editor of *Developments in Theoretical and Applied Mechanics*, *Volume XXI*.

Table of Contents

1 Mathematical Foundations: Vectors and Matrices

1.1 INTRODUCTION

This chapter provides an overview of mathematical relations, which will prove useful in the subsequent chapters. Chandrashekharaiah and Debnath (1994) provide a more complete discussion of the concepts introduced here.

1.1.1 Range and Summation Convention

Unless otherwise noted, repeated Latin indices imply summation over the range 1 to 3. For example:

$$a_i b_i = \sum_{i=1}^{3} a_i b_i = a_1 b_1 + a_2 b_2 + a_3 b_3 \tag{1.1}$$

$$a_{ij} b_{jk} = a_{i1} b_{1k} + a_{i2} b_{2k} + a_{i3} b_{3k} \tag{1.2}$$

The repeated index is "summed out" and, therefore, dummy. The quantity $a_{ij}b_{jk}$ in Equation (1.2) has two free indices, i and k (and later will be shown to be the ik^{th} entry of a second-order tensor). Note that Greek indices do not imply summation. Thus, $a_\alpha b_\alpha = a_1 b_1$ if $\alpha = 1$.

1.1.2 Substitution Operator

The quantity, δ_{ij}, later to be called the Kronecker tensor, has the property that

$$\delta_{ij} = \begin{cases} 1 & i = j \\ 0 & i \neq j \end{cases} \tag{1.3}$$

For example, $\delta_{ij} v_j = 1 \times v_i$, thus illustrating the substitution property.

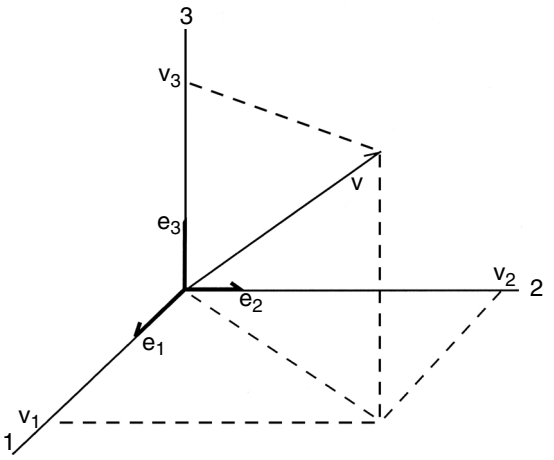

FIGURE 1.1 Rectilinear coordinate system.

1.2 VECTORS

1.2.1 NOTATION

Throughout this and the following chapters, orthogonal coordinate systems will be used. Figure 1.1 shows such a system, with base vectors $\mathbf{e}_1$, $\mathbf{e}_2$, and $\mathbf{e}_3$. The scalar product of vector analysis satisfies

$$\mathbf{e}_i \cdot \mathbf{e}_j = \delta_{ij} \tag{1.4}$$

The vector product satisfies

$$\mathbf{e}_i \times \mathbf{e}_j = \begin{cases} \mathbf{e}_k & i \neq j \text{ and } ijk \text{ in right-handed order} \\ -\mathbf{e}_k & i \neq j \text{ and } ijk \text{ not in right-handed order} \\ \mathbf{0} & i = j \end{cases} \tag{1.5}$$

It is an obvious step to introduce the alternating operator, ε_{ijk}, also known as the ijk^{th} entry of the permutation tensor:

$$\varepsilon_{ijk} = [\mathbf{e}_i \times \mathbf{e}_j] \cdot \mathbf{e}_k = \begin{cases} 1 & ijk \text{ distinct and in right-handed order} \\ -1 & ijk \text{ distinct but not in right-handed order} \\ 0 & ijk \text{ not distinct} \end{cases} \tag{1.6}$$

Consider two vectors, **v** and **w**. It is convenient to use two different types of notation. In **tensor indicial notation**, denoted by (*T), **v** and **w** are represented as

$$\text{*T)} \quad \mathbf{v} = v_i \mathbf{e}_i \qquad \mathbf{w} = w_i \mathbf{e}_i \tag{1.7}$$

Occasionally, base vectors are not displayed, so that **v** is denoted by v_i. By displaying base vectors, tensor indicial notation is explicit and minimizes confusion and ambiguity. However, it is also cumbersome.

In this text, the "default" is **matrix-vector** (*M) notation, illustrated by

$$\text{*M)} \quad \mathbf{v} = \begin{pmatrix} v_1 \\ v_2 \\ v_3 \end{pmatrix} \qquad \mathbf{w} = \begin{pmatrix} w_1 \\ w_2 \\ w_3 \end{pmatrix} \tag{1.8}$$

It is compact, but also risks confusion by not displaying the underlying base vectors. In *M notation, the transposes $\mathbf{v}^{\mathbf{T}}$ and $\mathbf{w}^{\mathbf{T}}$ are also introduced; they are displayed as "row vectors":

$$\text{*M)} \quad \mathbf{v}^{\mathbf{T}} = \{v_1 \quad v_2 \quad v_3\} \qquad \mathbf{w}^{\mathbf{T}} = \{w_1 \quad w_2 \quad w_3\} \tag{1.9}$$

The scalar product of **v** and **w** is written as

$$\begin{aligned} \text{*T)} \quad \mathbf{v} \cdot \mathbf{w} &= (v_i \mathbf{e}_i) \cdot (w_j \mathbf{e}_j) \\ &= v_i w_j \mathbf{e}_i \cdot \mathbf{e}_j \\ &= v_i w_j \delta_{ij} \\ &= v_i w_i \end{aligned} \tag{1.10}$$

The magnitude of **v** is defined by

$$\text{*T)} \quad |\mathbf{v}| = \sqrt{\mathbf{v} \cdot \mathbf{v}} \tag{1.11}$$

The scalar product of **v** and **w** satisfies

$$\text{*T)} \quad \mathbf{v} \cdot \mathbf{w} = |\mathbf{v}||\mathbf{w}| \cos\theta_{vw} \tag{1.12}$$

in which θ_{vw} is the angle between the vectors **v** and **w**. The scalar, or dot, product is

$$\text{*M)} \quad \mathbf{v} \cdot \mathbf{w} \rightarrow \mathbf{v}^{\mathbf{T}} \mathbf{w} \tag{1.13}$$

The vector, or cross, product is written as

$$\begin{aligned} \mathbf{v}\times\mathbf{w} &= v_i w_j \mathbf{e}_i \times \mathbf{e}_j \\ &= \varepsilon_{ijk} v_i w_j \mathbf{e}_k \end{aligned} \qquad \text{*T)} \tag{1.14}$$

Additional results on vector notation are presented in the next section, which introduces matrix notation. Finally, the vector product satisfies

$$|\mathbf{v}\times\mathbf{w}| = |\mathbf{v}||\mathbf{w}|\ \sin\theta_{vw} \qquad \text{*T)} \tag{1.15}$$

and **vxw** is colinear with **n** the unit normal vector perpendicular to the plane containing **v** and **w**. The area of the triangle defined by the vectors **v** and **w** is given by $\frac{1}{2}|\mathbf{v}\times\mathbf{w}|$.

1.2.2 Gradient, Divergence, and Curl

The derivative, $d\phi/d\mathbf{x}$, of a scalar ϕ with respect to a vector **x** is defined implicitly by

$$d\phi = \frac{d\phi}{d\mathbf{x}} d\mathbf{x} \qquad \text{*M)} \tag{1.16}$$

and it is a row vector whose i^{th} entry is $d\phi/dx_i$. In three-dimensional rectangular coordinates, the gradient and divergence operators are defined by

$$\nabla(\,) = \begin{pmatrix} \dfrac{\partial(\,)}{\partial x} \\ \dfrac{\partial(\,)}{\partial y} \\ \dfrac{\partial(\,)}{\partial z} \end{pmatrix} \qquad \text{*M)} \tag{1.17}$$

and clearly,

$$\left(\frac{d}{d\mathbf{x}}\right)^{\mathbf{T}}(\,) = \nabla(\,) \qquad \text{*M)} \tag{1.18}$$

The gradient of a scalar function ϕ satisfies the following integral relation:

$$\int \nabla\phi\, dV = \int \mathbf{n}\phi\, dS \tag{1.19}$$

The expression $\nabla\mathbf{v}^{\mathbf{T}}$ will be seen to be a tensor (see Chapter 2). Clearly,

$$\nabla\mathbf{v}^{\mathbf{T}} = [\nabla v_1 \quad \nabla v_2 \quad \nabla v_3] \tag{1.20}$$

from which we obtain the integral relation

$$\int \nabla \mathbf{v}^{\mathbf{T}} dV = \int \mathbf{n}\mathbf{v}^{\mathbf{T}} dS \tag{1.21}$$

Another important relation is the divergence theorem. Let V denote the volume of a closed domain, with surface S. Let $\mathbf{n}$ denote the exterior surface normal to S, and let $\mathbf{v}$ denote a vector-valued function of $\mathbf{x}$, the position of a given point within the body. The divergence of $\mathbf{v}$ satisfies

$$\text{*M)} \quad \oint \frac{d\mathbf{v}}{d\mathbf{x}} dV = \oint \mathbf{n}^{\mathbf{T}} \mathbf{v} dS \tag{1.22}$$

The curl of vector $\mathbf{v}$, $\nabla \times \mathbf{v}$, is expressed by

$$(\nabla \times \mathbf{v})_i = \varepsilon_{ijk} \frac{\partial}{\partial x_j} v_k \tag{1.23}$$

which is the conventional cross-product, except that the divergence operator replaces the first vector. The curl satisfies the curl theorem, analogous to the divergence theorem (Schey, 1973):

$$\int \nabla \times \mathbf{v} dV = \int \mathbf{n} \times \mathbf{v} dS \tag{1.24}$$

Finally, the reader may verify, with some effort that, for a vector $\mathbf{v}(\mathbf{X})$ and a path $\mathbf{X}(S)$ in which S is the length along the path,

$$\int \mathbf{v} \cdot d\mathbf{X}(S) = \int \mathbf{n} \cdot \nabla \times \mathbf{v}\, dS\ . \tag{1.25}$$

The integral between fixed endpoints is single-valued if it is path-independent, in which case $\mathbf{n} \cdot \nabla \times \mathbf{v}$ must vanish. However, $\mathbf{n}$ is arbitrary since the path is arbitrary, thus giving the condition for $\mathbf{v}$ to have a path-independent integral as

$$\nabla \times \mathbf{v} = \mathbf{0}. \tag{1.26}$$

1.3 MATRICES

An $n \times n$ matrix is simply an array of numbers arranged in rows and columns, also known as a second-order array. For the matrix $\mathbf{A}$, the entry a_{ij} occupies the intersection of the i^{th} row and the j^{th} column. We may also introduce the $n \times 1$ first-order array $\mathbf{a}$, in which a_i denotes the i^{th} entry. We likewise refer to the $1 \times n$ array, $\mathbf{a}^{\mathbf{T}}$, as first-order.

In the current context, a first-order array is not a vector unless it is associated with a coordinate system and certain transformation properties, to be introduced shortly. In the following, all matrices are real unless otherwise noted. Several properties of first- and second-order arrays are as follows:

The sum of two $n \times n$ matrices, **A** and **B**, is a matrix, **C**, in which $c_{ij} = a_{ij} + b_{ij}$.
The product of a matrix, **A**, and a scalar, q, is a matrix, **C**, in which $c_{ij} = qa_{ij}$.
The transpose of a matrix, **A**, denoted $\mathbf{A}^{\mathbf{T}}$, is a matrix in which $a_{ij}^{\mathbf{T}} = a_{ji}$. **A** is called symmetric if $\mathbf{A} = \mathbf{A}^{\mathbf{T}}$, and it is called antisymmetric if $\mathbf{A} = -\mathbf{A}^{\mathbf{T}}$.
The product of two matrices, **A** and **B**, is the matrix, **C**, for which

$$\text{*T)} \quad c_{ij} = a_{ik} b_{kj} \tag{1.27}$$

Consider the following to visualize matrix multiplication. Let the first-order array $\mathbf{a}_i^{\mathbf{T}}$ denote the i^{th} row of **A**, while the first-order array $\mathbf{b}_j$ denotes the j^{th} column of **B**. Then c_{ij} can be written as

$$\text{*T)} \quad c_{ij} = \mathbf{a}_i^{\mathbf{T}} \mathbf{b}_j \tag{1.28}$$

The product of a matrix **A** and a first-order array **c** is the first-order array **d** in which the i^{th} entry is $d_i = a_{ij} c_j$.
The ij^{th} entry of the identity matrix **I** is δ_{ij}. Thus, it exhibits ones on the diagonal positions ($i = j$) and zeroes off-diagonal ($i \neq j$). Thus, **I** is the matrix counterpart of the substitution operator.
The determinant of **A** is given by

$$\text{*T)} \quad \det(\mathbf{A}) = \frac{1}{6} \varepsilon_{ijk} \varepsilon_{pqr} a_{ip} a_{jq} a_{kr} \tag{1.29}$$

Suppose **a** and **b** are two non-zero, first-order $n \times 1$ arrays. If $\det(\mathbf{A}) = 0$, the matrix **A** is singular, in which case there is no solution to equations of the form $\mathbf{Aa} = \mathbf{b}$. However, if $\mathbf{b} = \mathbf{0}$, there may be multiple solutions. If $\det(\mathbf{A}) \neq 0$, then there is a unique, nontrivial solution **a**.

Let **A** and **B** be $n \times n$ nonsingular matrices. The determinant has the following useful properties:

$$\begin{gathered} \det(\mathbf{AB}) = \det(\mathbf{A}) \det(\mathbf{B}) \\ \text{*M)} \quad \det(\mathbf{A}^{\mathbf{T}}) = \det(\mathbf{A}) \\ \det(\mathbf{I}) = 1 \end{gathered} \tag{1.30}$$

If $\det(\mathbf{A}) \neq 0$, then $\mathbf{A}$ is nonsingular and there exists an inverse matrix, $\mathbf{A}^{-1}$, for which

$$*\text{M}) \quad \mathbf{A}\mathbf{A}^{-1} = \mathbf{A}^{-1}\mathbf{A} = \mathbf{I} \tag{1.31}$$

The transpose of a matrix product satisfies

$$*\text{M}) \quad (\mathbf{A}\mathbf{B})^{\mathbf{T}} = \mathbf{B}^{\mathbf{T}}\mathbf{A}^{\mathbf{T}} \tag{1.32}$$

The inverse of a matrix product satisfies

$$*\text{M}) \quad (\mathbf{A}\mathbf{B})^{-1} = \mathbf{B}^{-1}\mathbf{A}^{-1} \tag{1.33}$$

If $\mathbf{c}$ and $\mathbf{d}$ are two 3×1 vectors, the vector product $\mathbf{c} \times \mathbf{d}$ generates the vector $\mathbf{c} \times \mathbf{d} = \mathbf{C}\mathbf{d}$, in which $\mathbf{C}$ is an antisymmetric matrix given by

$$*\text{M}) \quad \mathbf{C} = \begin{bmatrix} 0 & -c_3 & c_2 \\ c_3 & 0 & -c_1 \\ -c_2 & c_1 & 0 \end{bmatrix} \tag{1.34}$$

Recalling that $\mathbf{c} \times \mathbf{d} = \varepsilon_{ikj} c_k d_j$, and noting that $\varepsilon_{ikj} c_k$ denotes the $(ij)^{th}$ component of an antisymmetric tensor, it is immediate that $[\mathbf{C}]_{ij} = \varepsilon_{ikj} c_k$.

If $\mathbf{c}$ and $\mathbf{d}$ are two vectors, the outer product $\mathbf{c}\mathbf{d}^{\mathbf{T}}$ generates the matrix $\mathbf{C}$ given by

$$*\text{M}) \quad \mathbf{C} = \begin{bmatrix} c_1 d_1 & c_1 d_2 & c_1 d_3 \\ c_2 d_1 & c_2 d_2 & c_2 d_3 \\ c_3 d_1 & c_3 d_2 & c_3 d_3 \end{bmatrix} \tag{1.35}$$

We will see later that $\mathbf{C}$ is a second-order tensor if $\mathbf{c}$ and $\mathbf{d}$ have the transformation properties of vectors.

An $n \times n$ matrix $\mathbf{A}$ can be decomposed into symmetric and antisymmetric matrices using

$$\mathbf{A} = \mathbf{A}_s + \mathbf{A}_a, \quad \mathbf{A}_s = \frac{1}{2}[\mathbf{A} + \mathbf{A}^{\mathbf{T}}], \quad \mathbf{A}_a = \frac{1}{2}[\mathbf{A} - \mathbf{A}^{\mathbf{T}}] \tag{1.36}$$

1.3.1 Eigenvalues and Eigenvectors

In this case, $\mathbf{A}$ is again an $n \times n$ tensor. The eigenvalue equation is

$$(\mathbf{A} - \lambda_j \mathbf{I})\mathbf{x}_j = \mathbf{0} \tag{1.37}$$

The solution for $\mathbf{x}_j$ is trivial unless $\mathbf{A} - \lambda_j \mathbf{I}$ is singular, in which event $\det(\mathbf{A} - \lambda_j \mathbf{I}) = 0$. There are n possible complex roots. If the magnitude of the eigenvectors is set to unity, they may likewise be determined. As an example, consider

$$\mathbf{A} = \begin{bmatrix} 2 & 1 \\ 1 & 2 \end{bmatrix} \tag{1.38}$$

The equation $\det(\mathbf{A} - \lambda_j \mathbf{I}) = 0$ is expanded as $(2 - \lambda_j)^2 - 1$, with roots $\lambda_{1,2} = 1, 3$, and

$$\mathbf{A} - \lambda_1 \mathbf{I} = \begin{bmatrix} 1 & 1 \\ 1 & 1 \end{bmatrix} \qquad \mathbf{A} - \lambda_2 \mathbf{I} = \begin{bmatrix} -1 & 1 \\ 1 & -1 \end{bmatrix} \tag{1.39}$$

Note that in each case, the rows are multiples of each other, so that only one row is independent. We next determine the eigenvectors. It is easily seen that magnitudes of the eigenvectors are arbitrary. For example, if $\mathbf{x}_1$ is an eigenvector, so is $10\mathbf{x}_1$. Accordingly, the magnitudes are arbitrarily set to unity. For $\mathbf{x}_1 = \{x_{11} \quad x_{12}\}^{\mathbf{T}}$,

$$x_{11} + x_{12} = 0 \qquad x_{11}^2 + x_{12}^2 = 1 \tag{1.40}$$

from which we conclude that $\mathbf{x}_1 = \{1 \quad -1\}^{\mathbf{T}}/\sqrt{2}$. A parallel argument furnishes $\mathbf{x}_2 = \{1 \quad 1\}^{\mathbf{T}}/\sqrt{2}$.

If $\mathbf{A}$ is symmetric, the eigenvalues and eigenvectors are real and the eigenvectors are orthogonal to each other: $\mathbf{x}_i^{\mathbf{T}}\mathbf{x}_j = \delta_{ij}$. The eigenvalue equations can be "stacked up," as follows.

$$\mathrm{A}[\mathrm{x}_1 : \mathrm{x}_2 : \ldots \mathrm{x}_n] = [\mathrm{x}_1 : \mathrm{x}_2 : \ldots \mathrm{x}_n] \begin{bmatrix} \lambda_1 & 0 & . & . & . \\ 0 & \lambda_2 & . & . & . \\ . & . & . & . & . \\ . & . & . & \lambda_{n-1} & 0 \\ . & . & . & 0 & \lambda_n \end{bmatrix} \tag{1.41}$$

With obvious identifications,

$$\mathbf{AX} = \mathbf{X\Lambda} \tag{1.42}$$

and $\mathbf{X}$ is the modal matrix. Let y_{ij} represent the ij^{th} entry of $\mathbf{Y} = \mathbf{X}^{\mathbf{T}}\mathbf{X}$

$$y_{ij} = \mathbf{x}_i^{\mathbf{T}}\mathbf{x}_j = \delta_{ij} \tag{1.43}$$

so that $\mathbf{Y} = \mathbf{I}$. We can conclude that $\mathbf{X}$ is an orthogonal tensor: $\mathbf{X}^{\mathbf{T}} = \mathbf{X}^{-1}$. Further,

$$\mathbf{X}^{\mathbf{T}}\mathbf{A}\mathbf{X} = \mathbf{\Lambda} \qquad \mathbf{A} = \mathbf{X}\,\mathbf{\Lambda}\,\mathbf{X}^{\mathbf{T}} \tag{1.44}$$

and $\mathbf{X}$ can be interpreted as representing a rotation from the reference axes to the principal axes.

1.3.2 Coordinate Transformations

Suppose that the vectors $\mathbf{v}$ and $\mathbf{w}$ are depicted in a second-coordinate system whose base vectors are denoted by $\mathbf{e}'_j$. Now, $\mathbf{e}'_j$ can be represented as a linear sum of the base vectors $\mathbf{e}_i$:

$$\text{*T)} \qquad \mathbf{e}'_j = q_{ji}\mathbf{e}_i \tag{1.45}$$

But then $\mathbf{e}_i \cdot \mathbf{e}'_j = q_{ij} = \cos(\theta_{ij'})$. It follows that $\delta_{ij} = \mathbf{e}'_i \cdot \mathbf{e}'_j = (q_{ik}\mathbf{e}_k) \cdot (q_{jl}\mathbf{e}_l) = q_{ik}q_{jl}\delta_{kl}$, so that

$$\begin{aligned} \text{*T)} \qquad q_{ik}q_{jk} &= q_{ik}q_{kj}^{\mathbf{T}} \\ &= \delta_{ij} \end{aligned}$$

In *M) notation, this is written as

$$\text{*M)} \qquad \mathbf{Q}\mathbf{Q}^{\mathbf{T}} = \mathbf{I} \tag{1.46}$$

in which case the matrix $\mathbf{Q}$ is called *orthogonal*. An analogous argument proves that $\mathbf{Q}^{\mathbf{T}}\mathbf{Q} = \mathbf{I}$. From Equation (1.30), $1 = \det(\mathbf{Q}\mathbf{Q}^{\mathbf{T}}) = \det(\mathbf{Q})\det(\mathbf{Q}^{\mathbf{T}}) = \det^2(\mathbf{Q})$. Right-handed rotations satisfy $\det(\mathbf{Q}) = 1$, in which case $\mathbf{Q}$ is called *proper orthogonal*.

1.3.3 Transformations of Vectors

The vector $\mathbf{v}'$ is the same as the vector $\mathbf{v}$, except that $\mathbf{v}'$ is referred to $\mathbf{e}'_j$, while $\mathbf{v}$ is referred to $\mathbf{e}_i$. Now

$$\begin{aligned} \mathbf{v}' &= v'_j\mathbf{e}'_j \\ \text{*T)} \qquad &= v'_j q_{ji}\mathbf{e}_i \\ &= v_i\mathbf{e}_i \end{aligned} \tag{1.47}$$

It follows that $v_i = v'_j q_{ji}$, and hence

$$*\text{M)} \quad \mathbf{v} = \mathbf{Q}^{\mathbf{T}}\mathbf{v}' \text{ (a)} \qquad \mathbf{v}' = \mathbf{Q}\mathbf{v} \text{ (b)} \tag{1.48}$$

in which q_{ij} is the ji^{th} entry of $\mathbf{Q}^{\mathbf{T}}$.

We can also state an alternate definition of a vector as a first-order tensor. Let $\mathbf{v}$ be an $n \times 1$ array of numbers referring to a coordinate system with base vectors $\mathbf{e}_i$. It is a vector if and only if, upon a rotation of the coordinate system to base vectors $\mathbf{e}'_j$, $\mathbf{v}'$ transforms according to Equation (1.48).

Since $(\frac{d\phi}{d\mathbf{x}})' d\mathbf{x}'$ is likewise equal to $d\phi$,

$$*\text{M)} \quad \left(\frac{d\phi}{d\mathbf{x}}\right)' = \left(\frac{d\phi}{d\mathbf{x}}\right)\mathbf{Q}^{\mathbf{T}} \tag{1.49}$$

for which reason $d\phi/d\mathbf{x}$ is called a contravariant vector, while $\mathbf{v}$ is properly called a covariant vector.

Finally, to display the base vectors to which the tensor $\mathbf{A}$ is referred (i.e., in tensor-indicial notation), we introduce the *outer product*

$$\mathbf{e}_i \wedge \mathbf{e}_j \tag{1.50}$$

with the matrix-vector counterpart $\mathbf{e}_i\mathbf{e}_j^{\mathbf{T}}$. Now

$$\mathbf{A} = a_{ij}\mathbf{e}_i \wedge \mathbf{e}_j \tag{1.51}$$

Note the useful result that

$$\mathbf{e}_i \wedge \mathbf{e}_j \cdot \mathbf{e}_k = \mathbf{e}_i \delta_{jk}$$

In this notation, given a vector $\mathbf{b} = b_k\mathbf{e}_k$,

$$\begin{aligned} \mathbf{A}\mathbf{b} &= a_{ij}\mathbf{e}_i \wedge \mathbf{e}_j \cdot b_k\mathbf{e}_k \\ &= a_{ij}b_k\mathbf{e}_i \wedge \mathbf{e}_j \cdot \mathbf{e}_k \\ &= a_{ij}b_k\mathbf{e}_i\delta_{jk} \\ &= a_{ij}b_j\mathbf{e}_i \end{aligned} \tag{1.52}$$

as expected.

1.3.4 Orthogonal Curvilinear Coordinates

The position vector of a point, P, referring to a three-dimensional, rectilinear, coordinate system is expressed in tensor-indicial notation as $\mathbf{R}_P = x_i\mathbf{e}_i$. The position vector connecting two "sufficiently close" points P and Q is given by

$$\Delta\mathbf{R} = \mathbf{R}_P - \mathbf{R}_Q \approx \mathbf{dR}_x \tag{1.53}$$

where

$$\mathbf{dR}_x = dx_i\mathbf{e}_i \tag{1.54}$$

with arc length

$$dS_x = \sqrt{dx_i dx_i} \tag{1.55}$$

Suppose now that the coordinates are transformed to y_j coordinates: $x_i = x_i(y_j)$. The same position vector, now referred to the transformed system, is

$$\begin{aligned}
\mathbf{dR}_y &= \sum_1^3 dy_\alpha \mathbf{g}_\alpha \\
\mathbf{g}_\alpha &= h_\alpha \boldsymbol{\gamma}_\alpha \\
h_\alpha &= \sqrt{\frac{dx_j}{dy_\alpha}\frac{dx_j}{dy_\alpha}}
\end{aligned} \tag{1.56}$$

$$\begin{aligned}
\boldsymbol{\gamma}_\alpha &= \frac{\frac{dx_i}{dy_\alpha}}{\sqrt{\frac{dx_j}{dy_\alpha}\frac{dx_j}{dy_\alpha}}}\mathbf{e}_i \\
&= \frac{1}{h_\alpha}\frac{dx_i}{dy_\alpha}\mathbf{e}_i
\end{aligned}$$

in which h_α is called the scale factor. Recall that the use of Greek letters for indices implies no summation. Clearly, $\boldsymbol{\gamma}_\alpha$ is a unit vector. Conversely, if the transformation is reversed,

$$\begin{aligned}
\mathbf{dR}_y &= \mathbf{g}_i dy_i \\
&= \frac{dy_i}{dx_j}\mathbf{g}_i dx_j
\end{aligned} \tag{1.57}$$

then the consequence is that

$$\mathbf{e}_j = \frac{dy_i}{dx_j}\mathbf{g}_i = \sum_\alpha \frac{dy_\alpha}{dx_j} h_\alpha \boldsymbol{\gamma}_\alpha \tag{1.58}$$

We restrict attention to orthogonal coordinate systems y_j, with the property that

$$\boldsymbol{\gamma}_\alpha^{\mathrm{T}} \boldsymbol{\gamma}_\beta = \delta_{\alpha\beta} \tag{1.59}$$

The length of the vector $\mathbf{dR}_y$ is now

$$dS_y = h_\alpha \sqrt{dy_i dy_i} \tag{1.60}$$

Under restriction to orthogonal coordinate systems, the initial base vectors $\mathbf{e}_i$ can be expressed in terms of $\boldsymbol{\gamma}_\alpha$ using

$$\begin{aligned} \mathbf{e}_i &= \left(\boldsymbol{\gamma}_j^{\mathrm{T}} \mathbf{e}_i\right)\boldsymbol{\gamma}_j \\ &= \frac{1}{h_i}\frac{\partial x_i}{\partial y_j}\boldsymbol{\gamma}_j \\ &= \frac{1}{h_i h_j}\frac{\partial x_i}{\partial y_j}\frac{\partial x_k}{\partial y_j}\mathbf{e}_k \end{aligned} \tag{1.61}$$

and furnishing

$$\frac{1}{h_i h_j}\frac{\partial x_i}{\partial y_j}\frac{\partial x_k}{\partial y_j} = \delta_{ik} \tag{1.62}$$

Also of interest is the volume element; the volume determined by the vector $\mathbf{dR}_y$ is given by the vector triple product

$$\begin{aligned} dV_y &= (h_1 dy_1 \boldsymbol{\gamma}_1)\cdot[h_2 dy_2 \boldsymbol{\gamma}_2 \times h_3 dy_3 \boldsymbol{\gamma}_3] \\ &= h_1 h_2 h_3 dy_1 dy_2 dy_3 \end{aligned} \tag{1.63}$$

and $h_1 h_2 h_3$ is known as the Jacobian of the transformation. For cylindrical coordinates using r, θ, and z, as shown in Figure 1.2, $x_1 = r\cos\theta$, $x_2 = r\sin\theta$, and $x_3 = z$. Simple manipulation furnishes that $h_r = 1$, $h_\theta = r$, $h_z = 1$, and

$$\mathbf{e}_r = \cos\theta\mathbf{e}_1 + \sin\theta\mathbf{e}_2 \qquad \mathbf{e}_\theta = -\sin\theta\mathbf{e}_1 + \cos\theta\mathbf{e}_2 \qquad \mathbf{e}_z = \mathbf{e}_3 \tag{1.64}$$

which, of course, are orthonormal vectors. Also of interest are the relations $\mathbf{de}_r = \mathbf{e}_\theta d\theta$ and $\mathbf{de}_\theta = -\mathbf{e}_r d\theta$.

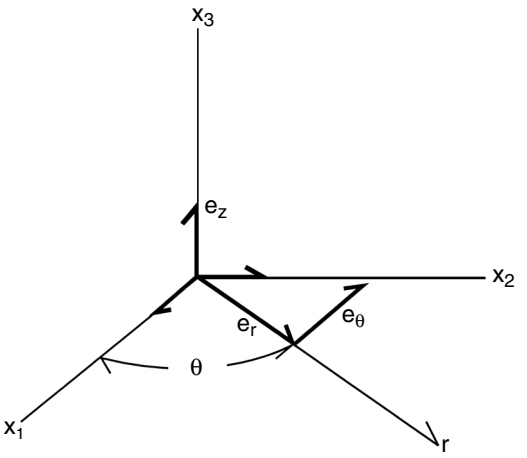

FIGURE 1.2 Cylindrical coordinate system.

Transformation of the coordinate system from rectilinear to cylindrical coordinates can be viewed as a rotation of the coordinate system through θ. Thus, if the vector $\mathbf{v}$ is referred to the reference rectilinear system and $\mathbf{v}'$ is the same vector referred to a cylindrical coordinate system, then in two dimensions,

$$\mathbf{v}' = \mathbf{Q}(\theta)\mathbf{v} \qquad \mathbf{Q}(\theta) = \begin{bmatrix} \cos\theta & \sin\theta & 0 \\ -\sin\theta & \cos\theta & 0 \\ 0 & 0 & 1 \end{bmatrix} \tag{1.65}$$

If $\mathbf{v}'$ is differentiated, for example, with respect to time t, there is a contribution from the rotation of the coordinate system: for example, if $\mathbf{v}$ and θ are functions of time t,

$$\begin{aligned} \frac{d}{dt}\mathbf{v}' &= \mathbf{Q}(\theta)\frac{d}{dt}\mathbf{v} + \frac{d\mathbf{Q}(\theta)}{dt}\mathbf{v} \\ &= \frac{\partial}{\partial t}\mathbf{v}' + \frac{d\mathbf{Q}(\theta)}{dt}\mathbf{Q}^{\mathrm{T}}(\theta)\mathbf{v}' \end{aligned} \tag{1.66}$$

where the partial derivative implies differentiation with θ instantaneously held fixed and

$$\frac{d\mathbf{Q}(\theta)}{dt} = \begin{bmatrix} -\sin\theta & \cos\theta & 0 \\ -\cos\theta & -\sin\theta & 0 \\ 0 & 0 & 1 \end{bmatrix} \frac{d\theta}{dt} \tag{1.67}$$

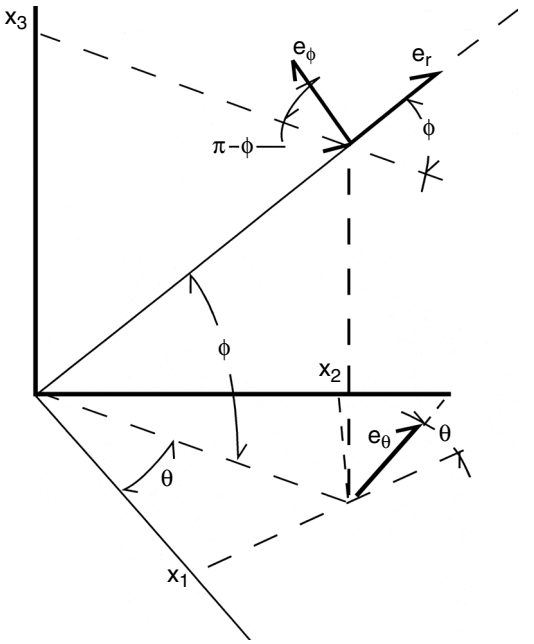

FIGURE 1.3 Spherical coordinate system.

Now $\frac{d\mathbf{Q}(\theta)}{dt}\mathbf{Q}^{\mathbf{T}}(\theta)$ is an antisymmetric matrix $\boldsymbol{\Omega}$ (to be identified later as a tensor) since

$$\mathbf{0} = \frac{d}{dt}(\mathbf{Q}(\theta)\mathbf{Q}^{\mathbf{T}}(\theta)) = \frac{d\mathbf{Q}(\theta)}{dt}\mathbf{Q}^{\mathbf{T}}(\theta) + \left[\frac{d\mathbf{Q}(\theta)}{dt}\mathbf{Q}^{\mathbf{T}}(\theta)\right]^{\mathbf{T}} \tag{1.68}$$

In fact,

$$\frac{d\mathbf{Q}(\theta)}{dt}\mathbf{Q}^{\mathbf{T}}(\theta) = \begin{pmatrix} 0 & 1 & 0 \\ -1 & 0 & 0 \\ 0 & 0 & 0 \end{pmatrix}\frac{d\theta}{dt} \tag{1.69}$$

It follows that

$$\frac{d}{dt}\mathbf{v}' = \frac{\partial}{\partial t}\mathbf{v}' + \boldsymbol{\omega}\times\mathbf{v}' \tag{1.70}$$

in which $\boldsymbol{\omega}$ is the axial vector of $\boldsymbol{\Omega}$.

Referring to Figure 1.3, spherical coordinates r, θ, and ϕ are introduced by the transformation

$$x_1 = r\cos\theta\cos\phi \qquad x_2 = r\sin\theta\cos\phi \qquad x_3 = r\sin\phi \tag{1.71}$$

The position vector is given by

$$\begin{aligned}\mathbf{r} &= x_1\mathbf{e}_1 + x_2\mathbf{e}_2 + x_3\mathbf{e}_3 \\ &= r\cos\theta\cos\phi\mathbf{e}_1 + r\sin\theta\cos\phi\mathbf{e}_2 + r\sin\phi\mathbf{e}_3\end{aligned} \tag{1.72}$$

Now $\mathbf{e}_r$ has the same direction as the position vector: $\mathbf{r} = r\mathbf{e}_r$. Thus, it follows that

$$\mathbf{e}_r = \cos\theta\cos\phi\mathbf{e}_1 + \sin\theta\cos\phi\mathbf{e}_2 + \sin\phi\mathbf{e}_3 \tag{1.73}$$

Following the general procedure in the preceding paragraphs,

$$\begin{array}{lll}\dfrac{\partial x_1}{\partial r} = \cos\theta\cos\phi & \dfrac{\partial x_1}{\partial\theta} = -r\sin\theta\cos\phi & \dfrac{\partial x_1}{\partial\phi} = -r\cos\theta\sin\phi \\ \dfrac{\partial x_2}{\partial r} = \sin\theta\cos\phi & \dfrac{\partial x_2}{\partial\theta} = r\cos\theta\cos\phi & \dfrac{\partial x_2}{\partial\phi} = -r\sin\theta\sin\phi \\ \dfrac{\partial x_3}{\partial r} = \sin\phi & \dfrac{\partial x_3}{\partial\theta} = 0 & \dfrac{\partial x_3}{\partial\phi} = r\cos\phi\end{array} \tag{1.74}$$

The differential of the position vector furnishes

$$d\mathbf{r} = dr\mathbf{e}_r + r\cos\phi\, d\theta\mathbf{e}_\theta + rd\phi\mathbf{e}_\phi \tag{1.75}$$

$$\mathbf{e}_r = \cos\theta\cos\phi\mathbf{e}_1 + \sin\theta\cos\phi\mathbf{e}_2 + \sin\phi\mathbf{e}_3 \quad \mathbf{e}_1 = \cos\theta\cos\phi\mathbf{e}_r - \sin\theta\mathbf{e}_\theta - \sin\phi\cos\theta\mathbf{e}_\phi$$

$$\mathbf{e}_\theta = -\sin\theta\mathbf{e}_1 + \cos\theta\mathbf{e}_2 \qquad \mathbf{e}_2 = \sin\theta\cos\phi\mathbf{e}_r + \cos\theta\mathbf{e}_\theta - \sin\phi\sin\theta\mathbf{e}_\phi$$

$$\mathbf{e}_\phi = -\sin\phi[\cos\theta\mathbf{e}_1 + \sin\theta\mathbf{e}_2] + \cos\phi\mathbf{e}_3 \quad \mathbf{e}_3 = \sin\phi\mathbf{e}_r + \cos\phi\mathbf{e}_\phi\,.$$

The scale factors are $h_r = 1$, $h_\theta = r\cos\phi$, $h_\phi = r$.

Consider a vector $\mathbf{v}$ in the rectilinear system, denoted as $\mathbf{v}'$ when referred to a spherical coordinate system:

$$\mathbf{v} = v_1\mathbf{e}_1 + v_2\mathbf{e}_2 + v_3\mathbf{e}_3 \qquad \mathbf{v}' = v_r\mathbf{e}_r + v_\theta\mathbf{e}_\theta + v_\phi\mathbf{e}_\phi. \tag{1.76}$$

Eliminating $\mathbf{e}_1$, $\mathbf{e}_2$, $\mathbf{e}_3$ in favor of $\mathbf{e}_r$, $\mathbf{e}_\theta$, $\mathbf{e}_\phi$ and using *M notation permits writing

$$\mathbf{v}' = \mathbf{Q}(\theta,\phi)\mathbf{v}, \qquad \mathbf{Q}(\theta,\phi) = \begin{bmatrix}\cos\theta\cos\phi & \sin\theta\cos\phi & \sin\phi \\ -\sin\theta & \cos\theta & 0 \\ -\sin\phi\cos\theta & -\sin\phi\sin\theta & \cos\phi\end{bmatrix}. \tag{1.77}$$

Suppose now that $\mathbf{v}(t)$, θ, and ϕ are functions of time. As in cylindrical coordinates,

$$\frac{d}{dt}\mathbf{v}' = \frac{\partial}{\partial t}\mathbf{v}' + \boldsymbol{\omega}\times\mathbf{v}' \tag{1.78}$$

where $\boldsymbol{\omega}$ is the axial vector of $\frac{d\mathbf{Q}(\theta)}{dt}\mathbf{Q}^{\mathrm{T}}(\theta)$. After some manipulation,

$$\begin{aligned}\frac{d\mathbf{Q}(\theta)}{dt} &= \begin{bmatrix} -\sin\theta\cos\phi & \cos\theta\cos\phi & 0 \\ -\cos\theta & -\sin\theta & 0 \\ \sin\theta\sin\phi & -\cos\theta\sin\phi & 0 \end{bmatrix}\frac{d\theta}{dt} \\ &+ \begin{bmatrix} -\cos\theta\sin\phi & -\sin\theta\sin\phi & \cos\phi \\ 0 & 0 & 0 \\ -\cos\theta\cos\phi & -\sin\theta\cos\phi & -\sin\phi \end{bmatrix}\frac{d\phi}{dt} \\ \frac{d\mathbf{Q}(\theta)}{dt}\mathbf{Q}^{\mathrm{T}}(\theta) &= \begin{bmatrix} 0 & \cos\phi & 0 \\ -\cos\phi & 0 & \sin\phi \\ 0 & -\sin\phi & 0 \end{bmatrix}\frac{d\theta}{dt} + \begin{bmatrix} 0 & 0 & 1 \\ 0 & 0 & 0 \\ -1 & 0 & 0 \end{bmatrix}\frac{d\phi}{dt}\end{aligned} \tag{1.79}$$

1.3.5 Gradient Operator

In rectilinear coordinates, let ψ be a scalar-valued function of $\mathbf{x}$: $\psi(\mathbf{x})$, starting with the chain rule

$$\begin{aligned} d\psi &= \frac{\partial\psi}{\partial x_i}dx_i \\ &= [\nabla\psi]\cdot d\mathbf{r}, \qquad d\mathbf{r} = \mathbf{e}_i dx_i \qquad \nabla\psi = \mathbf{e}_i\frac{\partial\psi}{\partial x_i} \end{aligned} \tag{1.80}$$

*T)

Clearly, $d\psi$ is a scalar and is unaffected by a coordinate transformation. Suppose that $\mathbf{x} = \mathbf{x}(\mathbf{y})$: $d\mathbf{r}' = \mathbf{g}_i dy_i$. Observe that

$$\begin{aligned} d\psi &= \frac{\partial\psi}{\partial x_i}dx_i \\ &= \sum_\alpha \frac{1}{h_\alpha}\frac{\partial\psi}{\partial y_\alpha}h_\alpha dy_\alpha \\ &= \left[\sum_\alpha \frac{\boldsymbol{\gamma}_\alpha}{h_\alpha}\frac{\partial\psi}{\partial y_\alpha}\right]\cdot\left[\sum_\beta h_\beta dy_\beta\boldsymbol{\gamma}_\beta\right] \end{aligned} \tag{1.81}$$

implying the identification

$$(\nabla\psi)' = \sum_{\alpha} \frac{\boldsymbol{\gamma}_\alpha}{h_\alpha} \frac{\partial \psi}{\partial y_\alpha} \tag{1.82}$$

For cylindrical coordinates in tensor-indicial notation with $\mathbf{e}_r = \boldsymbol{\gamma}_r$, $\mathbf{e}_\theta = \boldsymbol{\gamma}_\theta$, $\mathbf{e}_z = \boldsymbol{\gamma}_z$,

$$\nabla\psi = \mathbf{e}_r \frac{\partial \psi}{\partial r} + \frac{\mathbf{e}_\theta}{r} \frac{\partial \psi}{\partial \theta} + \mathbf{e}_z \frac{\partial \psi}{\partial z} \tag{1.83}$$

and in spherical coordinates

$$\nabla\psi = \mathbf{e}_r \frac{\partial \psi}{\partial r} + \frac{\mathbf{e}_\theta}{r\cos\phi} \frac{\partial \psi}{\partial \theta} + \frac{\mathbf{e}_z}{r} \frac{\partial \psi}{\partial \phi} \tag{1.84}$$

1.3.6 Divergence and Curl of Vectors

Under orthogonal transformations, the divergence and curl operators are invariant and satisfy the divergence and curl theorems, respectively. Unfortunately, the transformation properties of the divergence and curl operators are elaborate. The reader is referred to texts in continuum mechanics, such as Chung (1988). The development is given in Appendix I at the end of the chapter. Here, we simply list the results. Let $\mathbf{v}$ be a vector referred to rectilinear coordinates, and let $\mathbf{v}'$ denote the same vector referred to orthogonal coordinates. The divergence and curl satisfy

$$(\nabla \cdot \mathbf{v})' = \frac{1}{h_1 h_2 h_3}\left[\frac{\partial}{\partial y_1}(h_2 h_3 v_1') + \frac{\partial}{\partial y_2}(h_3 h_1 v_2') + \frac{\partial}{\partial y_3}(h_1 h_2 v_3')\right] \tag{1.85}$$

and

$$\begin{aligned}(\nabla \times \mathbf{v})' = \frac{1}{h_1 h_2 h_3}\Bigg[& h_1\left\{\frac{\partial}{\partial y_2}(h_3 v_3') - \frac{\partial}{\partial y_3}(h_2 v_2')\right\}\boldsymbol{\gamma}_1 \\ & - h_2\left\{\frac{\partial}{\partial y_1}(h_3 v_3') - \frac{\partial}{\partial y_3}(h_1 v_1')\right\}\boldsymbol{\gamma}_2 \\ & + h_3\left\{\frac{\partial}{\partial y_1}(h_2 v_2') - \frac{\partial}{\partial y_2}(h_1 v_1')\right\}\boldsymbol{\gamma}_3\Bigg]\end{aligned} \tag{1.86}$$

and in cylindrical coordinates:

$$(\nabla \cdot \mathbf{v}') = \frac{1}{r}\frac{\partial (r v_r)}{\partial r} + \frac{1}{r}\frac{\partial v_\theta}{\partial \theta} + \frac{\partial v_z}{\partial z} \tag{1.87}$$

and

$$(\nabla \times \mathbf{v})' = \frac{1}{r}\left[\left\{\frac{\partial v_z}{\partial \theta} - \frac{\partial (rv_\theta)}{\partial z}\right\}\mathbf{e}_r - \left\{\frac{\partial v_z}{\partial r} - \frac{\partial v_r}{\partial z}\right\}r\mathbf{e}_\theta + \left\{\frac{\partial (rv_\theta)}{\partial r} - \frac{\partial v_r}{\partial \theta}\right\}\mathbf{e}_z\right] \quad (1.88)$$

APPENDIX I: DIVERGENCE AND CURL OF VECTORS IN ORTHOGONAL CURVILINEAR COORDINATES

Derivatives of Base Vectors

In tensor-indicial notation, a vector **v** can be represented in rectilinear coordinates as $\mathbf{v} = v_k\mathbf{e}_k$. In orthogonal curvilinear coordinates, it is written as $\mathrm{v}' = \sum_\alpha v'_\alpha \boldsymbol{\gamma}_\alpha = \sum_\alpha v'_\alpha \frac{\mathbf{g}_\alpha}{h_\alpha}$.

A line segment $d\mathbf{r} = dx_i\mathbf{e}_i$ transforms to $d\mathbf{r}' = dy_k\mathbf{g}_k$. Recall that

$$\mathbf{e}_k = \frac{\partial y_l}{\partial x_k}\mathbf{g}_l = \sum_\beta h_\beta \frac{\partial y_\beta}{\partial x_k}\boldsymbol{\gamma}_\beta$$

$$\mathbf{g}_\alpha = \frac{\partial x_\alpha}{\partial y_k}\mathbf{e}_k \qquad h_\alpha = \sqrt{\mathbf{g}_\alpha \cdot \mathbf{g}_\alpha} \quad (a.1)$$

From Equation (a.1),

$$\frac{\partial \mathbf{g}_\alpha}{\partial y_j} = \frac{\partial^2 x_\alpha}{\partial y_k \partial y_j}\mathbf{e}_k$$

$$= \sum_\beta \begin{bmatrix} \alpha & & \beta \\ & j & \end{bmatrix} h_\beta \boldsymbol{\gamma}_\beta, \qquad \begin{bmatrix} \alpha & & \beta \\ & j & \end{bmatrix} = h_\beta \frac{\partial^2 x_\alpha}{\partial y_k \partial y_j}\frac{\partial y_\beta}{\partial x_k} \quad (a.2)$$

The bracketed quantities are known as Cristoffel symbols. From Equations (a.1 and a.2),

$$\frac{dh_\alpha}{dy_j} = \boldsymbol{\gamma}_\alpha \cdot \frac{d\mathbf{g}_\alpha}{dy_j}$$

$$= \begin{bmatrix} \alpha & & \alpha \\ & j & \end{bmatrix} h_\alpha \quad (a.3)$$

Continuing,

$$\frac{\partial \boldsymbol{\gamma}_\alpha}{\partial y_j} = \frac{1}{h_\alpha}\frac{\partial \mathbf{g}_\alpha}{\partial y_j} - \frac{\boldsymbol{\gamma}_\alpha}{h_\alpha}\frac{\partial h_\alpha}{\partial y_j}$$

$$= \sum_\beta c_{\alpha j\beta}\boldsymbol{\gamma}_\beta, \qquad c_{\alpha j\beta} = \frac{1}{h_\alpha}(1 - \delta_{\alpha\beta})\begin{bmatrix} \alpha & & \beta \\ & j & \end{bmatrix} h_\beta \quad (a.4)$$

Divergence

The development that follows is based on the fact that

$$\nabla \cdot \mathbf{v} = \nabla' \cdot \mathbf{v}' = tr\left(\frac{d\mathbf{v}'}{d\mathbf{r}'}\right) = tr\left(\frac{d\mathbf{v}}{d\mathbf{r}}\right) \tag{a.5}$$

The differential of $\mathbf{v}'$ is readily seen to be

$$d\mathbf{v}' = dv_j \boldsymbol{\gamma}_j + v_j d\boldsymbol{\gamma}_j \tag{a.6}$$

First, note that

$$\begin{aligned} dv_j \boldsymbol{\gamma}_j &= \frac{\partial v_j}{\partial y_k} \boldsymbol{\gamma}_j dy_k \\ &= \sum_\alpha \left(\frac{1}{h_\alpha} \frac{\partial v_j}{\partial y_\alpha} \boldsymbol{\gamma}_j \right) (h_\alpha dy_\alpha) \\ &= \sum_\alpha \left(\frac{1}{h_\alpha} \frac{\partial v_j}{\partial y_\alpha} \boldsymbol{\gamma}_j \wedge \boldsymbol{\gamma}_\alpha \right) \cdot \sum_\beta (h_\beta \boldsymbol{\gamma}_\beta dy_\beta) \\ &= \sum_\alpha \left(\frac{1}{h_\alpha} \frac{\partial v_j}{\partial y_\alpha} \boldsymbol{\gamma}_j \wedge \boldsymbol{\gamma}_\alpha \right) \cdot d\mathbf{r}' \end{aligned} \tag{a.7}$$

Similarly,

$$\begin{aligned} v_j d\boldsymbol{\gamma}_j &= v_j \frac{\partial \boldsymbol{\gamma}_j}{\partial y_k} dy_k \\ &= \sum_\alpha \left(\frac{v_j}{h_\alpha} \frac{\partial \boldsymbol{\gamma}_j}{\partial y_\alpha} \right) (h_\alpha dy_\alpha) \\ &= \sum_\alpha \left(\frac{v_j}{h_\alpha} \frac{\partial \boldsymbol{\gamma}_j}{\partial y_\alpha} \wedge \boldsymbol{\gamma}_\alpha \right) \cdot \sum_\beta (h_\beta \boldsymbol{\gamma}_\beta dy_\beta) \\ &= \sum_\alpha \left(\frac{v_j}{h_\alpha} \frac{\partial \boldsymbol{\gamma}_j}{\partial y_\alpha} \wedge \boldsymbol{\gamma}_\alpha \right) \cdot d\mathbf{r}' \\ &= \sum_\alpha \left[\frac{v_j}{h_\alpha} \left(\sum_\beta c_{j\alpha\beta} \boldsymbol{\gamma}_\beta \wedge \boldsymbol{\gamma}_\alpha \right) \right] \cdot d\mathbf{r}' \end{aligned} \tag{a.8}$$

Consequently,

$$\left[\frac{dv}{dr}\right]_{\beta\alpha} = \frac{1}{h_\alpha}\left[\frac{\partial v_j}{\partial y_\alpha}\delta_{j\beta} + v_j c_{j\beta\alpha}\right], \qquad \nabla\cdot\mathbf{v} = \sum_\alpha \frac{1}{h_\alpha}\left[\frac{\partial v_\alpha}{\partial y_\alpha} + v_j c_{j\alpha\alpha}\right] \tag{a.9}$$

Curl

In rectilinear coordinates, the individual entries of the curl can be expressed as a divergence, as follows. For the i^{th} entry,

$$\begin{aligned}[\nabla\times\mathbf{v}]_i &= \varepsilon_{ijk}\frac{\partial v_k}{\partial x_j} \\ &= \frac{\partial}{\partial x_j} w_j^{(i)} \qquad\qquad w_j^{(i)} = \varepsilon_{jki} v_k \\ &= \nabla\cdot\mathbf{w}^{(i)}\end{aligned} \tag{a.10}$$

Consequently, the curl of **v** can be written as

$$\nabla\times\mathbf{v} = \begin{pmatrix} \nabla\cdot\mathbf{w}^{(1)} \\ \nabla\cdot\mathbf{w}^{(2)} \\ \nabla\cdot\mathbf{w}^{(3)} \end{pmatrix} \tag{a.11}$$

The transformation properties of the curl can be readily induced from Equation (a.9).

1.4 EXERCISES

1. In the tetrahedron shown in Figure 1.4, A_1, A_2, and A_3 denote the areas of the faces whose normal vectors point in the $-\mathbf{e}_1$, $-\mathbf{e}_2$, and $-\mathbf{e}_3$ directions. Let A and **n** denote the area and normal vector of the inclined face, respectively. Prove that

$$\mathbf{n} = \frac{A_1}{A}\mathbf{e}_1 + \frac{A_2}{A}\mathbf{e}_2 + \frac{A_3}{A}\mathbf{e}_3$$

2. Prove that if $\boldsymbol{\sigma}$ is a symmetric tensor with entries σ_{ij}, that

$$\varepsilon_{ijk}\sigma_{jk} = 0, \quad i = 1,\ 2,\ 3.$$

3. If **v** and **w** are $n \times 1$ vectors, prove that $\mathbf{v}\times\mathbf{w}$ can be written as

$$\mathbf{v}\times\mathbf{w} = \mathbf{V}\mathbf{w}$$

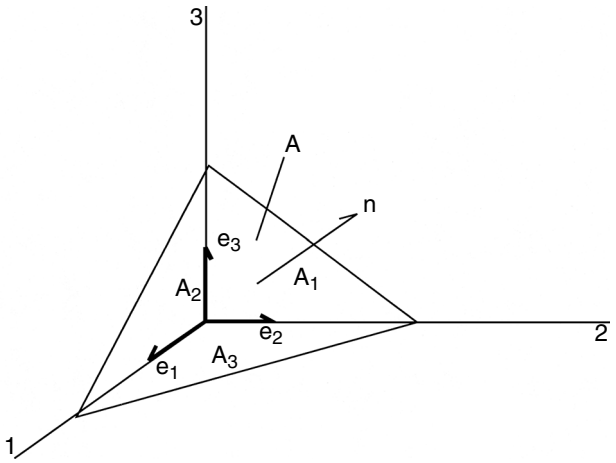

FIGURE 1.4 Geometry of a tetrahedron.

in which **V** is an antisymmetric tensor and **v** is the axial vector of **V**. Derive the expression for **V**.

4. Find the transposes of the matrices

$$\mathbf{A} = \begin{bmatrix} 1 & -1/2 \\ -1/3 & 1/4 \end{bmatrix} \qquad \mathbf{B} = \begin{bmatrix} 1 & 1/3 \\ 1/2 & 1/4 \end{bmatrix}$$

   (a) Verify that $\mathbf{AB} \neq \mathbf{BA}$.
   (b) Verify that $(\mathbf{AB})^{\mathbf{T}} = \mathbf{B}^{\mathbf{T}}\mathbf{A}^{\mathbf{T}}$.

5. Consider a matrix **C** given by

$$\mathbf{C} = \begin{bmatrix} a & b \\ c & d \end{bmatrix}$$

   Verify that its inverse is given by

$$\mathbf{C}^{-1} = \frac{1}{ad - bc}\begin{bmatrix} d & -b \\ -c & a \end{bmatrix}$$

6. For the matrices in Exercise 4, find the inverses and verify that

$$(\mathbf{AB})^{-1} = \mathbf{B}^{-1}\mathbf{A}^{-1}$$

7. Consider the matrix

$$\mathbf{Q} = \begin{bmatrix} \cos\theta & \sin\theta \\ -\sin\theta & \cos\theta \end{bmatrix}$$

Verify that
(a) $\mathbf{QQ}^{\mathbf{T}} = \mathbf{Q}^{\mathbf{T}}\mathbf{Q}$
(b) $\mathbf{Q}^{\mathbf{T}} = \mathbf{Q}^{-1}$
(c) For any 2×1 vector $\mathbf{a}$

$$|\mathbf{Qa}| = |\mathbf{a}|$$

[The relation in (c) is general, and $\mathbf{Qa}$ represents a rotation of $\mathbf{a}$.]

8. Using the matrix $\mathbf{C}$ from Exercise 5, and introducing the vectors (one-dimensional arrays)

$$\mathbf{a} = \begin{pmatrix} q \\ r \end{pmatrix} \qquad \mathbf{b} = \begin{pmatrix} s \\ t \end{pmatrix}$$

verify that

$$\mathbf{a}^{\mathbf{T}}\mathbf{Cb} = \mathbf{b}^{\mathbf{T}}\mathbf{C}^{\mathbf{T}}\mathbf{a}$$

9. Verify the divergence theorem using the following block, where

$$\mathbf{v} = \begin{bmatrix} x - y \\ x + y \end{bmatrix}$$

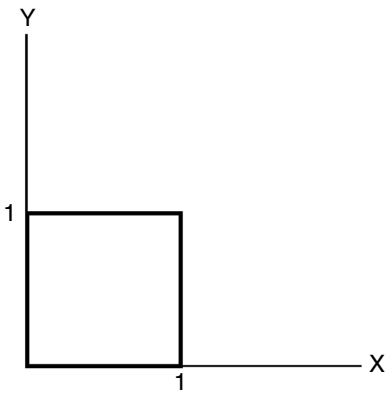

FIGURE 1.5 Test figure for the divergence theorem.

10. For the vector and geometry of Exercise 9, verify that

$$\int \mathbf{n} \times \mathbf{v} dS = \int \nabla \times \mathbf{v} dV$$

11. Using the geometry of Exercise 9, verify that

$$\int \mathbf{n} \times \mathbf{A} dS = \int \nabla \times \mathbf{A}^{\mathbf{T}} dV$$

using

$$a_{11} = x + y + x^2 + y^2$$

$$a_{12} = x + y + x^2 - y^2$$

$$a_{21} = x + y - x^2 - y^2$$

$$a_{22} = x - y - x^2 - y^2$$

12. Obtain the expressions for the gradient, divergence, and curl in spherical coordinates.

2 Mathematical Foundations: Tensors

2.1 TENSORS

We now consider two $n \times 1$ vectors, $\mathbf{v}$ and $\mathbf{w}$, and an $n \times n$ matrix, $\mathbf{A}$, such that $\mathbf{v} = \mathbf{Aw}$. We now make the important assumption that the underlying information in this relation is preserved under rotation. In particular, simple manipulation furnishes that

$$
\begin{aligned}
\mathbf{v}' &= \mathbf{Qv} \\
&= \mathbf{QAw} \\
&= \mathbf{QAQ^T Qw} \\
&= \mathbf{QAQ^T w}'.
\end{aligned}
\tag{2.1}
$$

*M)

The square matrix $\mathbf{A}$ is now called a second-order tensor if and only if $\mathbf{A}' = \mathbf{QAQ^T}$.

Let $\mathbf{A}$ and $\mathbf{B}$ be second-order $n \times n$ tensors. The manipulations that follow demonstrate that $\mathbf{A^T}$, $(\mathbf{A} + \mathbf{B})$, $\mathbf{AB}$, and $\mathbf{A^{-1}}$ are also tensors.

$$
\begin{aligned}
(\mathbf{A^T})' &= (\mathbf{QAQ^T})^\mathbf{T} \\
&= \mathbf{Q^{T^T} A^T Q^T}
\end{aligned}
\tag{2.2}
$$

$$
\begin{aligned}
\mathbf{A'B'} &= (\mathbf{QAQ^T})(\mathbf{QBQ^T}) \\
&= \mathbf{QA}(\mathbf{QQ^T})\mathbf{BQ^T} \\
&= \mathbf{QABQ^T}
\end{aligned}
\tag{2.3}
$$

$$
\begin{aligned}
(\mathbf{A}+\mathbf{B})' &= \mathbf{A}' + \mathbf{B}' \\
&= \mathbf{QAQ^T} + \mathbf{QBQ^T} \\
&= \mathbf{Q}(\mathbf{A}+\mathbf{B})\mathbf{Q^T}
\end{aligned}
\tag{2.4}
$$

$$
\begin{aligned}
\mathbf{A'^{-1}} &= (\mathbf{QAQ^T})^{-1} \\
&= \mathbf{Q^{T-1} A^{-1} Q^{-1}} \\
&= \mathbf{QA^{-1}Q^T}.
\end{aligned}
\tag{2.5}
$$

Let $\mathbf{x}$ denote an $n \times 1$ vector. The outer product, $\mathbf{x}\mathbf{x}^{\mathbf{T}}$, is a second-order tensor since

$$\begin{aligned}(\mathbf{x}\mathbf{x}^{\mathbf{T}})' &= \mathbf{x}'\mathbf{x}'^{\mathbf{T}} \\ &= (\mathbf{Q}\mathbf{x})(\mathbf{Q}\mathbf{x})^{\mathbf{T}} \\ &= \mathbf{Q}(\mathbf{x}\mathbf{x}^{\mathbf{T}})\mathbf{Q}^{\mathbf{T}}\end{aligned} \tag{2.6}$$

Next,

$$d^2\phi = d\mathbf{x}^{\mathbf{T}}\mathbf{H}d\mathbf{x} \qquad \mathbf{H} = \left(\frac{d}{d\mathbf{x}}\right)^{\mathbf{T}}\left(\frac{d\phi}{d\mathbf{x}}\right). \tag{2.7}$$

However,

$$\begin{aligned}d\mathbf{x}'^{\mathbf{T}}\mathbf{H}'d\mathbf{x}' &= (\mathbf{Q}d\mathbf{x})^{\mathbf{T}}\mathbf{H}'\mathbf{Q}d\mathbf{x} \\ &= d\mathbf{x}^{\mathbf{T}}(\mathbf{Q}^{\mathbf{T}}\mathbf{H}'\mathbf{Q})d\mathbf{x},\end{aligned} \tag{2.8}$$

from which we conclude that the Hessian $\mathbf{H}$ is a second-order tensor.

Finally, let $\mathbf{u}$ be a vector-valued function of $\mathbf{x}$. Then, $d\mathbf{u} = \frac{\partial \mathbf{u}}{\partial \mathbf{x}} d\mathbf{x}$, from which

$$d\mathbf{u}^{\mathbf{T}} = d\mathbf{x}^{\mathbf{T}}\left(\frac{\partial \mathbf{u}}{\partial \mathbf{x}}\right)^{\mathbf{T}} \tag{2.9}$$

and also

$$d\mathbf{u}^{\mathbf{T}} = d\mathbf{x}^{\mathbf{T}}\left(\frac{\partial}{\partial \mathbf{x}}\right)^{\mathbf{T}}\mathbf{u}^{\mathbf{T}}. \tag{2.10}$$

We conclude that

$$\left(\frac{\partial \mathbf{u}}{\partial \mathbf{x}}\right)^{\mathbf{T}} = \frac{\partial \mathbf{u}^{\mathbf{T}}}{\partial \mathbf{x}^{\mathbf{T}}}. \tag{2.11}$$

Furthermore, if $d\mathbf{u}'$ is a vector generated from $d\mathbf{u}$ by rotation in the opposite sense from the coordinate axes, then $d\mathbf{u}' = \mathbf{Q}d\mathbf{u}$ and $d\mathbf{x} = \mathbf{Q}d\mathbf{x}'$. Hence, $\mathbf{Q}$ is a tensor. Also, since $d\mathbf{u}' = \frac{\partial \mathbf{u}'}{\partial \mathbf{x}'} d\mathbf{x}'$, it is apparent that

$$\frac{\partial \mathbf{u}'}{\partial \mathbf{x}'} = \mathbf{Q}\frac{\partial \mathbf{u}}{\partial \mathbf{x}}\mathbf{Q}^{\mathbf{T}}, \tag{2.12}$$

from which we conclude that $\frac{\partial \mathbf{u}}{\partial \mathbf{x}}$ is a tensor. We can similarly show that $\mathbf{I}$ and $\mathbf{0}$ are tensors.

2.2 DIVERGENCE, CURL, AND LAPLACIAN OF A TENSOR

Suppose **A** is a tensor and **b** is an arbitrary, spatially constant vector of compatible dimension. The divergence and curl of a vector have already been defined. For later purposes, we need to extend the definition of the divergence and the curl to **A**.

2.2.1 DIVERGENCE

Recall the divergence theorem $\int \mathbf{c}^{\mathbf{T}}\mathbf{n}dS = \int \nabla^{\mathbf{T}}\mathbf{c}dV$. Let $\mathbf{c} = \mathbf{A}^{\mathbf{T}}\mathbf{b}$, in which **b** is an arbitrary constant vector. Now

$$\begin{aligned}\mathbf{b}^{\mathbf{T}}\int \mathbf{A}\mathbf{n}dS &= \int \nabla^{\mathbf{T}}(\mathbf{A}^{\mathbf{T}}\mathbf{b})dV \\ &= \int \nabla^{\mathbf{T}}\mathbf{A}^{\mathbf{T}}dV\mathbf{b} \\ &= \mathbf{b}^{\mathbf{T}}\int [\nabla^{\mathbf{T}}\mathbf{A}^{\mathbf{T}}]^{\mathbf{T}}dV. \end{aligned} \tag{2.13}$$

Consequently, we must define the divergence of **A** such that

$$^{*}\mathrm{M}) \qquad \int \mathbf{A}\mathbf{n}dS - \int [\nabla^{\mathbf{T}}\mathbf{A}^{\mathbf{T}}]^{\mathbf{T}}dV = \mathbf{0}. \tag{2.14}$$

In tensor-indicial notation,

$$\int b_i a_{ij} n_j dS - \int b_i \left[[\nabla^{\mathbf{T}}\mathbf{A}^{\mathbf{T}}]^{\mathbf{T}}\right]_i dV = 0. \tag{2.15}$$

Application of the divergence theorem to the vector $c_j = b_i a_{ij}$ furnishes

$$b_i \int \left[\frac{\partial}{\partial x_j}a_{ij} - \left[[\nabla^{\mathbf{T}}\mathbf{A}^{\mathbf{T}}]^{\mathbf{T}}\right]_i\right]dV = 0. \tag{2.16}$$

Since **b** is arbitrary, we conclude that

$$[\nabla^{\mathbf{T}}\mathbf{A}^{\mathbf{T}}]_i = \frac{\partial}{\partial x_j}a_{ij} = \frac{\partial}{\partial x_j}a_{ji}{}^{\mathbf{T}}. \tag{2.17}$$

Thus, if we are to write $\nabla \cdot \mathbf{A}$ as a (column) vector, mixing tensor- and matrix-vector notation,

$$\nabla \cdot \mathbf{A} = [\nabla^{\mathbf{T}}\mathbf{A}^{\mathbf{T}}]^{\mathrm{T}}. \tag{2.18}$$

It should be evident that $(\nabla\cdot)$ has different meanings when applied to a tensor as opposed to a vector.

Suppose **A** is written in the form

$$\mathbf{A} = \begin{pmatrix} \boldsymbol{\alpha}_1^{\mathbf{T}} \\ \boldsymbol{\alpha}_2^{\mathbf{T}} \\ \boldsymbol{\alpha}_3^{\mathbf{T}} \end{pmatrix}, \tag{2.19}$$

in which $\boldsymbol{\alpha}_i^{\mathbf{T}}$ corresponds to the i^{th} row of $\mathbf{A}$:$[\boldsymbol{\alpha}_i^{\mathbf{T}}]_j = a_{ij}$. It is easily seen that

$$\nabla^{\mathbf{T}}\mathbf{A}^{\mathbf{T}} = (\nabla^{\mathbf{T}}\boldsymbol{\alpha}_1 \quad \nabla^{\mathbf{T}}\boldsymbol{\alpha}_2 \quad \nabla^{\mathbf{T}}\boldsymbol{\alpha}_3). \tag{2.20}$$

2.2.2 Curl and Laplacian

The curl of vector **c** satisfies the curl theorem $\int \nabla\times\mathbf{c}\,dV = \int \mathbf{n}\times\mathbf{c}\,dS$. Using tensor-indicial notation,

$$\begin{aligned} \int \mathbf{n}\times\mathbf{c}\,dS &= \int \varepsilon_{ijk} n_j a_{kl} b_l\, dS \\ &= \left[\int \varepsilon_{ijk} n_j a_{kl}\, dS\right] b_l \\ &= \int c_{ij} n_j\, dS b_l, \quad c_{ij} = \varepsilon_{ijk} a_{kl} b_l. \end{aligned} \tag{2.21}$$

From the divergence theorem applied to the tensor $c_{ij} = \varepsilon_{ijk}\, a_{kl}\, b_l$,

$$\begin{aligned} \left[\int \mathbf{n}\times\mathbf{A}\mathbf{b}\,dS\right]_i &= \int \frac{\partial}{\partial x_j}(\varepsilon_{ijk} a_{kl} b_l)\,dV \\ &= \left[\int \varepsilon_{ijk}\frac{\partial a_{kl}}{\partial x_j}\,dV\right] b_l \\ &= \left[\int \nabla\times\mathbf{A}^{\mathbf{T}}\,dV\,\mathbf{b}\right]_i, \quad \text{if } [\nabla\times\mathbf{A}]_{il} = \varepsilon_{ijk}\frac{\partial}{\partial x_j} a_{kl}. \end{aligned} \tag{2.22}$$

Let $\boldsymbol{\alpha}_l^{\mathbf{T}}$ denote the row vector (array) corresponding to the l^{th} row of **A**: $[\boldsymbol{\alpha}_l^{\mathbf{T}}]_k = a_{lk}$. It follows that

$$\nabla\times\mathbf{A} = \left[\nabla\times\boldsymbol{\alpha}_1 \;\middle|\; \nabla\times\boldsymbol{\alpha}_2 \;\middle|\; \nabla\times\boldsymbol{\alpha}_3\right]. \tag{2.23}$$

If $\boldsymbol{\beta}_I$ is the array for the I^{th} column of $\mathbf{A}$, then

$$\nabla \times \mathbf{A}^{\mathbf{T}} = \left[\nabla \times \boldsymbol{\beta}_{\mathbf{1}} \;\middle|\; \nabla \times \boldsymbol{\beta}_{\mathbf{2}} \;\middle|\; \nabla \times \boldsymbol{\beta}_{\mathbf{3}}\right]. \tag{2.24}$$

The Laplacian applied to $\mathbf{A}$ is defined by

$$[\nabla^{\mathbf{2}}\mathbf{A}]_{ij} = \nabla^{\mathbf{2}} a_{ij}. \tag{2.25}$$

It follows, therefore, that

$$\nabla^{\mathbf{2}}\mathbf{A} = [\nabla^{\mathbf{2}}\boldsymbol{\beta}_{\mathbf{1}} \quad \nabla^{\mathbf{2}}\boldsymbol{\beta}_{\mathbf{2}} \quad \nabla^{\mathbf{2}}\boldsymbol{\beta}_{\mathbf{3}}]. \tag{2.26}$$

The vectors $\boldsymbol{\beta}_i$ satisfy the Helmholtz decomposition

$$\nabla^{\mathbf{2}}\boldsymbol{\beta}_i = \nabla(\nabla \cdot \boldsymbol{\beta}_i) - \nabla \times \nabla \times \boldsymbol{\beta}_i. \tag{2.27}$$

Observe from the following results that

$$\nabla^{\mathbf{2}}\mathbf{A} = \nabla(\nabla \cdot \mathbf{A}^{\mathbf{T}}) - \nabla \times [\nabla \times \mathbf{A}^{\mathbf{T}}]^{\mathbf{T}}. \tag{2.28}$$

An integral theorem for the Laplacian of a tensor is now found as

$$\int \nabla^{\mathbf{2}}\mathbf{A}\,dV = \int (\mathbf{n}\nabla^{\mathbf{T}})\mathbf{A}\,dS - \int \mathbf{n} \times [\nabla \times \mathbf{A}^{\mathbf{T}}]^{\mathbf{T}}\,dS. \tag{2.29}$$

2.3 INVARIANTS

Letting $\mathbf{A}$ denote a nonsingular, symmetric, 3×3 tensor, the equation $\det(\mathbf{A} - \lambda\mathbf{I}) = 0$ can be expanded as

$$\lambda^3 - I_1\lambda^2 + I_2\lambda - I_3 = 0, \tag{2.30}$$

in which

$$I_1 = tr(\mathbf{A}) \qquad I_2 = \frac{1}{2}[tr^2(\mathbf{A}) - tr(\mathbf{A}^2)] \qquad I_3 = \det(\mathbf{A}). \tag{2.31}$$

Here, $tr(\mathbf{A}) = \delta_{ij}a_{ij}$ denotes the *trace* of $\mathbf{A}$. Equation 2.30 also implies the Cayley-Hamilton theorem:

$$\mathbf{A}^3 - I_1\mathbf{A}^2 + I_2\mathbf{A} - I_3\mathbf{I} = \mathbf{0}, \tag{2.32}$$

from which

$$I_3 = \frac{1}{3}[tr(\mathbf{A}^3) - I_1 tr(\mathbf{A}^2) + I_2 tr(\mathbf{A})]$$
$$\mathbf{A^{-1}} = I_3^{-1}[\mathbf{A}^2 - I_1\mathbf{A} + I_2\mathbf{I}] \tag{2.33}$$

The trace of any $n \times n$ symmetric tensor $\mathbf{B}$ is invariant under orthogonal transformations (rotations), such as $tr(\mathbf{B}') = tr(\mathbf{B})$, since

$$\begin{aligned} a'_{pq}\delta_{pq} &= q_{pr}q_{qs}a_{rs}\delta_{pq} \\ &= a_{rs}q_{pr}q_{qs} \\ &= a_{rs}\delta_{rs}. \end{aligned} \tag{2.34}$$

Likewise, $tr(\mathbf{A}^2)$ and $tr(\mathbf{A}^3)$ are invariant since $\mathbf{A}$, $\mathbf{A}^2$, and $\mathbf{A}^3$ are tensors, thus I_1, I_2, and I_3 are invariants. Derivatives of invariants are presented in a subsequent section.

2.4 POSITIVE DEFINITENESS

In the finite-element method, an attractive property of some symmetric tensors is positive definiteness, defined as follows. The symmetric $n \times n$ tensor $\mathbf{A}$ is positive-definite, written $\mathbf{A} > \mathbf{0}$, if, for all nonvanishing $n \times 1$ vectors $\mathbf{x}$, the quadratic product $q(\mathbf{A}, \mathbf{x}) = \mathbf{x^T A x} > 0$. The importance of this property is shown in the following example. Let $\Pi = \frac{1}{2}\mathbf{x^T A x} - \mathbf{x^T f}$, in which $\mathbf{f}$ is known and $\mathbf{A} > \mathbf{0}$. After some simple manipulation,

$$\begin{aligned} d^2\Pi &= d\mathbf{x^T}\left[\left(\frac{d}{d\mathbf{x}}\right)^{\mathbf{T}} \frac{d}{d\mathbf{x}}\Pi\right]d\mathbf{x} \\ &= d\mathbf{x^T A}\,d\mathbf{x}. \end{aligned} \tag{2.35}$$

It follows that Π is a globally convex function that attains a minimum when $\mathbf{Ax} = \mathbf{f}$ ($d\Pi = 0$).

The following definition is equivalent to the statement that the symmetric $n \times n$ tensor $\mathbf{A}$ is positive-definite if and only if its eigenvalues are positive. For the sake of demonstration,

$$\begin{aligned} \mathbf{x^T A x} &= \mathbf{x^T X \Lambda \Lambda^T x} \\ &= \mathbf{y^T \Lambda y}, \quad (\mathbf{y} = \mathbf{X^T x}) \\ &= \sum_i \lambda_i y_i^2. \end{aligned} \tag{2.36}$$

The last expression can be positive for arbitrary **y** (arbitrary **x**) only if $\lambda_i > 0$, $i = 1, 2, \ldots, n$. The matrix **A** is semidefinite if $\mathbf{x}^T\mathbf{A}\mathbf{x} \geq 0$, and negative-definite (written $\mathbf{A} < \mathbf{0}$), if $\mathbf{x}^T\mathbf{A}\mathbf{x} < 0$. If **B** is a nonsingular tensor, then $\mathbf{B}^T\mathbf{B} > \mathbf{0}$, since $q(\mathbf{B}^T\mathbf{B}, \mathbf{x}) = \mathbf{x}^T\mathbf{B}^T\mathbf{B}\mathbf{x} = \mathbf{y}^T\mathbf{y} > 0$ (in which $\mathbf{y} = \mathbf{B}\mathbf{x}$ and Ω denotes the quadratic product). If **B** is singular, for example if $\mathbf{B} = \mathbf{y}\mathbf{y}^T$ where **y** is an $n \times 1$ vector, $\mathbf{B}^T\mathbf{B}$ is positive-semidefinite since a nonzero eigenvector **x** of **B** can be found for which the quadratic product $q(\mathbf{B}^T\mathbf{B}, \mathbf{x})$ vanishes.

Now suppose that **B** is a nonsingular, antisymmetric tensor. Multiplying through $\mathbf{B}\mathbf{x}_j = \lambda_j \mathbf{x}_j$ with $\mathbf{B}^T$ furnishes

$$\begin{aligned}\mathbf{B}^T\mathbf{B}\mathbf{x}_j &= \lambda_j \mathbf{B}^T\mathbf{x}_j \\ &= -\lambda_j \mathbf{B}\mathbf{x}_j \\ &= -\lambda_j^2 \mathbf{x}_j. \end{aligned} \tag{2.37}$$

Since $\mathbf{B}^T\mathbf{B}$ is positive-definite, it follows that $-\lambda_j^2 > 0$. Thus, λ_j is imaginary: $\lambda_j = i\mu_j$ using $i = \sqrt{-1}$. Consequently, $\mathbf{B}^2\mathbf{x}_j = \lambda_j^2\mathbf{x}_j = -\mu_j^2\mathbf{x}_j$, demonstrating that $\mathbf{B}^2$ is *negative-definite*.

2.5 POLAR DECOMPOSITION THEOREM

For an $n \times n$ matrix **B**, $\mathbf{B}^T\mathbf{B} > 0$. If the *modal matrix* of **B** is denoted by $\mathbf{X}_b$, we can write

$$\begin{aligned}\mathbf{B}^T\mathbf{B} &= \mathbf{X}_b^T\boldsymbol{\Delta}_b\mathbf{X}_b \\ &= \mathbf{X}_b^T(\boldsymbol{\Delta}_b)^{\frac{1}{2}}\mathbf{Y}\mathbf{Y}^T(\boldsymbol{\Delta}_b)^{\frac{1}{2}}\mathbf{X}_b \\ &= \left(\mathbf{X}_b^T(\boldsymbol{\Delta}_b)^{\frac{1}{2}}\mathbf{Y}\right)\left(\mathbf{X}_b^T(\boldsymbol{\Delta}_b)^{\frac{1}{2}}\mathbf{Y}\right)^T, \end{aligned} \tag{2.38a}$$

in which **Y** is an (unknown) orthogonal tensor. In general, we can write

$$\mathbf{B} = \mathbf{Y}^T(\boldsymbol{\Delta}_b)^{\frac{1}{2}}\mathbf{X}_b. \tag{2.38b}$$

To "justify" Equation 2.38b, we introduce the square root $\sqrt{\mathbf{B}^T\mathbf{B}}$ using

$$\sqrt{\mathbf{B}^T\mathbf{B}} = \mathbf{X}_b^T\boldsymbol{\Delta}_b^{\frac{1}{2}}\mathbf{X}_b, \qquad \boldsymbol{\Delta}_b^{\frac{1}{2}} = \begin{bmatrix} \sqrt{\lambda_1} & 0 & . & . & . \\ 0 & \sqrt{\lambda_2} & . & . & . \\ . & . & . & . & . \\ . & . & . & . & 0 \\ . & . & . & 0 & \sqrt{\lambda_n} \end{bmatrix}, \tag{2.38c}$$

in which the positive square roots are used. It is easy to verify that $(\sqrt{\mathbf{B}^{\mathbf{T}}\mathbf{B}})^2 = \mathbf{B}$ and that $\sqrt{\mathbf{B}^{\mathbf{T}}\mathbf{B}} > 0$. Note that

$$\left[\mathbf{B}\left(\sqrt{\mathbf{B}^{\mathbf{T}}\mathbf{B}}\right)^{-\frac{1}{2}}\right]\left[\mathbf{B}\left(\sqrt{\mathbf{B}^{\mathbf{T}}\mathbf{B}}\right)^{-\frac{1}{2}}\right]^{\mathbf{T}} = \left[\left(\sqrt{\mathbf{B}^{\mathbf{T}}\mathbf{B}}\right)^{-\frac{1}{2}}\right][\mathbf{B}^{\mathbf{T}}\mathbf{B}]\left[\left(\sqrt{\mathbf{B}^{\mathbf{T}}\mathbf{B}}\right)^{-\frac{1}{2}}\right]$$
$$= \mathbf{I}. \tag{2.38d}$$

Thus, $\mathbf{B}(\sqrt{\mathbf{B}^{\mathbf{T}}\mathbf{B}})^{-1/2}$ is an orthogonal tensor, called, for example, $\mathbf{Z}$, and hence we can write

$$\mathbf{B} = \mathbf{Z}\sqrt{\mathbf{B}^{\mathbf{T}}\mathbf{B}}$$
$$= \mathbf{Z}\mathbf{X}_b^{\mathbf{T}}\boldsymbol{\Delta}_b^{\frac{1}{2}}\mathbf{X}_b. \tag{2.38e}$$

Finally, noting that $(\mathbf{Z}\mathbf{X}_b^{\mathbf{T}})(\mathbf{Z}\mathbf{X}_b^{\mathbf{T}})^{\mathbf{T}} = \mathbf{Z}(\mathbf{X}_{\mathbf{b}}^{\mathbf{T}}\mathbf{X}_{\mathbf{b}})\mathbf{Z}^{\mathbf{T}} = \mathbf{Z}\mathbf{Z}^{\mathbf{T}} = \mathbf{I}$, we make the identification $\mathbf{Y}^{\mathbf{T}} = \mathbf{Z}\mathbf{X}_b^{\mathbf{T}}$ in Equation 2.38b. Equation 2.38 plays a major role in the interpretation of strain tensors, a concept that is introduced in subsequent chapters.

2.6 KRONECKER PRODUCTS ON TENSORS

2.6.1 *VEC* Operator and the Kronecker Product

Let $\mathbf{A}$ be an $n \times n$ (second-order) tensor. Kronecker product notation (Graham, 1981) reduces $\mathbf{A}$ to a first-order $n \times 1$ tensor (vector), as follows.

$$VEC(\mathbf{A}) = \{a_{11} \quad a_{21} \quad a_{31} \quad \cdots \quad a_{n,n-1} \quad a_{nn}\}^{\mathbf{T}}. \tag{2.39}$$

The inverse *VEC* operator, *IVEC*, is introduced by the obvious relation $IVEC(VEC(\mathbf{A})) = \mathbf{A}$. The Kronecker product of an $n \times m$ matrix $\mathbf{A}$ and an $r \times s$ matrix $\mathbf{B}$ generates an $nr \times ms$ matrix, as follows.

$$\mathbf{A} \otimes \mathbf{B} = \begin{bmatrix} a_{11}\mathbf{B} & a_{12}\mathbf{B} & . & . & a_{1m}\mathbf{B} \\ a_{21}\mathbf{B} & . & . & . & . \\ . & . & . & . & . \\ . & . & . & . & . \\ a_{n1}\mathbf{B} & . & . & . & a_{nm}\mathbf{B} \end{bmatrix}. \tag{2.40}$$

If m, n, r, and s are equal to n, and if $\mathbf{A}$ and $\mathbf{B}$ are tensors, then $\mathbf{A} \otimes \mathbf{B}$ transforms as a second-order $n^2 \times n^2$ tensor in a sense that is explained subsequently.

Equation 2.40 implies that the $n^2 \times 1$ Kronecker product of two $n \times 1$ vectors **a** and **b** is written as

$$\mathbf{a} \otimes \mathbf{b} = \begin{pmatrix} a_1\mathbf{b} \\ a_2\mathbf{b} \\ . \\ . \\ a_n\mathbf{b} \end{pmatrix}. \tag{2.41}$$

2.6.2 Fundamental Relations for Kronecker Products

Six basic relations are introduced, followed by a number of subsidiary relations. The proofs of the first five relations are based on Graham (1981).

Relation 1: Let **A** denote an $n \times m$ real matrix, with entry a_{ij} in the i^{th} row and j^{th} column. Let $I = (j-1)n + i$ and $J = (i-1)m + j$. Let $\mathbf{U}_{nm}$ denote the $nm \times nm$ matrix, independent of **A**, satisfying

$$u_{JK} = \begin{cases} 1, & K = I \\ 0, & K \neq I \end{cases} \qquad u_{IK} = \begin{cases} 1, & K = J \\ 0, & K \neq J \end{cases}. \tag{2.42}$$

Then,

$$VEC(\mathbf{A}^{\mathbf{T}}) = \mathbf{U}_{nm} VEC(\mathbf{A}). \tag{2.43}$$

Note that $u_{JK} = u_{JI} = 1$ and $u_{IK} = u_{IJ} = 1$, with all other entries vanishing. Hence if $m = n$, then $u_{JI} = u_{IJ}$, so that $\mathbf{U}_{nm}$ is symmetric if $m = n$.

Relation 2: If **A** and **B** are second-order $n \times n$ tensors, then

$$tr(\mathbf{AB}) = VEC^{\mathbf{T}}(\mathbf{A}^{\mathbf{T}}) VEC(\mathbf{B}). \tag{2.44}$$

Relation 3: If $\mathbf{I}_n$ denotes the $n \times n$ identity matrix, and if **B** denotes an $n \times n$ tensor, then

$$\mathbf{I}_n \otimes \mathbf{B}^{\mathbf{T}} = (\mathbf{I}_n \otimes \mathbf{B})^{\mathbf{T}}. \tag{2.45}$$

Relation 4: Let **A**, **B**, **C**, and **D**, respectively, denote $m \times n$, $r \times s$, $n \times p$, and $s \times q$ matrices. Then,

$$(\mathbf{A} \otimes \mathbf{B})\ (\mathbf{C} \otimes \mathbf{D}) = \mathbf{AC} \otimes \mathbf{BD}. \tag{2.46}$$

Relation 5: If **A**, **B**, and **C** are $n \times m$, $m \times r$, and $r \times s$ matrices, then

$$VEC(\mathbf{ACB}) = \mathbf{B}^{\mathbf{T}} \otimes \mathbf{A} VEC(\mathbf{C}). \tag{2.47}$$

Relation 6: If **a** and **b** are $n \times 1$ vectors, then

$$\mathbf{a} \otimes \mathbf{b} = VEC([\mathbf{ab}^{\mathbf{T}}]^{\mathbf{T}}). \tag{2.48}$$

As proof of Relation 6, if $I = (j-1)n + i$, then the I^{th} entry of $VEC(\mathbf{ba}^{\mathbf{T}})$ is $b_i a_j$. It is also the I^{th} entry of $\mathbf{a} \otimes \mathbf{b}$. Hence, $\mathbf{a} \otimes \mathbf{b} = VEC(\mathbf{ba}^{\mathbf{T}}) = VEC([\mathbf{ab}^{\mathbf{T}}]^{\mathbf{T}})$.

Symmetry of $\mathbf{U}_{nn}$ was established in Relation 1. Note that $VEC(\mathbf{A}) = \mathbf{U}_{nn} VEC(\mathbf{A}^{\mathbf{T}}) = \mathbf{U}_{nn}^2 VEC(\mathbf{A})$ if **A** is $n \times n$, and hence the matrix $\mathbf{U}_{nn}$ satisfies

$$\mathbf{U}_{nn}^2 = \mathbf{I}_{n^2} \qquad \mathbf{U}_{nn} = \mathbf{U}_{nn}^{\mathbf{T}} = \mathbf{U}_{nn}^{-\mathbf{1}}. \tag{2.49}$$

$\mathbf{U}_{nn}$ is hereafter called the permutation tensor for $n \times n$ matrices. If **A** is symmetric, then $(\mathbf{U}_{nn} - \mathbf{I}_{n^2})\, VEC(\mathbf{A}) = \mathbf{0}$. If **A** is antisymmetric, then $(\mathbf{U}_{nn} + \mathbf{I}_{nn}) VEC(\mathbf{A}) = \mathbf{0}$.

If **A** and **B** are second-order $n \times n$ tensors, then

$$\begin{aligned} tr(\mathbf{AB}) &= VEC^T(\mathbf{B}) VEC(\mathbf{A}^T) \\ &= VEC^T(\mathbf{B}) \mathbf{U}_{nn} VEC(\mathbf{A}) \\ &= [\mathbf{U}_{nn} VEC(\mathbf{B})]^T VEC(\mathbf{A}) \\ &= VEC^T(\mathbf{B}^T) VEC(\mathbf{A}) \\ &= tr(\mathbf{BA}), \end{aligned} \tag{2.50}$$

thereby recovering a well-known relation.

If $\mathbf{I}_n$ is the $n \times n$ identity tensor and $\mathbf{i}_n = VEC(\mathbf{I}_n)$, $VEC(\mathbf{A}) = \mathbf{I}_n \otimes \mathbf{A}\mathbf{i}_n$ since $VEC(\mathbf{A}) = VEC(\mathbf{AI}_n)$. If $\mathbf{I}_{nn}$ is the identity tensor in n^2-dimensional space, then $\mathbf{I}_n \otimes \mathbf{I}_n = \mathbf{I}_{nn}$ since $VEC(\mathbf{I}_n) = VEC(\mathbf{I}_n \mathbf{I}_n) = \mathbf{I}_n \otimes \mathbf{I}_n VEC(\mathbf{I}_n)$. Now, $\mathbf{i}_n = \mathbf{I}_n \mathbf{i}$, thus $\mathbf{I}_n \otimes \mathbf{I}_n = \mathbf{I}_{n^2}$.

If **A**, **B**, and **C** denote $n \times n$ tensors, then

$$\begin{aligned} VEC(\mathbf{ACB}^{\mathbf{T}}) &= \mathbf{I}_n \otimes \mathbf{A} VEC(\mathbf{CB}^{\mathbf{T}}) \\ &= (\mathbf{I}_n \otimes \mathbf{A})(\mathbf{B} \otimes \mathbf{I}_n) VEC(\mathbf{C}) \\ &= \mathbf{B} \otimes \mathbf{A} VEC(\mathbf{C}). \end{aligned} \tag{2.51}$$

However, by a parallel argument,

$$\begin{aligned} VEC[(\mathbf{ACB}^T)^T] &= VEC(\mathbf{BC}^T \mathbf{A}^T) \\ &= \mathbf{A} \otimes \mathbf{B} VEC(\mathbf{C}^T) \\ &= \mathbf{A} \otimes \mathbf{B} \mathbf{U}_{n^2} VEC(\mathbf{C}). \end{aligned} \tag{2.52}$$

The permutation tensor arises in the relation

$$VEC[(\mathbf{ACB}^T)^T] = \mathbf{U}_{n^2} VEC(\mathbf{ACB}^T). \tag{2.53}$$

Consequently, if $\mathbf{C}$ is arbitrary,

$$\mathbf{U}_{n^2}\mathbf{B} \otimes \mathbf{A} VEC(\mathbf{C}) = \mathbf{A} \otimes \mathbf{B}\mathbf{U}_{n^2} VEC(\mathbf{C}), \tag{2.54}$$

and, upon using the relation $\mathbf{U}_{n^2} = \mathbf{U}_{n^2}^{-1}$, we obtain an important result:

$$\mathbf{B} \otimes \mathbf{A} = \mathbf{U}_{n^2}\mathbf{A} \otimes \mathbf{B}\mathbf{U}_{n^2}. \tag{2.55}$$

If $\mathbf{A}$ and $\mathbf{B}$ are nonsingular $n \times n$ tensors, then

$$\begin{aligned}(\mathbf{A} \otimes \mathbf{B})(\mathbf{A}^{-1} \otimes \mathbf{B}^{-1}) &= \mathbf{A}\mathbf{A}^{-1} \otimes \mathbf{B}\mathbf{B}^{-1} \\ &= \mathbf{I}_n \otimes \mathbf{I}_n \\ &= \mathbf{I}_{n^2}.\end{aligned} \tag{2.56}$$

The Kronecker sum and difference appear frequently (for example, in control theory) and are defined as follows:

$$\mathbf{A} \oplus \mathbf{B} = \mathbf{A} \otimes \mathbf{I}_n + \mathbf{I}_n \otimes \mathbf{B} \qquad \mathbf{A} \ominus \mathbf{B} = \mathbf{A} \otimes \mathbf{I}_n - \mathbf{I}_n \otimes \mathbf{B}. \tag{2.57}$$

The Kronecker sum and difference of two $n \times n$ tensors are $n^2 \times n^2$ tensors, as explained in the following section.

2.6.3 Eigenstructures of Kronecker Products

Let α_j and β_k denote the eigenvalues of $\mathbf{A}$ and $\mathbf{B}$, and let $\mathbf{y}_j$ and $\mathbf{z}_k$ denote the corresponding eigenvectors. The Kronecker product, sum, and difference have the following eigenstructures:

expression	jk^{th} eigenvalue	jk^{th} eigenvector
$\mathbf{A} \otimes \mathbf{B}$	$\alpha_j \beta_k$	$\mathbf{y}_j \otimes \mathbf{z}_k$
$\mathbf{A} \oplus \mathbf{B}$	$\alpha_j + \beta_k$	$\mathbf{y}_j \otimes \mathbf{z}_k$
$\mathbf{A} \ominus \mathbf{B}$	$\alpha_j - \beta_k$	$\mathbf{y}_j \otimes \mathbf{z}_k$

(2.58)

As proof,

$$\begin{aligned}\alpha_j \mathbf{y}_j \otimes \beta_k \mathbf{z}_k &= \alpha_j \beta_k \mathbf{y}_j \otimes \mathbf{z}_k \\ &= \mathbf{A}\mathbf{y}_j \otimes \mathbf{B}\mathbf{z}_k \\ &= (\mathbf{A} \otimes \mathbf{B})(\mathbf{y}_j \otimes \mathbf{z}_k).\end{aligned} \tag{2.59}$$

Now, the eigenvalues of $\mathbf{A} \otimes \mathbf{I}_n$ are $1 \times \alpha_j$, while the eigenvectors are $\mathbf{y}_j \otimes \mathbf{w}_k$, in which $\mathbf{w}_k$ is an arbitrary unit vector (eigenvector of $\mathbf{I}_n$). The corresponding quantities for $\mathbf{I}_n \otimes \mathbf{B}$ are $\beta_k \times 1$ and $\mathbf{v}_j \times \mathbf{z}_k$, in which $\mathbf{v}_j$ is an arbitrary eigenvector of $\mathbf{I}_n$. Upon selecting $\mathbf{w}_k = \mathbf{z}_k$ and $\mathbf{v}_j = \mathbf{y}_j$, the Kronecker sum has eigenvalues $\alpha_j + \beta_k$ and eigenvectors $\mathbf{y}_j \otimes \mathbf{z}_k$.

2.6.4 Kronecker Form of Quadratic Products

Let $\mathbf{R}$ be a second-order $n \times n$ tensor. The quadratic product $\mathbf{a}^\mathbf{T}\mathbf{R}\mathbf{b}$ is easily derived: if $\mathbf{r} = VEC(\mathbf{R})$, then

$$\begin{aligned}\mathbf{a}^\mathbf{T}\mathbf{R}\mathbf{b} &= tr[\mathbf{b}\mathbf{a}^\mathbf{T}\mathbf{R}] \\ &= VEC^\mathbf{T}([\mathbf{b}\mathbf{a}^\mathbf{T}]^\mathbf{T})VEC(\mathbf{R}) \\ &= VEC^\mathbf{T}(\mathbf{a}\mathbf{b}^\mathbf{T})VEC(\mathbf{R}) \\ &= \mathbf{b}^\mathbf{T} \otimes \mathbf{a}^\mathbf{T}\mathbf{r}.\end{aligned} \tag{2.60}$$

2.6.5 Kronecker Product Operators for Fourth-Order Tensors

Let $\mathbf{A}$ and $\mathbf{B}$ be second-order $n \times n$ tensors, and let $\mathbf{C}$ be a fourth-order $n \times n \times n \times n$ tensor. Suppose that $\mathbf{A} = \mathbf{C}\mathbf{B}$, which is equivalent to $a_{ij} = c_{ijkl}b_{kl}$ in which the range of i, j, k, and l is $(1, n)$. The $TEN22$ operator is introduced implicitly using

$$VEC(\mathbf{A}) = TEN22(\mathbf{C})VEC(\mathbf{B}). \tag{2.61}$$

Note that

$$\begin{aligned}TEN22(\mathbf{ACB})VEC(\mathbf{D}) &= VEC(\mathbf{ACBD}) \\ &= \mathbf{I}_n \otimes \mathbf{A}\, VEC(\mathbf{CBD}) \\ &= \mathbf{I}_n \otimes \mathbf{A}\, TEN22(\mathbf{C})\, VEC(\mathbf{BD}) \\ &= \mathbf{I}_n \otimes \mathbf{A}\, TEN22(\mathbf{C})\mathbf{I}_n \otimes \mathbf{B}\, VEC(\mathbf{D}),\end{aligned} \tag{2.62}$$

hence, $TEN22(\mathbf{ACB}) = \mathbf{I}_n \otimes \mathbf{A}TEN22(\mathbf{C})\mathbf{I}_n \otimes \mathbf{B}$. Upon writing $\mathbf{B} = \mathbf{C}^{-1}\mathbf{A}$, it is obvious that $VEC(\mathbf{B}) = TEN22(\mathbf{C}^{-1})VEC(\mathbf{A})$. However, $TEN22(\mathbf{C})VEC(\mathbf{B}) = VEC(\mathbf{A})$, thus $VEC(\mathbf{B}) = [TEN22(\mathbf{C})]^{-1}VEC(\mathbf{A})$. We conclude that $TEN22(\mathbf{C}^{-1}) = TEN22^{-1}(\mathbf{C})$. Furthermore, by writing $\mathbf{A}^{\mathbf{T}} = \hat{\mathbf{C}}\mathbf{B}^{\mathbf{T}}$, it is also obvious that $\mathbf{U}_n\,\mathbf{a} = TEN22(\mathbf{C})\mathbf{U}_n\mathbf{b}$, thus $TEN22(\hat{\mathbf{C}}) = \mathbf{U}_{n^2}TEN22(\mathbf{C})\,\mathbf{U}_{n^2}$. The inverse of the $TEN22$ operator is introduced using the relation $ITEN22(TEN22(\mathbf{C})) = \mathbf{C}$.

2.6.6 Transformation Properties of *VEC* and *TEN22*

Suppose that $\mathbf{A}$ and $\mathbf{B}$ are true second-order $n \times n$ tensors and $\mathbf{C}$ is a fourth-order $n \times n \times n \times n$ tensor such that $\mathbf{A} = \mathbf{CB}$. All are referred to a coordinate system denoted as Y. Let the unitary matrix (tensor) $\mathbf{Q}_n$ represent a rotation that gives rise to a coordinate system Y'. Let $\mathbf{A}'$, $\mathbf{B}'$, and $\mathbf{C}'$ denote the counterparts of $\mathbf{A}$, $\mathbf{B}$, and $\mathbf{C}$. Now, since $\mathbf{A}' = \mathbf{Q}_n\,\mathbf{A}\mathbf{Q}_n^{\mathbf{T}}$,

$$VEC(\mathbf{A}') = \mathbf{Q} \otimes \mathbf{Q}VEC(\mathbf{A}). \tag{2.63}$$

However, note that $(\mathbf{Q} \otimes \mathbf{Q})^{\mathbf{T}} = \mathbf{Q}^{\mathbf{T}} \otimes \mathbf{Q}^{\mathbf{T}} = \mathbf{Q}^{-1} \otimes \mathbf{Q}^{-1} = (\mathbf{Q} \otimes \mathbf{Q})^{-1}$. Hence, $\mathbf{Q} \otimes \mathbf{Q}$ is a unitary matrix (tensor) in an n^2 vector space. However, not all rotations in n^2–dimensional space can be expressed in the form $\mathbf{Q} \otimes \mathbf{Q}$. It follows that $VEC(\mathbf{A})$ transforms as an $n^2 \times 1$ vector *under rotations of the form* $\mathbf{Q} \otimes \mathbf{Q}$.

Now write $\mathbf{A}' = \mathbf{C}'\,\mathbf{B}'$, from which

$$\mathbf{Q} \otimes \mathbf{Q}\,VEC(\mathbf{A}) = TEN22(\mathbf{C}')\mathbf{Q} \otimes \mathbf{Q}VEC(\mathbf{B}). \tag{2.64a}$$

It follows that

$$TEN22(\mathbf{C}') = \mathbf{Q} \otimes \mathbf{Q}\,TEN22(\mathbf{C})(\mathbf{Q} \otimes \mathbf{Q})^{\mathbf{T}}, \tag{2.64b}$$

thus $TEN22(\mathbf{C})$ transforms a second-order $n^2 \times n^2$ tensor *under rotations of the form* $\mathbf{Q} \otimes \mathbf{Q}$.

Finally, letting $\mathbf{C}_a$ and $\mathbf{C}_b$ denote third-order $n \times n \times n$ tensors, respectively, thereby satisfying relations of the form $\mathbf{A} = \mathbf{C}_a\mathbf{b}$ and $\mathbf{b} = \mathbf{C}_b\mathbf{A}$, it is readily shown that $TEN21(\mathbf{C_a})$ and $TEN12(\mathbf{C_b})$ satisfy

$$\begin{aligned} TEN21(\mathbf{C}'_a) &= \mathbf{Q} \otimes \mathbf{Q}TEN21(\mathbf{C}_a)\mathbf{Q}^{\mathbf{T}} && n^2 \times n \\ TEN12(\mathbf{C}'_b) &= \mathbf{Q}TEN12(\mathbf{C}_b)\mathbf{Q}^{\mathbf{T}} \otimes \mathbf{Q}^{\mathbf{T}} && n \times n^2, \end{aligned} \tag{2.65}$$

which we call tensors of order (2,1) and (1,2), respectively.

2.6.7 Kronecker Product Functions for Tensor Outer Products

Tensor outer products are commonly used in continuum mechanics. For example, Hooke's Law in isotropic linear elasticity with coefficients $\hat{\mu}$ and $\hat{\lambda}$ can be written as

$$T_{\mathrm{ij}} = \hat{\mu}(\delta_{\mathrm{ik}}\delta_{\mathrm{jl}} + \delta_{\mathrm{il}}\delta_{\mathrm{jk}})E_{\mathrm{kl}} + \hat{\lambda}\delta_{\mathrm{ij}}\delta_{\mathrm{kl}}E_{\mathrm{kl}} \qquad i, j = 1,\ 2,\ 3, \tag{2.66}$$

in which T_{ij} and E_{ij} are entries of the (small-deformation) stress and strain tensors denoted by **T** and **E**. Here, δ_{ij} denotes the substitution (Kronecker) tensor. Equation 2.66 exhibits three tensor outer products of the identity (Kronecker) tensor **I**: $\delta_{ik}\delta_{jl}$, $\delta_{il}\delta_{jk}$, and $\delta_{ij}\delta_{kl}$. In general, let **A** and **B** be two nonsingular $n \times n$ second-order tensors with entries a_{ij} and b_{ij}; let $\mathbf{a} = VEC(\mathbf{A})$ and $\mathbf{b} = VEC(\mathbf{B})$. There are 24 permutations of the indices ijkl corresponding to outer products of tensors **A** and **B**. Recalling the definitions of the Kronecker product, we introduce three basic Kronecker-product functions:

$$\mathbf{C_1}(\mathbf{A},\mathbf{B}) = \mathbf{ab^T} \qquad \mathbf{C_2}(\mathbf{A},\mathbf{B}) = \mathbf{A}\otimes\mathbf{B} \qquad \mathbf{C_3}(\mathbf{A},\mathbf{B}) = \mathbf{A}\otimes\mathbf{BU}_{n^2}. \tag{2.67}$$

Twenty-four outer product-Kronecker product pairs are obtained as follows:

$$\begin{array}{ll}
TEN22(a_{ij}b_{kl}) = \mathbf{C_1}(\mathbf{A},\mathbf{B}) & TEN22(b_{ij}a_{kl}) = \mathbf{C_1}(\mathbf{B},\mathbf{A}) \\
TEN22(a_{ji}b_{kl}) = \mathbf{C_1}(\mathbf{A^T},\mathbf{B}) & TEN22(b_{ji}a_{kl}) = \mathbf{C_1}(\mathbf{B^T},\mathbf{A}) \\
TEN22(a_{ij}b_{lk}) = \mathbf{C_1}(\mathbf{A},\mathbf{B^T}) & TEN22(b_{ij}a_{lk}) = \mathbf{C_1}(\mathbf{B},\mathbf{A^T}) \\
TEN22(a_{ji}b_{lk}) = \mathbf{C_1}(\mathbf{A^T},\mathbf{B^T}) & TEN22(b_{ji}a_{lk}) = \mathbf{C_1}(\mathbf{B^T},\mathbf{A^T}) \\
TEN22(a_{ik}b_{jl}) = \mathbf{C_2}(\mathbf{B},\mathbf{A}) & TEN22(b_{ik}a_{jl}) = \mathbf{C_2}(\mathbf{A},\mathbf{B}) \\
TEN22(a_{ki}b_{jl}) = \mathbf{C_2}(\mathbf{B},\mathbf{A^T}) & TEN22(b_{ki}a_{jl}) = \mathbf{C_2}(\mathbf{A},\mathbf{B^T}) \\
TEN22(a_{ik}b_{lj}) = \mathbf{C_2}(\mathbf{B^T},\mathbf{A}) & TEN22(b_{ik}a_{lj}) = \mathbf{C_2}(\mathbf{A^T},\mathbf{B}) \\
TEN22(a_{ki}b_{lj}) = \mathbf{C_2}(\mathbf{B^T},\mathbf{A^T}) & TEN22(b_{ki}a_{lj}) = \mathbf{C_2}(\mathbf{A^T},\mathbf{B^T}) \\
TEN22(a_{il}b_{jk}) = \mathbf{C_3}(\mathbf{B},\mathbf{A}) & TEN22(b_{il}a_{jk}) = \mathbf{C_3}(\mathbf{A},\mathbf{B}) \\
TEN22(a_{li}b_{jk}) = \mathbf{C_3}(\mathbf{B},\mathbf{A^T}) & TEN22(b_{li}a_{jk}) = \mathbf{C_3}(\mathbf{A},\mathbf{B^T}) \\
TEN22(a_{il}b_{kj}) = \mathbf{C_3}(\mathbf{B^T},\mathbf{A}) & TEN22(b_{il}a_{kj}) = \mathbf{C_3}(\mathbf{A^T},\mathbf{B}) \\
TEN22(a_{li}b_{kj}) = \mathbf{C_3}(\mathbf{B^T},\mathbf{A^T}) & TEN22(b_{li}a_{kj}) = \mathbf{C_3}(\mathbf{A^T},\mathbf{B^T})
\end{array}, \tag{2.68}$$

With $\boldsymbol{t} = VEC(\boldsymbol{T})$ and $\boldsymbol{e} = VEC(\boldsymbol{E})$, and noting that $\mathbf{U}_9\boldsymbol{e} = \boldsymbol{e}$ (since E is symmetric), we now restate Equation 2.66 as

$$\boldsymbol{t} = [\hat{\mu}[\mathbf{C}_2(\mathbf{I},\mathbf{I}) + \mathbf{C}_3(\mathbf{I},\mathbf{I})] + \hat{\lambda}\mathbf{C}_1(\mathbf{I},\mathbf{I})]\boldsymbol{e} \tag{2.69}$$

The proof is presented for several of the relations in Equation 2.68. We introduce tensors $\mathbf{R}$ and $\mathbf{S}$ with entries r_{ij} and s_{ij}. Also, let $\mathbf{s} = VEC(\mathbf{S})$ and $r = VEC(\mathbf{R})$.

a.) Suppose that $s_{ij} = a_{ij}b_{kl}r_{kl}$. However, $a_{ij}b_{kl}r_{kl} = a_{ij}b^{\mathbf{T}}_{lk}r_{kl}$, in which case $b^{\mathbf{T}}_{kl}$ is the kl^{th} entry of $\mathbf{B}^{\mathbf{T}}$. It follows that $\mathbf{S} = tr(\mathbf{B}^{\mathbf{T}}\mathbf{R})\mathbf{A}$. Hence,

$$\begin{aligned}\mathbf{s} &= VEC^{\mathbf{T}}[(\mathbf{B}^{\mathbf{T}})^{\mathbf{T}}]VEC(\mathbf{R})\mathbf{a}\\ &= VEC^{\mathbf{T}}(\mathbf{B})VEC(\mathbf{R})\mathbf{a}\\ &= \mathbf{a}\mathbf{b}^{\mathbf{T}}\mathbf{r}\\ &= \mathbf{C}_1(\mathbf{A},\mathbf{B})\mathbf{r}.\end{aligned} \tag{2.70}$$

Since $\mathbf{s} = TEN22(a_{ij}b_{kl})\mathbf{r}$, it follows that $TEN22(a_{ij}b_{kl}) = \mathbf{C}_1(\mathbf{A},\mathbf{B})$, as shown in Equation 2.68.

b.) Suppose that $s_{ij} = a_{ik}b_{jl}r_{kl}$. However, $a_{ik}b_{jl}r_{kl} = a_{ik}r_{kl}b^{\mathbf{T}}_{lj}$, thus $\mathbf{S} = \mathbf{A}\mathbf{R}\mathbf{B}^{\mathbf{T}}$. Now

$$\begin{aligned}\mathbf{s} &= VEC(\mathbf{A}\mathbf{R}\mathbf{B}^{\mathbf{T}})\\ &= \mathbf{I}\otimes\mathbf{A}VEC(\mathbf{R}\mathbf{B}^{\mathbf{T}})\\ &= \mathbf{I}\otimes\mathbf{A}\mathbf{B}\otimes\mathbf{I}\mathbf{r}\\ &= \mathbf{B}\otimes\mathbf{A}\mathbf{r}\\ &= \mathbf{C}_2(\mathbf{B},\mathbf{A})\mathbf{r},\end{aligned} \tag{2.71}$$

as shown in Equation 2.68.

c.) Suppose $s_{ij} = a_{il}b_{jk}r_{kl}$. However, $a_{il}b_{jk}r_{kl} = a_{il}r^{\mathbf{T}}_{lk}b_{kj}$, thus $\mathbf{S} = \mathbf{A}\mathbf{R}^{\mathbf{T}}\mathbf{B}^{\mathbf{T}}$. Now

$$\begin{aligned}\mathbf{s} &= VEC(\mathbf{A}\mathbf{R}^{\mathbf{T}}\mathbf{B}^{\mathbf{T}})\\ &= \mathbf{I}\otimes\mathbf{A}\mathbf{B}\otimes\mathbf{I}VEC(\mathbf{R}^{\mathbf{T}})\\ &= \mathbf{B}\otimes\mathbf{A}\mathbf{U}_9\mathbf{r}\\ &= \mathbf{C}_3(\mathbf{B},\mathbf{A})\mathbf{r},\end{aligned} \tag{2.72}$$

as shown in Equation 2.68.

2.6.8 Kronecker Expressions for Symmetry Classes in Fourth-Order Tensors

Let $\mathbf{C}$ denote a fourth-order tensor with entries c_{ijkl}. If the entries observe

$$\begin{aligned} c_{ijkl} &= c_{jikl} \qquad (a) \\ c_{ijkl} &= c_{ijlk} \qquad (b), \\ c_{ijkl} &= c_{klij} \qquad (c) \end{aligned} \tag{2.73}$$

then $\mathbf{C}$ is said to be *totally symmetric*. A fourth-order tensor $\mathbf{C}$ satisfying Equation 2.73a but not 2.73b or c is called symmetric.

Kronecker-product conditions for symmetry are now stated. The fourth-order tensor $\mathbf{C}$ is totally symmetric if and only if

$$\begin{aligned} TEN22(\mathbf{C}) &= TEN22^{T}(\mathbf{C}) \qquad (a) \\ \mathbf{U}_{n^2} TEN22(\mathbf{C}) &= TEN22(\mathbf{C}) \qquad (b)\ . \\ TEN22(\mathbf{C})\mathbf{U}_{n^2} &= TEN22(\mathbf{C}) \qquad (c) \end{aligned} \tag{2.74}$$

Equation 2.74a is equivalent to symmetry with respect to exchange of ij and kl in $\mathbf{C}$. Total symmetry also implies that, for any second-order $n \times n$ tensor $\mathbf{B}$, the corresponding tensor $\mathbf{A} = \mathbf{CB}$ is symmetric. Thus, if $\mathbf{a} = VEC(\mathbf{A})$ and $\mathbf{b} = VEC(\mathbf{B})$, then $\mathbf{a} = TEN22(\mathbf{C})\mathbf{b}$. However, $\mathbf{U}_{n^2}\mathbf{a} = TEN22(\mathbf{C})\mathbf{b}$. Multiplying through the later expression with $\mathbf{U}_{n^2}$ implies Equation 2.74b. For any $n \times n$ tensor $\mathbf{A}$, the tensor $\mathbf{B} = \mathbf{C}^{-1}\mathbf{A}$ is symmetric. It follows that $\mathbf{b} = TEN22(\mathbf{C}^{-1})\mathbf{a} = TEN22^{-1}(\mathbf{C})\mathbf{a}$, and $\mathbf{U}_{n^2}\mathbf{b} = TEN22^{-1}\mathbf{Ca}$. Thus, $TEN22(\mathbf{C}^{-1}) = \mathbf{U}_{n^2}\ TEN22^{-1}(\mathbf{C})$. Also, $TEN22(\mathbf{C}) = [\ \mathbf{U}_{n^2} TEN22^{-1}(\mathbf{C})]^{-1} = TEN22(\mathbf{C})\ \mathbf{U}_{n^2}$. We now draw the immediate conclusion that $\mathbf{U}_{n^2}\ TEN22(\mathbf{C})\ \mathbf{U}_{n^2} = TEN22(\mathbf{C})$ if $\mathbf{C}$ is totally symmetric.

We next prove the following:

$$\mathbf{C}^{-1} \text{ is totally symmetric if } \mathbf{C} \text{ is totally symmetric.} \tag{2.75}$$

Note that $TEN22(\mathbf{C})\ \mathbf{U}_{n^2} = TEN22(\mathbf{C})$ implies that $\mathbf{U}_{n^2} TEN22(\mathbf{C}^{-1}) = TEN22(\mathbf{C}^{-1})$, while $\mathbf{U}_{n^2} TEN22(\mathbf{C}) = TEN22(\mathbf{C})$ implies that $TEN22(\mathbf{C}^{-1})\ \mathbf{U}_{n^2} = TEN22(\mathbf{C}^{-1})$.

Finally, we prove the following: for a nonsingular $n \times n$ tensor $\mathbf{G}$,

$$\mathbf{GCG^T} \text{ is totally symmetric if } \mathbf{C} \text{ is totally symmetric.} \tag{2.76}$$

Equation 2.76 implies that $TEN22(\mathbf{GCG^{-T}}) = \mathbf{I} \otimes \mathbf{G}\ TEN22(\mathbf{C})\mathbf{I} \otimes \mathbf{G^T}$, so that $TEN22(\mathbf{GCG^T})$ is certainly symmetric. Next, consider whether $\mathbf{A}'$ given by

$$\mathbf{A}' = \mathbf{GCG^TB}' \tag{2.77}$$

is symmetric, in which case $\mathbf{B}'$ is a second-order, nonsingular $n \times n$ tensor. However, we can write

$$\mathbf{G}^{-1}\mathbf{A}'\mathbf{G}^{-\mathbf{T}} = \mathbf{C}\mathbf{G}^{-1}\mathbf{B}'\mathbf{G}^{-\mathbf{T}}. \tag{2.78}$$

Now $\mathbf{G}^{-1}\mathbf{A}'\mathbf{G}^{-\mathbf{T}}$ is symmetric since $\mathbf{C}$ is totally symmetric, and therefore $\mathbf{A}'$ is symmetric. Next, consider whether $\mathbf{B}'$ given by the following is symmetric:

$$\mathbf{B}' = \mathbf{G}^{-\mathbf{T}}\mathbf{C}^{-1}\mathbf{G}^{-1}\mathbf{A}' \tag{2.79}$$

However, we can write

$$\mathbf{G}^{\mathbf{T}}\mathbf{B}'\mathbf{G} = \mathbf{C}^{-1}\mathbf{G}^{-1}\mathbf{A}'\mathbf{G}. \tag{2.80}$$

Since $\mathbf{C}^{-1}$ is totally symmetric, it follows that $\mathbf{G}^{\mathbf{T}}\mathbf{B}'\mathbf{G}$ is symmetric, and hence $\mathbf{B}'$ is symmetric. We conclude that $\mathbf{G}\mathbf{C}\mathbf{G}^{\mathbf{T}}$ is totally symmetric.

2.6.9 Differentials of Tensor Invariants

Let $\mathbf{A}$ be a symmetric 3×3 tensor, with invariants $I_1(\mathbf{A})$, $I_2(\mathbf{A})$, and $I_3(\mathbf{A})$. For a scalar-valued function $f(\mathbf{A})$,

$$df(\mathbf{A}) = \frac{\partial f}{\partial a_{ij}}\, da_{ij} = tr\left(\frac{\partial f}{\partial \mathbf{A}}\, d\mathbf{A}\right), \quad \left(\frac{\partial f}{\partial \mathbf{A}}\right)_{ij} = \frac{\partial f}{\partial a_{ij}}. \tag{2.81}$$

However, with $\mathbf{a} = VEC(\mathbf{A})$, we can also write

$$\begin{aligned} df(\mathbf{A}) &= VEC^{\mathbf{T}}\left(\left[\frac{\partial f}{\partial \mathbf{A}}\right]^{\mathbf{T}}\right) VEC(d\mathbf{A}) \\ &= \frac{\partial f}{\partial \mathbf{a}}\, d\mathbf{a}. \end{aligned} \tag{2.82}$$

Taking this further,

$$\begin{aligned} \frac{\partial I_1}{\partial \mathbf{a}} &= \frac{\partial}{\partial \mathbf{a}}(\mathbf{i}^{\mathbf{T}}\mathbf{a}) = \mathbf{i}^{\mathbf{T}} \\ \frac{\partial I_2}{\partial \mathbf{a}} &= \frac{\partial}{\partial \mathbf{a}}\left[\frac{1}{2}(\mathbf{i}^{\mathbf{T}}\mathbf{a})^2 - \mathbf{a}^{\mathbf{T}}\mathbf{a}\right] \\ &= I_1\mathbf{i}^{\mathbf{T}} - \mathbf{a}^{\mathbf{T}} \end{aligned} \tag{2.83}$$

and

$$dI_3 = tr(\mathbf{A}^2 d\mathbf{A}) - I_1 tr(\mathbf{A}\, d\mathbf{A}) + I_2\, d\mathbf{A}$$
$$= tr(\mathbf{A}^{-1} d\mathbf{A}\, / I_3) \tag{2.84}$$

so that

$$\frac{\partial I_3}{\partial \mathbf{a}} = VEC(\mathbf{A}^{-1})\, / I_3 \tag{2.85}$$

2.7 EXERCISES

1. Given a symmetric $n \times n$ tensor $\boldsymbol{\sigma}$, prove that

$$tr(\boldsymbol{\sigma} - tr(\boldsymbol{\sigma}) I_n / n) = 0.$$

2. Prove that if $\boldsymbol{\sigma}$ is a symmetric tensor with entries σ_{ij},

$$\varepsilon_{ijk}\sigma_{jk} = 0, \quad i = 1,\ 2,\ 3.$$

3. Verify using 2×2 tensors that

$$tr(\mathbf{AB}) = tr(\mathbf{BA}).$$

4. Express I_3 as a function of I_1 and I_2.
5. Using 2×2 tensors and 2×1 vectors, verify the six relations given for Kronecker products.
6. Write out the 9×9 quantity *TEN*22*(C)* in Equation 2.66.
7. Using a 2×2 tensor $\mathbf{A}$, write out the differential of $ln(\mathbf{A})$.

3 Introduction to Variational and Numerical Methods

3.1 INTRODUCTION TO VARIATIONAL METHODS

Let $\mathbf{u}(\mathbf{x})$ be a vector-valued function of position vector $\mathbf{x}$, and consider a vector-valued function $\mathbf{F}(\mathbf{u}(\mathbf{x}), \mathbf{u}'(\mathbf{x}),\mathbf{x})$, in which $\mathbf{u}'(\mathbf{x}) = \partial\mathbf{u}/\partial\mathbf{x}$. Furthermore, let $\mathbf{v}(\mathbf{x})$ be a function such that $\mathbf{v}(\mathbf{x}) = \mathbf{0}$ when $\mathbf{u}(\mathbf{x}) = \mathbf{0}$ and $\mathbf{v}'(\mathbf{x}) = \mathbf{0}$ when $\mathbf{u}'(\mathbf{x}) = \mathbf{0}$, but which is otherwise arbitrary. The differential $d\mathbf{F}$ measures how much $\mathbf{F}$ changes if $\mathbf{x}$ changes. The variation $\delta\mathbf{F}$ measures how much $\mathbf{F}$ changes if $\mathbf{u}$ and $\mathbf{u}'$ change at fixed $\mathbf{x}$. Following Ewing, we introduce the vector-valued function $\boldsymbol{\phi}(e:\mathbf{F})$ as follows (Ewing, 1985):

$$\Phi(e{:}\mathbf{F}) = \mathbf{F}(\mathbf{u}(\mathbf{x}) + e\mathbf{v}(\mathbf{x}),\ \mathbf{u}'(\mathbf{x}) + e\mathbf{v}'(\mathbf{x}),\ \mathbf{x}) - \mathbf{F}(\mathbf{u}(\mathbf{x}),\ \mathbf{u}'(\mathbf{x}),\ \mathbf{x}) \tag{3.1}$$

The variation $\delta\mathbf{F}$ is defined by

$$\delta\mathbf{F} = \mathrm{e}\left(\frac{d\boldsymbol{\Phi}}{d\mathrm{e}}\right)_{|\mathrm{e}=0}, \tag{3.2}$$

with $\mathbf{x}$ fixed. Elementary manipulation demonstrates that

$$\delta\mathbf{F} = \frac{\partial\mathbf{F}}{\partial\mathbf{u}}\mathrm{e}\mathbf{v} + tr\left(\frac{\partial\mathbf{F}}{\partial\mathbf{u}'}\mathrm{e}\mathbf{v}'\right), \tag{3.3}$$

in which $\frac{\partial\mathbf{F}}{\partial\mathbf{u}'}\mathrm{e}\mathbf{v}' = \frac{\partial\mathbf{F}}{\partial u'_{ij}}\mathrm{e}\mathbf{v}'_{ij}$. If $\mathbf{F} = \mathbf{u}$, then $\delta\mathbf{F} = \delta\mathbf{u} = e\mathbf{v}$. If $\mathbf{F} = \mathbf{u}'$, then $\delta\mathbf{F} = \delta\mathbf{u}' = e\mathbf{v}'$. This suggests the form

$$\delta\mathbf{F} = \frac{\partial\mathbf{F}}{\partial\mathbf{u}}\delta\mathbf{u} + tr\left(\frac{\partial\mathbf{F}}{\partial\mathbf{u}'}\delta\mathbf{u}'\right). \tag{3.4}$$

The variational operator exhibits five important properties:

1. $\delta(.)$ commutes with linear differential operators and integrals. For example, if S denotes a prescribed contour of integration:

$$\int\delta(\,)dS = \delta\left[\int(\,)dS\right]. \tag{3.5}$$

2. $\delta(f)$ vanishes when its argument f is prescribed.
3. $\delta(.)$ satisfies the same operational rules as $d(.)$. For example, if the scalars q and r are both subject to variation, then

$$\delta(qr) = q\delta(r) + \delta(q)r. \tag{3.6}$$

4. If f is a prescribed function of (scalar) x, and if $u(x)$ is subject to variation, then

$$\delta(fu) = f\delta u. \tag{3.7}$$

5. Other than for number 2, the variation is arbitrary. For example, for two vectors $\mathbf{v}$ and $\mathbf{w}$, $\mathbf{v}^{\mathrm{T}} d\mathbf{w} = 0$ implies that $\mathbf{v}$ and $\mathbf{w}$ are orthogonal to each other. However, $\mathbf{v}^{\mathrm{T}}\delta\mathbf{w}$ implies that $\mathbf{v} = \mathbf{0}$, since only the zero vector can be orthogonal to an arbitrary vector.

As a simple example, Figure 3.1 depicts a rod of length L, cross-sectional area A, and elastic modulus E. At $x = 0$, the rod is built in, while at $x = L$, the tensile force P is applied. Inertia is neglected. The governing equations are in terms of displacement u, stress S, and (linear) strain E:

$$\begin{aligned} &\text{strain-displacement} && E = \frac{du}{dx} \\ &\text{stress-strain} && S = \mathrm{E}E \\ &\text{equilibrium} && \frac{d\sigma}{dx} = 0 \end{aligned} \tag{3.8}$$

Combining the equations furnishes

$$\mathrm{E}A\frac{d^2u}{dx^2} = 0. \tag{3.9}$$

The following steps serve to derive a variational equation that is equivalent to the differential equation and endpoint conditions (boundary conditions and constraints).

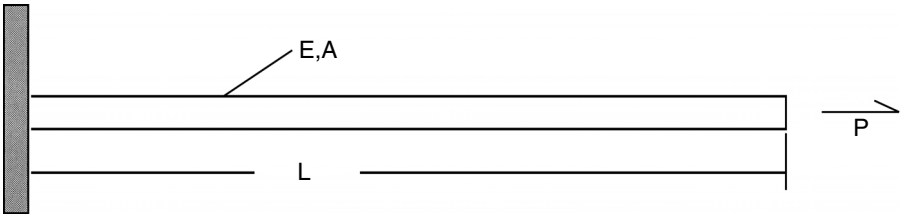

FIGURE 3.1 Rod under uniaxial tension.

Step 1: Multiply by the variation of the variable to be determined (u) and integrate over the domain.

$$\int_0^L \delta u \mathrm{E}A \frac{d^2u}{dx^2} A dx = 0. \tag{3.10}$$

Differential equations to be satisfied at every point in the domain are replaced with an integral equation whose integrand includes an arbitrary function.

Step 2: Integrate by parts, as needed, to render the argument in the domain integral positive definite.

$$\int_0^L \left[\frac{d}{dx}\left[\delta u \mathrm{E}A \frac{du}{dx} \right] - \left(\frac{d\delta u}{dx} \right) \mathrm{E}A \frac{du}{dx} \right] dx = 0 \tag{3.11}$$

However, the first term is the integral of a derivative, so that

$$\int_0^L \left[\left(\frac{d\delta u}{dx} \right) \mathrm{E}A \frac{du}{dx} \right] dx = \delta u \mathrm{E}A \frac{du}{dx}\Big|_0^L. \tag{3.12}$$

Step 3: Identify the primary and secondary variables. The primary variable is present in the endpoint terms (rhs) under the variational symbol, l, and is u. The conjugate secondary variable is $\mathrm{E}A\frac{du}{dx}$.

Step 4: Satisfy the constraints and boundary conditions. At $x = 0$, u is prescribed, thus $\delta u = 0$. At $x = L$, the load $P = \mathrm{E}A\frac{du}{dx}$ is prescribed. Also, note that $(\frac{du}{dx})\mathrm{E}A\frac{du}{dx} = \delta(\frac{1}{2}\mathrm{E}A(\frac{du}{dx})^2)$.

Step 5: Form the variational equation; the equations and boundary conditions are consolidated into one integral equation, $\delta F = 0$, where

$$F = \int_0^L \frac{1}{2}\mathrm{E}A\left(\frac{du}{dx}\right)^2 dx - Pu(L). \tag{3.13}$$

The j^{th} variation of a vector-valued quantity $\mathbf{F}$ is defined by

$$\delta^j \mathbf{F} = \mathrm{e}^j \left(\frac{\mathrm{d}^j \Phi}{\mathrm{de}^j} \right)_{|\mathrm{e}=0}. \tag{3.14}$$

It follows that $\delta^2\mathbf{u} = \mathbf{0}$ and $\delta^2\mathbf{u}' = \mathbf{0}$. By restricting $\mathbf{F}$ to a scalar-valued function F and $\mathbf{x}$ to reduce to x, we obtain

$$\delta^2 F = \{\delta\mathbf{u}^{\mathbf{T}} \quad \delta\mathbf{u}'^{\mathbf{T}}\}\mathbf{H}\begin{pmatrix}\delta\mathbf{u}\\ \delta\mathbf{u}'\end{pmatrix}, \qquad \mathbf{H} = \begin{bmatrix} \left(\frac{\partial}{\partial\mathbf{u}}\right)^{\mathbf{T}} \frac{\partial}{\partial\mathbf{u}} F & \left(\frac{\partial}{\partial\mathbf{u}}\right)^{\mathbf{T}} \frac{\partial}{\partial\mathbf{u}'} F \\ \left(\frac{\partial}{\partial\mathbf{u}'}\right)^{\mathbf{T}} \frac{\partial}{\partial\mathbf{u}} F & \left(\frac{\partial}{\partial\mathbf{u}'}\right)^{\mathbf{T}} \frac{\partial}{\partial\mathbf{u}'} F \end{bmatrix}, \tag{3.15}$$

and $\mathbf{H}$ is known as the Hessian matrix.

Now consider G given by

$$G = \int F(\mathbf{x},\ \mathbf{u}(\mathbf{x}),\ \mathbf{u}'(\mathbf{x}))dV + \int \mathbf{h}^{\mathbf{T}}(\mathbf{x})\mathbf{u}(\mathbf{x})\,dS, \tag{3.16}$$

in which V again denotes the volume of a domain and S denotes its surface area. In addition, $\mathbf{h}$ is a prescribed (known) function on S. G is called a *functional* since it generates a number for every function $\mathbf{u}(\mathbf{x})$. We first concentrate on a three-dimensional, rectangular coordinate system and suppose that $\delta G = 0$, as in the Principle of Stationary Potential Energy in elasticity. Note that

$$\frac{\partial}{\partial \mathbf{x}}\left[\frac{\partial \mathrm{F}}{\partial \mathbf{u}'}\delta\mathbf{u}\right] = tr\left(\frac{\partial \mathrm{F}}{\partial \mathbf{u}'}\delta\mathbf{u}'\right) + \frac{\partial}{\partial \mathbf{x}}\left(\frac{\partial}{\partial \mathbf{u}'}\mathrm{F}\right)\delta\mathbf{u}. \tag{3.17}$$

The first and last terms in Equation 3.17 can be recognized as divergences of vectors. We now invoke the divergence theorem to obtain

$$\begin{aligned} 0 &= \delta \mathrm{G} \\ &= \int\left[\frac{\partial \mathrm{F}}{\partial \mathbf{u}}\delta\mathbf{u} + tr\left(\frac{\partial \mathrm{F}}{\partial \mathbf{u}'}\delta\mathbf{u}'\right)\right]\mathrm{dV} + \int \mathbf{h}^{\mathbf{T}}(\mathbf{x})\delta\mathbf{u}(\mathbf{x})\,\mathrm{dS} \\ &= \int\left[\left(\frac{\partial \mathrm{F}}{\partial \mathbf{u}} - \frac{\partial}{\partial \mathbf{x}}\frac{\partial \mathrm{F}}{\partial \mathbf{u}'}\right)\delta\mathbf{u}\right]\mathrm{dV} + \int \mathbf{n}^{\mathbf{T}}\frac{\partial \mathrm{F}}{\partial \mathbf{u}'}\delta\mathbf{u}\mathrm{dS} + \int \mathbf{h}^{\mathbf{T}}(\mathbf{x})\delta\mathbf{u}(\mathbf{x})\,\mathrm{dS}. \end{aligned} \tag{3.18}$$

For suitable continuity properties of $\mathbf{u}$, arbitrariness of $\delta\mathbf{u}$ implies that $\delta G = 0$ is equivalent to the following *Euler equation, boundary conditions*, and *constraints* (the latter two are not uniquely determined by the variational principle):

$$\frac{\partial F}{\partial \mathbf{u}} - \frac{\partial}{\partial \mathbf{x}}\frac{\partial F}{\partial \mathbf{u}'} = \mathbf{0}^{\mathbf{T}}. \tag{3.19}$$

$$\begin{cases} \mathbf{u}(\mathbf{x})\textit{prescribed} & \boldsymbol{x} \text{ on } \boldsymbol{S}_1 \\ \mathbf{n}^{\mathbf{T}}\dfrac{\partial \mathrm{F}}{\partial \mathbf{u}'} + \mathbf{h}_1^{\mathbf{T}}(\mathbf{x}) = \mathbf{0}^{\mathbf{T}} \text{ on } \boldsymbol{S} & \boldsymbol{x} \text{ on } \boldsymbol{S} - \boldsymbol{S}_1 \end{cases}$$

Let $\mathbf{D} > \mathbf{0}$ denote a second-order tensor, and let $\boldsymbol{\pi}$ denote a vector that is a *nonlinear* function of a second vector $\mathbf{u}$, which is subject to variation. The function $F = \frac{1}{2}\boldsymbol{\pi}^{\mathbf{T}}\mathbf{D}\boldsymbol{\pi}$ satisfies

$$\delta \mathrm{F} = \delta\mathbf{u}^{\mathbf{T}}\frac{\partial \boldsymbol{\pi}^{\mathbf{T}}}{\partial \mathbf{u}^{\mathbf{T}}}\mathbf{D}\boldsymbol{\pi} \qquad \delta^2 \mathrm{F} = \delta\mathbf{u}^{\mathbf{T}}\frac{\partial \boldsymbol{\pi}^{\mathbf{T}}}{\partial \mathbf{u}^{\mathbf{T}}}\mathbf{D}\frac{\partial \boldsymbol{\pi}}{\partial \mathbf{u}}\delta\mathbf{u} + \delta\mathbf{u}^{\mathbf{T}}\left(\frac{\partial}{\partial \mathbf{u}}\left(\frac{\partial \boldsymbol{\pi}^{\mathbf{T}}}{\partial \mathbf{u}^{\mathbf{T}}}\right)\right)\delta\mathbf{u}\mathbf{D}\boldsymbol{\pi}. \tag{3.20}$$

Despite the fact that $\mathbf{D} > \mathbf{0}$, in the current nonlinear example, the specific vector $\mathbf{u}^*$ satisfying $\delta F = 0$ may correspond to a stationary point rather than a minimum.

3.2 NEWTON ITERATION AND ARC-LENGTH METHODS

3.2.1 Newton Iteration

Letting f and x denote scalars, consider the nonlinear algebraic equation $f(x; \lambda) = 0$, in which λ is a parameter we will call the load intensity. Such equations are often solved numerically by a two-track process: the load intensity λ is increased progressively using small increments. At each increment, the unknown x is computed using an iteration procedure. Suppose that at the n^{th} increment of λ, an accurate solution is achieved as x_n. Further suppose for simplicity's sake that x_n is "close" to the actual solution x_{n+1} for the $(n + 1)^{st}$ increment of λ. Using $x^{(0)} = x_n$ as the starting value, Newton iteration provides iterates according to the scheme

$$x^{(j+1)} = x^{(j)} - \left[\frac{df}{dx}\right]^{-1}_{|x^{(j)}} f(x^{(j)}). \tag{3.21}$$

Let $\Delta_{n+1,j}$ denote the increment $x^{(j+1)}_{n+1} - x^{(j)}_{n+1}$. Then, to first-order in the Taylor series

$$\begin{aligned}
\Delta_{\mathrm{n+1,j}} - \Delta_{\mathrm{n+1,j-1}} &= -\left[\left[\frac{\mathrm{df}}{\mathrm{dx}}\right]^{-1}_{|\mathrm{x^{(j)}}} \mathrm{f(x^{(j)})} - \left[\frac{\mathrm{df}}{\mathrm{dx}}\right]^{-1}_{|\mathrm{x^{(j-1)}}} \mathrm{f(x^{(j-1)})}\right] \\
&\approx -\left[\frac{\mathrm{df}}{\mathrm{dx}}\right]^{-1}_{|\mathrm{x^{(j)}}} \left[\mathrm{f(x^{(j)}) - f(x^{(j-1)})}\right] \\
&\approx -\left[\frac{\mathrm{df}}{\mathrm{dx}}\right]^{-1}_{|\mathrm{x^{(j)}}} \left[\frac{\mathrm{df}}{\mathrm{dx}}\right]_{|\mathrm{x^{(j)}}} \Delta_{\mathrm{n+1,j-1}} + 0^2 \\
&\approx \Delta_{\mathrm{n+1,j-1}} + 0^2
\end{aligned} \tag{3.22}$$

in which 0^2 refers to second-order terms in increments. It follows that $\Delta_{\mathrm{n+1,j}} \approx 0^2$. For this reason, Newton iteration is said to converge *quadratically* (presumably to the correct solution if the initial iterate is "sufficiently close"). When the iteration scheme converges to the solution, the load intensity is incremented again. Consider $f(x) = (x - 1)^2$. If $x^{(0)} = 1/2$, the iterates are 1/2, 3/4, 7/8, and 15/16. If $x^{(0)} = 2$, the iterates are 3/2, 5/4, 9/8, and 17/16. In both cases, the error is halved in each iteration.

The nonlinear, finite element poses nonlinear, algebraic equations of the form

$$\delta \mathbf{u}^T [\boldsymbol{\varphi}(\mathbf{u}) - \lambda \mathbf{v}] = 0, \tag{3.23}$$

in which $\mathbf{u}$ and $\boldsymbol{\varphi}$ are n × 1 vectors, $\mathbf{v}$ is a constant n × 1 unit vector, and λ represents "load intensity." The Newton iteration scheme provides the $(j + 1)^{st}$ iterate for $\mathbf{u}_{n+1}$ as

$$\Delta_{\mathrm{n+1,j}} = -\left[\left[\frac{\partial \boldsymbol{\varphi}}{\partial \mathbf{u}}\right]_{|\mathbf{u}^{(\mathrm{j})}_{\mathrm{n+1}}}\right]^{-1} \left[\boldsymbol{\varphi}\left(\mathbf{u}^{(\mathrm{j})}_{\mathrm{n+1}}\right) - \lambda_{\mathrm{j+1}} \mathbf{v}\right], \qquad \mathbf{u}^{(\mathrm{j+1})}_{\mathrm{n+1}} - \mathbf{u}^{(\mathrm{j})}_{\mathrm{n+1}} = \Delta_{\mathrm{n+1,j}}. \tag{3.24}$$

in which, for example, the initial iterate is $\mathbf{u}_n$. One can avoid the use of an explicit matrix inverse by solving the linear system

$$\left[\frac{\partial \varphi}{\partial \mathbf{u}}\right]_{\Big|\mathbf{u}_{n+1}^{(j)}} \Delta_{n+1,j} = \boldsymbol{\varphi}\left(\mathbf{u}_{n+1}^{(j)}\right) - \mathbf{v}_{j+1} \qquad \mathbf{u}_{n+1}^{(j+1)} = \mathbf{u}_{n+1}^{(j)} + \Delta_{n+1,j}. \tag{3.25}$$

3.2.2 Critical Points and the Arc-Length Method

A point λ^* at which the Jacobian matrix $\mathbf{J} = \frac{\partial \boldsymbol{\varphi}}{\partial \mathbf{u}}$ is singular is called a critical point, and corresponds to important phenomena such as buckling. There often is good reason to attempt to continue calculations through critical points, such as to compute a postbuckled configuration. Arc-length methods are suitable for doing so. Here, we present a version with a simple eigenstructure.

Suppose that the change in load intensity is regarded as a variable. Introduce the "constraint" on the size of the increment for the n^{th} load step:

$$\psi(\mathbf{u}, \lambda) = \beta^2[\lambda - \lambda_n] + \mathbf{v}^{\mathbf{T}}(\mathbf{u} - \mathbf{u}_n) - \Sigma^2 = 0, \tag{3.26}$$

in which Σ^2 is interpreted as the arc length in $n + 1$ dimensional space of $\mathbf{u}$ and λ. Also, $\beta > 0$. Now,

$$\begin{pmatrix} \boldsymbol{\varphi}(\mathbf{u}) - \lambda \mathbf{v} \\ \psi \end{pmatrix} = \begin{pmatrix} \mathbf{0} \\ \mathbf{0} \end{pmatrix}. \tag{3.27}$$

Newton iteration now is expressed as

$$\mathbf{J}' \begin{pmatrix} \mathbf{u}_{n+1}^{(j+1)} - \mathbf{u}_{n+1}^{(j)} \\ \lambda_{n+1}^{(j+1)} - \lambda_n^{(j)} \end{pmatrix} = -\begin{pmatrix} \boldsymbol{\varphi}\left(\mathbf{u}_{n+1}^{(j)}\right) - \lambda_{n+1}^{(j)} \mathbf{v} \\ \psi\left(\mathbf{u}_{n+1}^{(j)}, \lambda_{n+1}\right) \end{pmatrix}, \qquad \mathbf{J}' = \begin{bmatrix} \mathbf{J} & -\mathbf{v} \\ \mathbf{v}^{\mathbf{T}} & \beta^2 \end{bmatrix}. \tag{3.28}$$

An advantage is gained if $\mathbf{J}'$ can be made nonsingular even though $\mathbf{J}$ is singular. Suppose that $\mathbf{J}$ is symmetric and we can choose β such that $\mathbf{J} + \mathbf{v}\,\mathbf{v}^{\mathbf{T}}/\boldsymbol{\beta}^2 > \mathbf{0}$. Then $\mathbf{J}'$ admits the "triangularization"

$$\mathbf{J}' = \begin{pmatrix} \mathbf{J} + \mathbf{v}\,\mathbf{v}^{\mathbf{T}}/\boldsymbol{\beta}^2 & -\mathbf{v}/\boldsymbol{\beta} \\ \mathbf{0}^{\mathbf{T}} & \boldsymbol{\beta} \end{pmatrix} \begin{pmatrix} \mathbf{I} & \mathbf{0} \\ \mathbf{v}^{\mathbf{T}}/\boldsymbol{\beta} & \boldsymbol{\beta} \end{pmatrix}. \tag{3.29}$$

The determinant of $\mathbf{J}'$ is now $\boldsymbol{\beta}^2 \det(\mathbf{J} + \mathbf{v}\,\mathbf{v}^{\mathbf{T}}/\boldsymbol{\beta}^2)$. Ideally, β is chosen to maximize det ($\mathbf{J}'$).

3.3 EXERCISES

1. Directly apply variational calculus to F, given by

$$\mathrm{F} = \int_0^{\mathrm{L}} \frac{1}{2}\mathrm{EA}\left(\frac{du}{dx}\right)^2 dx - \mathrm{P}u(\mathrm{L})$$

to verify that $\delta\mathbf{F} = 0$ gives rise to the Euler equation

$$\mathrm{EA}\frac{d^2u}{dx^2} = 0$$

What endpoint conditions (not unique) are compatible with $\delta F = 0$?

2. The governing equation for an Euler-Bernoulli beam in Figure 3.2 is

$$\mathrm{EI}\frac{d^4w}{dx^4} = 0$$

in which w is the vertical displacement of the neutral (centroidal) axis. The shear force V and the bending moment M satisfy

$$\mathrm{M} = -\mathrm{EI}\frac{d^2w}{dx^2} \qquad \mathrm{V} = \mathrm{EI}\frac{d^3w}{dx^3}$$

Using integration by parts twice, obtain the function F such that $\delta\mathrm{F} = 0$ is equivalent to the foregoing differential equation together with the boundary conditions for a cantilevered beam of length L:

$$w(0) = w'(0) = 0 \qquad \mathrm{M}(\mathrm{L}) = 0, \quad \mathrm{V}(\mathrm{L}) = V_0.$$

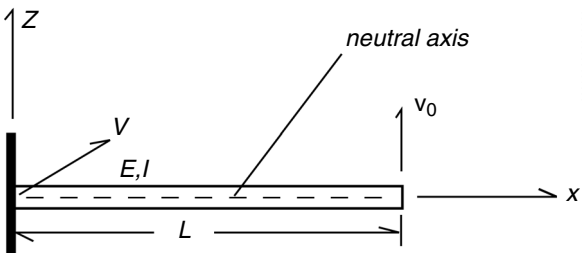

FIGURE 3.2 Cantilevered beam.

4 Kinematics of Deformation

The current chapter provides a review of the mathematics for describing deformation of continua. A more complete account is given, for example, in Chandrasekharaiah and Debnath (1994).

4.1 KINEMATICS

4.1.1 Displacement

In finite-element analysis for finite deformation, it is necessary to carefully distinguish between the current (or "deformed") configuration (i.e., at the current time or load step) and a reference configuration, which is usually considered strain-free. Here, both configurations are referred to the same orthogonal coordinate system characterized by the base vectors $\mathbf{e}_1, \mathbf{e}_2, \mathbf{e}_3$ (see Figure 1.1 in Chapter 1). Consider a body with volume V and surface S in the current configuration. The particle P occupies a position represented by the position vector $\mathbf{x}$, and experiences (empirical) temperature T. In the corresponding undeformed configuration, the position of P is described by $\mathbf{X}$, and the temperature has the value T_0 independent of $\mathbf{X}$. It is now assumed that $\mathbf{x}$ is a function of $\mathbf{X}$ and t and that T is also a function of $\mathbf{X}$ and t. The relations are written as $\mathbf{x}(\mathbf{X}, t)$ and $T(\mathbf{X}, t)$, and it is assumed that $\mathbf{x}$ and T are continuously differentiable in $\mathbf{X}$ and t through whatever order needed in the subsequent development.

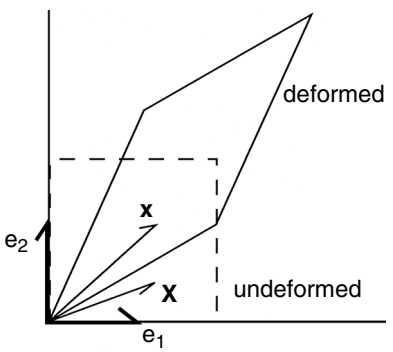

FIGURE 4.1 Position vectors in deformed and undeformed configurations.

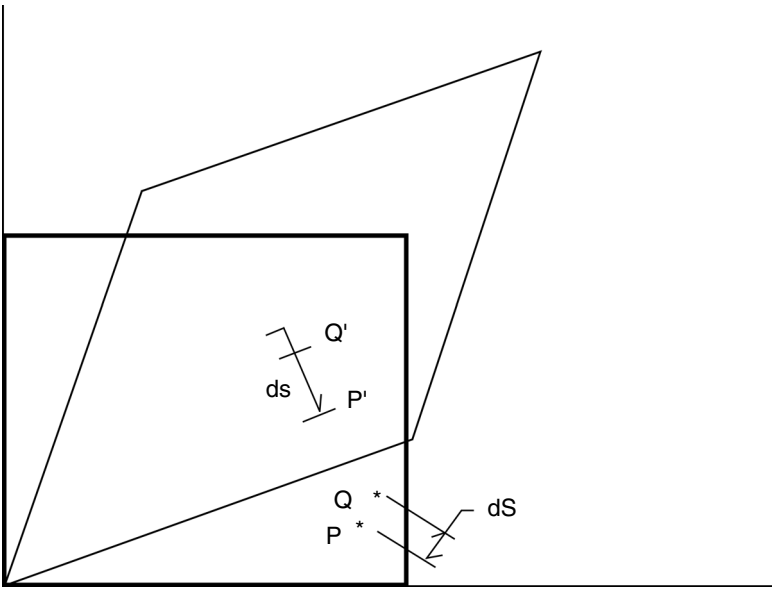

FIGURE 4.2 Deformed and undeformed distances between adjacent points.

4.1.2 Displacement Vector

The vector $u(\mathbf{X})$ represents the displacement from position $\mathbf{X}$ to $\mathbf{x}$:

$$\boldsymbol{u}(\mathbf{X},t) = \mathbf{x} - \mathbf{X}. \tag{4.1}$$

Now consider two close points, P and Q, in the undeformed configuration. The vector difference $\mathbf{X}_P - \mathbf{X}_Q$ is represented as a differential $d\mathbf{X}$ with squared length $dS^2 = d\mathbf{X}^T d\mathbf{X}$. The corresponding quantity in the deformed configuration is $d\mathbf{x}$, with $dS^2 = d\mathbf{x}^T d\mathbf{x}$.

4.1.3 Deformation Gradient Tensor

The deformation gradient tensor $\mathbf{F}$ is introduced as

$$d\mathbf{x} = \mathbf{F}d\mathbf{X} \qquad \mathbf{F} = \frac{\partial \mathbf{x}}{\partial \mathbf{X}} \tag{4.2}$$

$\mathbf{F}$ satisfies the polar-decomposition theorem:

$$\mathbf{F} = \mathbf{U}\Sigma\mathbf{V}^T, \tag{4.3}$$

in which $\mathbf{U}$ and $\mathbf{V}$ are orthogonal and $\boldsymbol{\Sigma}$ is a positive definite diagonal tensor whose

entries λ_j, the singular values of **F**, are called the principal stretches.

$$\Sigma = \begin{bmatrix} \lambda_1 & 0 & 0 \\ 0 & \lambda_2 & 0 \\ 0 & 0 & \lambda_3 \end{bmatrix} \tag{4.4}$$

Based on Equation 4.3, **F** can be visualized as representing a rotation, followed by a stretch, followed by a second rotation.

4.2 STRAIN

The deformation-induced change in squared length is given by

$$ds^2 - dS^2 = d\mathbf{X}^{\mathbf{T}} 2\boldsymbol{E} d\mathbf{X} \qquad \boldsymbol{E} = \frac{1}{2}[\mathbf{F}^{\mathbf{T}}\mathbf{F} - \mathbf{I}], \tag{4.5}$$

in which $\boldsymbol{E}$ denotes the *Lagrangian strain tensor*. Also of interest is the *Right Cauchy-Green strain* $\boldsymbol{C} = \mathbf{F}^{\mathbf{T}}\mathbf{F} = 2\boldsymbol{E} + \mathbf{I}$. Note that $\mathbf{F} = \mathbf{I} + \partial\mathbf{u}/\partial\mathbf{X}$. If quadratic terms in $\partial\mathbf{u}/\partial\mathbf{X}$ are neglected, the linear-strain tensor $\boldsymbol{E}_L$ is recovered as

$$\boldsymbol{E}_{\mathrm{L}} = \frac{1}{2}\left[\frac{\partial \mathbf{u}}{\partial \mathbf{X}} + \left(\frac{\partial \mathbf{u}}{\partial \mathbf{X}}\right)^{\mathbf{T}}\right]. \tag{4.6}$$

Upon application of Equation 4.3, $\boldsymbol{E}$ is rewritten as

$$\boldsymbol{E} = \mathbf{V}\left[\frac{1}{2}(\boldsymbol{\Sigma}^2 - \mathbf{I})\mathbf{V}^{\mathbf{T}}\right] \tag{4.7}$$

Under pure rotation $\mathbf{x} = \mathbf{QX}$, $\mathbf{F} = \mathbf{Q}$ and $\boldsymbol{E} = \frac{1}{2}[\mathbf{Q}^{\mathbf{T}}\mathbf{Q} - \mathbf{I}] = \mathbf{0}$. The case of pure rotation in small strain is considered in a subsequent section.

4.2.1 F, E, $\mathbf{E_L}$ and u in Orthogonal Coordinates

Let Y_1, Y_2, and Y_3 be orthogonal coordinates of a point in an undeformed configuration, with y_1, y_2, y_3 orthogonal coordinates in the deformed configuration. The corresponding orthonormal base vectors are $\boldsymbol{\Gamma}_1, \boldsymbol{\Gamma}_2, \boldsymbol{\Gamma}_3$ and $\boldsymbol{\gamma}_1, \boldsymbol{\gamma}_2, \boldsymbol{\gamma}_3$.

4.2.1.1 Deformation Gradient and Lagrangian Strain Tensors

Recalling relations introduced in Chapter 1 for orthogonal coordinates, the differential position vectors are expressed as

$$d\mathbf{R} = \sum_{\alpha} dY_\alpha H_\alpha \boldsymbol{\Gamma}_\alpha \qquad d\mathbf{r} = \sum_{\beta} dy_\beta h_\beta \boldsymbol{\gamma}_\beta \tag{4.8}$$

$$
\begin{aligned}
d\mathbf{r} &= \sum_{\alpha} dy_{\alpha} h_{\alpha} \boldsymbol{\gamma}_{\alpha} \\
&= \sum_{\beta} \sum_{\alpha} dy_{\alpha} h_{\alpha} (\gamma_{\alpha} \cdot \boldsymbol{\Gamma}_{\beta}) \boldsymbol{\Gamma}_{\beta} \\
&= \sum_{\beta} \sum_{\alpha} dy_{\alpha} h_{\alpha} q^{\mathbf{T}}_{\beta\alpha} \boldsymbol{\Gamma}_{\beta} \\
&= \sum_{\zeta} \sum_{\beta} \sum_{\alpha} q^{\mathbf{T}}_{\beta\alpha} \frac{h_{\alpha}}{H_{\zeta}} \frac{dy_{\alpha}}{dY_{\zeta}} H_{\zeta} dY_{\zeta} \boldsymbol{\Gamma}_{\beta} \\
&= \sum_{\zeta} \sum_{\beta} \sum_{\alpha} q^{\mathbf{T}}_{\beta\alpha} \frac{h_{\alpha}}{H_{\zeta}} \frac{dy_{\alpha}}{dY_{\zeta}} (\boldsymbol{\Gamma}_{\beta} \wedge \boldsymbol{\Gamma}_{\zeta}) H_{\zeta} dY_{\zeta} \boldsymbol{\Gamma}_{\zeta},
\end{aligned} \tag{4.9}
$$

in which $\boldsymbol{\Gamma}_{\beta}$ denotes the base vector in the curvilinear system used for the undeformed configuration.

This can be written as

$$
d\mathbf{r} = \mathbf{Q}^{\mathbf{T}} \mathbf{F}' d\mathbf{R}, \qquad [\mathbf{Q}^{\mathbf{T}}]_{\beta\alpha} = q^{\mathbf{T}}_{\beta\alpha} \qquad [\mathbf{F}']_{\alpha\zeta} = \frac{h_{\alpha}}{H_{\zeta}} \frac{\partial y_{\alpha}}{\partial Y_{\zeta}}, \tag{4.10}
$$

in which $\mathbf{Q}$ is the orthogonal tensor representing transformation from the undeformed to the deformed coordinate system. It follows that

$$
\boldsymbol{E} = \frac{1}{2}[\boldsymbol{F}^{\mathbf{T}} \boldsymbol{F} - \boldsymbol{I}] = \frac{1}{2}[\boldsymbol{F}'^{\mathbf{T}} \boldsymbol{F}' - \boldsymbol{I}],
$$

from which

$$
[\boldsymbol{E}]_{\mathrm{ij}} = \frac{1}{2}\left[\sum_{\beta}\left(\frac{\mathrm{h}_{\beta}^{2}}{\mathrm{H_i H_j}} \frac{\partial \mathrm{y}_{\beta}}{\partial \mathrm{Y_i}} \frac{\partial \mathrm{y}_{\beta}}{\partial \mathrm{Y_j}}\right) - \delta_{\mathrm{ij}}\right]. \tag{4.11}
$$

Displacement Vector

The position vectors can be written in the form $\mathbf{R} = \mathrm{Z}_i \boldsymbol{\Gamma}_i$, $\mathbf{r} = \mathrm{z}_j \boldsymbol{\gamma}_j$. The displacement vector referred to the undeformed base vectors is

$$
\mathbf{u} = [\mathrm{z}_j q_{ji} - \mathrm{Z}_i] \boldsymbol{\Gamma}_i, \qquad q_{ji} = \boldsymbol{\gamma}_j \cdot \boldsymbol{\Gamma}_i. \tag{4.12}
$$

Cylindrical Coordinates

In cylindrical coordinates,

$$
\mathbf{u} = [r\cos(\theta - \Theta) - R]\,\mathbf{e}_R + r\sin(\theta - \Theta)\mathbf{e}_{\theta} + (z - Z)\,\mathbf{e}_Z. \tag{4.13}
$$

We now apply the chain rule to ds^2 in cylindrical coordinates:

$$
\begin{aligned}
ds^2 &= d\mathbf{r}\cdot d\mathbf{r} = dr^2 + r^2 d\theta^2 + dz^2 \\
&= \left[\frac{dr}{dR}dR + \frac{1}{R}\frac{dr}{d\Theta}Rd\Theta + \frac{dr}{dZ}dZ\right]^2 + \left[r\frac{d\theta}{dR}dR + \frac{r}{R}\frac{d\theta}{d\Theta}Rd\Theta + r\frac{d\theta}{dZ}dZ\right]^2 \\
&\quad + \left[\frac{dz}{dR}dR + \frac{1}{R}\frac{dz}{d\Theta}Rd\Theta + \frac{dz}{dZ}dZ\right]^2 \\
&= \{dR \quad Rd\Theta \quad dZ\}\,\mathbf{C}\begin{Bmatrix} dR \\ Rd\Theta \\ dZ \end{Bmatrix},
\end{aligned}
\tag{4.14}
$$

in which

$$
\begin{aligned}
c_{RR} &= \left(\frac{dr}{dR}\right)^2 + \left(r\frac{d\theta}{dR}\right)^2 + \left(\frac{dz}{dR}\right)^2 & e_{RR} &= \frac{1}{2}(c_{RR}-1) \\
c_{\Theta\Theta} &= \left(\frac{1}{R}\frac{dr}{d\Theta}\right)^2 + \left(\frac{r}{R}\frac{d\theta}{d\Theta}\right)^2 + \left(\frac{1}{R}\frac{dz}{d\Theta}\right)^2 & e_{\Theta\Theta} &= \frac{1}{2}(c_{\Theta\Theta}-1) \\
c_{ZZ} &= \left(\frac{dr}{dZ}\right)^2 + \left(r\frac{d\theta}{dZ}\right)^2 + \left(\frac{dz}{dZ}\right)^2 & e_{ZZ} &= \frac{1}{2}(c_{ZZ}-1) \\
c_{R\Theta} &= \left(\frac{dr}{dR}\right)\left(\frac{1}{R}\frac{dr}{d\Theta}\right) + \left(r\frac{d\theta}{dR}\right)\left(\frac{r}{R}\frac{d\theta}{d\Theta}\right) + \left(\frac{dz}{dR}\right)\left(\frac{1}{R}\frac{dz}{d\Theta}\right) & e_{R\Theta} &= \frac{1}{2}c_{R\Theta} \\
c_{\Theta Z} &= \left(\frac{1}{R}\frac{dr}{d\Theta}\right)\left(\frac{dr}{dZ}\right) + \left(\frac{r}{R}\frac{d\theta}{d\Theta}\right)\left(r\frac{d\theta}{dZ}\right) + \left(\frac{1}{R}\frac{dz}{d\Theta}\right)\left(\frac{dz}{dZ}\right) & e_{\Theta Z} &= \frac{1}{2}c_{\Theta Z} \\
c_{ZR} &= \left(\frac{dr}{dZ}\right)\left(\frac{dr}{dR}\right) + \left(r\frac{d\theta}{dZ}\right)\left(r\frac{d\theta}{dR}\right) + \left(\frac{dz}{dZ}\right)\left(\frac{dz}{dR}\right) & e_{ZR} &= \frac{1}{2}c_{ZR}.
\end{aligned}
\tag{4.15}
$$

4.2.1.2 Linear-Strain Tensor in Cylindrical Coordinates

If quadratic terms in the displacements and their derivatives are neglected, then

$$
u_R \approx r - R \qquad \frac{u_\Theta}{R} \approx \theta - \Theta \qquad u_Z \approx z - Z,
\tag{4.16}
$$

$$
\begin{array}{lll}
\dfrac{dr}{dR} \approx 1 + \dfrac{du_R}{dR} & r\dfrac{d\theta}{dR} \approx R\dfrac{d}{dR}\left(\dfrac{u_\Theta}{R}\right) = \dfrac{du_\Theta}{dR} - \dfrac{u_\Theta}{R} & \dfrac{dz}{dR} \approx \dfrac{du_Z}{dR} \\
\dfrac{1}{R}\dfrac{dr}{d\Theta} \approx \dfrac{1}{R}\dfrac{du_R}{d\Theta} & \dfrac{r}{R}\dfrac{d\theta}{d\Theta} = \dfrac{R+u_R}{R}\left[1 + \dfrac{1}{R}\dfrac{du_\Theta}{d\Theta}\right] \approx 1 + \dfrac{u_R}{R} + \dfrac{1}{R}\dfrac{du_\Theta}{d\Theta} & \dfrac{1}{R}\dfrac{dz}{d\Theta} \approx \dfrac{1}{R}\dfrac{du_Z}{d\Theta} \\
\dfrac{dr}{dZ} \approx \dfrac{du_R}{dZ} & r\dfrac{d\theta}{dZ} \approx \dfrac{du_\Theta}{dZ} & \dfrac{dz}{dZ} \approx 1 + \dfrac{du_Z}{dZ}
\end{array}
$$

giving rise to the linear-strain tensor

$$\mathbf{E}_L = \begin{bmatrix} \dfrac{du_R}{dR} & \dfrac{1}{2}\left(\dfrac{du_\Theta}{dR} - \dfrac{u_\Theta}{R} + \dfrac{1}{R}\dfrac{\partial u_R}{\partial R}\right) & \dfrac{1}{2}\left[\dfrac{du_Z}{dR} + \dfrac{du_R}{dZ}\right] \\ \dfrac{1}{2}\left(\dfrac{du_\Theta}{dR} - \dfrac{u_\Theta}{R} + \dfrac{1}{R}\dfrac{\partial u_R}{\partial R}\right) & \dfrac{u_R}{R} + \dfrac{1}{R}\dfrac{du_\Theta}{d\Theta} & \dfrac{1}{2}\left[\dfrac{du_\Theta}{dZ} + \dfrac{1}{R}\dfrac{du_Z}{d\Theta}\right] \\ \dfrac{1}{2}\left[\dfrac{du_Z}{dR} + \dfrac{du_R}{dZ}\right] & \dfrac{1}{2}\left[\dfrac{du_\Theta}{dZ} + \dfrac{1}{R}\dfrac{du_Z}{d\Theta}\right] & \dfrac{du_Z}{dZ} \end{bmatrix}. \quad (4.17)$$

The divergence of $\mathbf{u}$ in cylindrical coordinates is given by $\nabla \cdot \mathbf{u} = trace\frac{d\mathbf{u}}{d\mathbf{r}} = trace(\boldsymbol{E}_L)$, from which

$$\nabla \cdot \mathbf{u} = \frac{du_R}{dR} + \frac{u_R}{R} + \frac{1}{R}\frac{du_\Theta}{d\Theta} + \frac{du_Z}{dZ}, \quad (4.18)$$

which agrees with the expression given in Schey (1973).

4.2.2 Velocity-Gradient Tensor, Deformation-Rate Tensor, and Spin Tensor

We now introduce the particle velocity $\mathbf{v} = \partial\mathbf{x}/\partial t$ and assume that it is an explicit function of $\mathbf{x}(t)$ and t. The velocity-gradient tensor $\mathbf{L}$ is introduced using $d\mathbf{v} = \mathbf{L}d\mathbf{x}$, from which

$$\begin{aligned} \mathbf{L} &= \frac{d\mathbf{v}}{d\mathbf{x}} \\ &= \frac{d\mathbf{v}}{d\mathbf{X}}\frac{d\mathbf{X}}{d\mathbf{x}} \\ &= \dot{\mathbf{F}}\mathbf{F}^{-1}. \end{aligned} \quad (4.19)$$

Its symmetric part, called the deformation-rate tensor,

$$\mathbf{D} = \frac{1}{2}[\mathbf{L} + \mathbf{L}^{\mathbf{T}}], \quad (4.20)$$

can be regarded as a strain rate referred to the current configuration. The corresponding strain rate referred to the undeformed configuration is the Lagrangian strain rate:

$$\begin{aligned} \dot{\boldsymbol{E}} &= \frac{1}{2}[\mathbf{F}^{\mathbf{T}}\dot{\mathbf{F}} + \dot{\mathbf{F}}^{\mathbf{T}}\mathbf{F}] \\ &= \mathbf{F}^{\mathbf{T}}\left\{\frac{1}{2}[\dot{\mathbf{F}}\mathbf{F}^{-1} + \mathbf{F}^{-\mathbf{T}}\dot{\mathbf{F}}^{\mathbf{T}}]\right\}\mathbf{F} \\ &= \mathbf{F}^{\mathbf{T}}\mathbf{D}\mathbf{F}. \end{aligned} \quad (4.21)$$

The antisymmetric portion of **L** is called the spin tensor **W**:

$$\mathbf{W} = \frac{1}{2}[\mathbf{L} - \mathbf{L}^{\mathbf{T}}]. \tag{4.22}$$

Suppose the deformation consists only of a time-dependent, rigid-body motion:

$$\mathbf{x}(t) = \mathbf{Q}(t)\mathbf{X} + \mathbf{b}(t), \qquad \mathbf{Q}^{\mathbf{T}}(t)\mathbf{Q}(t) = \mathbf{I}. \tag{4.23}$$

Clearly, $\mathbf{F} = \mathbf{Q}$ and $\boldsymbol{E} = \mathbf{0}$. Furthermore,

$$\mathbf{L} = \dot{\mathbf{Q}}\mathbf{Q}^{\mathbf{T}}, \tag{4.24}$$

which is antisymmetric since $\mathbf{0} = \dot{\mathbf{I}} = [\mathbf{Q}\mathbf{Q}^{\mathbf{T}}]^{\cdot} = \dot{\mathbf{Q}}\mathbf{Q}^{\mathbf{T}} + \mathbf{Q}\dot{\mathbf{Q}}^{\mathbf{T}} = \dot{\mathbf{Q}}\mathbf{Q}^{\mathbf{T}} + (\dot{\mathbf{Q}}\mathbf{Q}^{\mathbf{T}})^{\mathbf{T}}$. Hence, $\mathbf{D} = \mathbf{0}$ and $\mathbf{W} = \dot{\mathbf{Q}}\mathbf{Q}^{\mathbf{T}}$, thus explaining the name of **W**.

4.2.2.1 v, L, D, and W in Orthogonal Coordinates

The velocity $\mathbf{v}(\mathbf{y}, t)$ in orthogonal coordinates is given by

$$\mathbf{v}(\mathbf{y}, t) = \frac{d\mathbf{r}}{dt} = \sum_{\alpha} v_{\alpha}\boldsymbol{\gamma}_{\alpha}, \qquad v_{\alpha} = h_{\alpha}\frac{dy_{\alpha}}{dt}. \tag{4.25}$$

Based on what we learned in Chapter 1, with **v** denoting the velocity vector in orthogonal coordinates,

$$[\mathbf{L}]_{\beta\alpha} = \left[\frac{d\mathbf{v}}{d\mathbf{r}}\right]_{\beta\alpha} = \frac{1}{h_{\alpha}}\left[\frac{\partial v_j}{\partial y_{\alpha}}\delta_{j\beta} + v_j \mathbf{c}_{j\beta\alpha}\right].$$

$$\mathbf{c}_{\alpha j\beta} = \frac{1}{h_{\alpha}}(1 - \delta_{\alpha\beta})\begin{bmatrix}\alpha & & \beta\\ & j & \end{bmatrix}h_{\beta} \tag{4.26}$$

$$\begin{bmatrix}\alpha & & \beta\\ & j & \end{bmatrix} = h_{\beta}\frac{\partial^2 x_{\alpha}}{\partial y_k \partial y_j}\frac{\partial y_{\beta}}{\partial x_k}$$

Of course, $[\mathbf{D}]_{\beta\alpha} = \frac{1}{2}[[\mathbf{L}]_{\beta\alpha} + [\mathbf{L}]_{\alpha\beta}], [\mathbf{W}]_{\beta\alpha} = \frac{1}{2}[[\mathbf{L}]_{\beta\alpha} - [\mathbf{L}]_{\alpha\beta}]$.

4.2.2.2 Cylindrical Coordinates

The velocity vector in cylindrical coordinates is

$$\mathbf{v} = \frac{dr}{dt}\mathbf{e}_r + r\frac{d\theta}{dt}\mathbf{e}_{\theta} + \frac{dz}{dt}\mathbf{e}_z$$

$$= v_r\mathbf{e}_r + v_{\theta}\mathbf{e}_{\theta} + v_z\mathbf{e}_z. \tag{4.27}$$

Observe that

$$\begin{aligned} d\mathbf{v} &= dv_r\mathbf{e}_r + dv_\theta\mathbf{e}_\theta + dv_z\mathbf{e}_z + v_r d\mathbf{e}_r + v_\theta d\mathbf{e}_\theta \\ &= [dv_r - v_\theta d\theta]\mathbf{e}_r + [dv_\theta + v_r d\theta]\mathbf{e}_\theta + dv_z\mathbf{e}_z. \end{aligned} \tag{4.28}$$

Converting to matrix-vector notation, we get

$$\begin{aligned} d\boldsymbol{v} &= \begin{pmatrix} \frac{dv_r}{dr}dr + \frac{1}{r}\frac{dv_r}{d\theta}rd\theta + \frac{dv_r}{dz}dz - \frac{v_\theta}{r}rd\theta \\ \frac{dv_\theta}{dr}dr + \frac{1}{r}\frac{dv_\theta}{d\theta}rd\theta + \frac{dv_\theta}{dz}dz + \frac{v_r}{r}rd\theta \\ \frac{dv_z}{dr}dr + \frac{1}{r}\frac{dv_z}{d\theta}rd\theta + \frac{dv_z}{dz}dz \end{pmatrix} \\ &= \boldsymbol{L}\begin{pmatrix} dr \\ rd\theta \\ dz \end{pmatrix}, \qquad \boldsymbol{L} = \begin{bmatrix} \frac{dv_r}{dr} & \frac{1}{r}\frac{dv_r}{d\theta} - \frac{v_\theta}{r} & \frac{dv_r}{dz} \\ \frac{dv_\theta}{dr} & \frac{1}{r}\frac{dv_\theta}{d\theta} + \frac{v_r}{r} & \frac{dv_\theta}{dz} \\ \frac{dv_z}{dr} & \frac{1}{r}\frac{dv_z}{d\theta} & \frac{dv_z}{dz} \end{bmatrix}. \end{aligned} \tag{4.29}$$

4.2.2.3 Spherical Coordinates

Now

$$\begin{aligned} \mathbf{v} &= \frac{dr}{dt}\mathbf{e}_r + r\cos\phi\frac{d\theta}{dt}\mathbf{e}_\theta + r\frac{d\phi}{dt}\mathbf{e}_\phi \\ &= v_r\mathbf{e}_r + v_\theta\mathbf{e}_\theta + v_\phi\mathbf{e}_\phi \\ \mathbf{e}_r &= \cos\phi(\cos\theta\mathbf{e}_1 + \sin\theta\mathbf{e}_2) + \sin\phi\mathbf{e}_3 \\ \mathbf{e}_\theta &= -\sin\theta\mathbf{e}_1 + \cos\theta\mathbf{e}_2 \\ \mathbf{e}_\phi &= -\sin\phi(\cos\theta\mathbf{e}_1 + \sin\theta\mathbf{e}_2) + \cos\phi\mathbf{e}_3. \end{aligned} \tag{4.30}$$

Next,

$$\begin{aligned} &\mathbf{v}' = \mathbf{Q}\mathbf{v}, \quad \mathbf{v} = \begin{pmatrix} v_r \\ v_\theta \\ v_\phi \end{pmatrix}, \quad \mathbf{v}' \text{ referred to } \mathbf{e}_1,\ \mathbf{e}_2,\ \mathbf{e}_3 \\ &\mathbf{Q} = \begin{bmatrix} \cos\phi\cos\theta & \cos\phi\sin\theta & \sin\phi \\ -\sin\theta & \cos\theta & 0 \\ -\sin\phi\cos\theta & -\sin\phi\sin\theta & \cos\phi \end{bmatrix} \end{aligned} \tag{4.31}$$

$$d\mathbf{v} = \mathbf{Q}\mathbf{Q}^{\mathbf{T}} d\mathbf{v}^{*} + d\mathbf{Q}\mathbf{Q}^{\mathbf{T}}\mathbf{v}$$

$$= d\mathbf{v}^{*} + d\mathbf{Q}\mathbf{Q}^{\mathbf{T}}\mathbf{v}, \quad d\mathbf{v}^{*} = \begin{pmatrix} dv_r \\ dv_\theta \\ dv_\phi \end{pmatrix} \text{ referred to } \mathbf{e}_r,\ \mathbf{e}_\theta,\ \mathbf{e}_\phi \tag{4.32}$$

Recall that

$$\frac{d\mathbf{Q}(\theta)}{dt}\mathbf{Q}^{\mathbf{T}}(\theta) = \begin{bmatrix} 0 & \cos\phi & 0 \\ -\cos\phi & 0 & \sin\phi \\ 0 & -\sin\phi & 0 \end{bmatrix} \frac{d\theta}{dt} + \begin{bmatrix} 0 & 0 & 1 \\ 0 & 0 & 0 \\ -1 & 0 & 0 \end{bmatrix} \frac{d\phi}{dt}. \tag{4.33}$$

Thus, it follows that

$$d\mathbf{Q}\mathbf{Q}^{\mathbf{T}} = \frac{1}{r\cos\phi} \begin{bmatrix} 0 & \cos\phi & 0 \\ -\cos\phi & 0 & \sin\phi \\ 0 & -\sin\phi & 0 \end{bmatrix} r\cos\phi\, d\theta + \frac{1}{r} \begin{bmatrix} 0 & 0 & 1 \\ 0 & 0 & 0 \\ -1 & 0 & 0 \end{bmatrix} r\, d\phi \tag{4.34}$$

and

$$d\mathbf{Q}\mathbf{Q}^{\mathbf{T}}\mathbf{v} = \begin{pmatrix} \cos\phi v_\theta\, d\theta + v_\phi\, d\phi \\ -\cos\phi v_r\, d\theta + \sin\phi v_\phi\, d\theta \\ -\sin\phi v_\theta\, d\theta - v_r\, d\phi \end{pmatrix}$$

$$= \frac{1}{r} \begin{bmatrix} 0 & v_\theta & v_\phi \\ 0 & -v_r + \tan\phi v_\phi & 0 \\ 0 & -\tan\phi v_\theta & -v_r \end{bmatrix} \begin{pmatrix} dr \\ r\cos\phi\, d\theta \\ r\, d\phi \end{pmatrix}. \tag{4.35}$$

Finally,

$$dv^{*} = \begin{pmatrix} dv_r \\ dv_\theta \\ dv_\phi \end{pmatrix} = \begin{bmatrix} \frac{dv_r}{dr} & \frac{1}{r\cos\phi}\frac{dv_r}{d\theta} & \frac{1}{r}\frac{dv_r}{d\phi} \\ \frac{dv_\theta}{dr} & \frac{1}{r\cos\phi}\frac{dv_\theta}{d\theta} & \frac{1}{r}\frac{dv_\theta}{d\phi} \\ \frac{dv_\phi}{dr} & \frac{1}{r\cos\phi}\frac{dv_\phi}{d\theta} & \frac{1}{r}\frac{dv_\phi}{d\phi} \end{bmatrix} \begin{pmatrix} dr \\ r\cos\phi\, d\theta \\ r\, d\phi \end{pmatrix} \tag{4.36}$$

and

$$\mathbf{L} = \begin{bmatrix} \frac{dv_r}{dr} & \frac{1}{r\cos\phi}\frac{dv_r}{d\theta} & \frac{1}{r}\frac{dv_r}{d\phi} \\ \frac{dv_\theta}{dr} & \frac{1}{r\cos\phi}\frac{dv_\theta}{d\theta} & \frac{1}{r}\frac{dv_\theta}{d\phi} \\ \frac{dv_\phi}{dr} & \frac{1}{r\cos\phi}\frac{dv_\phi}{d\theta} & \frac{1}{r}\frac{dv_\phi}{d\phi} \end{bmatrix} + \frac{1}{r}\begin{bmatrix} 0 & v_\theta & v_\phi \\ 0 & -v_r + \tan\phi v_\phi & 0 \\ 0 & -\tan\phi v_\theta & -v_r \end{bmatrix}$$

$$= \begin{bmatrix} \frac{dv_r}{dr} & \frac{1}{r\cos\phi}\frac{dv_r}{d\theta} + \frac{v_\theta}{r} & \frac{1}{r}\frac{dv_r}{d\phi} + \frac{v_\phi}{r} \\ \frac{dv_\theta}{dr} & \frac{1}{r\cos\phi}\frac{dv_\theta}{d\theta} - \frac{v_r - \tan\phi v_\phi}{r} & \frac{1}{r}\frac{dv_\theta}{d\phi} \\ \frac{dv_\phi}{dr} & \frac{1}{r\cos\phi}\frac{dv_\phi}{d\theta} - \frac{\tan\phi v_\theta}{r} & \frac{1}{r}\frac{dv_\phi}{d\phi} - \frac{v_r}{r} \end{bmatrix}. \tag{4.37}$$

The divergence of **v** is given by *trace*(**L**), thus,

$$\nabla \cdot \mathbf{v} = \frac{dv_r}{dr} + \frac{1}{r\cos\phi}\frac{dv_\theta}{d\theta} - \frac{v_r - \tan\phi v_\phi}{r} + \frac{1}{r}\frac{dv_\phi}{d\phi}, \tag{4.38}$$

which is again in agreement with Schey (1973).

4.3 DIFFERENTIAL VOLUME ELEMENT

The volume spanned by the differential-position vector $d\mathbf{R}$ is given by the vector triple-product

$$\begin{aligned} dV_0 &= d\mathbf{X}_1 \cdot d\mathbf{X}_2 \times d\mathbf{X}_3 = d\mathbf{X}_1 d\mathbf{X}_2 d\mathbf{X}_3 \\ d\mathbf{X}_1 &= dX_1\mathbf{e}_1 \quad d\mathbf{X}_2 = dX_2\mathbf{e}_2 \quad d\mathbf{X}_3 = dX_3\mathbf{e}_3. \end{aligned} \tag{4.39}$$

The vectors $d\mathbf{X}_i$ deform into $d\mathbf{x}_j = \frac{dx_j}{d\mathbf{x}_i}\mathbf{e}_j d\mathbf{X}_i$. The deformed volume is now readily verified to be

$$\begin{aligned} dV &= d\mathbf{x}_1 \cdot d\mathbf{x}_2 \times d\mathbf{x}_3 \\ &= J dV_0, \quad J = det(\mathbf{F}) = det^{\frac{1}{2}}(\mathbf{C}), \end{aligned} \tag{4.40}$$

and J is called the Jacobian. To obtain J for small strain, we invoke invariance and $J = \sqrt{det(\boldsymbol{C})}$ to find

$$\begin{aligned} det^{\frac{1}{2}}(\mathbf{C}) &= det^{\frac{1}{2}}[\mathbf{I} + 2\boldsymbol{E}] \\ &= \sqrt{(1+2E_I)(1+2E_{II})(1+2E_{III})}, \end{aligned} \tag{4.41}$$

in which E_I, E_{II}, E_{III} are the eigenvalues of $\mathbf{E}_L$, assumed to be much less that unity. The linear-volume strain follows as

$$\begin{aligned} e_{vol} &= det^{\frac{1}{2}}(\mathbf{C}) - 1 \\ &= \sqrt{1 + 2(E_I + E_{II} + E_{III}) + quadratic\ terms} - 1 \\ &\approx tr(\boldsymbol{E}_L), \end{aligned} \tag{4.42}$$

using the approximation $\sqrt{1+x} \approx 1 + x/2$ if $x << 1$.

The time derivative of J is prominent in incremental formulations in continuum mechanics. Recalling that $J = \sqrt{I_3}$,

$$\begin{aligned} \frac{d}{dt} J &= \frac{1}{2J} \frac{dI_3}{dt} \\ &= \frac{J}{2} tr(\mathbf{C}^{-1}\dot{\mathbf{C}}) \\ &= \frac{J}{2} tr(\mathbf{F}^{-1}\mathbf{F}^{-\mathrm{T}}[\mathbf{F}^{\mathrm{T}}\dot{\mathbf{F}} + \dot{\mathbf{F}}^{\mathrm{T}}\mathbf{F}]) \\ &= \frac{J}{2} tr(\mathbf{F}^{-1}\dot{\mathbf{F}} + \mathbf{F}^{-1}\mathbf{F}^{-\mathrm{T}}\dot{\mathbf{F}}^{\mathrm{T}}\mathbf{F}) \\ &= \frac{J}{2} [tr(\mathbf{F}^{-1}\dot{\mathbf{F}}) + tr(\mathbf{F}^{-1}\mathbf{F}^{-\mathrm{T}}\dot{\mathbf{F}}^{\mathrm{T}}\mathbf{F})] \\ &= J\, tr\left(\frac{\mathbf{F}^{-1}\dot{\mathbf{F}} + \mathbf{F}^{-\mathrm{T}}\dot{\mathbf{F}}^{\mathrm{T}}}{2} \right) \\ &= J\, tr(\mathbf{D}). \end{aligned} \tag{4.43}$$

4.4 DIFFERENTIAL SURFACE ELEMENT

Let dS denote a surface element in the deformed configuration, with exterior unit normal $\mathbf{n}$, as illustrated in Figure 4.3. The corresponding quantities from the reference configuration are dS_0 and $\mathbf{n}_0$. A surface element dS obeys the transformation (Chandrashekharaiah and Debnath, 1994):

$$\mathbf{n}\, dS = J\mathbf{F}^{-\mathrm{T}}\mathbf{n}_0\, dS_0, \tag{4.44}$$

from which we conclude that

$$dS = J\sqrt{\mathbf{n}_0^{\mathrm{T}}\mathbf{C}^{-1}\mathbf{n}_0}\, dS_0 \qquad \mathbf{n} = \frac{\mathbf{F}^{-\mathrm{T}}\mathbf{n}_0}{\sqrt{\mathbf{n}_0^{\mathrm{T}}\mathbf{C}^{-1}\mathbf{n}_0}}. \tag{4.45}$$

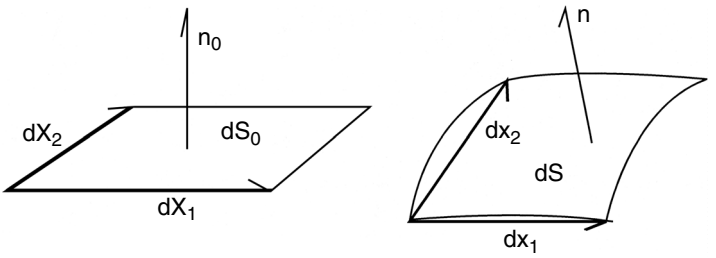

FIGURE 4.3 Surface patches in undeformed and deformed configurations.

During deformation, the surface normal changes direction, a fact which is important, for example, in contact problems. In incremental variational methods, we consider the differential $\frac{d\mathbf{n}}{dt}$ and $d(\mathbf{n}dS)$:

$$\frac{d}{dt}[\mathbf{n}dS] = \frac{dJ}{dt}\mathbf{F}^{-\mathbf{T}}\mathbf{n}_0\,dS_0 + J\frac{d\mathbf{F}^{-\mathbf{T}}}{dt}\mathbf{n}_0\,dS_0. \tag{4.46}$$

However, recalling Equation 4.43,

$$\frac{dJ}{dt} = J\,tr(\mathbf{D})$$

$$\frac{dJ}{dt}\mathbf{F}^{-\mathbf{T}}\mathbf{n}_0\,dS_0 = tr(\mathbf{D})J\mathbf{F}^{-\mathbf{T}}\mathbf{n}_0\,dS_0$$

$$= tr(\mathbf{D})\mathbf{n}\,dS. \tag{4.47}$$

Also, since $d(\mathbf{F}^{\mathbf{T}}\mathbf{F}^{-\mathbf{T}}) = \mathbf{0}$, then

$$\frac{d\mathbf{F}^{-T}}{dt} = -\mathbf{F}^{-T}\frac{d\mathbf{F}^{T}}{dt}\mathbf{F}^{-T}$$

$$= -\mathbf{L}^{T}\mathbf{F}^{-T}. \tag{4.48}$$

Finally, we have

$$\frac{\mathrm{d}[\mathbf{n}dS]}{\mathrm{dt}} = [tr(\mathbf{D})\mathbf{I} - \mathbf{L}^{T}]\mathbf{n}dS. \tag{4.49}$$

Next, we find with some effort that

$$\frac{\mathrm{d}\mathbf{n}}{\mathrm{dt}} = \frac{\mathrm{d}\mathbf{F}^{-\mathbf{T}}}{\mathrm{dt}}\frac{\mathbf{n}_0}{\sqrt{\mathbf{n}_0^{\mathbf{T}}\mathbf{C}^{-\mathbf{1}}\mathbf{n}_0}} - \frac{\mathbf{F}^{-\mathbf{T}}\mathbf{n}_0}{\sqrt{\mathbf{n}_0^{\mathbf{T}}\mathbf{C}^{-\mathbf{1}}\mathbf{n}_0}}\frac{\mathbf{n}_0^{\mathbf{T}}\frac{\mathrm{d}\mathbf{C}^{-\mathbf{1}}}{\mathrm{dt}}\mathbf{n}_0}{\mathbf{n}_0^{\mathbf{T}}\mathbf{C}^{-\mathbf{1}}\mathbf{n}_0}$$

$$= [(\mathbf{n}^{\mathbf{T}}\mathbf{D}\mathbf{n})\mathbf{I} - \mathbf{L}^{\mathbf{T}}]\mathbf{n}. \tag{4.50}$$

4.5 ROTATION TENSOR

Elementary manipulation furnishes

$$\begin{aligned} d\mathbf{u} &= \frac{d\mathbf{u}}{d\mathbf{X}} d\mathbf{X} \\ &= [\boldsymbol{E}_{\mathrm{L}} + \boldsymbol{\omega}] d\mathbf{X}, \end{aligned} \tag{4.51}$$

in which the antisymmetric rotation tensor $\boldsymbol{\omega}$ appears:

$$\boldsymbol{\omega} = \frac{1}{2}\left[\frac{\partial \mathbf{u}}{\partial \mathbf{X}} - \left(\frac{\partial \mathbf{u}}{\partial \mathbf{X}}\right)^{\mathrm{T}}\right]. \tag{4.52}$$

Consider pure rotation with small angle θ:

$$\begin{aligned} \mathbf{x} &= \begin{bmatrix} \cos\theta & \sin\theta & 0 \\ -\sin\theta & \cos\theta & 0 \\ 0 & 0 & 1 \end{bmatrix} \mathbf{X} \\ &\approx \begin{bmatrix} 1-\frac{\theta^2}{2} & \theta & 0 \\ -\theta & 1-\frac{\theta^2}{2} & 0 \\ 0 & 0 & 1 \end{bmatrix} \mathbf{X}, \end{aligned} \tag{4.53}$$

thus,

$$\mathbf{u} = \begin{bmatrix} -\frac{\theta^2}{2} & 0 & 0 \\ 0 & -\frac{\theta^2}{2} & 0 \\ 0 & 0 & 0 \end{bmatrix} \mathbf{X} + \begin{bmatrix} 0 & \theta & 0 \\ -\theta & 0 & 0 \\ 0 & 0 & 0 \end{bmatrix} \mathbf{X} \tag{4.54}$$

$$\boldsymbol{E}_L = \begin{bmatrix} -\frac{\theta^2}{2} & 0 & 0 \\ 0 & -\frac{\theta^2}{2} & 0 \\ 0 & 0 & 0 \end{bmatrix}, \quad \boldsymbol{\omega} = \begin{bmatrix} 0 & \theta & 0 \\ -\theta & 0 & 0 \\ 0 & 0 & 0 \end{bmatrix}. \tag{4.55}$$

Evidently, the normal strains do not vanish, but are second-order in θ, while $\boldsymbol{\omega}$ is first-order in θ. Under the assumption of small deformation, nonlinear terms are neglected so that $\mathbf{E}_{\mathrm{L}}$ is regarded as vanishing.

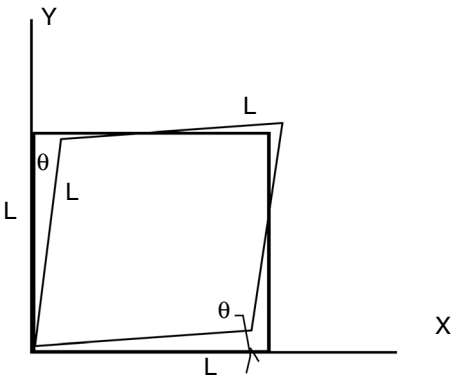

FIGURE 4.4 Element in undeformed and deformed configurations.

Consider as a second example the following derivation in which the sides of the unit square rotate toward each other by 2θ.

The deformation can be described by the relations

$$\begin{aligned} x &= (1-\cos\theta)X + \sin\theta Y \approx \left[1-\frac{\theta^2}{2}\right]X + \theta Y \\ y &= \sin\theta X + (1-\cos\theta)Y \approx \theta X + \left[1-\frac{\theta^2}{2}\right]Y, \end{aligned} \tag{4.56}$$

from which we conclude that

$$\boldsymbol{E}_L = \begin{bmatrix} -\frac{\theta^2}{2} & \theta & 0 \\ \theta & -\frac{\theta^2}{2} & 0 \\ 0 & 0 & 0 \end{bmatrix}. \tag{4.57}$$

Upon neglecting quadratic terms, we conclude that linear-shear strain is a measure of how much the axes rotate toward each other, while the rotation tensor is a measure of how much the axes rotate in the same sense.

4.6 COMPATIBILITY CONDITIONS FOR E_L AND D

The following paragraphs present the compatibility equations for the linear-strain tensor, allowing $\boldsymbol{E}_L$ to be integrated to produce a displacement field $\mathbf{u}(\mathbf{X})$, which is unique to within a rigid-body motion. It should be evident that a parallel argument produces exactly the same result for the velocity vector $\mathbf{v}(\mathbf{x})$ starting from a given deformation-rate tensor $\mathbf{D}(\mathbf{x})$.

There are two major "paths" to solutions of problems in continuum mechanics. For example,

Assume/approximate **u**. Apply the strain-displacement relations to estimate ***E***, apply the stress-strain relations to estimate ***S***, and then apply equilibrium relations to obtain the field equation. Solve the field equation applying boundary conditions and constraints.

Assume/approximate ***S***, and then estimate ***E*** using the strain-displacement relations. Apply compatibility relations to obtain the field equation, and then solve the field equation and boundary conditions and constraints.

To understand the second solution path, we focus on the following compatibility relation. Suppose the linear strains are known as functions of the position **X**. Under what circumstances can the strain-displacement relations be integrated to produce a displacement field that is unique to within a rigid-body displacement? Recall that

$$\begin{aligned} \mathrm{d}\mathbf{u} &= \frac{\mathrm{d}\mathbf{u}}{\mathrm{d}\mathbf{X}}\mathrm{d}\mathbf{X} \\ &= [\boldsymbol{E}_{\mathrm{L}} + \boldsymbol{\omega}]\mathrm{d}\mathbf{X} \end{aligned} \tag{4.58}$$

Evidently, $\boldsymbol{E}_{\mathrm{L}}$ is only part of the derivative of **u**. In 2-D rectilinear coordinates, we will see that the compatibility equation, guaranteeing unique **u** to within a rigid-body motion, is given by:

$$\frac{\partial^2 E_{12}}{\partial x_1 \partial x_2} = \frac{1}{2}\left[\frac{\partial^2 E_{11}}{\partial x_2^2} + \frac{\partial^2 E_{22}}{\partial x_1^2}\right] \tag{4.59}$$

The proof of the compatibility equation is as follows. We consider a path in the physical (X_1, X_2, X_3) space, along which the arc length is denoted by λ. Accordingly, the position vector **X** is a function of λ. The integral of $d\mathbf{u}$, taken from $\lambda = 0$ to λ^* is

$$\begin{aligned} \mathbf{u}(\mathbf{X}(\lambda^*)) &= \mathbf{u}(0) + \int_0^{\mathbf{X}(\lambda^*)} \frac{d\mathbf{u}}{d\mathbf{X}} d\mathbf{X} \\ &= \mathbf{u}(0) + \int_0^{\mathbf{X}(\lambda^*)} \boldsymbol{E}(\mathbf{X}(\lambda^*)) d\mathbf{X} + \int_0^{\mathbf{X}(\lambda\lambda^*)} \boldsymbol{\omega}(\mathbf{X}) d\mathbf{X}. \end{aligned} \tag{4.60}$$

The term $\mathbf{u}(0)$ can be interpreted as the rigid-body translation. The first integral can be evaluated since $\boldsymbol{E}(\mathbf{X})$ and $\mathbf{X}(\lambda)$ are given functions. The second integral can be rewritten using an elementary transformation as

$$\int_0^{\mathbf{X}(\lambda^*)} \boldsymbol{\omega}(\mathbf{X})\mathrm{d}\mathbf{X} = -\int_{\mathbf{X}(\lambda^*)}^{0} \boldsymbol{\omega}(\mathbf{X}^* - \mathbf{X})\mathrm{d}(\mathbf{X}^* - \mathbf{X}). \tag{4.61}$$

Note the following:

$$d[\boldsymbol{\omega}(\mathbf{X})(\mathbf{X}^* - \mathbf{X})] = \boldsymbol{\omega}(\mathbf{X})d(\mathbf{X}^* - \mathbf{X}) + [(\mathbf{X}^* - \mathbf{X})^T d\boldsymbol{\omega}^T(\mathbf{X}^* - \mathbf{X})]^T$$
$$= \boldsymbol{\omega}(\mathbf{X})d(\mathbf{X}^* - \mathbf{X}) - [(\mathbf{X}^* - \mathbf{X})^T d\boldsymbol{\omega}(\mathbf{X}^* - \mathbf{X})]^T$$
$$= \boldsymbol{\omega}(\mathbf{X})d(\mathbf{X}^* - \mathbf{X}) - \left[(\mathbf{X}^* - \mathbf{X})^T \frac{d\boldsymbol{\omega}(\mathbf{X}^* - \mathbf{X})}{d(\mathbf{X}^* - \mathbf{X})} d(\mathbf{X}^* - \mathbf{X})\right]^T. \tag{4.62}$$

Consequently, integration by parts furnishes

$$-\int_{\mathbf{X}(\lambda^*)}^{0} \boldsymbol{\omega}(\mathbf{X})d(\mathbf{X}^* - \mathbf{X}) = \boldsymbol{\omega}(\mathbf{X}(0))(\mathbf{X}(\lambda^*) - \mathbf{X}(0))$$
$$+\left[\int_{\mathbf{X}(\lambda^*)-\mathbf{X}(0)}^{0} (\mathbf{X}^* - \mathbf{X})^T \frac{d\boldsymbol{\omega}(\mathbf{X}^* - \mathbf{X})}{d(\mathbf{X}^* - \mathbf{X})} d(\mathbf{X}^* - \mathbf{X})\right]^T. \tag{4.63}$$

The term $\boldsymbol{\omega}(\mathbf{X}(0))(\mathbf{X}(\lambda^*) - \mathbf{X}(0))$ can be identified as a rigid-body rotation since the rotation tensor $\boldsymbol{\omega}(\mathbf{X}(0))$ is independent of position. We now focus on the second term. Now that rigid-body translation and rotation have been accommodated, the integral should give a unique value regardless of the path. Consider two paths, path 1 and path 2, from $\lambda = 0$ to λ^*. The integral over these paths should produce the same unique values. Therefore, the closed path 0 to λ^* along path 1 followed by λ^* to 0 in a negative sense along path 2 should vanish. Furthermore, path 1 and path 2 are arbitrary, except for terminating at the same points. It follows that along any closed path

$$\oint (\mathbf{X}^* - \mathbf{X})^T \frac{d\boldsymbol{\omega}(\mathbf{X}^* - \mathbf{X})}{d(\mathbf{X}^* - \mathbf{X})} d(\mathbf{X}^* - \mathbf{X}) = \mathbf{0}^T. \tag{4.64}$$

Let us now write $\boldsymbol{\omega}(\mathbf{X})$ as $\boldsymbol{\omega}(\mathbf{X}) = \{\boldsymbol{\omega}_1(\mathbf{X}) \quad \boldsymbol{\omega}_2(\mathbf{X}) \quad \boldsymbol{\omega}_3(\mathbf{X})\}$, in which $\boldsymbol{\omega}_i$ denotes the vector corresponding to the i^{th} column of $\boldsymbol{\omega}$. The compatibility condition can now be written as

$$\oint (\mathbf{X}^* - \mathbf{X})^T \frac{d\boldsymbol{\omega}_j(\mathbf{X}^* - \mathbf{X})}{d(\mathbf{X}^* - \mathbf{X})} d(\mathbf{X}^* - \mathbf{X}) = 0, \quad j = 1,2,3. \tag{4.65}$$

For a suitable differential function $\Psi(\mathrm{X})$, the condition for $\oint \boldsymbol{\Psi} \cdot \mathrm{d}\mathbf{X} = 0$ over an arbitrary contour is that the curl of Ψ vanishes, from which we express the compatibility conditions as

$$\nabla \times \left[(\mathbf{X}^* - \mathbf{X})^{\mathbf{T}} \frac{d\boldsymbol{\omega}_j(\mathbf{X})}{d(\mathbf{X}^* - \mathbf{X})}\right] = 0, \quad j = 1,2,3. \tag{4.66}$$

This can be expanded at considerable effort to derive 81 compatibility equations, including Equation 4.59.

4.7 SAMPLE PROBLEMS

1. Referring to Figure 4.5, determine **u**, **F**, J, and $\boldsymbol{E}$ as functions of **X** and **Y**. Use $H = 1.0$, $W = 1.0$, $a = 0.1$, $b = 0.1$, $c = 0.3$, $d = 0.2$, $e = 0.2$, $f = 0.1$. Assume a unit thickness in the Z-direction in both the deformed and undeformed configurations.

Solution: Since straight sides are deformed into straight sides, the deformation pattern can be assumed in the form

$$x = \alpha X + \beta Y + \gamma XY \qquad y = \delta X + \varepsilon Y + \zeta XY,$$

and it is necessary to determine α, β, γ, δ, ε, and ζ from the coordinates of the vertices in the deformed configuration.

$$\text{At } (X,Y) = (W,0) \quad : \quad W + a = \alpha W \qquad\qquad b = \delta W$$

$$\text{At } (X,Y) = (0,H) \quad : \quad e = \beta H \qquad\qquad H + f = \varepsilon H$$

$$\text{At } (X,Y) = (W,H) \quad : \quad W + c = \alpha H + \beta H + \gamma WH \qquad H + d = \delta W + \varepsilon H + \zeta WH$$

After elementary manipulation,

$$\alpha = 1 + \frac{a}{W} = 1.1 \qquad \beta = \frac{e}{H} = 0.2 \qquad \delta = \frac{b}{W} = 0.1$$

$$\varepsilon = 1 + \frac{f}{H} = 1.2 \qquad \gamma = \frac{W + c - (W + a) - e}{WH} = 0.4 \qquad \zeta = \frac{H + d - b - (H + f)}{WH} = 0.$$

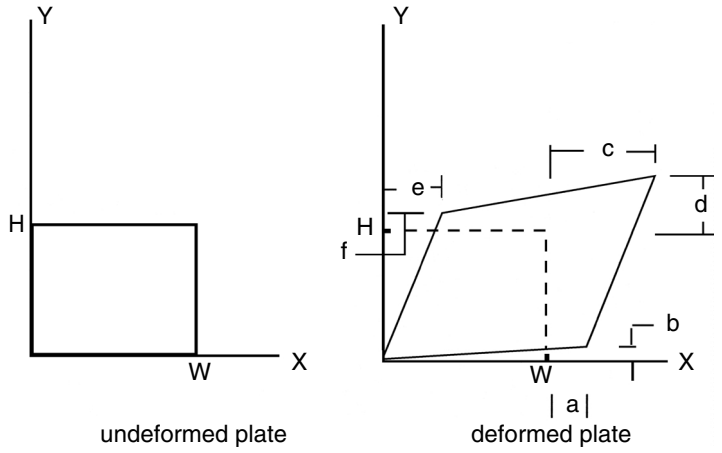

FIGURE 4.5 Plate elements in undeformed and deformed states.

The 2×2 deformation gradient tensor $\mathbf{F}$ and its determinant are now:

$$\mathbf{F} = \begin{bmatrix} \alpha + \gamma Y & \beta + \gamma X \\ \delta + \zeta Y & \varepsilon + \zeta X \end{bmatrix} = \begin{bmatrix} 1.1 + 0.4Y & 0.2 + 0.4X \\ 0.1 & 1.2 \end{bmatrix}.$$

$$J = 1.3 + 0.48Y - 0.04X$$

The displacement vector is

$$\mathbf{u} = \begin{pmatrix} x - X \\ y - Y \end{pmatrix} = \begin{pmatrix} (\alpha - 1)X + \beta Y + \gamma XY \\ \delta X + (\varepsilon - 1)Y + \zeta XY \end{pmatrix} = \begin{pmatrix} 0.1X + 0.2Y + 0.4XY \\ 0.1X + 0.2Y \end{pmatrix}.$$

The Lagrangian strain $\boldsymbol{E} = \frac{1}{2}[\mathbf{F}^{\mathrm{T}}\mathbf{F} - \mathbf{I}]$ is

$$\boldsymbol{E} = \frac{1}{2}\begin{bmatrix} 1.1 + 0.4Y & 0.1 \\ 0.2 + 0.4X & 1.2 \end{bmatrix}\begin{bmatrix} 1.1 + 0.4Y & 0.2 + 0.4X \\ 0.1 & 1.2 \end{bmatrix} - \frac{1}{2}\begin{bmatrix} 1 & 0 \\ 0 & 1 \end{bmatrix}$$

$$= \begin{bmatrix} 0.11 + 0.44Y + 0.08Y^2 & 0.17 + 0.22X + 0.04Y + 0.08XY \\ 0.17 + 0.22X + 0.04Y + 0.08XY & 0.24 + 0.08X + 0.08X^2 \end{bmatrix}$$

2. Figure 4.6 shows a square element at time t and at $t + dt$. Estimate **L**, **D**, and **W** at time t. Use $a = 0.1dt$, $b = 1 + 0.2dt$, $c = 0.2dt$, $d = 1 + 0.4dt$, $e = 0.05dt$, $f = 0.1dt$, $g = 1 - 0.1dt$, $h = 1 + 0.5dt$. Assume a unit thickness in the Z-direction in both the deformed and undeformed configurations.

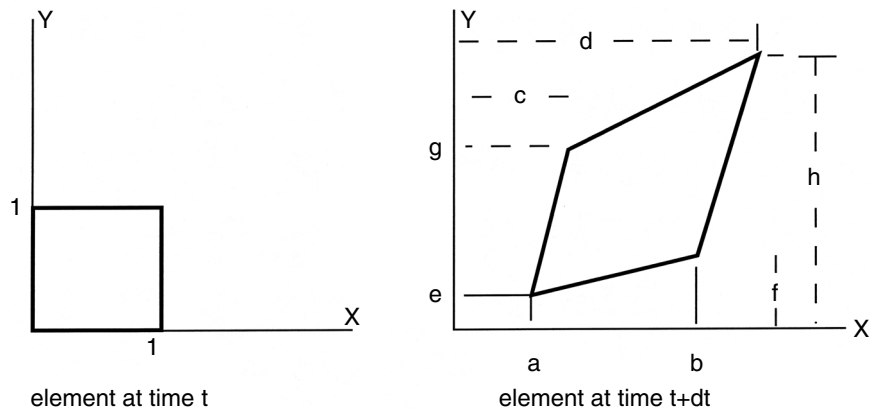

FIGURE 4.6 Element experiencing rigid body motion and deformation.

Solution: First, represent the deformed position vectors in terms of the undeformed position vectors using eight coefficients determined using the given geometry. In particular,

$$x = \alpha + \beta X + \gamma Y + \delta XY \qquad y = \varepsilon + \zeta X + \eta Y + \theta XY.$$

Following procedures analogous to Problem 1, we find:

$$\begin{aligned} \alpha &= 0.1dt & \varepsilon &= 0.05dt \\ \beta &= 1 + 0.2dt & \zeta &= 0.1dt \\ \gamma &= 0.2dt & \eta &= 1 - 0.1dt \\ \delta &= -0.5dt & \theta &= -0.05dt. \end{aligned}$$

The velocities can be estimated using $v_x \approx \frac{x - X}{dt}$ and $v_y \approx \frac{y - Y}{dt}$, from which

$$\begin{aligned} v_x &= 0.1 + 0.2X + 0.2Y - 0.5XY \\ v_y &= 0.05 + 0.1X - 0.1Y - 0.05XY. \end{aligned}$$

The tensors **L**, **D**, and **W** are now readily found as:

$$\mathbf{L} = \begin{bmatrix} 0.2 - 0.5Y & 0.2 - 0.5X \\ 0.1 - 0.05Y & -0.1 - 0.05X \end{bmatrix}$$

$$\mathbf{D} = \begin{bmatrix} 0.2 - 0.5Y & 0.15 - 0.25X - 0.025Y \\ 0.15 - 0.25X - 0.025Y & -0.1 - 0.05X \end{bmatrix}$$

$$\mathbf{W} = \begin{bmatrix} 0 & -0.4 - 0.25X + 0.025Y \\ 0.4 + 0.25X - 0.025Y & 0 \end{bmatrix}.$$

4.8 EXERCISES

1. Consider a one-dimensional deformation in which $x = (1 + \lambda)X$. What value of λ is the linear-strain ε_L error by 5% relative to the Lagrangian strain $\boldsymbol{E}$? Use the error measure

$$\text{error} = \frac{E - E_{\text{L}}}{E}.$$

2. A 1×1 square plate has a constant (2×2) Lagrangian-strain tensor $\boldsymbol{E}$. What is the deformed length of the diagonal? What is the volume change?

If the linear strain $\boldsymbol{E}_{\mathrm{L}}$ is now approximated as $\boldsymbol{E}$, what is the diagonal and what is the volume change? Take

$$\boldsymbol{E} = \begin{pmatrix} 0.1 & 0.05 \\ 0.05 & 0.1 \end{pmatrix}.$$

3. Verify that the expressions in the text for $\mathbf{F}$ and $\boldsymbol{E}$ in cylindrical coordinates are consistent with the equation

$$\mathbf{F} = \mathbf{Q}\,\mathbf{F}', \quad [\mathbf{Q}^{\mathbf{T}}]_{\beta\alpha} = q^{\mathbf{T}}_{\beta\alpha} \quad [\mathbf{F}']_{\alpha\zeta} = \frac{h_\alpha}{H_\zeta}\frac{\partial y_\alpha}{\partial Y_\zeta},$$

in which $\mathbf{Q}$ is the orthogonal tensor representing transformation from the undeformed to the deformed coordinate system, and also with

$$[\boldsymbol{E}]_{ij} = \frac{1}{2}\left[\sum_\beta \left(\frac{h_\beta^2}{H_i H_j}\frac{\partial y_\beta}{\partial Y_i}\frac{\partial y_\beta}{\partial Y_j}\right) - \delta_{ij}\right].$$

4. Obtain expressions for $\mathbf{u}$, $\mathbf{F}$, $\boldsymbol{E}$, and $\boldsymbol{E}_{\mathrm{L}}$ in spherical coordinates.
5. For cylindrical coordinates, determine the Lagrangian strain in the following two cases:

   (*a*) Pure radial expansion: $r = \lambda R, \quad \theta = \Theta, \quad z = Z$

   (*b*) Torsion: $r = R, \quad \theta = \Theta + \lambda Z, \quad z = Z$

6. In spherical coordinates, determine the Lagrangian strain for pure radial expansion.

$$r = \lambda R, \quad \theta = \Theta, \quad \phi = \Phi$$

7. Obtain $\mathbf{v}$, $\mathbf{L}$, $\mathbf{D}$, and $\mathbf{W}$ in spherical coordinates.
8. For cylindrical coordinates, find $\mathbf{L}$, $\mathbf{D}$, and $\mathbf{W}$ for the following flows:

   (a) pure radial flow: $v_r = f(r), \quad v_\theta = 0, \quad v_z = 0$

   (b) pipe flow: $v_r = 0, \quad v_\theta = 0, \quad v_z = f(r)$

   (c) cylindrical flow: $v_r = 0, \quad v_\theta = f(r), \quad v_z = 0$

   (d) torsional flow: $v_r = 0, \quad v_\theta = f(z), \quad v_z = 0$

9. In spherical coordinates, find $\mathbf{L}$, $\mathbf{D}$, and $\mathbf{W}$ for pure radial expansion:

$$v_r = f(r), \quad v_\theta = 0, \quad v_\phi = 0$$

10. For linear strain in rectilinear coordinates and 2-D, the compatibility relation is

$$\frac{\partial^2 E_{12}}{\partial x_1 \partial x_2} = \frac{1}{2}\left[\frac{\partial^2 E_{11}}{\partial x_2^2} + \frac{\partial^2 E_{22}}{\partial x_1^2}\right].$$

Find the implications of this relation for a linear-strain field assumed to be given by

$$E_{11} = a_1 X^2 + a_2 XY + a_3 Y^2$$

$$E_{22} = b_1 X^2 + b_2 XY + b_3 Y^2$$

$$E_{12} = c_1 X^2 + c_2 XY + c_3 Y^2.$$

11. Consider a square $L \times L$ plate (undeformed configuration) with linear strains

$$E_{11} = a_1 + a_2 X + a_3 Y$$

$$E_{22} = b_1 + b_2 X + b_3 Y$$

$$E_{12} = c_1 + c_2 X + c_3 Y.$$

Assuming that the origin does not move, find the deformed position of $(X, Y) = (L, L)$.

5 Mechanical Equilibrium and the Principle of Virtual Work

5.1 TRACTION AND STRESS

5.1.1 Cauchy Stress

Consider a differential tetrahedron enclosing the point x in the deformed configuration. The area of the inclined face is dS, and dS_i is the area of the face whose exterior normal vector is $-\mathbf{e}_i$. Simple vector analysis serves to derive that $n_i = dS_i/dS$ (see Exercise 1 in Chapter 1). Next, let $d\mathbf{P}$ denote the force on a surface element dS, and let $d\mathbf{P}^{(i)}$ denote the force on area dS_i. The traction vector is introduced by $\boldsymbol{\tau} = d\mathbf{P}/dS$. As the tetrahedron shrinks to a point, the contribution of volume forces, such as inertia, decays faster than surface forces. Balance of forces on the tetrahedron now requires that

$$dP_j = \sum_i dP_j^i. \tag{5.1}$$

The traction vector acting on the inclined face is defined by

$$\boldsymbol{\tau} = \frac{d\mathbf{P}}{dS}, \tag{5.2}$$

from which

$$\begin{aligned} \tau_j &= \sum_i \frac{dP_j^{(i)}}{dS} \\ &= \sum_i \frac{dP_j^{(i)}}{dS_i}\frac{dS_i}{dS} \\ &= T_{ij}n_i. \end{aligned} \tag{5.3}$$

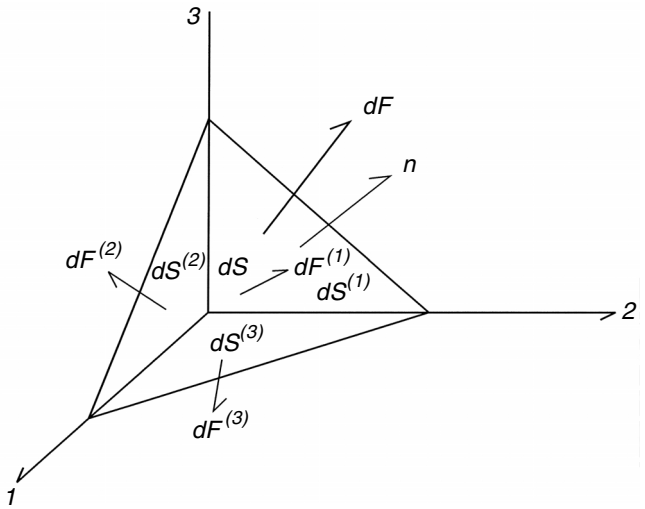

FIGURE 5.1 Equilibrium of a tetrahedron.

with

$$T_{ij} = \frac{dP_j^{(i)}}{dS_i}. \tag{5.4}$$

It is readily seen that T_{ij} can be interpreted as the intensity of the force acting in the j direction on the facet pointing in the $-i$ direction, and is recognized as the ij^{th} entry of the Cauchy stress $\boldsymbol{T}$. In matrix-vector notation, the stress-traction relation is written as

$$\boldsymbol{\tau} = \boldsymbol{T}^{\mathrm{T}}\mathbf{n}. \tag{5.5}$$

The next section will show that $\boldsymbol{T}$ is symmetric by virtue of the balance of angular momentum. Equation 5.5 implies that $\boldsymbol{T}^{\mathrm{T}}$ is a tensor, thus, it follows that $\boldsymbol{T}$ is a tensor. To visualize $\boldsymbol{T}$, consider a differential cube. Positive stresses are shown on faces pointing in positive directions, as shown in Figure 5.2.

In traditional depictions, the stresses on the back faces are represented by arrows pointing in negative directions. However, this depiction can be confusing—the arrows actually represent the directions of the traction components. Consider the one-dimensional bar in Figure 5.3. The traction vector $t\mathbf{e}_1$ acts at $x = L$, while the traction vector $-t\mathbf{e}_1$ acts at $x = 0$. At $x = L$, the corresponding stress is $t_{11} = t\mathbf{e}_1 \cdot \mathbf{e}_1 = t$. At $x = 0$, the stress is given by $(-t\mathbf{e}_1) \cdot (\mathbf{e}_1) = t$. Clearly, the stress at both ends, and in fact throughout the bar, is positive (tensile).

We will see later that the stress tensor is symmetric by virtue of the balance of angular momentum.

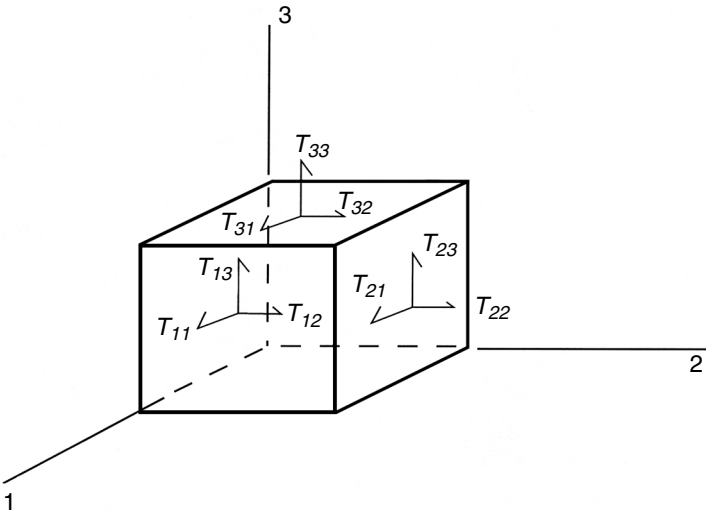

FIGURE 5.2 Illustration of the stress tensor.

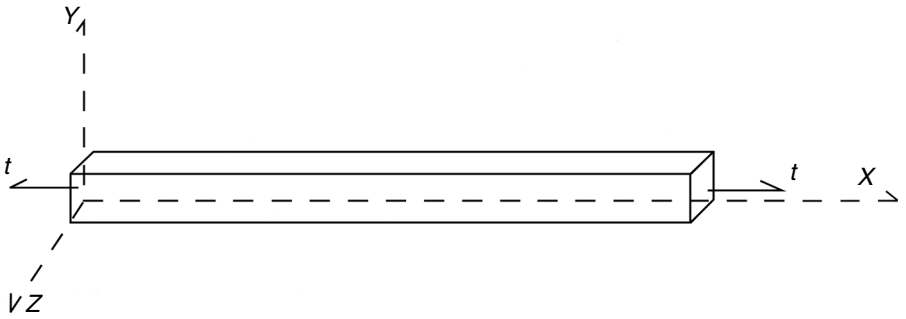

FIGURE 5.3 Tractions on a bar experiencing uniaxial tension.

5.1.2 1st Piola-Kirchhoff Stress

The transformation to undeformed coordinates is now considered. In Chapter 3, we saw that

$$\begin{aligned} \boldsymbol{\tau} dS &= \boldsymbol{T}^{\mathrm{T}} \mathbf{n} dS \\ &= \boldsymbol{T}^{\mathrm{T}} \mathbf{J} \mathbf{F}^{-\mathrm{T}} \mathbf{n}_0 dS_0 \\ &= \bar{\boldsymbol{S}}^{\mathrm{T}} \mathbf{n}_0 dS_0, \qquad \bar{\boldsymbol{S}} = \mathbf{J} \mathbf{F}^{-1} \boldsymbol{T}. \end{aligned} \tag{5.6}$$

$\bar{\boldsymbol{S}}$ is known as the 1st Piola-Kirchhoff stress tensor, and it is not symmetric.

5.1.3 2nd Piola-Kirchhoff Stress

We next derive the stress tensor that is conjugate to the Lagrangian-strain rate, i.e., corresponds to the correct amount of work per unit undeformed volume. At a segment dS at $\mathbf{x}$ on the deformed boundary, assuming static conditions, the rate of work $d\dot{W}$ of the tractions is

$$\begin{aligned} d\dot{W} &= d\mathbf{P}^T\dot{\mathbf{u}} \\ &= \boldsymbol{\tau}^T\dot{\mathbf{u}}\, dS. \end{aligned} \tag{5.7}$$

Over the surface S, shifting to tensor-indicial notation and invoking the divergence theorem, we find

$$\begin{aligned} \dot{W} &= \int \boldsymbol{\tau}^{\mathbf{T}}\dot{\mathbf{u}}\, dS \\ &= \int T_{ij}n_i\dot{u}_j dS \\ &= \int \frac{\partial \dot{u}_j}{\partial x_i} T_{ij}\, dV + \int \dot{u}_j \frac{\partial T_{ij}}{\partial x_i} dV. \end{aligned} \tag{5.8}$$

We will shortly see that static equilibrium implies that $\frac{\partial T_{ij}}{\partial x_i} = 0$, which enables us to conclude that

$$\dot{W} = \int \frac{\partial \dot{u}_j}{\partial x_i} T_{ij}\, dV. \tag{5.9}$$

Returning to matrix-vector notation, since $\frac{\partial \dot{u}_j}{\partial x_i} = [\mathbf{L}]_{ji}$, then

$$\begin{aligned} \dot{\mathrm{W}} &= \int tr(\boldsymbol{T}\mathbf{L}^{\mathbf{T}})\mathrm{dV} \\ &= \int tr[\boldsymbol{T}(\mathbf{D}-\mathbf{W})]\mathrm{dV}, \\ &= \int tr[\boldsymbol{T}\mathbf{D}]\mathrm{dV} \end{aligned} \tag{5.10}$$

since the trace vanishes for the product of a symmetric and antisymmetric tensor.

To convert to undeformed coordinates,

$$\begin{aligned}\dot{\mathrm{W}} &= \int tr(\boldsymbol{T}\mathbf{D})\mathrm{dV} \\ &= \int tr(J\boldsymbol{T}\mathbf{F}^{-1}\dot{\boldsymbol{E}}\mathbf{F}^{-\mathbf{T}})\mathrm{dV}_0 \\ &= \int tr(J\mathbf{F}^{-\mathbf{T}}\boldsymbol{T}\mathbf{F}^{-1}\dot{\boldsymbol{E}})\mathrm{dV}_0 \\ &= \int tr(\boldsymbol{S}\dot{\boldsymbol{E}})\mathrm{dV}, \quad \mathbf{S} = \mathrm{J}\mathbf{F}^{-\mathbf{T}}\boldsymbol{T}\mathbf{F}^{-\mathbf{1}}.\end{aligned} \tag{5.11}$$

The tensor $\boldsymbol{S}$ is called the 2nd Piola-Kirchhoff stress tensor. It is symmetric if $\boldsymbol{T}$ is symmetric.

Note that $J\,tr(\boldsymbol{T}\mathbf{L}) = J\,tr(\boldsymbol{T}\dot{\mathbf{F}}\mathbf{F}^{-1}) = J\,tr(\mathbf{F}^{-1}\boldsymbol{T}\dot{\mathbf{F}}) = tr(\bar{S}\dot{\mathbf{F}})$, so that the 1st Piola-Kirchhoff stress is said to be conjugate to the deformation-gradient tensor **F**.

5.2 STRESS FLUX

Consider two deformations, $\mathbf{x}_1$ and $\mathbf{x}_2$, differing only by a rigid body motion:

$$\mathbf{x}_2 = \mathbf{V}(t)\mathbf{x}_1 + \mathbf{b}(t)\,, \tag{5.12}$$

in which $\mathbf{V}(t)$ is orthogonal. A tensor $\mathbf{A}(\mathbf{x})$ is objective (see Eringen) if

$$\mathbf{A}(\mathbf{x}_2) = \mathbf{V}\mathbf{A}(\mathbf{x}_1)\mathbf{V}^{\mathbf{T}}\,. \tag{5.13}$$

It turns out that the matrix of time derivatives of the Cauchy stress, $\dot{\boldsymbol{T}}$, is not objective, while the deformation rate tensor, **D**, is. Thus, if $\boldsymbol{\xi}$ is a fourth-order tensor, a constitutive equation of the form $\dot{\mathbf{T}} = \boldsymbol{\xi}\mathbf{D}$ would be senseless. Instead, the time derivative is replaced with an objective stress flux, as explained in the following. First, note that

$$\mathbf{F}_2 = \mathbf{V}\mathbf{F}_1 \tag{5.14}$$

$$\begin{aligned}\mathbf{L}_2 &= \dot{\mathbf{F}}_2\mathbf{F}_2^{-1} \\ &= [\dot{\mathbf{V}}\mathbf{V}^{\mathbf{T}}\mathbf{V}\mathbf{F}_1 + \mathbf{V}\dot{\mathbf{F}}_1]\mathbf{F}_1^{-1}\mathbf{V}^{\mathbf{T}} \\ &= \boldsymbol{\Omega} + \mathbf{V}\mathbf{L}_1\mathbf{V}^{\mathbf{T}}, \quad \boldsymbol{\Omega} = \dot{\mathbf{V}}\mathbf{V}^{\mathbf{T}}.\end{aligned}$$

The tensor $\boldsymbol{\Omega}$ is antisymmetric since $d\mathbf{I}/dt = \mathbf{0} = \boldsymbol{\Omega} + \boldsymbol{\Omega}^{\mathbf{T}}$.

We seek a stress flux affording the simplest conversion from deformed to undeformed coordinates. Note that

$$\frac{d\boldsymbol{S}}{dt} = \frac{d}{dt}[J\mathbf{F}^{-T}\boldsymbol{T}\mathbf{F}^{-1}]$$
$$= J tr(\mathbf{D})\mathbf{F}^{-T}\boldsymbol{T}\mathbf{F}^{-1} + J\dot{\mathbf{F}}^{-T}\boldsymbol{T}\mathbf{F}^{-1} + J\mathbf{F}^{-T}\dot{\boldsymbol{T}}\mathbf{F}^{-1} + J\mathbf{F}^{-T}\boldsymbol{T}\dot{\mathbf{F}}^{-1}. \tag{5.15}$$

However, $(\mathbf{F}^{-1}\mathbf{F})^{\bullet} = \mathbf{0}$ so that $\dot{\mathbf{F}}^{-1} = -\mathbf{F}^{-1}\dot{\mathbf{F}}\mathbf{F}^{-1}$ and $\dot{\mathbf{F}}^{-T} = -\mathbf{F}^{-T}\dot{\mathbf{F}}^{T}\mathbf{F}^{-T}$. Now,

$$\frac{d\boldsymbol{S}}{dt} = J\mathbf{F}^{-T}\,\mathring{\boldsymbol{T}}\,\mathbf{F}^{-1}, \tag{5.16a}$$

in which

$$\mathring{\boldsymbol{T}} = \dot{\boldsymbol{T}} + tr(\boldsymbol{D})\boldsymbol{T} - \mathbf{L}\boldsymbol{T} - \boldsymbol{T}\mathbf{L}^{T}, \tag{5.16b}$$

is known as the *Truesdell stress flux*. Under pure rotation, $\mathbf{F} = \mathbf{Q}$ and $\dot{\mathbf{S}} = J\mathbf{Q}\,\mathring{\boldsymbol{T}}\,\mathbf{Q}^{T}$.

To prove the objectivity of $\mathring{\boldsymbol{T}}$, note that

$$\mathring{\boldsymbol{T}}_2 = \dot{\boldsymbol{T}}_2 + \boldsymbol{T}_2 tr(\mathbf{D}_2) - \mathbf{L}_2\boldsymbol{T}_2 - \boldsymbol{T}_2\mathbf{L}_2^{T}$$
$$= [\mathbf{V}\boldsymbol{T}_1\mathbf{V}^{T}]^{\bullet} + \mathbf{V}\boldsymbol{T}\mathbf{V}^{T} tr(\mathbf{D}_1) - [\mathbf{V}\mathbf{L}_1\mathbf{V}^{T} + \boldsymbol{\Omega}]\mathbf{V}\boldsymbol{T}_1\mathbf{V}^{T} - \mathbf{V}\boldsymbol{T}_1^{T}\mathbf{V}^{T}\left[\mathbf{V}\mathbf{L}_1^{T}\mathbf{V}^{T} - \boldsymbol{\Omega}\right]$$
$$= \mathbf{V}\dot{\boldsymbol{T}}_1\mathbf{V}^{T} + \boldsymbol{\Omega}\mathbf{V}\boldsymbol{T}_1\mathbf{V}^{T} - \mathbf{V}\boldsymbol{T}_1\mathbf{V}^{T}\boldsymbol{\Omega} + \mathbf{V}\boldsymbol{T}_1\mathbf{V}^{T} tr(\mathbf{D}_1)$$
$$- \mathbf{V}\mathbf{L}_1\boldsymbol{T}_1\mathbf{V}^{T} - \mathbf{V}\boldsymbol{T}_1\mathbf{L}_1^{T}\mathbf{V}^{T} - \boldsymbol{\Omega}\mathbf{V}\boldsymbol{T}_1\mathbf{V}^{T} + \mathbf{V}\boldsymbol{T}_1\mathbf{V}^{T}\boldsymbol{\Omega}$$
$$= \mathbf{V}\,\mathring{\boldsymbol{T}}_1\,\mathbf{V}^{T}. \tag{5.16c}$$

The choice of stress flux is not unique. For example, the stress flux given by

$$\overset{\square}{\boldsymbol{T}} = \mathring{\boldsymbol{T}} - \boldsymbol{T} tr(\mathbf{D})$$
$$= \dot{\boldsymbol{T}} - \mathbf{L}\boldsymbol{T} - \boldsymbol{T}\mathbf{L}^{T} \tag{5.17}$$

is also objective, as is the widely used Jaumann stress flux:

$$\overset{\Delta}{\boldsymbol{T}} = \dot{\boldsymbol{T}} + \mathbf{W}\boldsymbol{T} - \boldsymbol{T}\mathbf{W}, \qquad \mathbf{W} = \frac{1}{2}(\mathbf{L} - \mathbf{L}^{T}). \tag{5.18}$$

5.3 BALANCE OF MASS, LINEAR MOMENTUM, AND ANGULAR MOMENTUM

5.3.1 Balance of Mass

Balance of mass requires that the total mass of an isolated body not change. For example,

$$\frac{d}{dt}\int \rho \, dV = 0, \tag{5.19}$$

in which $\rho(\mathbf{x},t)$ is the mass density. Since $dV = JdV_0$, it follows that $\rho J = \rho_0$. In addition,

$$\begin{aligned} 0 &= \frac{d}{dt}(\rho J) \\ &= \frac{\partial}{\partial t}(\rho J) + \frac{\partial}{\partial \mathbf{x}}(\rho J)\mathbf{v}(\mathbf{x},t), \qquad \mathbf{v}(\mathbf{x},t) = \frac{\partial \mathbf{x}}{\partial t}. \end{aligned} \tag{5.20}$$

5.3.2 Rayleigh Transport Theorem

Let $\mathbf{w}(\mathbf{x},t)$ denote a vector-valued function. Conversion of the volume integral from deformed to undeformed coordinates is achieved as

$$\int_V \rho \mathbf{w}(\mathbf{x},t) dV = \int_{V_0} \rho_0 \mathbf{w}(\mathbf{x},t) dV_0 \, . \tag{5.21}$$

The *Rayleigh Transport Theorem* is

$$\frac{d}{dt}\int \rho \mathbf{w}(\mathbf{x},t) dV = \int \rho \left[\frac{d}{dt} \mathbf{w}(\mathbf{x},t) \right] dV = \mathbf{0} \, . \tag{5.22}$$

5.3.3 Balance of Linear Momentum

In a fixed-coordinate system, balance of linear momentum requires that the total force on a body with volume V and surface S be equal to the rate of change of linear momentum:

$$\boldsymbol{P} = \int \boldsymbol{\tau} \, dS = \frac{d}{dt}\int \rho \frac{d\boldsymbol{u}}{dt} dV \, . \tag{5.23}$$

Invoking Equation 5.22 yields

$$\int \boldsymbol{\tau} \, dS = \int \rho \frac{d^2\boldsymbol{u}}{dt^2} dV \, . \tag{5.24}$$

In current coordinates, application of the divergence theorem furnishes the equilibrium equation

$$\int \boldsymbol{\tau} \mathrm{d}S = \int \boldsymbol{T}^{\mathbf{T}} \mathbf{n} \, \mathrm{d}S$$

$$= \int [\nabla^{\mathbf{T}} \boldsymbol{T}^{\mathbf{T}}]^T \mathrm{d}V. \tag{5.25}$$

Equation 5.24 now becomes

$$\int \left[\nabla^{\mathbf{T}} \boldsymbol{T}^{\mathbf{T}} - \rho \frac{\mathrm{d}^2 \mathbf{u}^{\mathrm{T}}}{\mathrm{dt}^2} \right] \mathrm{d}V = \mathbf{0}^{\mathbf{T}}. \tag{5.26}$$

Since this equation applies not only to the whole body, but also to arbitrary subdomains of the body, the argument of the integral in Equation 5.26 must vanish pointwise:

$$\nabla^{\mathbf{T}} \boldsymbol{T}^{\mathbf{T}} = \rho \frac{\mathrm{d}^2 \mathbf{u}^T}{\mathrm{dt}^2}. \tag{5.27}$$

To convert to undeformed coordinates, the 1st Piola-Kirchhoff stress is invoked to furnish

$$\int \bar{\boldsymbol{S}}^{\mathbf{T}} \mathbf{n}_{\mathbf{0}} \mathrm{d}S_0 = \int \rho_0 \frac{\mathrm{d}^2 \mathbf{u}^{\mathbf{T}}}{\mathrm{dt}^2} \mathrm{d}V_0, \tag{5.28}$$

and the divergence theorem furnishes

$$\nabla_0^{\mathbf{T}} \bar{\boldsymbol{S}}^{\mathbf{T}} = \rho_0 \frac{\mathrm{d}^2 \mathbf{u}^{\mathbf{T}}}{\mathrm{dt}^2}, \tag{5.29}$$

in which ∇_o denotes the divergence operator referred to undeformed coordinates. This equation will later be the starting point in the formulation of incremental variational principles.

5.3.4 Balance of Angular Momentum

Assuming that only surface forces are present, relative to the origin, the total moment of the traction is equal to the rate of change of angular momentum:

$$\int \boldsymbol{x} \times \boldsymbol{\tau} \, dS = \frac{d}{dt} \int \boldsymbol{x} \times \rho \dot{\boldsymbol{x}} \, dV. \tag{5.30}$$

To examine this principle further, it is convenient to use tensor-indicial notation. First, note using the divergence theorem that

$$\begin{aligned}\int \boldsymbol{x} \times \boldsymbol{\tau} dS &= \int \varepsilon_{ijk} x_j \boldsymbol{\tau}_k dS \\ &= \int \varepsilon_{ijk} x_j T_{lk} n_l \, dS \\ &= \int \frac{\partial}{\partial x_l} (\varepsilon_{ijk} x_j T_{lk}) dV \\ &= \int \varepsilon_{ijk} \delta_{jl} T_{lk} dV + \int \varepsilon_{ijk} x_j \frac{\partial}{\partial x_l} T_{lk} \, dV \\ &= \int \varepsilon_{ijk} T_{jk} dV + \int \varepsilon_{ijk} x_j \frac{\partial}{\partial x_l} T_{lk} \, dV. \end{aligned} \tag{5.31}$$

Continuing,

$$\begin{aligned}\frac{d}{dt} \int \mathbf{x} \times \rho \dot{\mathbf{x}} \, dV &= \int \mathbf{x} \times \rho \ddot{\mathbf{x}} \, dV + \int \dot{\mathbf{x}} \times \rho \dot{\mathbf{x}} \, dV \\ &= \int \mathbf{x} \times \rho \ddot{\mathbf{x}} \, dV \\ &= \int \varepsilon_{ijk} x_j \rho \ddot{x}_k dV. \end{aligned} \tag{5.32}$$

Balance of angular momentum can thus be restated as

$$0 = \int \varepsilon_{ijk} T_{jk} dV + \int \varepsilon_{ijk} x_j \left[\frac{\partial}{\partial x_l} T_{lk} - \rho \ddot{x}_k \right] dV \, . \tag{5.33}$$

The second term vanishes by virtue of balance of linear momentum (see Equation 5.27), leaving

$$\varepsilon_{ijk} T_{jk} = 0 \, , \tag{5.34}$$

which implies that $\boldsymbol{T}$ is symmetric: $\boldsymbol{T} = \boldsymbol{T}^{\mathrm{T}}$ (see exercises in Chapter 1). It follows from Equation 5.6 and Equation 5.11 that $\boldsymbol{S}$ is also symmetric, but that $\overline{\boldsymbol{S}}$ is not symmetric.

5.4 PRINCIPLE OF VIRTUAL WORK

The balance of linear and angular momentum leads to auxiliary variational principles that are fundamental to the finite-element method. Variational methods were introduced in Chapter 3. We recall the balance of linear momentum in rectilinear coordinates as

$$\frac{\partial}{\partial x_l} T_{kl} - \rho \ddot{u}_k = 0\,, \tag{5.35}$$

and $T_{lk} = T_{kl}$ by virtue of the balance of angular momentum. We have tacitly assumed that $\ddot{x} = \ddot{u}_k$, which is to say that deformed positions are referred to a coordinate system that does not translate or rotate. A variational principle is sought from

$$\int \delta u_k \left[\frac{\partial}{\partial x_l} T_{kl} - \rho \ddot{u}_k \right] dV = 0\,, \tag{5.36}$$

in which δu_k is an admissible variation of u_k. Consider the spatial dependence of u_k to be subject to variation, but not the temporal dependence. For example, if u_k can be represented, at least locally, as

$$\mathbf{u} = \mathbf{N}^{\mathbf{T}}(\mathrm{x})\boldsymbol{\gamma}(\mathrm{t})\,, \tag{5.37a}$$

then

$$\delta \mathrm{u}_{\mathrm{k}} = [\mathbf{N}^{\mathbf{T}}(\mathbf{x})]_{\mathrm{kl}}\, \delta\gamma_{\mathrm{l}}(\mathrm{t}). \tag{5.37b}$$

The second term in the variational equation remains as $-\int \delta u_k \rho \ddot{u}_k dV$. The first term is integrated by parts only once for reasons that will be identified shortly: it becomes $\int \frac{\partial}{\partial x_l}[\delta u_k T_{lk}]dV - \int \frac{\partial \delta u_k}{\partial x_l} T_{lk} dV$. From the divergence theorem,

$$\begin{aligned} \int \frac{\partial}{\partial x_l}[\delta u_k T_{lk}]dV &= \int n_l [\delta u_k T_{lk}]dS \\ &= \int \delta u_k \tau_k dS, \end{aligned} \tag{5.38}$$

which can be interpreted as the virtual work of the tractions on the exterior boundary. Next, since $\boldsymbol{T}$ is symmetric,

$$\begin{aligned} \int \frac{\partial \delta u_k}{\partial x_l} T_{lk} dV &= \int \delta 3_{kl} T_{lk} dV \\ 3_{kl} &= \frac{1}{2}\left[\frac{\partial u_k}{\partial x_l} + \frac{\partial u_l}{\partial x_k} \right], \end{aligned} \tag{5.39}$$

and we call 3_{kl} the Eulerian strain. The term $\int \delta 3_{kl} T_{lk} dV$ can be called the virtual work of the stresses. Next, to evaluate $\int \delta u_k \tau_k dS$, we suppose that the exterior boundary consists of three zones: $S = S_1 + S_2 + S_3$. On S_1, the displacement u_k is prescribed, causing the integral over S_1 to vanish. On S_2, suppose that the traction is prescribed as $\bar{\tau}_k(\mathbf{s})$. The contribution is $\int_{S_2} \delta u_k \bar{\tau}_k(\mathbf{s}) dS$. Finally, on S_3, suppose that $\tau_k = \bar{\tau}_k(\mathbf{s}) - [\mathbf{A}(\mathbf{s})]_{kl} u_l(\mathbf{s})$, thus furnishing $\int_{S_3} \delta u_k \bar{\tau}_k(\mathbf{s}) dS - \int_{S_3} \delta u_k [\mathbf{A}(\mathbf{s})]_{kl} u_l(\mathbf{s}) dS$. The various contributions are consolidated into the *Principle of Virtual Work* (Zienkiewicz and Taylor, 1989) as

$$\int \delta 3_{kl} T_{lk} dV + \int \delta u_k \rho \ddot{u}_k dV = \int_{S_2} \delta u_k \bar{\tau}_k(s) dS + \int_{s_3} \delta u_k \bar{\tau}_k(s) dS - \int_{s_3} \delta u_k [A(s)]_{kl} u_l(s) dS \tag{5.40}$$

Now consider the case in which, as in classical elasticity,

$$T_{lk} = \mathrm{d}_{lkmn} 3_{mn} \qquad \boldsymbol{T} = \boldsymbol{D3}, \tag{5.41}$$

in which d_{lkmn} are the entries of a fourth-order, constant, positive-definite tensor D. The first term in Equation 5.40 now becomes $\delta \int \frac{1}{2} 3_{kl} \mathrm{d}_{lkmn} 3_{mn} \mathrm{d}V$, with a positive-definite integrand. Achieving this outcome is the motivation behind integrating by parts just once. In the language of Chapter 3, u_k is the primary variable and τ_k is the secondary variable: on any boundary point, either u_k or τ_k should be specified, or, more generally, τ_k should be specified as a function of u_k. Finally, application of the interpolation model (see Equation 5.37) and cancellation of $\delta \boldsymbol{\gamma}^{\mathbf{T}}$ furnishes the ordinary differential equation

$$\mathbf{M}\ddot{\boldsymbol{\gamma}} + [\mathbf{K} + \mathbf{H}]\boldsymbol{\gamma} = \mathbf{f}(t)\,, \tag{5.42}$$

in which

$$\begin{aligned} \mathbf{M} &= \int \rho \mathbf{N}(\mathbf{x}) \mathbf{N}^{\mathbf{T}}(\mathbf{x}) dV \qquad & \mathbf{K} &= \int \mathbf{B} \boldsymbol{D} \mathbf{B}^{\mathbf{T}} dV \\ \mathbf{H} &= \int_{S_3} \mathbf{N}(\mathbf{x}) \mathbf{A} \mathbf{N}^{\mathbf{T}}(\mathbf{x}) dV & \mathbf{f}(t) &= \int_{S_2+S_3} \mathbf{N}(\mathbf{s}) \bar{\boldsymbol{\tau}}_k(\mathbf{s}) dS \end{aligned} \tag{5.43}$$

and in which $VEC(\boldsymbol{T}) = \chi VEC(\mathbf{3})$, $\chi = TEN22(\mathrm{D})$. In addition, $VEC(\mathbf{3}) = \mathbf{B}^{\mathbf{T}}(\mathbf{x})\boldsymbol{\gamma}$. **B** is derived from the strain-displacement relations, and **M** is the positive-definite *mass matrix.* **K** is the positive-definite matrix representing the domain contribution to the *stiffness matrix.* **H** is the boundary contribution to the *stiffness matrix*, and **f** is a *consistent force vector.* These notions will be addressed in greater detail in subsequent chapters.

To convert the Principle of Virtual Work to undeformed coordinates,

$$\int \delta u_k \rho \ddot{u}_k dV \to \int \delta u_k \rho_0 \ddot{u}_k dV_0$$
$$\int_{S_2} \delta u_k \bar{\tau}_k(\mathbf{s}) dS + \int_{S_3} \delta u_k \bar{\tau}_k(\mathbf{s}) dS \to \int_{S_{20}} \delta u_k \bar{\tau}_k^0(\mathbf{s}_0) dS_0 + \int_{S_{30}} \delta u_k \bar{\tau}_k^0(\mathbf{s}_0) dS_0, \tag{5.44}$$

using, from Chapter 3,

$$\bar{\tau}_k^0 = \mu \bar{\tau}_k \qquad \mu = J\sqrt{\mathbf{n_0^T C^{-1} n_0}}\,. \tag{5.45}$$

Next,

$$\int_{S_3} \delta u_k [\mathbf{A}(\mathbf{s})]_{kl} u_l(\mathbf{s}) dS \to \int_{S_3} \delta u_k [\mu \mathbf{A}(\mathbf{s})]_{kl} u_l(\mathbf{s}_0) dS_0. \tag{5.46}$$

Some manipulation is required to convert the virtual work of the stresses. Observe that

$$\begin{aligned}
\delta\mathbf{3} &= \frac{1}{2}\left[\frac{\partial \delta \mathbf{u}}{\partial \mathbf{x}} + \left(\frac{\partial \delta \mathbf{u}}{\partial \mathbf{x}}\right)^{\mathbf{T}}\right] \\
&= \frac{1}{2}\left[\frac{\partial \delta \mathbf{u}}{\partial \mathbf{X}}\frac{\partial \mathbf{X}}{\partial \mathbf{x}} + \left(\frac{\partial \delta \mathbf{u}}{\partial \mathbf{X}}\frac{\partial \mathbf{X}}{\partial \mathbf{x}}\right)^{\mathbf{T}}\right] \\
&= \frac{1}{2}[\delta \mathbf{F}\mathbf{F}^{-1} + \mathbf{F}^{-\mathbf{T}}\delta \mathbf{F}^{\mathbf{T}}] \\
&= \mathbf{F}^{-\mathbf{T}}\left[\frac{1}{2}[\mathbf{F}^{\mathbf{T}}\delta \mathbf{F} + \delta \mathbf{F}^{\mathbf{T}}\mathbf{F}]\right]\mathbf{F}^{-1} \\
&= \mathbf{F}^{-\mathbf{T}}\delta \boldsymbol{E}\mathbf{F}^{-1}.
\end{aligned} \tag{5.47}$$

Now

$$\begin{aligned}
\int \delta 3_{kl} T_{lk} dV &= \int tr(\delta \mathbf{3}\mathbf{T}) dV \\
&= \int tr(\mathbf{F}^{-\mathbf{T}}\delta \boldsymbol{E}\mathbf{F}^{-1}\mathbf{T}) J dV_0 \\
&= \int tr(\delta \mathbf{E} J \mathbf{F}^{-1}\boldsymbol{T}\mathbf{F}^{-\mathbf{T}}) dV_0 \\
&= \int tr(\delta \boldsymbol{E}\boldsymbol{S}) dV_0 \\
&= \int \delta E_{ji} S_{ij} dV_0.
\end{aligned} \tag{5.48}$$

Consolidating the terms, the Principle of Virtual Work in undeformed coordinates is

$$\int \delta E_{ji} S_{ij} dV_0 + \int \delta u_k \rho_0 \ddot{u}_k dV_0 = \int_{S_{20}} \delta u_k \bar{\tau}_k^0(s_0) dS_0 + \int_{S_{30}} \delta u_k \bar{\tau}_k^0(s_0) dS_0 - \int_{S_{30}} \delta u_k [\mu \mathbf{A}(\mathbf{s}_0)]_{kl} u_l(s_0) dS_0. \quad (5.49)$$

5.5 SAMPLE PROBLEMS

1. The following plate is subject to the tractions shown. At B, there is a frictionless roller support. Find the reactions at A and B. Assume that the plate has thickness W.

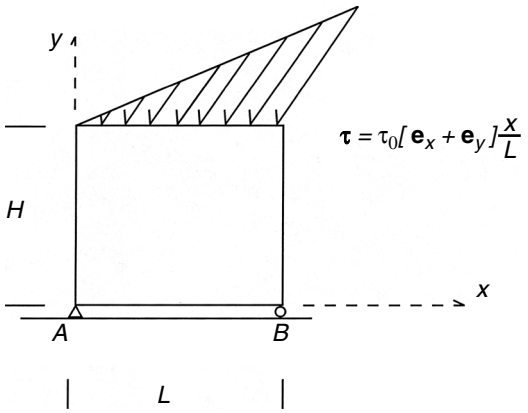

FIGURE 5.4 Plate under traction.

Solution: The reactions are denoted as R_{Ax}, R_{Ay}, R_{Bx}, and R_{By} and are all assumed to be positive. Clearly, $R_{Bx} = 0$. Force equilibrium requires that

$$R_{Ax} - tW\int_0^L \frac{x}{L} dx = 0 \Rightarrow R_{Ax} = \frac{tW}{2L}$$

$$R_{Ay} + R_{By} - tW\int_0^L \frac{x}{L} dx = 0 \Rightarrow R_{Ay} + R_{By} = \frac{tW}{2L}.$$

Balance of moments about A requires that

$$LR_{By} + tW\int_0^L \frac{x^2}{L} dx = 0 \Rightarrow R_{By} = -\frac{tW}{3L}.$$

Accordingly, $R_{Ay} = \frac{5}{6}\frac{tW}{L}$.

2. The figure shows a square plate of uniform thickness W. It experiences Cauchy stresses given by

$$\boldsymbol{T} = \begin{bmatrix} T_{11} & T_{12} & 0 \\ T_{21} & 0 & 0 \\ 0 & 0 & 0 \end{bmatrix}.$$

On diagonal AB, find the total transverse force and moment about A.

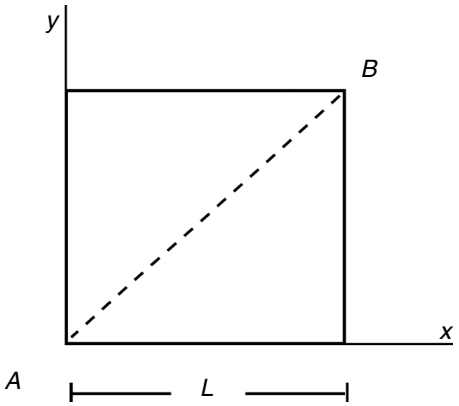

FIGURE 5.5 Plate element under stress.

Solution: The axes are rotated through 45 degrees so that the x-axis coincides with the diagonal (x'-axis). Now,

$$T_{x'x'} = \frac{T_{xx}}{2} + T_{xy} \qquad T_{y'y'} = \frac{T_{xx}}{2} - T_{xy} \qquad T_{x'y'} = -\frac{T_{xx}}{2}.$$

The transverse force is

$$F_{y'} = \left(\frac{T_{xx}}{2} - T_{xy}\right)\sqrt{2}WL.$$

The moment about A is

$$M = \frac{\sqrt{2}}{2} LF_{y'}.$$

3. The plate illustrated has thickness W, width *dx*, and height *dy*. The stresses T_{xz}, T_{yz}, and T_{zz} vanish. Find the equations resulting from balancing forces and moments. In particular, prove that

$$T_{xy} = T_{yx}\,.$$

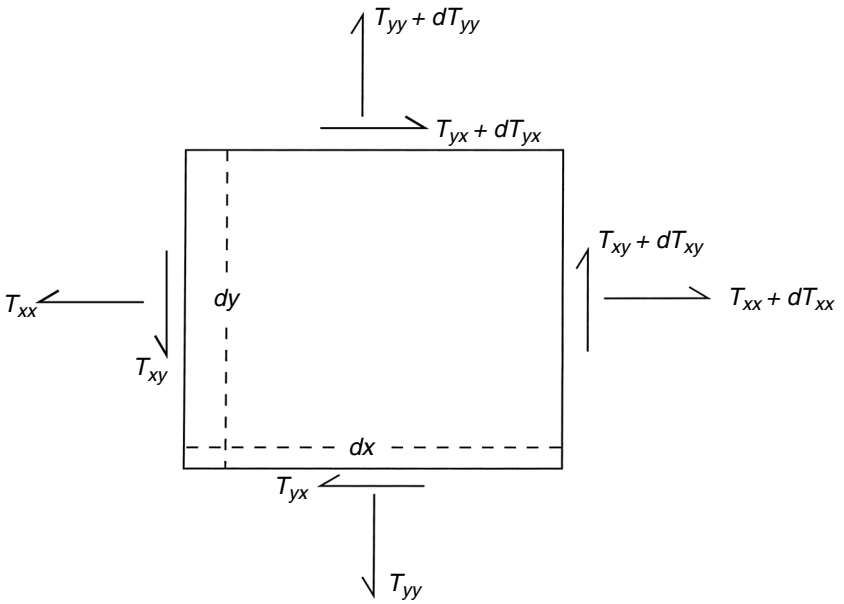

FIGURE 5.6 Moment balance on a plate element under nonuniform stress.

Solution: For the x-direction forces,

$$W\left[T_{xx} + \frac{dT_{xx}}{dx}dx - T_{xx}\right]dy + W\left[T_{yx} + \frac{dT_{yx}}{dy}dy - T_{yx}\right]dx = 0 \Rightarrow \frac{dT_{xx}}{dx} + \frac{dT_{yx}}{dy} = 0\,.$$

For y-direction forces,

$$W\left[T_{xy} + \frac{dT_{xy}}{dx}dx - T_{xy}\right]dy + W\left[T_{yy} + \frac{dT_{yy}}{dy}dy - T_{yy}\right]dx = 0 \Rightarrow \frac{dT_{xy}}{dx} + \frac{dT_{yy}}{dy} = 0\,.$$

For moments about A,

$$-W\left[T_{xx} + \frac{dT_{xx}}{dx}dx - T_{xx}\right]dy\frac{dy}{2} - W\left[T_{yx} + \frac{dT_{yx}}{dy}dy\right]dxdy$$

$$+ W\left[T_{xy} + \frac{dT_{xy}}{dx}dx\right]dydx + W\left[T_{yy} + \frac{dT_{yy}}{dy}dy - T_{yy}\right]dx\frac{dx}{2} = 0.$$

Consequently, neglecting terms of third order in differentials,

$$-WT_{yx}dxdy + WT_{xy}dydx = 0 \Rightarrow T_{xy} = T_{yx}\,.$$

4. At point (0,0,0), the tractions $\boldsymbol{\tau}_1$, $\boldsymbol{\tau}_2$, $\boldsymbol{\tau}_3$ act on planes with normal vectors $\mathbf{n}_1$, $\mathbf{n}_2$, and $\mathbf{n}_3$. Find the Cauchy stress tensor $\boldsymbol{T}$ given

$$\mathbf{n}_1 = \frac{1}{\sqrt{3}}[\mathbf{e}_1 + \mathbf{e}_2 + \mathbf{e}_3] \qquad \boldsymbol{\tau}_1 = \frac{1}{\sqrt{3}}[6\mathbf{e}_1 + 9\mathbf{e}_2 + 15\mathbf{e}_3]$$

$$\mathbf{n}_2 = \frac{1}{\sqrt{3}}[\mathbf{e}_1 + \mathbf{e}_2 - \mathbf{e}_3] \qquad \boldsymbol{\tau}_2 = \frac{1}{\sqrt{3}}[0\mathbf{e}_1 + 1\mathbf{e}_2 + 3\mathbf{e}_3]$$

$$\mathbf{n}_3 = \frac{1}{\sqrt{3}}[\mathbf{e}_1 - \mathbf{e}_2 - \mathbf{e}_3] \qquad \boldsymbol{\tau}_3 = -\frac{1}{\sqrt{3}}[4\mathbf{e}_1 + 5\mathbf{e}_2 + 7\mathbf{e}_3].$$

Solution: This problem requires application of the stress-traction relation. Now

$$\frac{1}{\sqrt{3}}\begin{pmatrix}6\\9\\12\end{pmatrix} = \begin{bmatrix}T_{11} & T_{12} & T_{13}\\ T_{21} & T_{22} & T_{23}\\ T_{31} & T_{32} & T_{33}\end{bmatrix}\frac{1}{\sqrt{3}}\begin{pmatrix}1\\1\\1\end{pmatrix}$$

$$\Rightarrow T_{11} + T_{12} + T_{13} = 6 \quad (1) \quad T_{21} + T_{22} + T_{23} = 9 \quad (2) \quad T_{31} + T_{32} + T_{33} = 1 \quad (3).$$

Similarly,

$$\frac{1}{\sqrt{2}}\begin{pmatrix}3\\5\\7\end{pmatrix} = \begin{bmatrix}T_{11} & T_{12} & T_{13}\\ T_{21} & T_{22} & T_{23}\\ T_{31} & T_{32} & T_{33}\end{bmatrix}\frac{1}{\sqrt{2}}\begin{pmatrix}1\\1\\0\end{pmatrix}$$

$$\Rightarrow T_{11} + T_{12} = 3 \quad (4) \qquad T_{21} + T_{22} = 5 \quad (5) \qquad T_{31} + T_{32} = 7 \quad (6)$$

$$\frac{1}{\sqrt{3}}\begin{pmatrix}-4\\-5\\-6\end{pmatrix} = \begin{bmatrix}T_{11} & T_{12} & T_{13}\\ T_{21} & T_{22} & T_{23}\\ T_{31} & T_{32} & T_{33}\end{bmatrix}\frac{1}{\sqrt{3}}\begin{pmatrix}1\\-1\\-1\end{pmatrix}$$

$$\Rightarrow T_{11} - T_{12} - T_{13} = -4 \quad (7) \qquad T_{21} - T_{22} - T_{23} = -5 \quad (8) \qquad T_{31} - T_{32} - T_{33} = -6 \quad (9)$$

The solution is straightforward. For example, adding (1) and (7) furnishes $T_{11} = 1$, from which (4) implies $T_{12} = 2$.
Solving the equations furnishes us with

$$\boldsymbol{T} = \begin{bmatrix} 1 & 2 & 3 \\ 2 & 3 & 4 \\ 3 & 4 & 5 \end{bmatrix}.$$

5. Given the Cauchy stress $\boldsymbol{T}$, find $\bar{\boldsymbol{S}}$ and $\boldsymbol{S}$ if $\mathbf{x}(t) = \mathbf{Q}(t)\mathbf{X}$, $\mathbf{Q}(t)\mathbf{Q}(t)^{\mathbf{T}} = \mathbf{I}$.

Solution: Clearly $\mathbf{F} = \mathbf{Q}$, thus $J = 1$. Also, $\mathbf{F}^{-\mathbf{T}} = \mathbf{Q}$. It is immediate that $\bar{\boldsymbol{S}} = \mathbf{Q}(\mathrm{t})\boldsymbol{T}$ and $\boldsymbol{S} = \mathbf{Q}(\mathrm{t})\boldsymbol{T}\mathbf{Q}(\mathrm{t})^{\mathbf{T}}$.

5.6 EXERCISES

1. In classical linear elasticity, introduce the isotropic stress and isotropic linear strain as

$$\mathbf{s} = tr(\boldsymbol{S}) \qquad \mathbf{e} = tr(\boldsymbol{E}_{\mathbf{L}}),$$

and introduce the deviatoric stress and strain using

$$\mathbf{s}_{\mathbf{d}} = \mathbf{s} - \frac{1}{3}\mathrm{s}\mathbf{i} \qquad \mathbf{e}_{\mathbf{d}} = \mathbf{e} - \frac{1}{3}es\mathbf{i}.$$

Verify that, if $\dot{\mathbf{s}} = z\mu\dot{\mathbf{e}} + \lambda tr(\boldsymbol{\varepsilon})\mathbf{i}$

$$\mathbf{i}^{\mathbf{T}}\mathbf{s}_{\mathbf{d}} = 0 \qquad \mathbf{i}^{\mathbf{T}}\boldsymbol{e}_{\mathbf{d}} = 0$$

$$\mathbf{s}_{\mathbf{d}} = 2\mu\mathbf{e}_{\mathbf{d}}$$

$$s = (2\mu + 3\lambda)e\ .$$

2. Find the reaction forces in the following problem. There is a frictionless roller support at B.

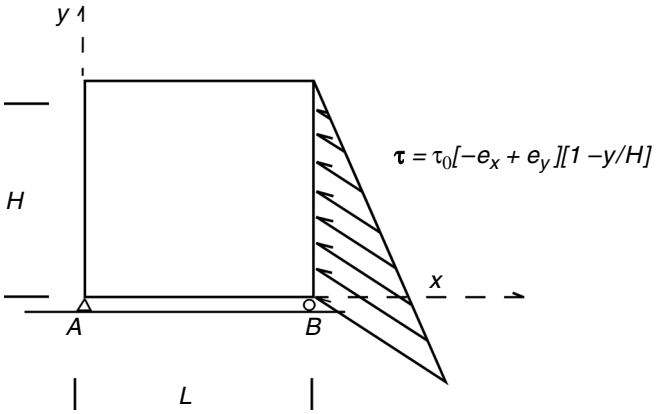

FIGURE 5.7 Plate element under traction.

3. Find the net force and moment about A (thickness = W) on the diagonal in the following plate, given the Cauchy stresses

$$T = \begin{bmatrix} x & y & 0 \\ y & xy & 0 \\ 0 & 0 & 0 \end{bmatrix}.$$

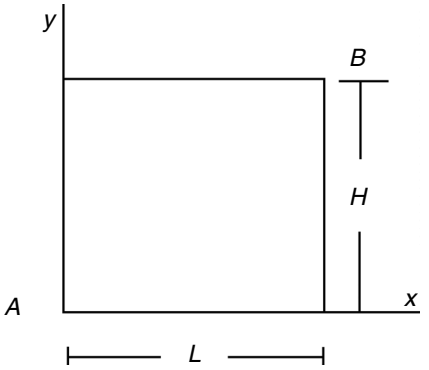

FIGURE 5.8 Plate element experiencing stress.

4. At point (0,0,0), the tractions $\boldsymbol{\tau}_1$, $\boldsymbol{\tau}_2$, $\boldsymbol{\tau}_3$ act on planes with normal vectors $\mathbf{n}_1$, $\mathbf{n}_2$, and $\mathbf{n}_3$. Find the Cauchy stress tensor $\boldsymbol{T}$, given,

$$\mathbf{n}_1 = \frac{1}{\sqrt{3}}[\mathbf{e_1} + \mathbf{e}_2 + \mathbf{e}_3] \qquad \boldsymbol{\tau}_1 = \frac{1}{\sqrt{3}}[2\mathbf{e_1} - 5\mathbf{e}_2 + 6\mathbf{e}_3]$$

$$\mathbf{n}_2 = \frac{1}{\sqrt{2}}[\mathbf{e_1} + \mathbf{e}_2] \qquad \boldsymbol{\tau}_2 = \frac{1}{\sqrt{2}}[\mathbf{e_1} - \mathbf{e}_2 + \mathbf{e}_3]$$

$$\mathbf{n}_3 = \frac{1}{\sqrt{3}}[\mathbf{e_1} - \mathbf{e}_2 - \mathbf{e}_3] \qquad \boldsymbol{\tau}_3 = -\frac{1}{\sqrt{3}}[6\mathbf{e_1} - 1\mathbf{e}_2 + 2\mathbf{e}_3].$$

5. Given the Cauchy stress tensor $\boldsymbol{T}$, find the 1st and 2nd Piola-Kirchhoff stress tensors if $\mathbf{x}(t) = \mathbf{Q}(t)\boldsymbol{\Delta}(t)\mathbf{X}$, in which

$$\boldsymbol{\Delta}(t) = \begin{bmatrix} 1+at & 0 & 0 \\ 0 & 1+bt & 0 \\ 0 & 0 & 1+ct \end{bmatrix}.$$

6. The Cauchy stress tensor is given by

$$\boldsymbol{T} = \begin{bmatrix} T_{11} & T_{12} & 0 \\ T_{12} & T_{22} & 0 \\ 0 & 0 & 0 \end{bmatrix}.$$

Now suppose the 1-2 axes are rotated through $+\theta$ degrees around the z-axis, to furnish $1' - 2'$ axes.
Prove that

$$T_{1'1'} = \frac{T_{11}+T_{22}}{2} + \frac{T_{11}-T_{22}}{2}\cos 2\theta + T_{12}\sin 2\theta$$

$$T_{2'2'} = \frac{T_{11}+T_{22}}{2} - \frac{T_{11}-T_{22}}{2}\cos 2\theta - T_{12}\sin 2\theta$$

$$T_{1'2'} = -\frac{T_{11}-T_{22}}{2}\sin 2\theta + T_{12}\cos 2\theta$$

7. Verify that

$$E_{ij}^{(L)} = \frac{1}{2\mu}\left[T_{ij} - \frac{\lambda}{2\mu+3\lambda}T_{kk}\delta_{ij}\right]$$

is the inverse of $T_{ij} = 2\mu E_{ij}^{(L)} + \lambda E_{kk}^{(L)}\delta_{ij}$.

8. In undeformed coordinates and Kronecker Product (VEC) notation, the 2nd Piola-Kirchhoff stress for incompressible hyperelastic materials can be written as

$$\mathbf{s} = \frac{\partial w'}{\partial \mathbf{e}} = 2\varphi_1'\mathbf{n}_1' + 2\varphi_2'\mathbf{n}_2' - pI_3\mathbf{n}_3 .$$

Find the corresponding expression in deformed coordinates. Derive ψ_1' and ψ_2', in which direct transformation furnishes

$$\mathbf{t} = 2\psi_1'\mathbf{m}_1' + 2\psi_2'\mathbf{m}_2' - p\mathbf{i} .$$

9. Prove that, under uniaxial tension in an isotropic, linearly elastic material, $E_{22} = E_{33}$.
10. Obtain λ in terms of E and ν. (See Problem 7.)
11. The bulk modulus κ is defined by $t_{kk} = 3\kappa e_{kk}^{(L)}$. Obtain κ as a function of E and ν. (See Problem 7.)
12. The 2" × 2" × 2" cube shown in Figure 5.9 is confined on its sides facing the ± x faces by rigid, frictionless walls. The sides facing the ±z faces are free. The top and bottom faces are subjected to a compressive force of 100 lbf. Take E = 10^7 psi and $\nu = 1/3$. Find all nonzero stresses and strains. What is the volume change? What are the principal stresses and strains? What is the maximum shear stress?

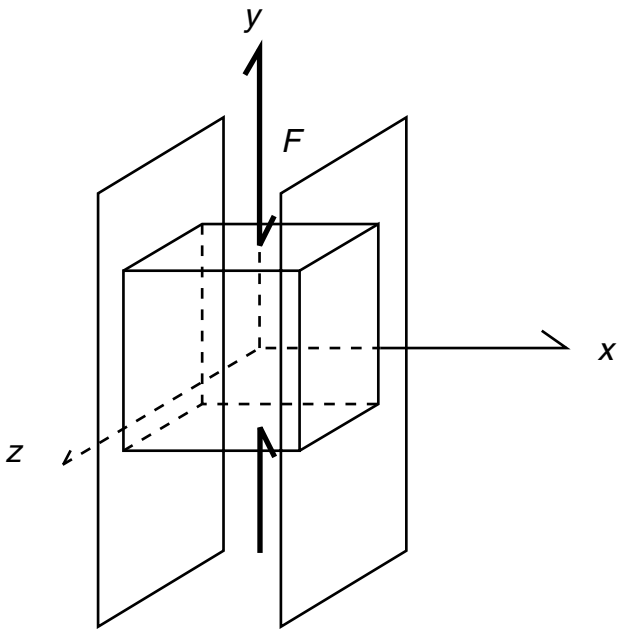

FIGURE 5.9 Strain in a constrained cube.

13. Write out the proof of the Principle of Virtual Work in deformed coordinates.
14. Write out the conversion of the Principle of Virtual Work to undeformed coordinates.
15. Write out the steps whereby the Principle of Virtual Work leads to

$$\mathbf{M}\ddot{\boldsymbol{\gamma}} + [\mathbf{K} + \mathbf{H}]\boldsymbol{\gamma} = \mathbf{f}(t) \ .$$

16. Suppose that $\mathbf{u} = \mathbf{N}^{\mathbf{T}}(\mathbf{x})\boldsymbol{\gamma}(t)$ and assume two dimensions. In 2-D, find $\mathbf{B}^{\mathbf{T}}$ in terms of the derivatives of $\mathbf{N}^{\mathbf{T}}(\mathbf{x})$, in which

$$\begin{pmatrix} 3_{11} \\ 3_{21} \\ 3_{12} \\ 3_{22} \end{pmatrix} = \mathbf{B}^{\mathbf{T}}(\mathbf{x})\boldsymbol{\gamma}(t), \qquad \begin{pmatrix} u_1 \\ u_2 \end{pmatrix} = \mathbf{N}^{\mathbf{T}}(\mathbf{x})\boldsymbol{\gamma}(t)$$

$$\mathbf{N}^{\mathbf{T}}(\mathbf{x}) = \begin{bmatrix} 1 & x & y & 0 & 0 & 0 \\ 0 & 0 & 0 & 1 & x & y \end{bmatrix} \begin{bmatrix} \boldsymbol{\Phi} & \mathbf{0} \\ \mathbf{0} & \boldsymbol{\Phi} \end{bmatrix}.$$

$\boldsymbol{\Phi}$ is a $1 \times n$ constant matrix (row vector); $\boldsymbol{\gamma}$ is $n \times 1$.

6 Stress-Strain Relation and the Tangent-Modulus Tensor

6.1 STRESS-STRAIN BEHAVIOR: CLASSICAL LINEAR ELASTICITY

Under the assumption of linear strain, the distinction between the Cauchy and Piola-Kirchhoff stresses vanishes. The stress is assumed to be given as a linear function of linear strain by the relation

$$T_{ij} = c_{ijkl} E^{(L)}_{kl}, \tag{6.1}$$

in which c_{ijkl} are constants and are the entries of a $3 \times 3 \times 3 \times 3$ fourth-order tensor, $\mathbf{C}$. If $\boldsymbol{T}$ and $\boldsymbol{E}_{\mathbf{L}}$ were not symmetrical, $\mathbf{C}$ might have as many as 81 distinct entries. However, due to the symmetry of $\boldsymbol{T}$ and $\boldsymbol{E}_{\mathbf{L}}$ there are no more than 36 distinct entries. Thermodynamic arguments in subsequent sections will provide a rationale for the *Maxwell* relations:

$$\frac{\partial T_{ij}}{\partial E_{kl}} = \frac{\partial T_{kl}}{\partial E_{ij}}. \tag{6.2}$$

It follows that $c_{ijkl} = c_{klij}$, which implies that there are, at most, 21 distinct coefficients. There are no further arguments from general principles for fewer coefficients. Instead, the number of distinct coefficients is specific to a material, and reflects the degree of symmetry in the material. The smallest number of distinct coefficients is achieved in the case of isotropy, which can be explained physically as follows. Suppose a thin plate of elastic material is tested such that thin strips are removed at several angles and then subjected to uniaxial tension. If the measured stress-strain curves are the same and independent of the orientation at which they are cut, the material is isotropic. Otherwise, it exhibits anisotropy, but may still exhibit limited types of symmetry, such as transverse isotropy or orthotropy. The notion of isotropy is illustrated in Figure 6.1.

In isotropic, linear-elastic materials (which implies linear strain), the number of distinct coefficients can be reduced to two, μ and λ, as illustrated by Lame's equation,

$$T_{ij} = 2\mu E^{(L)}_{ij} + \lambda E^{(L)}_{kk} \delta_{ij}. \tag{6.3}$$

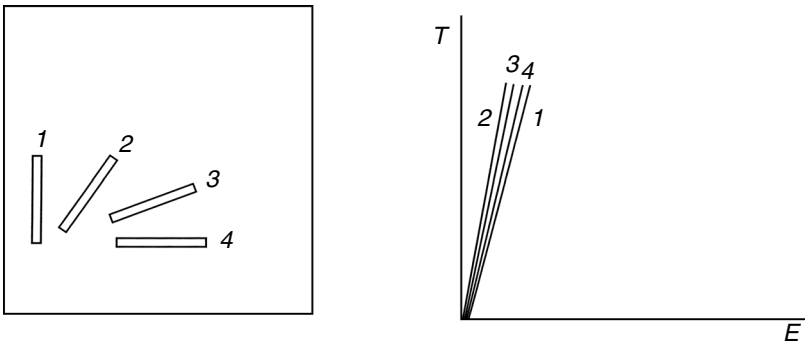

FIGURE 6.1 Illustration of isotropy.

This can be inverted to furnish

$$E_{ij}^{(L)} = \frac{1}{2\mu}\left[T_{ij} - \frac{\lambda}{2\mu+3\lambda}T_{kk}\delta_{ij}\right]. \tag{6.4}$$

The classical elastic modulus E_0 and Poisson's ratio ν represent response *under uniaxial tension only*, provided that $T_{11} = T$, $T_{ij} = 0$. Otherwise,

$$E = \frac{T_{11}}{E_{11}^{(L)}} \qquad \nu = -\frac{E_{22}^{(L)}}{E_{11}^{(L)}} = -\frac{E_{33}^{(L)}}{E_{11}^{(L)}}. \tag{6.5}$$

It is readily verified that

$$\frac{1}{E} = \frac{1}{2\mu}\left[1 - \frac{\lambda}{2\mu+3\lambda}\right] \qquad \frac{\nu}{E} = \frac{1}{2\mu}\frac{\lambda}{2\mu+3\lambda}, \tag{6.6}$$

from which it is immediate that

$$\frac{1}{2\mu} = \frac{1+\nu}{E}, \tag{6.7}$$

Leaving the case of uniaxial tension for the normal (diagonal) stresses and strains, we can write

$$E_{11}^{(L)} = \frac{1}{2\mu}\left[1 - \frac{\lambda}{2\mu+3\lambda}\right]T_{11} - \frac{1}{2\mu}\frac{\lambda}{2\mu+3\lambda}(T_{22}+T_{33})$$

$$= \frac{1}{E}[T_{11} - \nu(T_{22}+T_{33})], \tag{6.8}$$

$$E_{22}^{(L)} = \frac{1}{E}[T_{22} - \nu(T_{33}+T_{11})], \tag{6.9}$$

and

$$E_{33}^{(L)} = \frac{1}{\mathrm{E}}[T_{33} - \nu(T_{11} + T_{22})], \tag{6.10}$$

and the off-diagonal terms satisfy

$$E_{12}^{(L)} = \frac{1+\nu}{\mathrm{E}} T_{12} \qquad E_{23}^{(L)} = \frac{1+\nu}{\mathrm{E}} T_{23} \qquad E_{31}^{(L)} = \frac{1+\nu}{\mathrm{E}} T_{31}. \tag{6.11}$$

6.2 ISOTHERMAL TANGENT-MODULUS TENSOR

6.2.1 Classical Elasticity

Under small deformation, the fourth-order tangent-modulus tensor $\boldsymbol{D}$ in linear elasticity is defined by

$$\mathrm{d}\boldsymbol{T} = \boldsymbol{D}\mathrm{d}\boldsymbol{E}_{\mathbf{L}}. \tag{6.12}$$

In linear isotropic elasticity, the stress-strain relations are written in the Lame's form as

$$\boldsymbol{T} = 2\mu\boldsymbol{E}_{\mathbf{L}} + \lambda tr(\boldsymbol{E}_{\mathbf{L}})\mathbf{I}. \tag{6.13}$$

Using Kronecker Product notation from Chapter 2, this can be rewritten as

$$VEC(\boldsymbol{T}) = [2\mu\mathbf{I}\otimes\mathbf{I} + \lambda\mathbf{i}\mathbf{i}^{\mathbf{T}}]VEC(\boldsymbol{E}_{\mathbf{L}}), \tag{6.14}$$

from which we conclude that

$$\boldsymbol{D} = ITEN22(2\mu\mathbf{I}\otimes\mathbf{I} + \lambda\mathbf{i}\mathbf{i}^{\mathbf{T}}). \tag{6.15}$$

6.2.2 Compressible Hyperelastic Materials

In isotropic hyperelasticity, which is descriptive of compressible rubber elasticity, the 2nd Piola-Kirchhoff stress is taken to be derivable from a strain-energy function that depends on the principal invariants I_1, I_2, I_3 of the Right Cauchy-Green strain tensor:

$$\begin{aligned} &\boldsymbol{S} = \frac{\mathrm{d}w}{\mathrm{d}\boldsymbol{E}} = 2\frac{\mathrm{d}w}{\mathrm{d}\boldsymbol{C}} \quad \boldsymbol{s}^{\mathbf{T}} = \frac{\mathrm{d}w}{\mathrm{d}\boldsymbol{e}} = 2\frac{\mathrm{d}w}{\mathrm{d}\boldsymbol{c}} && \text{(a)} \\ &\boldsymbol{s} = VEC(\boldsymbol{S}) \qquad \boldsymbol{e} = VEC(\boldsymbol{E}) \qquad \boldsymbol{c} = VEC(\boldsymbol{C}). && \text{(b)} \end{aligned} \tag{6.16}$$

Now,

$$\mathbf{s} = 2\phi_i \mathbf{n}_i, \qquad \phi_i = \frac{\partial w}{\partial \mathrm{I}_i}, \qquad \mathbf{n}_i^{\mathrm{T}} = \frac{\partial \mathrm{I}_i}{\partial \boldsymbol{c}}. \tag{6.17}$$

From Chapter 2,

$$\mathbf{n}_1 = \mathbf{i} \qquad \mathbf{n}_2 = I_1\mathbf{i} - \mathbf{c} \qquad \mathbf{n}_3 = VEC(\mathbf{C}^{-1})I_3. \tag{6.18}$$

The tangent-modulus tensor $\boldsymbol{D}_o$, referred to the undeformed configuration, is given by

$$\mathrm{d}\boldsymbol{S} = \boldsymbol{D}_o \mathrm{d}\boldsymbol{E} \qquad \mathrm{d}\boldsymbol{s} = TEN22(\boldsymbol{D}_o)\mathrm{d}\boldsymbol{E}, \tag{6.19}$$

and now

$$TEN22(\boldsymbol{D}_o) = 4\phi_{ij}\mathbf{n}_i\mathbf{n}_j^{\mathrm{T}} + 4\phi_i\mathbf{A}_i, \qquad \mathbf{A}_i = \frac{\mathrm{d}\mathbf{n}_i}{\mathrm{d}\boldsymbol{c}}. \tag{6.20}$$

Finally,

$$\begin{aligned}
\mathbf{A}_1 &= \frac{\mathrm{d}\mathbf{i}}{\mathrm{d}\boldsymbol{c}} = \mathbf{0}^{\mathrm{T}} && \text{(a)}\\
\mathbf{A}_2 &= \frac{\mathrm{d}}{\mathrm{d}\boldsymbol{c}} I_2 \\
&= \frac{\mathrm{d}}{\mathrm{d}\boldsymbol{c}}[I_1\mathbf{i} - \boldsymbol{c}] \\
&= \mathbf{i}\mathbf{i}^{\mathrm{T}} - \mathbf{I}_9 && \text{(b)}\\
\mathbf{A}_3 &= \frac{\mathrm{d}}{\mathrm{d}\mathbf{c}}[VEC(\boldsymbol{C}^{-1})I_3] \\
&= \frac{\mathrm{d}}{\mathrm{d}\boldsymbol{c}}[I_2\mathbf{i} - I_1\boldsymbol{c} + VEC(\boldsymbol{C}^2)] \\
&= \mathbf{i}\mathbf{n}_2^{\mathrm{T}} - \boldsymbol{c}\mathbf{i}^{\mathrm{T}} + \boldsymbol{C} \oplus \boldsymbol{C} \\
&= I_1[\mathbf{i}\mathbf{i}^{\mathrm{T}} - \mathbf{I}_9] - [\mathbf{i}\boldsymbol{c}^{\mathrm{T}} + \boldsymbol{c}\mathbf{i}^{\mathrm{T}}] + \boldsymbol{C} \oplus \boldsymbol{C} && \text{(c)}
\end{aligned} \tag{6.21}$$

In deriving $\mathbf{A}_3$ we have taken advantage of the Cayley-Hamilton theorem (see Chapter 2).

6.3 INCOMPRESSIBLE AND NEAR-INCOMPRESSIBLE HYPERELASTIC MATERIALS

Polymeric materials, such as natural rubber, are often nearly incompressible. For some applications, they can be idealized as incompressible. However, for applications involving confinement, such as in the corners of seal wells, it may be necessary to accommodate the small degree of incompressibility to achieve high accuracy. Incompressibility and near-incompressibility represent *internal constraints*. The principal (e.g., Lagrangian) strains are not independent, and the stresses are not determined completely by the strains. Instead, differences in the principal stresses are determined by differences in principal strains (Oden, 1972). An additional field must be introduced to enforce the internal constraint, and we will see that this internal field can be taken as the hydrostatic pressure (referred to the current configuration).

6.3.1 INCOMPRESSIBILITY

The constraint of incompressibility is expressed by the relation $J = 1$. Now,

$$\begin{aligned} J &= \det \mathbf{F} \\ &= \sqrt{\det^2(\mathbf{F})} \\ &= \sqrt{\det(\mathbf{F})\det(\mathbf{F}^{\mathbf{T}})} \\ &= \sqrt{\det^2(\mathbf{F}^{\mathbf{T}}\mathbf{F})} \\ &= \sqrt{I_3}, \end{aligned} \tag{6.22}$$

and consequently,

$$I_3 = 1. \tag{6.23}$$

The constraint of incompressibility can be enforced using a Lagrange multiplier (see Oden, 1972), denoted here as p. The multiplier depends on $\mathbf{X}$ and is, in fact, the additional field just mentioned. Oden (1972) proposed introducing an augmented strain-energy function, w', similar to

$$w' = w(I_1', I_2') - \frac{1}{2}\, p(I_3 - 1), \qquad I_1' = \frac{I_1}{I_3^{1/3}}, \qquad I_2' = \frac{I_2}{I_3^{2/3}}, \tag{6.24}$$

in which w is interpreted as the conventional strain-energy function, but with dependence on I_3 (=1) removed. I_1' and I_2' are called the deviatoric invariants. For reasons to be explained in a later chapter presenting variational principles, this form serves

to enforce incompressibility, with $\boldsymbol{S}$ now given by

$$\begin{aligned}\boldsymbol{s} &= \frac{\partial w'}{\partial \boldsymbol{e}} \\ &= 2\phi_1'\mathbf{n}_1' + 2\phi_2'\mathbf{n}_2' - p\mathrm{I}_3\mathbf{n}_3 \end{aligned} \tag{6.25}$$

$$\phi_1' = \frac{\partial w}{\partial I_1'} \qquad \phi_2' = \frac{\partial w}{\partial I_2'} \qquad \mathbf{n}_1' = \left[\frac{\partial I_1'}{\partial \boldsymbol{c}}\right]^{\mathbf{T}} \qquad \mathbf{n}_2' = \left[\frac{\partial I_2'}{\partial \boldsymbol{c}}\right]^{\mathbf{T}}.$$

To convert to deformed coordinates, recall that $\boldsymbol{S} = \mathrm{J}\mathbf{F}^{-1}\boldsymbol{T}\mathbf{F}^{-\mathbf{T}}$. It is left to the reader in an exercise to derive ψ_1' and ψ_2' in which

$$\mathbf{t} = VEC(\boldsymbol{T}) = 2\psi_1'\mathbf{m}_1' + 2\psi_2'\mathbf{m}_2' - p\mathbf{i} \tag{6.26}$$

in which $\mathbf{i}^{\mathbf{T}}\mathbf{m}_1' = 0$ and $\mathbf{i}^{\mathbf{T}}\mathbf{m}_2' = 0$. It follows that $p = -tr(\boldsymbol{T})/3$ since

$$\begin{aligned} tr(\boldsymbol{T}) &= \mathbf{i}^{\mathbf{T}}\mathbf{t} \\ &= 2\psi_1'\mathbf{i}^{\mathbf{T}}\mathbf{m}_1' + 2\psi_2'\mathbf{i}^{\mathbf{T}}\mathbf{m}_2' - p\mathbf{i}^{\mathbf{T}}\mathbf{i} \\ &= -\mathbf{i}^{\mathbf{T}}\mathbf{i}p \\ &= -3p. \end{aligned} \tag{6.27}$$

Evidently, the Lagrange multiplier enforcing incompressibility is the "true" hydrostatic pressure.

Finally, the tangent-modulus tensor is somewhat more complicated because d$\boldsymbol{S}$ depends on d$\boldsymbol{E}$ and dp. We will see in subsequent chapters that it should be defined as $\boldsymbol{D}^*$ using

$$TEN22(\boldsymbol{D}^*) = \begin{bmatrix} \dfrac{\mathrm{d}\boldsymbol{s}}{\mathrm{d}\boldsymbol{e}} & \dfrac{\mathrm{d}\boldsymbol{s}}{\mathrm{d}p} \\ -\left(\dfrac{\mathrm{d}\boldsymbol{s}}{\mathrm{d}p}\right)^{\mathbf{T}} & \mathbf{0} \end{bmatrix}$$

$$\begin{aligned} \frac{\mathrm{d}\boldsymbol{s}}{\mathrm{d}\boldsymbol{e}} &= 4[\phi_1'\mathbf{A}_1' + \phi_2'\mathbf{A}_2' + \phi_{11}'\mathbf{n}_1'(\mathbf{n}_1')^{\mathbf{T}} + \phi_{12}'\mathbf{n}_1'(\mathbf{n}_2')^{\mathbf{T}} \\ &\quad + \phi_{21}'\mathbf{n}_2'(\mathbf{n}_1')^{\mathbf{T}} + \phi_{22}'\mathbf{n}_2'(\mathbf{n}_2')^{\mathbf{T}}] \end{aligned} \tag{6.28}$$

$$\frac{\mathrm{d}\boldsymbol{s}}{\mathrm{d}p} = -I_3 n_3.$$

Example: Uniaxial Tension

Consider the Neo-Hookean elastomer satisfying

$$w = \alpha\left[\mathrm{I}_1 - 3\right] \qquad \text{and subject to} \qquad I_3 = 1. \tag{6.29}$$

We seek the relation between s_1 and e_1, which will be obtained twice: once by enforcing the incompressibility constraint *a priori*, and the second by enforcing the constraint *a posteriori*.

a priori: Assume for the sake of brevity that $\mathbf{e}_2 = \mathbf{e}_3$. $I_3 = 1$ implies that $c_2 = 1/\sqrt{c_1}$. The strain-energy function now is $w = \alpha[c_1 + \frac{2}{\sqrt{c_1}} - 3]$. The stress, s_1, is now found as

$$s_1 = 2\frac{\mathrm{d}w}{\mathrm{d}c_1} = 2\alpha\left[1 - \frac{1}{c_1^{3/2}}\right]. \tag{6.30}$$

a posteriori: Use the augmented function

$$w' = \alpha[I_1 - 3] - \frac{p}{2}[I_3 - 1]. \tag{6.31}$$

Now

$$\begin{aligned} s_1 &= 2\frac{\mathrm{d}w'}{\mathrm{d}c_1} = 2\alpha - p/c_1 \\ 0 = s_2 &= 2\frac{\mathrm{d}w'}{\mathrm{d}c_2} = 2\alpha - p/c_2 \\ 0 = s_3 &= 2\frac{\mathrm{d}w'}{\mathrm{d}c_3} = 2\alpha - p/c_3 \\ 0 &= \frac{\mathrm{d}w'}{\mathrm{d}p} = 0 \rightarrow I_3 = 1. \end{aligned} \tag{6.32}$$

Thus, it follows that $c_2 = c_3 = 1/\sqrt{c_1}$ and $p/c_2 = 2\alpha$. We conclude that

$$\begin{aligned} s_1 &= 2\alpha - p/c_1 \\ &= 2\alpha - \frac{c_2}{c_1}p/c_2 \\ &= 2\alpha\left[1 - \frac{c_2}{c_1}\right] \\ &= 2\alpha\left[1 - \frac{1}{c_1^{3/2}}\right]. \end{aligned} \tag{6.33}$$

a posteriori with deviatoric invariants: Consider the augmented function with deviatoric invariants:

$$w' = \alpha\left[I_1/I_3^{1/3} - 3\right] - \frac{p}{2}[I_3 - 1] \qquad \text{(a)}$$

$$s_1 = 2\frac{\mathrm{d}w'}{\mathrm{d}c_1} = 2\alpha\left[\frac{1}{I_3^{1/3}} - \frac{1}{3}\frac{I_1}{I_3^{4/3}}\frac{I_3}{c_1}\right] - p\frac{I_3}{c_1} \qquad \text{(b)}$$

$$0 = s_2 = 2\frac{\mathrm{d}w'}{\mathrm{d}c_2} = 2\alpha\left[\frac{1}{I_3^{1/3}} - \frac{1}{3}\frac{I_1}{I_3^{4/3}}\frac{I_3}{c_2}\right] - p\frac{I_3}{c_2} \qquad \text{(c)} \qquad (6.34)$$

$$0 = s_3 = 2\frac{\mathrm{d}w'}{\mathrm{d}c_3} = 2\alpha\left[\frac{1}{I_3^{1/3}} - \frac{1}{3}\frac{I_1}{I_3^{4/3}}\frac{I_3}{c_3}\right] - p\frac{I_3}{c_3} \qquad \text{(d)}$$

Hence, $c_2 = c_3$. Furthermore,

$$\frac{\mathrm{d}w'}{\mathrm{d}p} = 0 \rightarrow I_3 = 1. \qquad (6.34e)$$

Equation 6.34 now implies that

$$\frac{2\alpha}{3}\left[\frac{c_2 - c_1}{c_2}\right] = \frac{p}{c_2}, \qquad (6.35)$$

and substitution into Equation 6.34b furnishes

$$s_1 = 2\alpha\left[1 - \frac{1}{c_1^{3/2}}\right], \qquad (6.36)$$

as in the *a priori* case and in the first *a posteriori* case. Now, the Lagrange multiplier p can be interpreted as the pressure referred to current coordinates.

6.3.2 Near-Incompressibility

As will be seen in Chapter 18, the augmented strain-energy function

$$w'' = w(I_1', I_2') - \frac{1}{2}p[I_3 - 1] - \frac{p^2}{2\kappa} \qquad (6.37)$$

serves to enforce the constraint

$$p = -\kappa\left[I_3 - 1\right]. \qquad (6.38)$$

Here, κ is the bulk modulus, and it is assumed to be quite large compared to, for example, the small strain-shear modulus. The tangent-modulus tensor is now

$$TEN22\left(\boldsymbol{D}^{*}\right)=\begin{bmatrix} \dfrac{\mathrm{d}\boldsymbol{s}}{\mathrm{d}\boldsymbol{e}} & \dfrac{\mathrm{d}\boldsymbol{s}}{\mathrm{d}p} \\ -\left(\dfrac{\mathrm{d}\boldsymbol{s}}{\mathrm{d}p}\right)^{\mathbf{T}} & \dfrac{1}{\kappa} \end{bmatrix}. \tag{6.39}$$

6.4 NONLINEAR MATERIALS AT LARGE DEFORMATION

Suppose that the constitutive relations are measured at a constant temperature in the current configuration as

$$\mathring{\boldsymbol{T}} = \boldsymbol{D}\mathbf{D}, \tag{6.40}$$

in which the fourth-order tangent-modulus tensor $\boldsymbol{D}$ can, in general, be a function of stress, strain, temperature, and internal-state variables (discussed in subsequent chapters). This form is attractive since $\mathring{\boldsymbol{T}}$ and $\mathbf{D}$ are both objective. Conversion to undeformed coordinates is realized by

$$\begin{aligned} \dot{\boldsymbol{S}} &= \mathrm{J}\mathbf{F}^{-1}\boldsymbol{D}\mathbf{D}\mathbf{F}^{-\mathbf{T}} \\ &= \mathrm{J}\mathbf{F}^{-1}\boldsymbol{D}\mathbf{F}^{-\mathbf{T}}\dot{\boldsymbol{E}}\mathbf{F}^{-1}\mathbf{F}^{-\mathbf{T}}. \end{aligned} \tag{6.41}$$

If $\mathbf{s} = VEC(\boldsymbol{S})$ and $\mathbf{e} = VEC(\boldsymbol{E})$, then

$$\begin{aligned} \dot{\mathbf{s}} &= \mathrm{J}\mathbf{I}\otimes\mathbf{F}^{-1}VEC(\boldsymbol{D}\mathbf{F}^{-\mathbf{T}}\dot{\boldsymbol{E}}\mathbf{F}^{-1}\mathbf{F}^{-\mathbf{T}}) \\ &= \mathrm{J}\mathbf{I}\otimes\mathbf{F}^{-1}\mathbf{F}^{-1}\otimes\mathbf{I}TEN22(\boldsymbol{D})VEC(\mathbf{F}^{-\mathbf{T}}\dot{\boldsymbol{E}}\mathbf{F}^{-1}) \\ &= \mathrm{J}\mathbf{F}^{-1}\otimes\mathbf{F}^{-1}TEN22(\boldsymbol{D})(\mathbf{F}^{-\mathbf{T}}\otimes\mathbf{I})(\mathbf{I}\otimes\mathbf{F}^{-\mathbf{T}})VEC(\dot{\boldsymbol{E}}) \\ &= \mathrm{J}\mathbf{F}^{-1}\otimes\mathbf{F}^{-1}TEN22(\boldsymbol{D})\mathbf{F}^{-\mathbf{T}}\otimes\mathbf{F}^{-\mathbf{T}}\dot{\mathbf{e}} \\ &= TEN22(\boldsymbol{D}_{o})\dot{\mathbf{e}}. \end{aligned} \tag{6.42}$$

Recalling Chapter 2, it follows that

$$\dot{\boldsymbol{S}} = \boldsymbol{D}_{o}\dot{\boldsymbol{E}}, \tag{6.43}$$

in which

$$\boldsymbol{D}_{o} = ITEN22(\mathrm{J}\mathbf{F}^{-1}\otimes\mathbf{F}^{-1}TEN22(\boldsymbol{D})\mathbf{F}^{-\mathbf{T}}\otimes\mathbf{F}^{-\mathbf{T}}) \tag{6.44}$$

is the tangent-modulus tensor $\boldsymbol{D}_{o}$ referred to undeformed coordinates.

Suppose instead that the Jaumann stress flux is used and that

$$\overset{\vartriangle}{\boldsymbol{T}} = \boldsymbol{D}\mathbf{D}. \tag{6.45}$$

Now

$$\begin{aligned}\dot{\boldsymbol{S}} &= \mathrm{J}\mathbf{F}^{-\mathbf{T}}\left[\overset{\vartriangle}{\boldsymbol{T}} + \boldsymbol{T}tr(\boldsymbol{D}) - (\mathbf{L}+\mathbf{W})\boldsymbol{T} - \boldsymbol{T}(\mathbf{L}^{\mathbf{T}} - \mathbf{W})\right]\mathbf{F}^{-1} \\ &= \mathrm{J}\mathbf{F}^{-\mathbf{T}}\left[\boldsymbol{D}\mathbf{F}^{-\mathbf{T}}\dot{\boldsymbol{E}}\mathbf{F}^{-1} + \boldsymbol{T}tr(\mathbf{F}^{-\mathbf{T}}\dot{\boldsymbol{E}}\mathbf{F}^{-1}) - (\mathbf{L}+\mathbf{W})\boldsymbol{T} - \boldsymbol{T}(\mathbf{L}^{\mathbf{T}} - \mathbf{W})\right]\mathbf{F}^{-1}.\end{aligned} \tag{6.46}$$

For this flux, there does not appear to be any way that $\dot{\boldsymbol{S}}$ can be written in the form of Equation 6.42, i.e., is determined by $\dot{\boldsymbol{E}}$. To see this, consider

$$\begin{aligned} VEC(\dot{\boldsymbol{S}}) &= TEN22(\boldsymbol{D}')VEC(\dot{\boldsymbol{E}}) - TEN22(\boldsymbol{D}'')VEC(\mathbf{L}+\mathbf{W}) && \text{(a)} \\ TEN22(\boldsymbol{D}') &= [\mathbf{I}\otimes(\mathbf{F}^{-\mathbf{T}})^2\, TEN22(\mathrm{J}\mathbf{F}^{-\mathbf{T}}\boldsymbol{D}\mathbf{F}^{-\mathbf{T}}) + VEC(\boldsymbol{T})VEC^{\mathbf{T}}(\mathbf{F}\mathbf{F}^{-\mathbf{T}})] && \text{(b)} \\ TEN22(\boldsymbol{D}'') &= \mathrm{J}[\mathbf{I}\otimes\mathbf{F}^{-1}]^2[\boldsymbol{T}\otimes\mathbf{I} - \mathbf{I}\otimes\boldsymbol{T}\mathbf{U}_9] && \text{(c)}\end{aligned} \tag{6.47}$$

In the second term in Equation 6.47a, $VEC(\mathbf{L}+\mathbf{W})$ cannot be eliminated in favor of $VEC(\mathbf{D})$, and hence in favor of $VEC(\dot{\boldsymbol{E}})$. Note that

$$VEC(\mathbf{D}) = \frac{1}{2}VEC(\mathbf{L}+\mathbf{L}^{\mathbf{T}}) = \frac{1}{2}(\mathbf{I}+\mathbf{U}_9)VEC(\mathbf{L}). \tag{6.48}$$

$\mathbf{I}+\mathbf{U}_9$ is singular, as seen in the following argument. Recall that $\mathbf{U}_9$ is symmetric and thus has real eigenvalues. However, $\mathbf{U}_9^2 = \mathbf{I}$ and thus the eigenvalues of $\mathbf{U}_9$ are either 1 or −1. Some of the eigenvalues must be −1. Otherwise, $\mathbf{U}_9$ would be the identity matrix, in which case it would not, in general, have the permutation property identified in Chapter 2. Thus, some of the eigenvalues of $\mathbf{I}+\mathbf{U}_9$ vanish. Instead, we write

$$VEC(\dot{\boldsymbol{S}}) = \boldsymbol{D}'VEC(\dot{\mathbf{E}}) - \boldsymbol{D}''VEC(\mathbf{D}) - \boldsymbol{D}''VEC(\boldsymbol{D}+2\mathbf{W}), \tag{6.49}$$

and we see that if the Jaumann stress flux is used, $\dot{\boldsymbol{S}}$ is determined by $\dot{\boldsymbol{E}}$ *and the spin* $\mathbf{W}$. Recall that the spin does not vanish under rigid-body rotation.

6.5 EXERCISES

1. In classical linear elasticity, introduce the isotropic stress and isotropic linear strain as

$$\mathbf{s} = tr(\boldsymbol{S}) \qquad \mathbf{e} = tr(\boldsymbol{E}_{\mathbf{L}}),$$

and introduce the deviatoric stress and strain using

$$\mathbf{s_d} = \mathbf{s} - \frac{1}{3}s\mathbf{i} \qquad \mathbf{e_d} = \mathbf{e} - \frac{1}{3}e\mathbf{i}.$$

Verify that

$$\mathbf{i}^{\mathrm{T}}\mathbf{s_d} = 0 \qquad \mathbf{i}^{\mathrm{T}}\mathbf{e_d} = 0$$

$$\mathbf{s_d} = 2\mu\mathbf{e_d}$$

$$s = (2\mu + 3\lambda)e.$$

2. Verify that Equation 6.3 can be inverted to furnish

$$\mathbf{e} = \frac{1}{2\mu}\left[\mathbf{t} - \frac{\lambda}{(2\mu + 3\lambda)}(\mathbf{i}^{\mathrm{T}}\mathbf{t})\mathbf{i}\right], \quad \mathbf{t} = VEC(\boldsymbol{T})$$

3. In classical linear elasticity, under uniaxial stress, the elastic modulus E and Poisson's ratio ν are defined by

$$E = \frac{\sigma_{11}}{\varepsilon_{11}} \qquad \nu = -\frac{\varepsilon_{22}}{\varepsilon_{11}} = -\frac{\varepsilon_{33}}{\varepsilon_{11}}, \qquad \begin{cases} \sigma_{11} \neq 0 \\ \sigma_{ij} = 0 \quad ij \neq 11. \end{cases}$$

Prove that

$$\frac{1}{E} = \frac{1}{2\mu}\left[1 - \frac{\lambda}{(2\mu + 3\lambda)}\right] \qquad \nu = -\frac{\lambda}{2(\mu + \lambda)} \qquad \mu = \frac{E}{2(1+\nu)}.$$

4. Obtain **v**, **L**, **D**, and **W** in spherical coordinates.
5. For cylindrical coordinates, find **L**, **D**, and **W** for the following flows:

(a) pure radial flow: $v_r = f(r), \quad v_\theta = 0, \quad v_z = 0$

(b) pipe flow: $v_r = 0, \quad v_\theta = 0, \quad v_z = f(r)$

(c) cylindrical flow: $v_r = 0, \quad v_\theta = f(r), \quad v_z = 0$

(d) torsional flow: $v_r = 0, \quad v_\theta = f(z), \quad v_z = 0$

6. In undeformed coordinates, the 2nd Piola-Kirchhoff stress for an incompressible, hyperelastic material is given by

$$\mathbf{s} = \frac{\partial w'}{\partial \mathbf{e}} = 2\varphi_1'\mathbf{n}_1' + 2\varphi_2'\mathbf{n}_2' - pI_3\mathbf{n}_3.$$

Find the corresponding expression in deformed coordinates: derive ψ_1' and ψ_2', in which direct transformation furnishes

$$\mathbf{t} = 2\psi_1'\mathbf{m}_1' + 2\psi_2'\mathbf{m}_2' - p\mathbf{i}.$$

7. Prove that under uniaxial tension in an isotropic linearly elastic material $e_{22} = e_{33}$. (Problem 9, Chapter 5.)
8. Obtain λ in terms of E and ν. (Problem 10, Chapter 5.)
9. The bulk modulus K is defined by $t_{kk} = 3\mathrm{K}e_{kk}^{(L)}$. Obtain K as a function of E and ν. (Problem 11, Chapter 5.)
10. The 2" × 2" × 2" shown in Figure 6.2 is confined on its sides facing the $\pm x$ faces by rigid, frictionless walls. The sides facing the $\pm z$ faces are free. The top and bottom faces are subjected to a compressive force of 100 lbf. Take E = 10∧7 psi and ν = 1/3. Find all nonzero stresses and strains. What is the volume change? What are the principal stresses and strains? What is the maximum shear stress? (Problem 12, Chapter 5.)

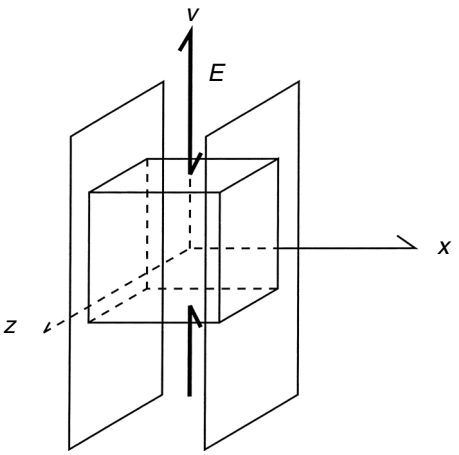

FIGURE 6.2 Strain in a constrained plate.

7 Thermal and Thermomechanical Response

7.1 BALANCE OF ENERGY AND PRODUCTION OF ENTROPY

7.1.1 Balance of Energy

The total energy increase in a body, including internal energy and kinetic energy, is equal to the corresponding work done on the body and the heat added to the body. In rate form,

$$\dot{\mathfrak{K}} + \dot{\Xi} = \dot{W} + \dot{Q}, \tag{7.1}$$

in which:

Ξ is the internal energy with density ξ

$$\dot{\Xi} = \int \rho \dot{\xi} dV; \tag{7.2a}$$

$\dot{W}$ is the rate of mechanical work, satisfying

$$\dot{W} = \int \dot{\mathbf{u}}^{\mathbf{T}} \boldsymbol{\tau} dS, \tag{7.2b}$$

$\dot{Q}$ is the rate of heat input, with heat production h and heat flux $\mathbf{q}$, satisfying

$$\dot{Q} = \int \rho h dV - \int \mathbf{n}^{\mathbf{T}} \mathbf{q} dS, \text{ and} \tag{7.2c}$$

$\dot{\mathfrak{K}}$ is the rate of increase in the kinetic energy,

$$\dot{\mathfrak{K}} = \int \rho \dot{\mathbf{u}}^{\mathbf{T}} \frac{d\dot{\mathbf{u}}}{dt} dV. \tag{7.2d}$$

It has been tacitly assumed that all work is done on S, and that body forces do no work.

Invoking the divergence theorem and balance of linear momentum furnishes

$$\int \left[\rho \dot{\xi} + \dot{\mathbf{u}}^T \left[\rho \frac{d\dot{\mathbf{u}}}{dt} - \nabla^T \boldsymbol{T} \right] - tr(\boldsymbol{T}\mathbf{D}) - \rho h + \nabla^T \mathbf{q} \right] dV = 0. \tag{7.3}$$

The inner bracketed term inside the integrand vanishes by virtue of the balance of linear momentum. The relation holds for arbitrary volumes, from which the local form of balance of energy, referred to undeformed coordinates, is obtained as

$$\rho \dot{\xi} = tr(\boldsymbol{T}\mathbf{D}) - \nabla^{\mathbf{T}} \mathbf{q} + \rho \mathrm{h}. \tag{7.4}$$

To convert to undeformed coordinates, note that

$$\begin{aligned} \int \mathbf{n}^{\mathbf{T}} \mathbf{q} dS &= \int \mathbf{q}^{\mathbf{T}} J \mathbf{F}^{-\mathbf{T}} \mathbf{n}_0 dS_0 \\ &= \int \mathbf{q}_0^{\mathbf{T}} \mathbf{n}_0 dS_0 \qquad \mathbf{q}_0 = J\mathbf{F}^{-1}\mathbf{q}. \end{aligned} \tag{7.5}$$

In undeformed coordinates, Equation 7.3 is rewritten as

$$\int \left[\rho_0 \dot{\xi} - tr(\boldsymbol{S}\dot{\boldsymbol{E}}) - \rho_0 \mathrm{h} + \nabla_0^{\mathbf{T}} \mathbf{q}_0 \right] dV_0 = 0, \tag{7.6a}$$

furnishing the *local form*

$$\rho_0 \dot{\xi} - tr(\boldsymbol{S}\dot{\boldsymbol{E}}) - \rho_0 \mathrm{h} + \nabla_0^{\mathbf{T}} \mathbf{q}_0 = 0. \tag{7.6b}$$

7.1.2 Entropy Production Inequality

Following the thermodynamics of ideal and non-ideal gases, the entropy production inequality is introduced as follows (see Callen, 1985):

$$\dot{H} = \int \rho \dot{\eta} \mathrm{dV} \geq \int \frac{\mathrm{h}}{\mathrm{T}} \mathrm{dV} - \int \frac{\mathbf{n}^{\mathbf{T}} \mathbf{q}}{\mathrm{T}} \mathrm{dS}, \tag{7.7a}$$

in which H is the total entropy, η is the specific entropy per unit mass, and T is the absolute temperature. This relation provides a "framework" for describing the irreversible nature of dissipative processes, such as heat flow and plastic deformation. We apply the divergence theorem to the surface integral and obtain the local form of the entropy production inequality:

$$\rho \mathrm{T} \dot{\eta} \geq \mathrm{h} - \nabla^{\mathbf{T}} \mathbf{q} + \mathbf{q}^{\mathbf{T}} \nabla \mathrm{T}/\mathrm{T}. \tag{7.7b}$$

The corresponding relation in undeformed coordinates is

$$\rho_0 \mathrm{T}\dot{\eta} \geq \mathrm{h} - \nabla_0^{\mathbf{T}}\mathbf{q}_0 + \mathbf{q}_0^{\mathbf{T}}\nabla_0 \mathrm{T}/\mathrm{T}. \tag{7.7c}$$

7.1.3 Thermodynamic Potentials

The Balance of Energy introduces the internal energy Ξ, which is an extensive variable—its value accumulates over the domain. The mass and volume averages of extensive variables are also referred to as extensive variables. This contrasts with intensive, or pointwise, variables, such as the stresses and the temperature. Another extensive variable is the entropy H. In reversible elastic systems, the heat flux is completely converted into entropy according to

$$\dot{Q} = \mathrm{T}\dot{H}. \tag{7.8}$$

(We shall consider several irreversible effects, such as plasticity, viscosity, and heat conduction.) In undeformed coordinates, the balance of energy for reversible processes can be written as

$$\rho_0 \dot{\xi} = tr(\boldsymbol{S}\dot{\boldsymbol{E}}) + \rho_0 \mathrm{T}\dot{\eta}. \tag{7.9}$$

We call this equation the thermal equilibrium equation. It is assumed to be integrable, so that the internal energy is dependent on the current state represented by the current values of the state variables $\boldsymbol{E}$ and η. For the sake of understanding, we can think of T as a thermal stress and η as a thermal strain. Clearly, $\dot{\eta} = 0$ if there is no heat input across the surface or generated in the volume. Consequently, the entropy is a convenient state variable for representing adiabatic processes.

In Callen (1985), a development is given for the stability of thermodynamic equilibrium, according to which, under suitable conditions, the strain and the entropy density assume values that maximize the internal energy. Other thermodynamic potentials, depending on alternate state variables, can be introduced by a Lorentz transformation, as illustrated in the following equation. Doing so is attractive if the new state variables are accessible to measurement. For example, the Gibbs Free Energy (density) is a function of the intensive variables $\boldsymbol{S}$ and T:

$$\rho_0 g = \rho_0 \xi - tr(\boldsymbol{S}\boldsymbol{E}) - \rho_0 \mathrm{T}\eta, \tag{7.10a}$$

from which

$$\rho_0 \dot{g} = -tr(\boldsymbol{E}\dot{\boldsymbol{S}}) - \rho_0 \eta \dot{\mathrm{T}}. \tag{7.10b}$$

Stability of thermodynamic equilibrium requires that $\boldsymbol{S}$ and T assume values that minimize g under suitable conditions. This potential is of interest in fluids experiencing adiabatic conditions since the pressure (stress) is accessible to measurement using, for example, pitot tubes.

In solid continua, the stress is often more difficult to measure than the strain. Accordingly, for solids, the Helmholtz Free Energy (density) f is introduced using

$$\rho_0 f = \rho_0 \xi - \rho_0 \mathrm{T}\eta, \tag{7.11a}$$

furnishing

$$\rho_0 \dot{f} = tr(\boldsymbol{S}\dot{\boldsymbol{E}}) - \rho_0 \eta \dot{\mathrm{T}}. \tag{7.11b}$$

It is evident that f is a function of both an intensive and an extensive variable. At thermodynamic equilibrium, it exhibits a (stationary) saddle point rather than a maximum or a minimum. Finally, for the sake of completeness, we mention a fourth potential, known as the enthalpy $\rho_0 h = \rho_0 \xi - tr(\boldsymbol{SE})$, and

$$\rho_0 \dot{\mathrm{h}} = -tr(\boldsymbol{E}\dot{\boldsymbol{S}}) + \rho_0 \mathrm{T}\dot{\eta}. \tag{7.12}$$

The enthalpy also is a function of an extensive variable and an intensive variable and exhibits a saddle point at equilibrium. It is attractive in fluids under adiabatic conditions.

7.2 CLASSICAL COUPLED LINEAR THERMOELASTICITY

The classical theory of coupled thermoelasticity in isotropic media corresponds to the restriction to the linear-strain tensor, $\boldsymbol{E} \approx \dot{\boldsymbol{E}}_L$ and to the stress-strain temperature relation

$$\boldsymbol{T} = 2\mu\boldsymbol{E} + \lambda[tr(\boldsymbol{E}) - \alpha(\mathrm{T} - \mathrm{T}_0)]\mathbf{I}. \tag{7.13}$$

Here, α is the volumetric coefficient of thermal expansion, typically a small number in metals. If the temperature increases without stress being applied, the strain increases according to $e_{\mathrm{vol}} = tr(\mathbf{E}) = \alpha(T - T_0)$. Thermoelastic processes are assumed to be reversible, in which case, $-\nabla \cdot \mathbf{q} + h = \rho T\dot{\eta}$. It is also assumed that the specific heat at constant strain, c_e, given by

$$c_e = T\frac{\partial \eta}{\partial T}, \tag{7.14}$$

is constant. The balance of energy is restated as

$$\rho_0 \dot{\xi} = tr(\boldsymbol{T}\dot{\boldsymbol{E}}) - \rho \mathrm{T}\dot{\eta} \tag{7.15}$$

Recalling that ξ is a function of the extensive variables $\boldsymbol{E}$ and η, to convert to $\boldsymbol{E}$ and T as state variables, which are accessible to measurement, we recall the

Helmholtz Free Energy $f = e + T\eta$. Since $\dot{f}$ is an exact differential, to ensure path independence, we infer the Maxwell relation:

$$-\rho \left.\frac{\partial \eta}{\partial \boldsymbol{E}}\right|_{\mathrm{T}} = \left.\frac{\partial \boldsymbol{T}}{\partial \mathrm{T}}\right|_{\dot{\mathbf{E}}}. \tag{7.16}$$

Returning to the energy-balance equation,

$$\begin{aligned}\rho\dot{\xi} &= tr\left(\rho\left.\frac{\partial \xi}{\partial \boldsymbol{E}}\right|_{\eta}\dot{\boldsymbol{E}}\right) + \rho\left.\frac{\partial \xi}{\partial \eta}\right|_{\mathbf{E}}\dot{\eta} \\ &= tr\left(\left[\rho\left.\frac{\partial \xi}{\partial \boldsymbol{E}}\right|_{\eta} + \rho\left.\frac{\partial \xi}{\partial \eta}\right|_{\mathbf{E}}\left.\frac{\partial \eta}{\partial \boldsymbol{E}}\right|_{\mathbf{T}}\right]\dot{\boldsymbol{E}}\right) + \rho\left[\left.\frac{\partial \xi}{\partial \eta}\right|_{\mathbf{E}}\left.\frac{\partial \eta}{\partial \mathrm{T}}\right|_{\mathbf{E}}\right]\dot{\mathrm{T}}.\end{aligned} \tag{7.17}$$

Also, note that

$$\boldsymbol{T} = \left.\frac{\partial \xi}{\partial E}\right|_{\eta} \qquad \mathrm{T} = \left.\frac{\partial \xi}{\partial \eta}\right|_{\mathbf{E}}, \tag{7.18a}$$

thus

$$\begin{aligned}\rho\dot{\xi} &= tr\left(\left[\rho\left.\frac{\partial \xi}{\partial \boldsymbol{E}}\right|_{\eta} + \rho\left.\frac{\partial \xi}{\partial \eta}\right|_{\mathbf{E}}\left.\frac{\partial \eta}{\partial \boldsymbol{E}}\right|_{\mathbf{T}}\right]\dot{\mathbf{E}}\right) + \rho\left[\left.\frac{\partial \xi}{\partial \eta}\right|_{\mathbf{E}}\left.\frac{\partial \eta}{\partial \mathbf{T}}\right|_{\mathbf{E}}\right]\dot{\mathbf{T}} \\ &= tr\left(\left[\boldsymbol{T} - \mathrm{T}\left.\frac{\partial \boldsymbol{T}}{\partial \mathrm{T}}\right|_{E}\right]\dot{\boldsymbol{E}}\right) + \rho\mathrm{T}\left.\frac{\partial \eta}{\partial \mathbf{T}}\right|_{\mathbf{E}}\dot{\mathbf{T}}.\end{aligned} \tag{7.18b}$$

We previously identified the coefficient of specific heat, assumed constant, as $c_e = T\left.\frac{\partial \eta}{\partial \mathbf{T}}\right|_{\mathbf{E}}$, so that

$$\rho\dot{\xi} = tr\left(\left[\boldsymbol{T} - \mathrm{T}\frac{\partial \boldsymbol{T}}{\partial \mathrm{T}}\right]\dot{\mathbf{E}}\right) + \rho c_e\dot{\mathrm{T}}. \tag{7.19}$$

From Equation 7.13, upon approximating T as T_0, $\mathrm{T}_0\frac{\partial \boldsymbol{T}}{\partial \mathrm{T}} = -\alpha\lambda T_0\mathbf{I}$. From Fourier's Law, $\mathbf{q} = -k\nabla T$. Thus, the thermal-field equation now can be written as

$$k\nabla^2\mathrm{T} = \alpha\lambda\mathrm{T}_0 tr(\dot{\mathbf{E}}) + \rho\mathrm{c}_\mathrm{e}\dot{\mathrm{T}}. \tag{7.20}$$

The balance of linear momentum, together with the stress-strain and strain-displacement relations of linear isotropic thermoelasticity, imply that

$$\frac{\partial}{\partial x_j}\left[2\mu\left[\frac{1}{2}\left(\frac{\partial u_i}{\partial x_j}+\frac{\partial u_j}{\partial x_i}\right)\right]+\lambda\left[\frac{\partial u_k}{\partial x_k}-\alpha(\mathrm{T}-\mathrm{T}_0)\delta_{ij}\right]\right]=\rho\frac{\partial u_i}{\partial t^2}, \tag{7.21}$$

from which we obtain the mechanical-field equation (Navier's Equation for Thermoelasticity):

$$\mu\nabla^2\mathbf{u}+(\lambda+\mu)\nabla tr(\boldsymbol{E})-\alpha\lambda\nabla\mathrm{T}=\rho\frac{\partial\mathbf{u}}{\partial\mathrm{t}^2}. \tag{7.22}$$

The thermal-field equation depends on the mechanical field through the term $\alpha\lambda\mathrm{T}_0 tr(\dot{\boldsymbol{E}})$. Consequently, if $\boldsymbol{E}$ is static, there is no coupling. Similarly, the mechanical field depends on the thermal field through $\alpha\lambda\nabla T$, which often is quite small in, for example, metals, if the assumption of reversibility is a reasonable approximation.

We next derive the entropy. Since $c_e=\mathrm{T}\frac{\partial\eta}{\partial\mathrm{T}}\Big|_{\mathbf{E}}$ is constant, we conclude that it has the form

$$\rho\eta=\rho\eta_0+\rho\mathrm{c}_\mathrm{e}\ln(\mathrm{T}/\mathrm{T}_0)+\rho\eta^*(\boldsymbol{E}), \tag{7.23}$$

where $\eta^*(\boldsymbol{E})$ remains to be determined. We take η_0 to vanish. However, $\rho\frac{\partial\eta}{\partial\boldsymbol{E}}\Big|_{\mathbf{T}}=\rho\frac{\partial\eta^*}{\partial\boldsymbol{E}}=-\frac{\partial\boldsymbol{T}}{\partial\mathrm{T}}\Big|_{\boldsymbol{E}}=\alpha\lambda\mathbf{I}$, implying that

$$\rho\eta=\rho\eta_0+\rho\mathrm{c}_\mathrm{e}\ln(\mathrm{T}/\mathrm{T}_0)+\alpha\lambda tr(\boldsymbol{E}). \tag{7.24}$$

Now consider f, for which the fundamental relation in Equation 7.11b implies

$$\frac{\partial f}{\partial\mathrm{T}}\Big|_E=-\eta\qquad\rho\frac{\partial f}{\partial\boldsymbol{E}}\Big|_{\mathbf{T}}=\boldsymbol{T}. \tag{7.25}$$

Integrating the entropy,

$$\rho f=\rho f_0-\rho\mathrm{c}_e[\mathrm{T}\ln(\mathrm{T}/\mathrm{T}_0)-1]-\alpha\lambda tr(\mathbf{E})\mathrm{T}+\rho f^*(\boldsymbol{E}), \tag{7.26}$$

in which $f^*(\boldsymbol{E})$, remains to be determined. Integrating the stress,

$$\rho f=\mu\,tr(\boldsymbol{E}^2)+\frac{\lambda}{2}tr^2(\mathbf{E})-\alpha\lambda\,tr(\boldsymbol{E})(\mathrm{T}-\mathrm{T}_0)+\rho f^{**}(\mathrm{T}), \tag{7.27}$$

in which $f^{**}(\mathrm{T})$ also remains to be determined. However, reconciling the two forms furnishes (taking $f_0 = 0$)

$$\rho f = \mu\, tr(\mathbf{E}^2) + \frac{\lambda}{2} tr^2(\mathbf{E}) - \alpha\lambda\, tr(\mathbf{E})\mathrm{T} - \rho \mathrm{c_e}[\mathrm{T}\ln(\mathrm{T}/\mathrm{T}_0) - 1]. \tag{7.28}$$

7.3 THERMAL AND THERMOMECHANICAL ANALOGS OF THE PRINCIPLE OF VIRTUAL WORK

7.3.1 Conductive Heat Transfer

For a linear, isotropic, thermoelastic medium, the Fourier Heat Conduction Law becomes $\mathbf{q} = -k_T \nabla \mathrm{T}$, in which k_T is the thermal conductance, assumed positive. Neglecting coupling to the mechanical field, the thermal-field equation in an isotropic medium experiencing small deformation can be written as

$$-\nabla^{\mathbf{T}} k_T \nabla \mathrm{T} + \rho c_e \dot{\mathrm{T}} = 0. \tag{7.29}$$

We now construct a thermal counterpart of the principle of virtual work. Multiplying by $\delta\mathrm{T}$ and using integration by parts, we obtain

$$\int \delta\nabla^{\mathbf{T}}\mathrm{T} k_T \nabla \mathrm{T} dV + \int \delta \mathrm{T} \rho c_e \dot{\mathrm{T}} dV = \int \delta \mathrm{T} \mathbf{n}^{\mathbf{T}} \mathbf{q} dS \tag{7.30}$$

Clearly, T is regarded as the primary variable, and the associated secondary variable is $\mathbf{q}$. Suppose that the boundary is decomposed into three segments: $S = S_I + S_{II} + S_{III}$. On S_I, the temperature T is prescribed as, for example, T_0. It follows that $\delta\mathrm{T} = 0$ on S_I. On S_{II}, the heat flux $\mathbf{q}$ is prescribed as $\mathbf{q}_0$. Consequently, $\delta \mathrm{T}\mathbf{n}^{\mathbf{T}}\mathbf{q} \rightarrow \delta\,\mathrm{T}\mathbf{n}^{\mathbf{T}}\mathbf{q}_0$. On S_{III}, the heat flux is dependent on the surface temperature through a heat-transfer vector: $\boldsymbol{h}$: $\mathbf{q} = \mathbf{q}_0 - \boldsymbol{h}(\mathrm{T} - \mathrm{T}_0)$. The right side of Equation 7.30 now becomes

$$\int_S \delta \mathrm{T}\mathbf{n}^{\mathbf{T}}\mathbf{q} dS = \int_{S_{II}} \delta \mathrm{T}\mathbf{n}^{\mathbf{T}}\mathbf{q}_0 dS + \int_{S_{III}} \delta \mathrm{T}\mathbf{n}^{\mathbf{T}}\mathbf{q}_0 dS - \int_{S_{III}} \delta \mathrm{T}\mathbf{n}^{\mathbf{T}}\boldsymbol{h}(\mathrm{T} - \mathrm{T}_0) dS. \tag{7.31}$$

We now suppose that T is approximated using an interpolation function of the form

$$\mathrm{T} - \mathrm{T}_0 \sim \mathbf{N}_{\mathbf{T}}^{\mathbf{T}}(\mathbf{x})\boldsymbol{\theta}(t) \quad \delta\mathrm{T} \sim \mathbf{N}_{\mathbf{T}}^{\mathbf{T}}(\mathbf{x})\delta\boldsymbol{\theta}(t), \tag{7.32}$$

from which we obtain

$$\nabla \mathrm{T} \sim \mathbf{B}_T^T(\mathbf{x})\boldsymbol{\theta}(t) \quad \delta\nabla\mathrm{T} \sim \mathbf{B}_T^T(\mathbf{x})\delta\boldsymbol{\theta}(t), \tag{7.33}$$

in which $\mathbf{B}_\mathbf{T}$ is the thermal analog of the strain-displacement matrix. Upon substitution of the interpolation models, the thermal-field equation now reduces to the system of ordinary differential equations:

$$\mathbf{K}_\mathbf{T}\boldsymbol{\theta}(t) + \mathbf{M}_\mathbf{T}\dot{\boldsymbol{\theta}}(t) = \mathbf{f}_\mathbf{T}, \tag{7.34}$$

in which

$\mathbf{K}_\mathbf{T} = \mathbf{K}_{\mathbf{T}1} + \mathbf{K}_{\mathbf{T}2}$	Thermal Stiffness Matrix
$\mathbf{K}_{\mathbf{T}1} = \int \mathbf{B}_\mathbf{T}(\mathbf{x}) k_T \mathbf{B}_\mathbf{T}^\mathbf{T}(\mathbf{x}) dV$	Conductance Matrix
$\mathbf{K}_{\mathbf{T}2} = \int_{S_{III}} \mathbf{N}_\mathbf{T}(\mathbf{x}) \mathbf{n}^\mathbf{T} \boldsymbol{h} \mathbf{N}_\mathbf{T}^\mathbf{T}(\mathbf{x}) dS$	Surface Conductance Matrix
$\mathbf{M}_\mathbf{T} = \int \mathbf{N}_\mathbf{T}(\mathbf{x}) \rho c_e \mathbf{N}_\mathbf{T}^\mathbf{T}(\mathbf{x}) dV$	Thermal Mass Matrix; Capacitance Matrix
$\mathbf{f}_\mathbf{T} = \int_{S_{II}} \mathbf{N}_\mathbf{T}(\mathbf{x}) \mathbf{n}^\mathbf{T} \mathbf{q}_0 dS + \int_{S_{III}} \mathbf{N}_\mathbf{T}(\mathbf{x}) \mathbf{n}^\mathbf{T} \mathbf{q}_0 dS$	Consistent Thermal Force; Consistent Heat Flux

7.3.2 Coupled Linear Isotropic Thermoelasticity

The thermal-field equation is repeated as

$$-k_\mathbf{T} \nabla^2 \mathrm{T} = \alpha \lambda \mathrm{T}_0 tr(\dot{\boldsymbol{E}}) + \rho \mathrm{c}_\mathrm{e} \dot{\mathrm{T}}. \tag{7.35}$$

Following the same steps used for conductive heat transfer furnishes the variational principle

$$\int \delta \nabla^\mathbf{T} \mathrm{T} k_\mathrm{T} \nabla \mathrm{T} dV + \int \delta \mathrm{T} \rho \mathrm{c}_\mathrm{e} \dot{\mathrm{T}} dV + \int \delta \mathrm{T} \alpha \lambda \mathrm{T}_0 tr(\dot{\boldsymbol{E}}) dV = \int \delta \mathrm{T} \mathbf{n}^\mathbf{T} \mathbf{q} dS. \tag{7.36}$$

The principle of virtual work for the mechanical field is recalled as

$$\int tr(\delta \boldsymbol{E} \boldsymbol{T}) dV + \int \delta \mathbf{u}^\mathbf{T} \rho \ddot{\mathbf{u}} dV = \int_S \delta \mathbf{u}^\mathbf{T} \boldsymbol{\tau}(\mathbf{s}) dS. \tag{7.37}$$

Also, recall that $\boldsymbol{T} = 2\mu\mathbf{E} + \lambda[tr(\mathbf{E}) - \alpha(\mathrm{T} - \mathrm{T}_0)]\mathbf{I}$. Consequently,

$$\int tr(\delta \mathbf{E}[2\mu \mathbf{E} + \lambda\, tr(\mathbf{E})\mathbf{I}]) dV - \int tr(\delta \mathbf{E} \lambda \alpha (\mathrm{T} - \mathrm{T}_0)\mathbf{I}) dV + \int \delta \mathbf{u}^T \rho \ddot{\mathbf{u}} dV = \int_S \delta \mathbf{u}^T \boldsymbol{\tau}(\mathbf{s}) dS. \tag{7.38}$$

Then introduce the interpolation models,

$$\mathbf{u}(\mathbf{x}) = \mathbf{N}^{\mathbf{T}}(\mathbf{x})\boldsymbol{\gamma}(t), \tag{7.39}$$

from which we can derive $\mathbf{B}(\mathbf{x})$ and $\mathbf{b}(\mathbf{x})$, thus satisfying

$$VEC(\boldsymbol{E}) = \mathbf{B}^{\mathbf{T}}(\mathbf{x})\boldsymbol{\gamma}(t) \quad tr(\boldsymbol{E}) = \mathbf{b}^{\mathbf{T}}(\mathbf{x})\boldsymbol{\gamma}(t). \tag{7.40}$$

It follows that

$$\mathbf{K}\boldsymbol{\gamma}(t) + \mathbf{M}\ddot{\boldsymbol{\gamma}}(t) - \boldsymbol{\Omega}^{\mathbf{T}}\boldsymbol{\theta}(t) = \mathbf{f}. \tag{7.41}$$

We assume that the traction $\boldsymbol{\tau}(\mathbf{S})$ is specified everywhere as $\boldsymbol{\tau}_0(\mathbf{S})$ on S. Here,

$$\begin{aligned}
\mathbf{K} &= \int \mathbf{B}^{\mathbf{T}}(\mathbf{x})\boldsymbol{D}\mathbf{B}(\mathbf{x})dV && \textit{Stiffness Matrix} \\
\mathbf{M} &= \int \mathbf{N}(\mathbf{x})\rho\mathbf{N}^{\mathbf{T}}(\mathbf{x})dV && \textit{Mass Matrix} \\
\boldsymbol{\Omega} &= \int \alpha\lambda\mathbf{b}^{\mathbf{T}}(\mathbf{x})\mathbf{N}_{\mathbf{T}}(\mathbf{x})dV && \textit{Thermoelastic Matrix} \\
\mathbf{f} &= \int \mathbf{N}(\mathbf{x})\boldsymbol{\tau}dS && \textit{Consistent Force Vector}.
\end{aligned} \tag{7.42}$$

For the thermal field, assuming that the heat flux $\mathbf{q}$ is specified as $\mathbf{q_0}$ on the surface, variational methods, together with the interpolation models, furnish the equation

$$\frac{1}{\mathrm{T}_0}\mathbf{K}_{\mathbf{T}}\boldsymbol{\theta}(t) + \frac{1}{\mathrm{T}_0}\mathbf{M}_{\mathbf{T}}\dot{\boldsymbol{\theta}}(t) + \boldsymbol{\Omega}\dot{\boldsymbol{\gamma}}(t) = \frac{1}{\mathrm{T}_0}\mathbf{f}_{\mathbf{T}}, \quad \mathbf{f}_{\mathbf{T}} = \int \mathbf{N}_{\mathbf{T}}(\mathbf{x})\mathbf{n}^{\mathbf{T}}\mathbf{q}_{\mathbf{0}}dS. \tag{7.43}$$

The combined equations for a thermoelastic medium are now written in state (first-order) form as

$$\begin{gathered}
\mathbf{W}_1\frac{d}{dt}\begin{pmatrix}\dot{\boldsymbol{\gamma}}(t)\\ \boldsymbol{\gamma}(t)\\ \boldsymbol{\theta}(t)\end{pmatrix} + \mathbf{W}_2\begin{pmatrix}\dot{\boldsymbol{\gamma}}(t)\\ \boldsymbol{\gamma}(t)\\ \boldsymbol{\theta}(t)\end{pmatrix} = \begin{pmatrix}\mathbf{f}(t)\\ \mathbf{0}\\ \frac{1}{\mathrm{T}_0}\mathbf{f}_{\mathbf{T}}(t)\end{pmatrix} \\
\mathbf{W}_1 = \begin{bmatrix}\mathbf{M} & \mathbf{0} & \mathbf{0}\\ \mathbf{0} & \mathbf{K} & \mathbf{0}\\ \mathbf{0} & \mathbf{0} & \frac{1}{\mathrm{T}_0}\mathbf{M}_{\mathbf{T}}\end{bmatrix}, \qquad \mathbf{W}_2 = \begin{bmatrix}\mathbf{0} & \mathbf{K} & -\boldsymbol{\Omega}^{\mathbf{T}}\\ -\mathbf{K} & \mathbf{0} & \mathbf{0}\\ \boldsymbol{\Omega} & \mathbf{0} & \frac{1}{\mathrm{T}_0}\mathbf{M}_{\mathbf{T}}\end{bmatrix}.
\end{gathered} \tag{7.44}$$

Note that $\mathbf{W_1}$ is positive-definite and symmetric, while $\frac{1}{2}(\mathbf{W_2} + \mathbf{W_2^T})$ is positive-semidefinite, implying that coupled linear thermoelasticity is at least marginally stable, whereas a strictly elastic system is strictly marginally stable. Thus, thermal conduction has a stabilizing effect, which can be shown to be analogous to viscous dissipation.

7.4 EXERCISES

1. Express the thermal equilibrium equation in:
   (a) cylindrical coordinates
   (b) spherical coordinates
2. Derive the specific heat at constant stress, rather than at constant strain.
3. Write down the coupled thermal and elastic equations for a one-dimensional member.

8 Introduction to the Finite-Element Method

8.1 INTRODUCTION

In thermomechanical members and structures, finite-element analysis (FEA) is typically invoked to compute displacement and temperature fields from known applied loads and heat fluxes. FEA has emerged in recent years as an essential resource for mechanical and structural designers. Its use is often mandated by standards such as the ASME Pressure Vessel Code, by insurance requirements, and even by law. Its acceptance has benefited from rapid progress in related computer hardware and software, especially computer-aided design (CAD) systems. Today, a number of highly developed, user-friendly finite-element codes are available commercially. The purpose of this chapter is to introduce finite-element theory and practice. The next three chapters focus on linear elasticity and thermal response, both static and dynamic, of basic structural members. After that, nonlinear thermomechanical response is considered.

In FEA practice, a design file developed using CAD is often "imported" into finite-element codes, from which point little or no additional effort is required to develop the finite-element model and perform sophisticated thermomechanical analysis and simulation. CAD integrated with an analysis tool, such as FEA, is an example of computer-aided engineering (CAE). CAE is a powerful resource with the potential of identifying design problems much more efficiently and rapidly than by "trial and error."

A major FEM application is the determination of stresses and temperatures in a component or member in locations where failure is thought most likely. If the stresses or temperatures exceed allowable or safe values, the product can be redesigned and then reanalyzed. Analysis can be diagnostic, supporting interpretation of product-failure data. Analysis also can be used to assess performance, for example, by determining whether the design-stiffness coefficient for a rubber spring is attained.

8.2 OVERVIEW OF THE FINITE-ELEMENT METHOD

Consider a thermoelastic body with force and heat applied to its exterior boundary. The finite-element method serves to determine the displacement vector $\mathbf{u}(\mathbf{X}, t)$ and the temperature $T(\mathbf{X}, t)$ as functions of the undeformed position $\mathbf{X}$ and time t. The process of creating a finite-element model to support the design of a mechanical system can be viewed as having (at least) eight steps:

1. The body is first discretized, i.e., it is modeled as a mesh of finite elements connected at nodes.
2. Within each element, interpolation models are introduced to provide approximate expressions for the unknowns, typically $\mathbf{u}(\mathbf{X}, t)$ and $T(\mathbf{X}, t)$,

in terms of their nodal values, which now become the unknowns in the finite-element model.
3. The strain-displacement relation and its thermal analog are applied to the approximations for **u** and T to furnish approximations for the (Lagrangian) strain and the thermal gradient.
4. The stress-strain relation and its thermal analog (Fourier's Law) are applied to obtain approximations to stress **S** and heat flux **q** in terms of the nodal values of **u** and T.
5. Equilibrium principles in variational form are applied using the various approximations within each element, leading to *element equilibrium equations*.
6. The element equilibrium equations are assembled to provide a *global equilibrium equation*.
7. Prescribed kinematic and temperature conditions on the boundaries (*constraints*) are applied to the global equilibrium equations, thereby reducing the number of degrees of freedom and eliminating "rigid-body" modes.
8. The resulting global equilibrium equations are then solved using computer algorithms.

The output is postprocessed. Initially, the output should be compared to data or benchmarks, or otherwise validated, to establish that the model correctly represents the underlying mechanical system. If not satisfied, the analyst can revise the finite-element model and repeat the computations. When the model is validated, postprocessing, with heavy reliance on graphics, then serves to interpret the results, for example, determining whether the underlying design is satisfactory. If problems with the design are identified, the analyst can then choose to revise the design. The revised design is modeled, and the process of validation and interpretation is repeated.

8.3 MESH DEVELOPMENT

Finite-element simulation has classically been viewed as having three stages: *preprocessing, analysis*, and *postprocessing*. The input file developed at the preprocessing stage consists of several elements:

1. control information (type of analysis, etc.)
2. material properties (e.g., elastic modulus)
3. mesh (element types, nodal coordinates, connectivities)
4. applied force and heat flux data
5. supports and constraints (e.g., prescribed displacements)
6. initial conditions (dynamic problems)

In problems without severe stress concentrations, much of the mesh data can be developed conveniently using automatic-mesh generation. With the input file developed, the analysis processor is activated and "raw" output files are generated. The postprocessor module typically contains (interfaces to) graphical utilities, thus facilitating display of output in the form chosen by the analyst, for example, contours of the Von Mises stress. Two problems arise at this stage: *validation* and *interpretation*.

The analyst can use benchmark solutions, special cases, or experimental data to validate the analysis. With validation, the analyst gains confidence in, for example, the mesh. He or she still may face problems of interpretation, particularly if the output is voluminous. Fortunately, current graphical-display systems make interpretation easier and more reliable, such as by displaying high stress regions in vivid colors. Postprocessors often allow the analyst to "zoom in" on regions of high interest, for example, where rubber is highly confined. More recent methods based on virtual-reality technology enable the analyst to fly through and otherwise become immersed in the model.

The goal of mesh design is to select the number and location of finite-element nodes and element types so that the associated analyses are sufficiently accurate. Several methods include automatic-mesh generation with adaptive capabilities, which serve to produce and iteratively refine the mesh based on a user-selected error tolerance. Even so, satisfactory meshes are not necessarily obtained, so that model editing by the analyst may be necessary. Several practical rules are as follows:

1. Nodes should be located where concentrated loads and heat fluxes are applied.
2. Nodes should be located where displacements and temperatures are constrained or prescribed in a concentrated manner, for example, where "pins" prevent movement.
3. Nodes should be located where concentrated springs and masses and their thermal analogs are present.
4. Nodes should be located along lines and surface patches, over which pressures, shear stresses, compliant foundations, distributed heat fluxes, and surface convection are applied.
5. Nodes should be located at boundary points where the applied tractions and heat fluxes experience discontinuities.
6. Nodes should be located along lines of symmetry.
7. Nodes should be located along interfaces between different materials or components.
8. Element-aspect ratios (ratio of largest to smallest element dimensions) should be no greater than, for example, five.
9. Symmetric configurations should have symmetric meshes.
10. The density of elements should be greater in domains with higher gradients.
11. Interior angles in elements should not be excessively acute or obtuse, for example, less than 45° or greater than 135°.
12. Element-density variations should be gradual rather than abrupt.
13. Meshes should be uniform in subdomains with low gradients.
14. Element orientations should be staggered to prevent "bias."

In modeling a configuration, a good practice is initially to develop the mesh locally in domains expected to have high gradients, and thereafter to develop the mesh in the intervening low-gradient domains, thereby "reconciling" the high-gradient domains.

There are two classes of errors in finite-element analysis:

Modeling error ensues from inaccuracies in such input data as the material properties, boundary conditions, and initial values. In addition, there often are compromises in the mesh, for example, modeling sharp corners as rounded.

Numerical error is primarily due to truncation and round-off. As a practical matter, error in a finite-element simulation is often assessed by comparing solutions from two meshes, the second of which is a refinement of the first.

The sensitivity of finite-element computations to error is to some extent controllable. If the condition number of the stiffness matrix (the ratio of the maximum to the minimum eigenvalue) is modest, sensitivity is reduced. Typically, the condition number increases rapidly as the number of nodes in a system grows. In addition, highly irregular meshes tend to produce high-condition numbers. Models mixing soft components, for example, rubber, with stiff components, such as steel plates, are also likely to have high-condition numbers. Where possible, the model should be designed to reduce the condition number.

9 Element Fields in Linear Problems

This chapter presents interpolation models in physical coordinates for the most part, for the sake of simplicity and brevity. However, in finite-element codes, the physical coordinates are replaced by natural coordinates using relations similar to interpolation models. Natural coordinates allow use of Gaussian quadrature for integration and, to some extent, reduce the sensitivity of the elements to geometric details in the physical mesh. Several examples of the use of natural coordinates are given.

9.1 INTERPOLATION MODELS

9.1.1 One-Dimensional Members

9.1.1.1 Rods

The governing equation for the displacements in rods (also bars, tendons, and shafts) is

$$\mathrm{E}A\frac{\partial^2 u}{\partial x^2} = \rho A\frac{\partial^2 u}{\partial t^2}, \tag{9.1}$$

in which $u(x, t)$ denotes the radial displacement, E, A and ρ are constants, x is the spatial coordinate, and t denotes time. Since the displacement is governed by a second-order differential equation, in the spatial domain, it requires two (time-dependent) constants of integration. Applied to an element, the two constants can be supplied implicitly using two nodal displacements as functions of time. We now approximate $u(x, t)$ using its values at x_e and x_{e+1}, as shown in Figure 9.1.

The lowest-order interpolation model consistent with two integration constants is linear, in the form

$$u(x,t) = \boldsymbol{\varphi}_{m1}^T(x)\boldsymbol{\Phi}_{m1}\boldsymbol{\gamma}_{m1}(t), \quad \boldsymbol{\gamma}_{m1}(t) = \begin{pmatrix} u_e(t) \\ u_{e+1}(t) \end{pmatrix}, \quad \boldsymbol{\varphi}_{m1}^T(x) = (1 \quad x). \tag{9.2}$$

We seek to identify $\boldsymbol{\Phi}_{\mathrm{m1}}$ in terms of the nodal values of u. Letting $u_e = u(x_e)$ and $u_{e+1} = u(x_{e+1})$, furnishes

$$u_e(t) = (1 \quad x_e)\boldsymbol{\Phi}_{m1}\boldsymbol{\gamma}_{m1}(t), \quad u_{e+1}(t) = \begin{pmatrix} 1 & x_{e+1} \end{pmatrix}\boldsymbol{\Phi}_{m1}\boldsymbol{\gamma}_{m1}(t). \tag{9.3}$$

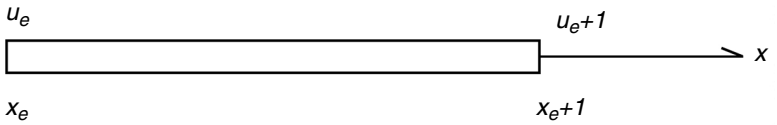

FIGURE 9.1 Rod element.

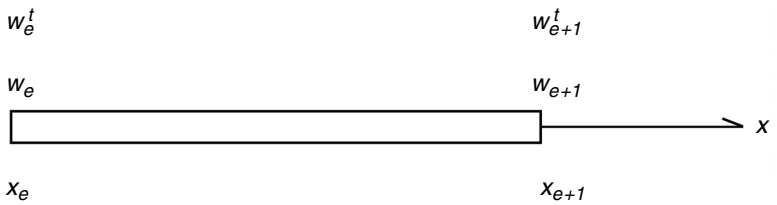

FIGURE 9.2 Beam element.

However, from the meaning of $\boldsymbol{\gamma}_{m1}(t)$, we conclude that

$$\boldsymbol{\Phi}_{m1} = \begin{bmatrix} 1 & x_e \\ 1 & x_{e+1} \end{bmatrix}^{-1} = \frac{1}{l_e}\begin{bmatrix} x_{e+1} & -x_e \\ -1 & 1 \end{bmatrix}, \qquad l_e = x_{e+1} - x_e. \tag{9.4}$$

9.1.1.2 Beams

The equation for a beam, following Euler-Bernoulli theory, is:

$$\mathrm{E}I\frac{\partial^4 w}{\partial x^4} + \rho A\frac{\partial^2 u}{\partial t^2} = 0, \tag{9.5}$$

in which $w(x, t)$ denotes the transverse displacement of the beam's neutral axis, and I is a constant. In the spatial domain, there are four constants of integration. In an element, they can be supplied implicitly by the values of w and $w' = \partial w/\partial x$ at each of the two element nodes. Referring to Figure 9.2, we introduce the interpolation model for $w(x, t)$:

$$w(x,t) = \boldsymbol{\varphi}_{b1}^{\mathbf{T}}(x)\boldsymbol{\Phi}_{b1}\boldsymbol{\gamma}_{b1}(t), \qquad \boldsymbol{\varphi}_{b1}^{\mathbf{T}}(x) = \begin{pmatrix} 1 & x & x^2 & x^3 \end{pmatrix}, \qquad \boldsymbol{\gamma}_{m1}(t) = \begin{pmatrix} w_e \\ -w_e' \\ w_{e+1} \\ -w_{e+1}' \end{pmatrix}. \tag{9.6}$$

Enforcing this model at x_e and at x_{e+1} furnishes

$$\mathbf{\Phi}_{\mathrm{b1}} = \begin{bmatrix} 1 & x_e & x_e^2 & x_e^3 \\ 0 & -1 & -2x_e & -3x_e^2 \\ 1 & x_{e+1} & x_{e+1}^2 & x_{e+1}^3 \\ 0 & -1 & -2x_{e+1} & -3x_{e+1}^2 \end{bmatrix}^{-1}. \tag{9.7}$$

9.1.1.3 Beam Columns

Beam columns are of interest, among other reasons, in predicting buckling according to the Euler criterion. The z–displacement w of the neutral axis is assumed to depend only on x and the x–displacement. Also, u is modeled as

$$u(x,\, z) = u_0(x) - z\frac{\partial w(x)}{\partial x}, \tag{9.8}$$

in which $u_0(x)$ represents the stretching of the neutral axis. It is necessary to know $u_0(x)$, $w(x)$ and $\frac{\partial w(x)}{\partial x}$ at x_e and x_{e+1}. The interpolation model is now

$$u(x,\, z,\, t) = (1 \quad x)\mathbf{\Phi}_{m1}\boldsymbol{\gamma}_{m1} - z(1 \quad x \quad x^2 \quad x^3)\mathbf{\Phi}_{b1}\boldsymbol{\gamma}_{b1}, \tag{9.9}$$

$$\boldsymbol{\gamma}_{m1} = \begin{pmatrix} u_e(t) \\ u_{e+1}(t) \end{pmatrix}, \quad \boldsymbol{\gamma}_{b1} = \begin{pmatrix} w_e \\ -w_e' \\ w_{e+1} \\ -w_{e+1}' \end{pmatrix},$$

and

$$\mathbf{\Phi}_{\mathrm{m1}} = \frac{1}{l_e}\begin{bmatrix} x_{e+1} & -x_e \\ -1 & 1 \end{bmatrix}, \quad \mathbf{\Phi}_{\mathrm{b1}} = \begin{bmatrix} 1 & x_e & x_e^2 & x_e^3 \\ 0 & -1 & -2x_e & -3x_e^2 \\ 1 & x_{e+1} & x_{e+1}^2 & x_{e+1}^3 \\ 0 & -1 & -2x_{e+1} & -3x_{e+1}^2 \end{bmatrix}^{-1}.$$

9.1.1.4 Temperature Model: One Dimension

The temperature variable to be determined is $\mathrm{T} - \mathrm{T}_0$, in which T_0 is a reference temperature assumed to be independent of x. The governing equation for a one-dimensional conductor is

$$kA\frac{\partial^2 \mathrm{T}}{\partial x^2} = \rho A c_e \frac{\partial \mathrm{T}}{\partial t}. \tag{9.10}$$

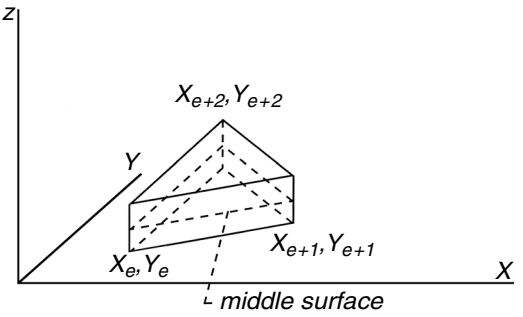

FIGURE 9.3 Triangular plate element.

This equation is formally the same as for a rod equation (see Equation 9.1), furnishing the interpolation model for the element as

$$\mathrm{T}(x,\ t) - \mathrm{T}_0 = \boldsymbol{\varphi}_{m1}^{\mathbf{T}}(x)\boldsymbol{\Phi}_{m1}\boldsymbol{\theta}_1(t), \qquad \boldsymbol{\theta}_1(t) = \begin{pmatrix} \mathrm{T}_e(t) - \mathrm{T}_0 \\ \mathrm{T}_{e+1}(t) - \mathrm{T}_0 \end{pmatrix}. \tag{9.11}$$

9.1.2 Interpolation Models: Two Dimensions

9.1.2.1 Membrane Plate

Now suppose that the displacements $u(x, y, t)$ and $v(x, y, t)$ are modeled on the triangular plate element in Figure 9.3, using the values $u_e(t)$, $v_e(t)$, $u_{e+1}(t)$, $v_{e+1}(t)$, $u_{e+2}(t)$, and $v_{e+2}(t)$. This element arises in plane stress and plane strain, and is called a membrane plate element. A linear model suffices for each quantity because it provides three coefficients to match three nodal values. The interpolation model now is

$$\begin{pmatrix} u(x, y, t) \\ v(x, y, t) \end{pmatrix} = \begin{bmatrix} \boldsymbol{\varphi}_{m2}^{\mathbf{T}} & \mathbf{0}^{\mathbf{T}} \\ \mathbf{0}^{\mathbf{T}} & \boldsymbol{\varphi}_{m2}^{\mathbf{T}} \end{bmatrix} \begin{bmatrix} \boldsymbol{\Phi}_{m2}^{\mathbf{T}} & \mathbf{0}^{\mathbf{T}} \\ \mathbf{0}^{\mathbf{T}} & \boldsymbol{\Phi}_{m2}^{\mathbf{T}} \end{bmatrix} \begin{pmatrix} \boldsymbol{\gamma}_u(t) \\ \boldsymbol{\gamma}_v(t) \end{pmatrix} \tag{9.12}$$

$$\boldsymbol{\gamma}_{\mathrm{u}}(t) = \begin{pmatrix} u_e(t) \\ u_{e+1}(t) \\ u_{e+2}(t) \end{pmatrix}, \quad \boldsymbol{\gamma}_{\mathrm{v}}(t) = \begin{pmatrix} v_e(t) \\ v_{e+1}(t) \\ v_{e+2}(t) \end{pmatrix}, \quad \boldsymbol{\varphi}_{\mathrm{m2}} = \begin{pmatrix} 1 \\ x \\ y \end{pmatrix}, \quad \boldsymbol{\Phi}_{\mathrm{m2}}^{\mathbf{T}} = \begin{bmatrix} 1 & x_e & y_e \\ 1 & x_{e+1} & y_{e+1} \\ 1 & x_{e+2} & y_{e+2} \end{bmatrix}^{-1}.$$

9.1.2.2 Plate with Bending Stresses

In a plate element experiencing bending only, the in-plane displacements, u and v, are expressed by

$$u(x, y, z, t) = -z\frac{\partial w}{\partial x}, \quad v(x, y, z, t) = -z\frac{\partial w}{\partial y}, \tag{9.13}$$

in which $z = 0$ at the middle plane. The out-of-plane displacement, w, is assumed to be a function of x and y only.

An example of an interpolation model is introduced as follows to express $w(x, y)$ throughout the element in terms of the nodal values of w, $\frac{\partial w}{\partial x}$ and $\frac{\partial w}{\partial y}$:

$$w(x,y,t) = \boldsymbol{\varphi}_{b2}^{\mathbf{T}}(x,y)\boldsymbol{\Phi}_{b2}\boldsymbol{\gamma}_{b2}(t) \tag{9.14}$$

$$\boldsymbol{\varphi}_{b2}^{\mathbf{T}}(x,y) = \begin{pmatrix} 1 & x & y & x^2 & xy & y^2 & x^3 & \frac{1}{2}(x^2y + y^2x) & y^3 \end{pmatrix}$$

$$\boldsymbol{\gamma}_{b2}^{\mathbf{T}}(t) = \begin{pmatrix} w_e & -\left(\frac{\partial w}{\partial x}\right)_e & -\left(\frac{\partial w}{\partial y}\right)_e & w_{e+1} & -\left(\frac{\partial w}{\partial x}\right)_{e+1} \\ -\left(\frac{\partial w}{\partial y}\right)_{e+1} & w_{e+2} & -\left(\frac{\partial w}{\partial x}\right)_{e+2} & -\left(\frac{\partial w}{\partial y}\right)_{e+2} \end{pmatrix}$$

$$\boldsymbol{\Phi}_{b2}^{-1} = \begin{bmatrix} 1 & x_e & y_e & x_e^2 & x_e y_e & y_e^2 & x_e^3 & \frac{1}{2}x_e y_e(x_e + y_e) & y_e^3 \\ 0 & -1 & 0 & -2x_e & -y_e & 0 & -3x_e^2 & -(x_e y_e + \frac{1}{2}y_e^2) & 0 \\ 0 & 0 & -1 & 0 & -x_e & -2x_e & 0 & -(\frac{1}{2}x_e^2 + x_e y_e) & -3y_e^2 \\ 1 & x_{e+1} & y_{e+1} & x_{e+1}^2 & x_{e+1}y_{e+1} & y_{e+1}^2 & x_{e+1}^3 & \frac{1}{2}x_{e+1}y_{e+1}(x_{e+1} + y_{e+1}) & y_{e+1}^3 \\ 0 & -1 & 0 & -2x_{e+1} & -y_{e+1} & 0 & -3x_{e+1}^2 & -(x_{e+1}y_{e+1} + \frac{1}{2}y_{e+1}^2) & 0 \\ 0 & 0 & -1 & 0 & -x_{e+1} & -2y_{e+1} & 0 & -(\frac{1}{2}x_{e+1}^2 + x_{e+1}y_{e+1}) & -3y_{e+1}^2 \\ 1 & x_{e+2} & y_{e+2} & x_{e+2}^2 & x_{e+2}y_{e+2} & y_{e+2}^2 & x_{e+2}^3 & \frac{1}{2}x_{e+2}y_{e+2}(x_{e+2} + y_{e+2}) & y_{e+2}^3 \\ 0 & -1 & 0 & -2x_{e+2} & -y_{e+2} & 0 & -3x_{e+2}^2 & -(x_{e+2}y_{e+2} + \frac{1}{2}y_{e+2}^2) & 0 \\ 0 & 0 & -1 & 0 & -x_{e+2} & -2y_{e+2} & 0 & -(\frac{1}{2}x_{e+2}^2 + x_{e+2}y_{e+2}) & -3y_{e+2}^2 \end{bmatrix}.$$

It follows that

$$\begin{pmatrix} \mathrm{u(x,\ y,\ z,\ t)} \\ \mathrm{v(x,\ y,\ z,\ t)} \\ \mathrm{w(x,\ y,\ z,\ t)} \end{pmatrix} = \begin{pmatrix} -\mathrm{z}\dfrac{\partial \boldsymbol{\varphi}_{\mathrm{b2}}^{\mathbf{T}}}{\partial \mathrm{x}} \\ -\mathrm{z}\dfrac{\partial \boldsymbol{\varphi}_{\mathrm{b2}}^{\mathbf{T}}}{\partial \mathrm{y}} \\ \boldsymbol{\varphi}_{\mathrm{b2}}^{\mathbf{T}} \end{pmatrix} \boldsymbol{\Phi}_{\mathrm{b2}}\boldsymbol{\gamma}_{\mathrm{b2}}(\mathrm{t}). \tag{9.15}$$

9.1.2.3 Plate with Stretching and Bending

Finally, for a plate experiencing both stretching and bending, the displacements are assumed to satisfy

$$u(x,\ y,\ z,\ t) = u_0(x,\ y,\ z,\ t) - z\frac{\partial w}{\partial x}, \qquad v(x,\ y,\ z,\ t) = v_0(x,\ y,\ z,\ t) - z\frac{\partial w}{\partial y} \tag{9.16}$$

and w is a function only of x, y, and t(not z). Here, $z = 0$ at the middle surface, while u_0 and v_0 represent the in-plane displacements. Using the nodal values of u_0, v_0, and w_0, a combined interpolation model is obtained as

$$\begin{pmatrix} u(x, y, z, t) \\ v(x, y, z, t) \\ w(x, y, z, t) \end{pmatrix} = \begin{pmatrix} u_0(x, y, t) \\ v_0(x, y, t) \\ w_0(x, y, t) \end{pmatrix} + \begin{pmatrix} -z\dfrac{\partial \boldsymbol{\varphi}_{b2}^{\mathbf{T}}}{\partial x} \\ -z\dfrac{\partial \boldsymbol{\varphi}_{b2}^{\mathbf{T}}}{\partial y} \\ \boldsymbol{\varphi}_{b2}^{\mathbf{T}} \end{pmatrix} \boldsymbol{\Phi}_{b2}\boldsymbol{\gamma}_{b2}(t)$$

$$= \begin{bmatrix} \boldsymbol{\varphi}_{m2}^{\mathbf{T}} & \mathbf{0}^{\mathbf{T}} & -z\dfrac{\partial \boldsymbol{\varphi}_{b2}^{\mathbf{T}}}{\partial x} \\ \mathbf{0}^{\mathbf{T}} & \boldsymbol{\varphi}_{m2}^{\mathbf{T}} & -z\dfrac{\partial \boldsymbol{\varphi}_{b2}^{\mathbf{T}}}{\partial y} \\ \mathbf{0}^{\mathbf{T}} & \mathbf{0}^{\mathbf{T}} & \boldsymbol{\varphi}_{b2}^{\mathbf{T}} \end{bmatrix} \begin{bmatrix} \boldsymbol{\Phi}_{m2} & \mathbf{0} & \mathbf{0} \\ \mathbf{0} & \boldsymbol{\Phi}_{m2} & \mathbf{0} \\ \mathbf{0} & \mathbf{0} & \boldsymbol{\Phi}_{b2} \end{bmatrix} \begin{pmatrix} \boldsymbol{\gamma}_u(t) \\ \boldsymbol{\gamma}_v(t) \\ \boldsymbol{\gamma}_w(t) \end{pmatrix}. \quad (9.17)$$

9.1.2.4 Temperature Field in Two Dimensions

In the two-dimensional, triangular element illustrated in Figure 9.3, the linear interpolation model for the temperature is

$$\mathrm{T} - \mathrm{T}_0 = \boldsymbol{\varphi}_{m2}^{\mathbf{T}}\boldsymbol{\Phi}_{m2}\boldsymbol{\theta}_2, \qquad \boldsymbol{\theta}_2^{\mathbf{T}} = (\mathrm{T}_e - \mathrm{T}_0 \quad \mathrm{T}_{e+1} - \mathrm{T}_0 \quad \mathrm{T}_{e+2} - \mathrm{T}_0). \quad (9.18)$$

9.1.2.5 Axisymmetric Elements

An axisymmetric element is displayed in Figure 9.4. It is applicable to bodies that are axisymmetric and are submitted to axisymmetric loads, such as all-around pressure. The radial displacement is denoted by u, and the axial displacement is denoted by w. The tangential displacement v vanishes, while radial and axial displacements are independent of θ. Now u and w depend on r, z, and t.

There are two distinct situations that require distinct interpolation models. In the first case, none of the nodes are on the axis of revolution ($r = 0$), while in the second case, one or two nodes are, in fact, on the axis. In the first case, the linear

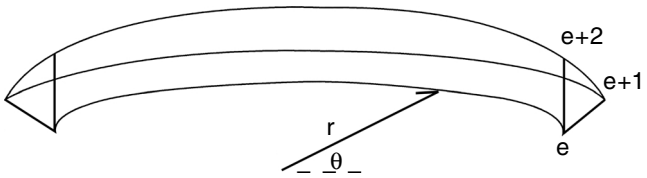

FIGURE 9.4 Axisymmetric element.

interpolation model is given by

$$\begin{pmatrix} u(r,\,z,\,t) \\ w(r,\,z,\,t) \end{pmatrix} = \begin{bmatrix} \boldsymbol{\varphi}_{a1}^{\mathbf{T}} & \mathbf{0}^{\mathbf{T}} \\ \mathbf{0}^{\mathbf{T}} & \boldsymbol{\varphi}_{a1}^{\mathbf{T}} \end{bmatrix} \begin{bmatrix} \boldsymbol{\Phi}_{a1}^{\mathbf{T}} & \mathbf{0}^{\mathbf{T}} \\ \mathbf{0}^{\mathbf{T}} & \boldsymbol{\Phi}_{a1}^{\mathbf{T}} \end{bmatrix} \begin{pmatrix} \boldsymbol{\gamma}_{ua1}(t) \\ \boldsymbol{\gamma}_{wa1}(t) \end{pmatrix}. \tag{9.19}$$

$$\boldsymbol{\varphi}_{a1}^{\mathbf{T}} = (1 \quad r \quad z), \quad \boldsymbol{\Phi}_{a1} = \begin{bmatrix} 1 & r_e & z_e \\ 1 & r_{e+1} & z_{e+1} \\ 1 & r_{e+2} & z_{e+2} \end{bmatrix}^{-1}, \quad \boldsymbol{\gamma}_{ua1} = \begin{pmatrix} u_e \\ u_{e+1} \\ u_{e+2} \end{pmatrix}, \quad \boldsymbol{\gamma}_{wa1} = \begin{pmatrix} w_e \\ w_{e+1} \\ w_{e+2} \end{pmatrix}$$

Now suppose that there are nodes on the axis, and note that the radial displacements are constrained to vanish on the axis. For reasons shown later, it is necessary to enforce the symmetry constraints *a priori* in the formulation of the displacement model. In particular, suppose that node e is on the axis, with nodes $e + 1$ and $e + 2$ defined counterclockwise at the other vertices. The linear interpolation model is now

$$\begin{pmatrix} u(r,\,z,\,t) \\ w(r,\,z,\,t) \end{pmatrix} = \begin{bmatrix} \boldsymbol{\varphi}_{a2}^{\mathbf{T}} & \mathbf{0}^{\mathbf{T}} \\ \mathbf{0}^{\mathbf{T}} & \boldsymbol{\varphi}_{a2}^{\mathbf{T}} \end{bmatrix} \begin{bmatrix} \boldsymbol{\Phi}_{a2}^{\mathbf{T}} & \mathbf{0}^{\mathbf{T}} \\ \mathbf{0}^{\mathbf{T}} & \boldsymbol{\Phi}_{a2}^{\mathbf{T}} \end{bmatrix} \begin{pmatrix} \boldsymbol{\gamma}_{ua2}(t) \\ \boldsymbol{\gamma}_{wa2}(t) \end{pmatrix} \tag{9.20}$$

$$\boldsymbol{\varphi}_{a2}^{\mathbf{T}} = (r \quad z - z_e), \quad \boldsymbol{\Phi}_{a2} = \begin{bmatrix} r_{e+1} & z_{e+1} - z_e \\ r_{e+2} & z_{e+2} - z_e \end{bmatrix}^{-1}.$$

A similar formulation can be used if two nodes are on the axis of symmetry so that the u displacement in the element is modeled using only one nodal displacement, with a coefficient vanishing at each of the nodes on the axis of revolution.

9.1.3 Interpolation Models: Three Dimensions

We next consider the tetrahedron illustrated in Figure 9.5.

A linear interpolation model for the temperature can be expressed as

$$\mathrm{T} - \mathrm{T}_0 = \boldsymbol{\varphi}_{3T}^{\mathbf{T}} \boldsymbol{\Phi}_{3T} \boldsymbol{\theta}_3 \tag{9.21}$$

$$\boldsymbol{\varphi}_{3\mathrm{T}}^{\mathbf{T}} = (1 \quad x \quad y \quad z)$$

$$\boldsymbol{\Phi}_{3\mathrm{T}} = \begin{bmatrix} 1 & x_e & y_e & z_e \\ 1 & x_{e+1} & y_{e+1} & z_{e+1} \\ 1 & x_{e+2} & y_{e+2} & z_{e+2} \\ 1 & x_{e+3} & y_{e+3} & z_{e+3} \end{bmatrix}^{-1}$$

$$\theta_{3\mathrm{T}}^{\mathrm{T}} = \{\mathrm{T}_e - \mathrm{T}_o \quad \mathrm{T}_{e+1} - \mathrm{T}_o \quad \mathrm{T}_{e+2} - \mathrm{T}_o \quad \mathrm{T}_{e+3} - \mathrm{T}_o\}$$

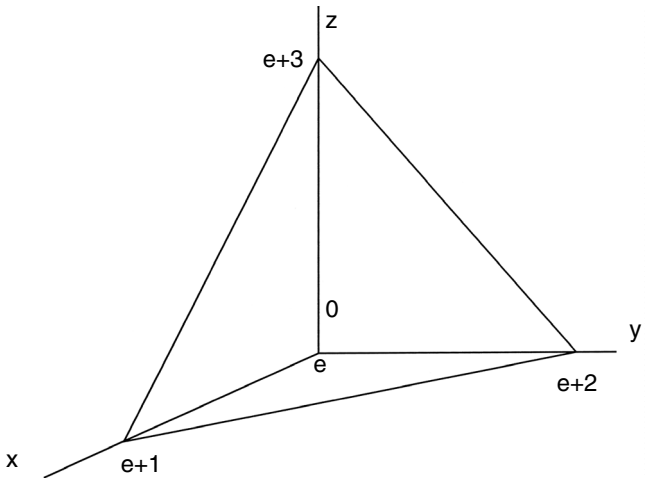

FIGURE 9.5 Tetrahedral element.

For elasticity with displacements u, v, and w, the corresponding interpolation model is

$$\begin{pmatrix} u(x, y, z, t) \\ v(x, y, z, t) \\ w(x, y, z, t) \end{pmatrix} = \begin{bmatrix} \boldsymbol{\varphi}_3^{\mathbf{T}} & \mathbf{0}^{\mathbf{T}} & \mathbf{0}^{\mathbf{T}} \\ \mathbf{0}^{\mathbf{T}} & \boldsymbol{\varphi}_3^{\mathbf{T}} & \mathbf{0}^{\mathbf{T}} \\ \mathbf{0}^{\mathbf{T}} & \mathbf{0}^{\mathbf{T}} & \boldsymbol{\varphi}_3^{\mathbf{T}} \end{bmatrix} \begin{bmatrix} \boldsymbol{\Phi}_3 & \mathbf{0} & \mathbf{0} \\ \mathbf{0} & \boldsymbol{\Phi}_3 & \mathbf{0} \\ \mathbf{0} & \mathbf{0} & \boldsymbol{\Phi}_3 \end{bmatrix} \begin{pmatrix} \boldsymbol{\gamma}_u(t) \\ \boldsymbol{\gamma}_v(t) \\ \boldsymbol{\gamma}_w(t) \end{pmatrix} \tag{9.22}$$

$$\boldsymbol{\gamma}_u(t) = \begin{pmatrix} u_e(t) \\ u_{e+1}(t) \\ u_{e+2}(t) \\ u_{e+3}(t) \end{pmatrix}, \quad \boldsymbol{\gamma}_v(t) = \begin{pmatrix} v_e(t) \\ v_{e+1}(t) \\ v_{e+2}(t) \\ v_{e+3}(t) \end{pmatrix}, \quad \boldsymbol{\gamma}_w(t) = \begin{pmatrix} w_e(t) \\ w_{e+1}(t) \\ w_{e+2}(t) \\ w_{e+3}(t) \end{pmatrix}$$

9.2 STRAIN-DISPLACEMENT RELATIONS AND THERMAL ANALOGS

9.2.1 Strain-Displacement Relations: One Dimension

For the rod, the strain is given by $\varepsilon = E_{11} = \frac{\partial u}{\partial x}$. An estimate for ε implied by the interpolation model in Equation 9.3 has the form

$$\varepsilon(x, t) = \boldsymbol{\beta}_{\mathrm{m1}}^{\mathbf{T}}(x)\boldsymbol{\Phi}_{\mathrm{m1}}\boldsymbol{\gamma}_{\mathrm{m1}}(\mathrm{t}), \tag{9.23}$$

$$\boldsymbol{\beta}_{m1}^{\mathbf{T}} = \frac{d\boldsymbol{\varphi}_{m1}^{\mathbf{T}}}{dx} = (0 \quad 1)$$

For the beam, the corresponding relation is

$$\varepsilon(x,\, z,\, t) = -z\frac{\partial w}{\partial x}, \tag{9.24}$$

from which the consistent approximation is obtained:

$$\varepsilon(x,z,t) = -z\boldsymbol{\beta}_{b1}^{\mathbf{T}}(x)\boldsymbol{\Phi}_{b1}\boldsymbol{\gamma}_{b1}(\mathrm{t}), \tag{9.25}$$

$$\boldsymbol{\beta}_{b1}^{\mathbf{T}} = \frac{d\boldsymbol{\varphi}_{b1}^{\mathbf{T}}}{dx} = (0 \quad 1 \quad 2x \quad 3x^2)$$

For the beam column, the strain is given by

$$\varepsilon(x,\, z,\, t) = -z\boldsymbol{\beta}_{\mathrm{m}b1}^{\mathbf{T}}(x)\boldsymbol{\Phi}_{\mathrm{m}b1}\boldsymbol{\gamma}_{\mathrm{m}b1}(\mathrm{t}), \tag{9.26}$$

$$\boldsymbol{\beta}_{mb1}^{\mathbf{T}} = \begin{pmatrix}\boldsymbol{\beta}_{m1}^{\mathbf{T}} & -z\boldsymbol{\beta}_{b1}^{\mathbf{T}}\end{pmatrix}\begin{bmatrix}\boldsymbol{\Phi}_{m1} & \mathbf{0}\\ \mathbf{0} & \boldsymbol{\Phi}_{mb1}\end{bmatrix}\begin{pmatrix}\boldsymbol{\gamma}_{m1}(t)\\ \boldsymbol{\gamma}_{b1}(t)\end{pmatrix}$$

9.2.2 Strain-Displacement Relations: Two Dimensions

In two dimensions, the (linear) strain tensor is given by

$$\boldsymbol{E}(x,\, y) = \begin{bmatrix}E_{xx} & E_{xy}\\ E_{xy} & E_{yy}\end{bmatrix} = \begin{bmatrix}\frac{\partial u}{\partial x} & \frac{1}{2}\left(\frac{\partial u}{\partial y} + \frac{\partial v}{\partial x}\right)\\ \frac{1}{2}\left(\frac{\partial u}{\partial y} + \frac{\partial v}{\partial x}\right) & \frac{\partial v}{\partial y}\end{bmatrix}. \tag{9.27}$$

We will see later the two important cases of plane stress and plane strain. In the latter case, E_{zz} vanishes and s_{zz} is not needed to achieve a solution. In the former case, s_{zz} vanishes and E_{zz} is not needed for solution.

In traditional finite-element notation, we obtain [cf. (Zienkiewicz and Taylor, 1989)]

$$\boldsymbol{\varepsilon}' = \begin{pmatrix}E_{xx}\\ E_{yy}\\ E_{xy}\end{pmatrix} = \boldsymbol{\beta}_{\mathrm{m}2}^{\mathrm{T}}\hat{\boldsymbol{\Phi}}_{\mathrm{m}2}\begin{pmatrix}\boldsymbol{\gamma}_{\mathrm{u}2}\\ \boldsymbol{\gamma}_{\mathrm{v}2}\end{pmatrix} \tag{9.28}$$

$$\boldsymbol{\beta}_{\mathrm{m2}}^{\mathbf{T}} = \begin{bmatrix} \dfrac{\partial \boldsymbol{\varphi}_{\mathrm{m2}}^{\mathbf{T}}}{\partial \mathrm{x}} & \mathbf{0}^{\mathbf{T}} \\ \mathbf{0}^{\mathbf{T}} & \dfrac{\partial \boldsymbol{\varphi}_{\mathrm{m2}}^{\mathbf{T}}}{\partial \mathrm{y}} \\ \dfrac{1}{2}\dfrac{\partial \boldsymbol{\varphi}_{\mathrm{m2}}^{\mathbf{T}}}{\partial \mathrm{y}} & \dfrac{1}{2}\dfrac{\partial \boldsymbol{\varphi}_{\mathrm{m2}}^{\mathbf{T}}}{\partial \mathrm{x}} \end{bmatrix}, \quad \hat{\boldsymbol{\Phi}}_{\mathrm{m2}} = \begin{bmatrix} \boldsymbol{\Phi}_{\mathrm{m2}} & \mathbf{0} \\ \mathbf{0} & \boldsymbol{\Phi}_{\mathrm{m2}} \end{bmatrix}$$

The prime in $\mathbf{e}'$ is introduced temporarily to call attention to the fact that it does not equal $VEC(\boldsymbol{E}_{\mathrm{L}})$. Hereafter, the prime will not be displayed.

For a plate with bending stresses only,

$$\boldsymbol{e}'(x,\ y,\ z,\ t) = -z \begin{pmatrix} \dfrac{\partial^2 w}{\partial x^2} \\ \dfrac{\partial^2 w}{\partial y^2} \\ \dfrac{\partial^2 w}{\partial x \partial y} \end{pmatrix}, \tag{9.29}$$

from which

$$\boldsymbol{e}'(x,\ y,\ z,\ t) = -z\boldsymbol{\beta}_{b2}^{T}(x)\boldsymbol{\Phi}_{b2}\boldsymbol{\gamma}_{b2}(t), \quad \boldsymbol{\beta}_{b2} = \begin{pmatrix} \dfrac{\partial^2 \boldsymbol{\varphi}_{b2}^{T}}{\partial x^2} \\ \dfrac{\partial^2 \boldsymbol{\varphi}_{b2}^{T}}{\partial y^2} \\ \dfrac{\partial^2 \boldsymbol{\varphi}_{b2}^{T}}{\partial x \partial y} \end{pmatrix}. \tag{9.30}$$

For a plate experiencing both membrane and bending stresses, the relations can be combined to furnish

$$\boldsymbol{e}'(x,\ y,\ z,\ t) = \boldsymbol{\beta}_{mb2}^{\mathbf{T}}(x,\ y,\ z)\boldsymbol{\Phi}_{mb2}\boldsymbol{\gamma}_{mb2}(t) \tag{9.31}$$

$$\boldsymbol{\beta}_{\mathrm{mb2}}^{\mathbf{T}} = \begin{pmatrix} \boldsymbol{\beta}_{\mathrm{m2}}^{\mathbf{T}} & -z\boldsymbol{\beta}_{\mathrm{b2}}^{\mathbf{T}} \end{pmatrix}, \quad \boldsymbol{\Phi}_{\mathrm{mb2}} = \begin{bmatrix} \boldsymbol{\Phi}_{\mathrm{m2}} & \mathbf{0} \\ \mathbf{0} & \boldsymbol{\Phi}_{\mathrm{b2}} \end{bmatrix}, \quad \boldsymbol{\gamma}_{\mathrm{mb2}}(\mathrm{t}) = \begin{pmatrix} \boldsymbol{\gamma}_{\mathrm{m2}}(\mathrm{t}) \\ \boldsymbol{\gamma}_{\mathrm{b2}}(\mathrm{t}) \end{pmatrix}$$

9.2.3 Axisymmetric Element on Axis of Revolution

For the toroidal element with a triangular cross section, it is necessary to consider two cases. If there are no nodes on the axis of revolution, then

$$\boldsymbol{e}(r,\ z,\ t) = \begin{pmatrix} \dfrac{\partial u}{\partial r} \\ \dfrac{u}{r} \\ \dfrac{\partial w}{\partial z} \\ \dfrac{1}{2}\left(\dfrac{\partial u}{\partial z} + \dfrac{\partial w}{\partial r}\right) \end{pmatrix} = \boldsymbol{\beta}_{a1}^{\mathbf{T}} \begin{bmatrix} \boldsymbol{\Phi}_{a1} & \mathbf{0} \\ \mathbf{0} & \boldsymbol{\Phi}_{a1} \end{bmatrix} \begin{pmatrix} \boldsymbol{\gamma}_{ua1}(t) \\ \boldsymbol{\gamma}_{wa1}(t) \end{pmatrix} \tag{9.32}$$

$$\boldsymbol{\beta}_{a1}^{\mathbf{T}} = \begin{bmatrix} 0 & 1 & 0 & 0 & 0 & 0 \\ \frac{1}{2} & 1 & \frac{z}{r} & 0 & 0 & 0 \\ 0 & 0 & 0 & 0 & 0 & 1 \\ 0 & 0 & \frac{1}{2} & 0 & \frac{1}{2} & 0 \end{bmatrix}$$

in which the prime is no longer displayed. If element e is now located on the axis of revolution, we obtain

$$\boldsymbol{e}(r, z, t) = \boldsymbol{b}_{a2}^{\mathbf{T}} \begin{bmatrix} \boldsymbol{\Phi}_{a2} & \mathbf{0} \\ \mathbf{0} & \boldsymbol{\Phi}_{a1} \end{bmatrix} \begin{pmatrix} \boldsymbol{\gamma}_{ua2}(t) \\ \boldsymbol{\gamma}_{wa1}(t) \end{pmatrix} \tag{9.33}$$

$$\boldsymbol{\beta}_{a2}^{\mathbf{T}} = \begin{bmatrix} 1 & 0 & 0 & 0 & 0 \\ 1 & \frac{z-z_e}{r} & 0 & 0 & 0 \\ 0 & 0 & 0 & 0 & 1 \\ 0 & \frac{1}{2} & 0 & \frac{1}{2} & 0 \end{bmatrix}$$

9.2.4 Thermal Analog in Two Dimensions

The thermal analog of the strain is the temperature gradient satisfying

$$\nabla \mathrm{T} = \boldsymbol{\beta}_{T2}^{T} \boldsymbol{\Phi}_{T2} \boldsymbol{\theta}_2, \quad \boldsymbol{\beta}_{T2}^{\mathbf{T}} = \begin{bmatrix} 0 & 1 & 0 \\ 0 & 0 & 1 \end{bmatrix}. \tag{9.34}$$

9.2.5 Three-Dimensional Elements

Recalling the tetrahedral element in the previous section, the strain relation can be written as

$$\boldsymbol{e} = \begin{pmatrix} E_{xx} \\ E_{yy} \\ E_{zz} \\ E_{xy} \\ E_{yz} \\ E_{zx} \end{pmatrix} = \begin{pmatrix} \frac{\partial u}{\partial x} \\ \frac{\partial v}{\partial y} \\ \frac{\partial w}{\partial z} \\ \frac{1}{2}\left(\frac{\partial u}{\partial y} + \frac{\partial v}{\partial x}\right) \\ \frac{1}{2}\left(\frac{\partial v}{\partial z} + \frac{\partial w}{\partial y}\right) \\ \frac{1}{2}\left(\frac{\partial w}{\partial x} + \frac{\partial u}{\partial z}\right) \end{pmatrix} = \boldsymbol{\beta}_3^{\mathbf{T}} \begin{bmatrix} \boldsymbol{\Phi}_3 & \mathbf{0} & \mathbf{0} \\ \mathbf{0} & \boldsymbol{\Phi}_3 & \mathbf{0} \\ \mathbf{0} & \mathbf{0} & \boldsymbol{\Phi}_3 \end{bmatrix} \begin{pmatrix} \boldsymbol{\gamma}_{u3} \\ \boldsymbol{\gamma}_{v3} \\ \boldsymbol{\gamma}_{w3} \end{pmatrix} \tag{9.35}$$

9.2.6 Thermal Analog in Three Dimensions

Again referring to the tetrahedral element, the relation for the temperature gradient is

$$\nabla \mathrm{T} = \boldsymbol{\beta}_{3T}^{\mathbf{T}} \Phi_{3T} \boldsymbol{\theta}_3, \qquad \boldsymbol{\beta}_{3T}^{\mathbf{T}} = \begin{bmatrix} 0 & 1 & 0 & 0 & 0 & 0 & 0 & 0 & 0 & 0 & 0 & 0 \\ 0 & 0 & 0 & 0 & 0 & 0 & 1 & 0 & 0 & 0 & 0 & 0 \\ 0 & 0 & 0 & 0 & 0 & 0 & 0 & 0 & 0 & 0 & 0 & 1 \end{bmatrix}. \tag{9.36}$$

9.3 STRESS-STRAIN-TEMPERATURE RELATIONS IN LINEAR THERMOELASTICITY

9.3.1 Overview

If $\boldsymbol{S}$ is the stress tensor under small deformation, the stress-strain relation for a linearly elastic, isotropic solid under small strain is given in Lame's form by

$$\boldsymbol{S} = 2\mu \boldsymbol{E}_L + \lambda tr(\boldsymbol{E}_L)\mathbf{I}, \tag{9.37}$$

in which $\mathbf{I}$ is the identity tensor. The Lame's coefficients are denoted by λ and μ, and are given in terms of the familiar elastic modulus $\mathbf{E}$ and Poisson ratio ν as

$$\mu = \frac{\mathrm{E}}{2(1+\nu)}, \qquad \lambda = \frac{\nu \mathrm{E}}{(1-2\nu)(1+\nu)}. \tag{9.38}$$

Letting $\boldsymbol{s} = VEC(\boldsymbol{S})$ and $\mathbf{e} = VEC(\boldsymbol{E}_L)$, the stress-strain relations are written using Kronecker product operators as

$$\boldsymbol{s} = \mathbf{D}\boldsymbol{e}, \qquad \mathbf{D} = 2\mu \mathbf{I}_9 + \lambda \mathbf{i}\mathbf{i}^{\mathbf{T}}, \tag{9.39}$$

and $\mathbf{D}$ is the tangent-modulus tensor introduced in the previous chapters.

9.3.2 One-Dimensional Members

For a beam column, recalling the strain-displacement model,

$$S_{11} = \sigma(x, z, t) = \mathrm{E}\varepsilon = -z\mathrm{E}\boldsymbol{\beta}_{\mathrm{mb1}}^{\mathbf{T}}(x)\boldsymbol{\Phi}_{\mathrm{mb1}}\boldsymbol{\gamma}_{\mathrm{mb1}}(t). \tag{9.40}$$

The cases of a rod and a beam are recovered by setting $\boldsymbol{\gamma}_{m1}$ or $\boldsymbol{\gamma}_{b1}$ equal to zero vectors, respectively.

9.3.3 Two-Dimensional Elements

9.3.3.1 Membrane Response

In two-dimensional elements, several cases can be distinguished. We first consider elements in plane stress. It is convenient to use Hooke's Law in the form

$$\begin{aligned} E_{xx} &= \frac{1}{\mathrm{E}}[S_{xx} - \nu(S_{yy} + S_{zz})] \\ E_{yy} &= \frac{1}{\mathrm{E}}[S_{yy} - \nu(S_{yy} + S_{zz})] \\ E_{zz} &= \frac{1}{\mathrm{E}}[S_{zz} - \nu(S_{xx} + S_{yy})] \\ E_{xy} &= \frac{1+\nu}{\mathrm{E}} S_{xy} \\ E_{yz} &= \frac{1+\nu}{\mathrm{E}} S_{yz} \\ E_{zx} &= \frac{1+\nu}{\mathrm{E}} S_{zx} \end{aligned} \tag{9.41}$$

Under plane stress, $S_{xz} = S_{yz} = S_{zz} = 0$. Now, $E_{zz} \neq 0$, but we will see that it is not of present interest since it does not influence the solution process. Later on, for reasons such as tolerances, we may wish to calculate it, but this is a postprocessing issue. Consequently, in plane stress, the stress-strain relations reduce to

$$\begin{aligned} E_{xx} &= \frac{1}{\mathrm{E}}(S_{xx} - \nu S_{yy}) \\ E_{yy} &= \frac{1}{\mathrm{E}}(S_{yy} - \nu S_{xx}) \\ E_{xy} &= \frac{1+\nu}{\mathrm{E}} S_{xy} \end{aligned} \tag{9.42}$$

In traditional finite-element notation, this can be written as

$$\begin{pmatrix} S_{xx} \\ S_{yy} \\ S_{xy} \end{pmatrix} = \boldsymbol{D}_{m21} \begin{pmatrix} E_{xx} \\ E_{yy} \\ E_{xy} \end{pmatrix}. \tag{9.43}$$

in which

$$\boldsymbol{D}_{m21} = \mathrm{E} \begin{bmatrix} 1 & -\nu & 0 \\ -\nu & 1 & 0 \\ 0 & 0 & 1+\nu \end{bmatrix}^{-1} = \frac{\mathrm{E}}{1-\nu^2} \begin{bmatrix} 1 & \nu & 0 \\ \nu & 1 & 0 \\ 0 & 0 & 1+\nu \end{bmatrix} \tag{9.44}$$

can be called the tangent-modulus *matrix* under plane stress (note that, unlike the previous definition, it is not based on the *VEC* operator and is not a tensor).

Under plane strain, $E_{xz} = E_{yz} = E_{zz} = 0$. Now, $S_{zz} \neq 0$. However, this stress is not of great interest since its value is not needed for attaining a solution. The quantity may be of interest later, e.g., to check whether yield conditions in plasticity are met, but it can be obtained at that point by a postprocessing procedure. The equations of plane strain are

$$\begin{pmatrix} \mathrm{S_{xx}} \\ \mathrm{S_{yy}} \\ \mathrm{S_{xy}} \end{pmatrix} = \boldsymbol{D}_{m22} \begin{pmatrix} \mathrm{E_{xx}} \\ \mathrm{E_{yy}} \\ \mathrm{E_{xy}} \end{pmatrix}, \tag{9.45}$$

$$\boldsymbol{D}_{m22} = \frac{\mathrm{E}^*}{1-\nu^{*2}} \begin{bmatrix} 1 & \nu^* & 0 \\ \nu^* & 1 & 0 \\ 0 & 0 & 1+\nu^* \end{bmatrix}, \quad \mathrm{E}^* = \frac{\mathrm{E}}{1-\nu^2}, \quad \nu^* = \frac{\nu}{1-\nu}$$

and $\boldsymbol{D}_{m22}$ is the tangent-modulus tensor in plane strain.

However, in the finite-element method, we will see that we are interested in a slightly different quantity from $\boldsymbol{D}_{m21}$ or $\boldsymbol{D}_{m22}$, as follows. The Principle of Virtual Work uses the strain-energy density given by $\frac{1}{2} S_{ij} E_{ij}$. However, elementary manipulation serves to prove that

$$\frac{1}{2} S_{ij} E_{ij} = \frac{1}{2} (S_{xx} \quad S_{yy} \quad S_{zz}) \begin{bmatrix} 1 & 0 & 0 \\ 0 & 1 & 0 \\ 0 & 0 & 2 \end{bmatrix} \begin{pmatrix} E_{xx} \\ E_{yy} \\ E_{xy} \end{pmatrix}. \tag{9.46}$$

In the Principle of Virtual Work, the tangent-modulus tensor in plane stress is replaced by

$$\boldsymbol{D}'_{m21} = \frac{\mathrm{E}}{1-\nu^2} \begin{bmatrix} 1 & \nu & 0 \\ \nu & 1 & 0 \\ 0 & 0 & 2(1+\nu) \end{bmatrix} \tag{9.47}$$

and similarly for plane strain. (This peculiarity is an artifact of traditional finite-element notation and does not appear if *VEC* notation is used.) The stresses are now given in terms of nodal displacements by

$$\begin{pmatrix} S_{\mathrm{xx}}(\mathrm{x},\mathrm{y},\mathrm{t}) \\ S_{\mathrm{yy}}(\mathrm{x},\mathrm{y},\mathrm{t}) \\ S_{\mathrm{xy}}(\mathrm{x},\mathrm{y},\mathrm{t}) \end{pmatrix} = \boldsymbol{D}_{m2i} \begin{pmatrix} E_{\mathrm{xx}} \\ E_{\mathrm{yy}} \\ E_{\mathrm{xy}} \end{pmatrix} = \boldsymbol{D}'_{m2i} \boldsymbol{\beta}^{\mathrm{T}}_{m2} \hat{\boldsymbol{\Phi}}_{m2} \begin{pmatrix} \boldsymbol{\gamma}_{u2} \\ \boldsymbol{\gamma}_{v2} \end{pmatrix}, \quad i = \begin{cases} 1 & \text{plane stress} \\ 2 & \text{plane strain} \end{cases} \tag{9.48}$$

9.3.3.2 Two-Dimensional Members: Bending Response

Thin plates experiencing bending only are assumed to be in a state of plane stress. The tangent-modulus matrix is given in Equation 9.47, and an approximation for the strain is obtained as

$$\begin{pmatrix} S_{\mathrm{xx}} \\ S_{\mathrm{yy}} \\ S_{\mathrm{xy}} \end{pmatrix} = \boldsymbol{D}_{m21} \begin{pmatrix} E_{\mathrm{xx}} \\ E_{\mathrm{yy}} \\ E_{\mathrm{xy}} \end{pmatrix} - z\boldsymbol{D}_{m21}\boldsymbol{\beta}_{b2}^{\mathrm{T}}\hat{\boldsymbol{\Phi}}_{b2}\boldsymbol{\gamma}_{b2}(t). \tag{9.49}$$

9.3.4 Element for Plate with Membrane and Bending Response

Plane stress is also applicable, consequently:

$$\begin{pmatrix} S_{xx} \\ S_{yy} \\ S_{xy} \end{pmatrix} = \boldsymbol{D}_{m21} \begin{pmatrix} E_{xx} \\ E_{yy} \\ E_{xy} \end{pmatrix} = \boldsymbol{D}_{m21}\boldsymbol{\beta}_{mb2}^{\mathrm{T}}(x,y,z)\hat{\boldsymbol{\Phi}}_{mb2}\boldsymbol{\gamma}_{mb2}(t). \tag{9.50}$$

9.3.5 Axisymmetric Element

It is sufficient to consider the case in which none of the nodes of the element are located on the axis of revolution.

$$\begin{pmatrix} S_{rr} \\ S_{\theta\theta} \\ S_{zz} \\ S_{rz} \end{pmatrix} = \boldsymbol{D}_a \begin{pmatrix} E_{rr} \\ E_{\theta\theta} \\ E_{zz} \\ E_{rz} \end{pmatrix} = \boldsymbol{D}_a\boldsymbol{\beta}_{a1}^{\mathrm{T}} \begin{bmatrix} \hat{\boldsymbol{\Phi}}_{a1} & \mathbf{0} \\ \mathbf{0} & \hat{\boldsymbol{\Phi}}_{a1} \end{bmatrix} \begin{pmatrix} \boldsymbol{\gamma}_{ua1}(t) \\ \boldsymbol{\gamma}_{wa1}(t) \end{pmatrix}, \tag{9.51}$$

$$\boldsymbol{D}_a = \mathrm{E} \begin{bmatrix} 1 & -\nu & -\nu & 0 \\ -\nu & 1 & -\nu & 0 \\ -\nu & -\nu & 1 & 0 \\ 0 & 0 & 0 & 1+\nu \end{bmatrix}^{-1}$$

For use in the Principle of Virtual Work, $\boldsymbol{D}_a$ is modified to furnish $\boldsymbol{D}'_a$, given by

$$\boldsymbol{D}'_a = \mathrm{E}\begin{bmatrix}1&0&0&0\\0&1&0&0\\0&0&1&0\\0&0&0&\sqrt{2}\end{bmatrix}\begin{bmatrix}1&-\nu&-\nu&0\\-\nu&1&-\nu&0\\-\nu&-\nu&1&0\\0&0&0&1+\nu\end{bmatrix}^{-1}\begin{bmatrix}1&0&0&0\\0&1&0&0\\0&0&1&0\\0&0&0&\sqrt{2}\end{bmatrix}. \tag{9.52}$$

9.3.6 Three-Dimensional Element

All six stresses and strains are now present. Using traditional notation, we write

$$\begin{pmatrix}S_{xx}\\S_{yy}\\S_{zz}\\S_{xy}\\S_{yz}\\S_{zx}\end{pmatrix} = \boldsymbol{D}_3\begin{pmatrix}E_{xx}\\E_{yy}\\E_{zz}\\E_{xy}\\E_{yz}\\E_{zx}\end{pmatrix} = \boldsymbol{D}_3\boldsymbol{\beta}_3^{\mathrm{T}}\begin{bmatrix}\boldsymbol{\Phi}_3&\mathbf{0}&\mathbf{0}\\\mathbf{0}&\boldsymbol{\Phi}_3&\mathbf{0}\\\mathbf{0}&\mathbf{0}&\boldsymbol{\Phi}_3\end{bmatrix}\begin{pmatrix}\boldsymbol{\gamma}_{u3}\\\boldsymbol{\gamma}_{v3}\\\boldsymbol{\gamma}_{w3}\end{pmatrix} \tag{9.53}$$

$$\boldsymbol{D}_3 = \mathrm{E}\begin{bmatrix}1&-\nu&-\nu&0&0&0\\-\nu&1&-\nu&0&0&0\\-\nu&-\nu&1&0&0&0\\0&0&0&1+\nu&0&0\\0&0&0&0&1+\nu&0\\0&0&0&0&0&1+\nu\end{bmatrix}^{-1}$$

and for the Principle of Virtual Work,

$$\boldsymbol{D}'_3 = \mathrm{E}\mathbf{J}_6\begin{bmatrix}1&-\nu&-\nu&0&0&0\\-\nu&1&-\nu&0&0&0\\-\nu&-\nu&1&0&0&0\\0&0&0&1+\nu&0&0\\0&0&0&0&1+\nu&0\\0&0&0&0&0&1+\nu\end{bmatrix}^{-1}\mathbf{J}_6 \tag{9.54}$$

$$\mathbf{J}_6 = \begin{bmatrix} 1 & 0 & 0 & 0 & 0 & 0 \\ 0 & 1 & 0 & 0 & 0 & 0 \\ 0 & 0 & 1 & 0 & 0 & 0 \\ 0 & 0 & 0 & \sqrt{2} & 0 & 0 \\ 0 & 0 & 0 & 0 & \sqrt{2} & 0 \\ 0 & 0 & 0 & 0 & 0 & \sqrt{2} \end{bmatrix}$$

9.3.7 Elements for Conductive Heat Transfer

Assuming the isotropic version of Fourier's Law, the heat-flux vector, which can be considered the thermal analog of the stress, satisfies

$$\mathbf{q} = -k \begin{cases} \boldsymbol{\beta}_{T1}^{\mathbf{T}} \boldsymbol{\Phi}_{T1} \boldsymbol{\theta}_1 & 1-D \\ \boldsymbol{\beta}_{T2}^{\mathbf{T}} \boldsymbol{\Phi}_{T2} \boldsymbol{\theta}_2 & 2-D \\ \boldsymbol{\beta}_{T3}^{\mathbf{T}} \boldsymbol{\Phi}_{T3} \boldsymbol{\theta}_3 & 3-D. \end{cases} \tag{9.55}$$

9.4 EXERCISES

1. Modify the rod element to replace the physical coordinate x with the "natural coordinate" ξ in which

$$\xi = ax + b, \qquad \xi(x_e) = -1, \qquad \xi(x_{e+1}) = +1.$$

   Rewrite the interpolation model using natural coordinates, and perform the inverse to obtain $\boldsymbol{\Phi}_{m1}$.
2. Rewrite the Euler-Bernoulli equation for the beam using the previous transformation. Rewrite the interpolation model using natural coordinates, and perform the inverse to obtain $\boldsymbol{\Phi}_{b1}$.
3. Verify that the inverse given in Equation 9.44 is correct.
4. Invert Equation 9.39 to express $\boldsymbol{E}$ as a function of $\boldsymbol{s}$. Find the correct expression for $\boldsymbol{D}^{-1}$.
5. Write out the 9×9 tensors $\boldsymbol{D}$ and $\boldsymbol{D}^{-1}$ that correspond to Lame's equation.
6. For the axisymmetric triangular element, find the strain-displacement matrix $\boldsymbol{\beta}^{\mathbf{T}}$ in the cases in which two of the nodes are located on the axis of revolution. Note that for axisymmetric problems, $u_r = 0$ at $r = 0$.

7. The stress-strain relations in two-dimensional plane stress can be written as

$$\begin{pmatrix} E_{xx} \\ E_{yy} \\ E_{xy} \end{pmatrix} = \frac{1}{\mathrm{E}} \begin{bmatrix} 1 & -\nu & 0 \\ -\nu & 1 & 0 \\ 0 & 0 & 1+\nu \end{bmatrix} \begin{pmatrix} S_{xx} \\ S_{yy} \\ S_{xy} \end{pmatrix}$$

Prove that in plane strain

$$\begin{pmatrix} E_{xx} \\ E_{yy} \\ E_{xy} \end{pmatrix} = \frac{1}{\mathrm{E}^*} \begin{bmatrix} 1 & -\nu^* & 0 \\ -\nu^* & 1 & 0 \\ 0 & 0 & 1+\nu^* \end{bmatrix} \begin{pmatrix} S_{xx} \\ S_{yy} \\ S_{xy} \end{pmatrix},$$

where

$$\mathrm{E}^* = \mathrm{E}/(1-\nu^2), \quad \nu^* = \nu/(1-\nu) .$$

8. If

$$\begin{pmatrix} E_{xx} \\ E_{yy} \end{pmatrix} = \frac{1}{\mathrm{E}} \begin{bmatrix} 1-\nu^2 & -\nu(1+\nu) \\ -\nu(1+\nu) & 1-\nu^2 \end{bmatrix} \begin{pmatrix} S_{xx} \\ S_{yy} \end{pmatrix},$$

find the matrix $\hat{\boldsymbol{D}}$ such that

$$\begin{pmatrix} S_{xx} \\ S_{yy} \end{pmatrix} = \frac{E}{(1+\nu)(1-2\nu)} \hat{\mathrm{D}} \begin{pmatrix} E_{xx} \\ E_{yy} \end{pmatrix}.$$

What happens if $\nu \to 1/2$?

10 Element and Global Stiffness and Mass Matrices

10.1 APPLICATION OF THE PRINCIPLE OF VIRTUAL WORK

Elements of variational calculus were discussed in Chapter 3, and the Principle of Virtual Work was introduced in Chapter 5. Under static conditions, the principle is repeated here as

$$\int \delta E_{ij} S_{ij} dV + \int \delta u_i \rho \ddot{u}_i dV = \int \delta u_i \tau_i dS. \tag{10.1}$$

As before, δ represents the variational operator. We assume for our purposes that the displacement, the strain, and the stress satisfy representations of the form

$$\mathbf{u}(\mathbf{x}, t) = \boldsymbol{\varphi}^{\mathbf{T}}(\mathbf{x})\boldsymbol{\Phi}\boldsymbol{\gamma}(t), \qquad \boldsymbol{E} = \boldsymbol{\beta}^{\mathbf{T}}(\mathbf{x})\boldsymbol{\Phi}\boldsymbol{\gamma}(t), \qquad \boldsymbol{S} = \mathbf{D}\boldsymbol{E}, \tag{10.2}$$

in which $\boldsymbol{E}$ and $\boldsymbol{S}$ are written as one-dimensional arrays in accordance with traditional finite-element notation. For use in the Principle of Virtual Work, we need $\boldsymbol{D'}$, which introduces the factor 2 into the entries corresponding to shear. We suppose that the boundary is decomposed into four segments: $S = S_I + S_{II} + S_{III} + S_{IV}$. On S_I, $\mathbf{u}$ is prescribed, in which event $\delta\mathbf{u}$ vanishes. On S_{II}, the traction $\boldsymbol{\tau}$ is prescribed as $\boldsymbol{\tau}_0$. On S_{III}, there is an elastic foundation described by $\boldsymbol{\tau} = \boldsymbol{\tau}_0 - \mathbf{A}(\mathbf{x})\mathbf{u}$, in which $\mathbf{A}(\mathbf{x})$ is a known matrix function of $\mathbf{x}$. On S_{IV}, there are inertial boundary conditions, by virtue of which $\boldsymbol{\tau} = \boldsymbol{\tau}_0 - \mathbf{B}\ddot{\mathbf{u}}$. The term on the right now becomes

$$\begin{aligned}\int \delta u_i \tau_i dS = \delta\boldsymbol{\gamma}^{\mathbf{T}} &\int_{S_{II}+S_{III}+S_{IV}} \boldsymbol{\Phi}^{\mathbf{T}}\boldsymbol{\varphi}(\mathbf{x})\boldsymbol{\tau}_0 dS \\ &- \delta\boldsymbol{\gamma}^{\mathbf{T}} \int_{S_{III}} \boldsymbol{\Phi}^{\mathbf{T}}\boldsymbol{\varphi}(\mathbf{x})\mathbf{A}\boldsymbol{\varphi}^{\mathbf{T}}(\mathbf{x})\boldsymbol{\Phi} dS\boldsymbol{\gamma}(t) \\ &- \delta\boldsymbol{\gamma}^{\mathbf{T}} \int_{S_{IV}} \boldsymbol{\Phi}^{\mathbf{T}}\boldsymbol{\varphi}(\mathbf{x})\mathbf{B}\boldsymbol{\varphi}^{\mathbf{T}}(\mathbf{x})\boldsymbol{\Phi} dS\ddot{\boldsymbol{\gamma}}(t).\end{aligned} \tag{10.3}$$

The term on the left in Equation 10.1 becomes

$$\int \delta E_{ij} S_{ij} dV = \boldsymbol{\delta\gamma}^{\mathbf{T}} \mathbf{K} \boldsymbol{\gamma}(\mathrm{t}), \qquad \mathbf{K} = \int \boldsymbol{\Phi}^{\mathbf{T}} \boldsymbol{\beta}(\mathbf{x}) \mathbf{D}' \boldsymbol{\beta}^{\mathbf{T}}(\mathbf{x}) \boldsymbol{\Phi} \, \mathrm{dV}$$
$$\int \delta u_i \rho \ddot{\mathrm{u}}_i dV = \boldsymbol{\delta\gamma}^{\mathbf{T}} \mathbf{M} \ddot{\boldsymbol{\gamma}}(\mathrm{t}), \qquad \mathbf{M} = \int \boldsymbol{\rho\Phi}^{\mathbf{T}} \boldsymbol{\varphi}(\mathbf{x}) \boldsymbol{\varphi}^{\mathbf{T}}(\mathbf{x}) \boldsymbol{\Phi} \, \mathrm{dV}, \tag{10.4}$$

in which **K** is called the stiffness matrix and **M** is called the mass matrix. Canceling the arbitrary variation and bringing terms with unknowns to the left side furnishes the equation as follows:

$$(\mathbf{K} + \mathbf{K}_S)\boldsymbol{\gamma}(t) + (\mathbf{M} + \mathbf{M}_S)\ddot{\boldsymbol{\gamma}}(t) = \mathbf{f}$$
$$\mathbf{f} = \int_{S_{II}+S_{III}} \boldsymbol{\Phi}^{\mathbf{T}} \boldsymbol{\varphi}(\mathbf{x}) \boldsymbol{\tau}_0 dS$$
$$\mathbf{K}_S = \int_{S_{III}} \boldsymbol{\Phi}^{\mathbf{T}} \boldsymbol{\varphi}(\mathbf{x}) \mathbf{A} \boldsymbol{\varphi}^{\mathbf{T}}(\mathbf{x}) \boldsymbol{\Phi} dS \tag{10.5}$$
$$\mathbf{M}_S = \int_{S_{IV}} \boldsymbol{\Phi}^{\mathbf{T}} \boldsymbol{\varphi}(\mathbf{x}) \mathbf{B} \boldsymbol{\varphi}^{\mathbf{T}}(\mathbf{x}) \boldsymbol{\Phi} dS.$$

Clearly, elastic supports on S_{III} furnish a boundary contribution to the stiffness matrix, while mass on the boundary segment S_{IV} furnishes a contribution to the mass matrix.

Sample Problem 1: One element rod

Consider a rod with modulus E, mass density ρ, area A, and length L. It is built in at $x = 0$. At $x = L$, there is a concentrated mass m to which is attached a spring of stiffness k, as illustrated in Figure 10.1. The stiffness and mass matrices, from the domain, reduce to the scalar values $\mathbf{K} \rightarrow EA/L$, $\mathbf{M} \rightarrow \rho AL/3$, $\mathbf{M}_S \rightarrow m$, $\mathbf{K}_S \rightarrow k$. The governing equation is $(\frac{EA}{L} + k)\gamma + (\frac{\rho AL}{3} + m)\ddot{\gamma} = f$.

Sample Problem 2: Beam element

Consider a one-element model of a cantilevered beam to which a solid disk is welded at $x = L$. Attached at L is a linear spring and a torsional spring, the latter having the property that the moment developed is proportional to the slope of the beam.

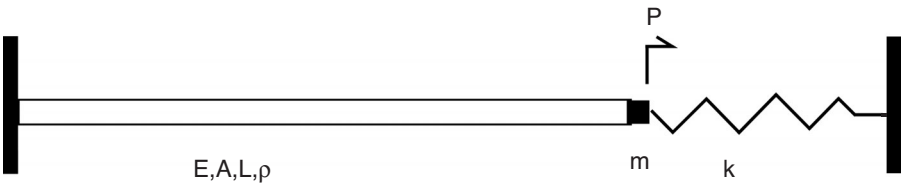

FIGURE 10.1 Rod with inertial and compliant boundary conditions.

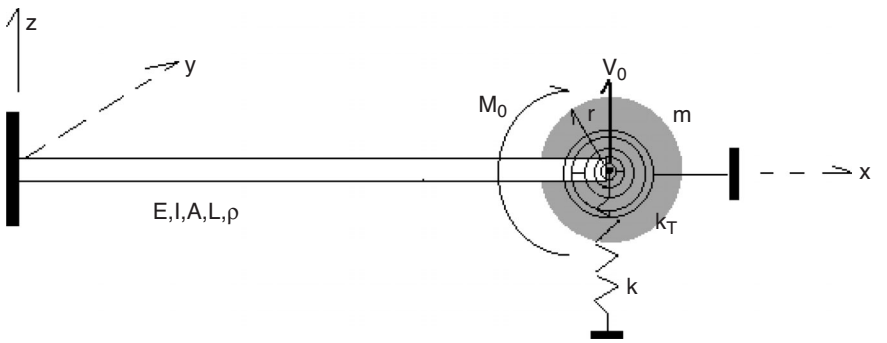

FIGURE 10.2 Beam with translational and rotational inertial and compliant boundary conditions.

The shear force V_0 and the moment M_0 act at L. The interpolation model, incorporating the constraints $w(0, t) = -w'(0, t) = 0$ *a priori*, is

$$w(x,t) = (x^2 x^3)\begin{bmatrix} L^2 & L^3 \\ -2L & -3L^2 \end{bmatrix}^{-1}\begin{pmatrix} w(L,t) \\ -w'(L,t) \end{pmatrix}. \tag{10.6}$$

The stiffness and mass matrices, due to the domain, are readily shown to be

$$\mathbf{K} = \frac{EI}{L^3}\begin{bmatrix} 12 & 6L \\ 6L & 4L^2 \end{bmatrix}, \qquad \mathbf{M} = \rho AL\begin{bmatrix} \frac{13}{35} & \frac{11}{210}L \\ \frac{11}{210}L & \frac{1}{105}L^2 \end{bmatrix}. \tag{10.7}$$

The stiffness and mass contributions from the boundary conditions are

$$\mathbf{K}_S = \begin{bmatrix} k & 0 \\ 0 & k_T \end{bmatrix}, \qquad \mathbf{M}_S = \begin{bmatrix} m & 0 \\ 0 & \frac{mr^2}{2} \end{bmatrix}. \tag{10.8}$$

The governing equation is now

$$(\mathbf{M}+\mathbf{M}_S)\begin{pmatrix} \ddot{w}(L,t) \\ -\ddot{w}'(L,t) \end{pmatrix} + (\mathbf{K}+\mathbf{K}_S)\begin{pmatrix} w(L,t) \\ -w'(L,t) \end{pmatrix} = \begin{pmatrix} V_0 \\ M_0 \end{pmatrix}. \tag{10.9}$$

10.2 THERMAL COUNTERPART OF THE PRINCIPLE OF VIRTUAL WORK

For our purposes, we focus on the equation of conductive heat transfer as

$$k\nabla^2 \mathrm{T} = \rho c_e \frac{\partial \mathrm{T}}{\partial t}. \tag{10.10}$$

Multiplying by the variation of $T - T_0$, integrating by parts, and applying the divergence theorem furnishes

$$\int \delta\nabla^{\mathbf{T}}\mathrm{T}k\nabla\mathrm{T}dV + \int \delta\,\mathrm{T}\rho c_e\,\frac{\partial \mathrm{T}}{\partial t}\,dV = \int \delta\,\mathrm{T}\mathbf{n}^{\mathbf{T}}\mathbf{q}dS. \tag{10.11}$$

Now suppose that the interpolation models for temperature in the current element furnish a relation of the form

$$\mathrm{T} - \mathrm{T}_0 = \boldsymbol{\varphi}_T^{\mathbf{T}}(\mathbf{x})\boldsymbol{\Phi}_T\boldsymbol{\theta}(t), \quad \nabla\mathrm{T} = \boldsymbol{\beta}_T^{\mathbf{T}}(\mathbf{x})\boldsymbol{\Phi}_T\boldsymbol{\theta}(t), \quad \mathbf{q} = -k_T^{\mathbf{T}}(\mathbf{x})\boldsymbol{\Phi}_T\boldsymbol{\theta}(t). \tag{10.12}$$

The terms on the left in Equation 10.11 can now be written as

$$\begin{aligned}
&\int \delta\nabla^T\mathrm{T}k\nabla\mathrm{T}dV \to \delta\boldsymbol{\theta}^{\mathbf{T}}(t)\mathbf{K}_T\boldsymbol{\theta}(t), \qquad \mathbf{K}_T = \int k\boldsymbol{\Phi}_T^{\mathbf{T}}\boldsymbol{\beta}_T\boldsymbol{\beta}_T^{\mathbf{T}}\boldsymbol{\Phi}_T dV \\
&\int \delta\mathrm{T}\rho c_e\,\frac{\partial \mathrm{T}}{\partial t}\,dV \to \delta\boldsymbol{\theta}^{\mathbf{T}}(t)\mathbf{M}_T\dot{\boldsymbol{\theta}}(t), \qquad \mathbf{M}_T = \int \rho c_e\boldsymbol{\Phi}_T^{\mathbf{T}}\boldsymbol{\varphi}_T\boldsymbol{\varphi}_T^{\mathbf{T}}\boldsymbol{\Phi}_T dV.
\end{aligned} \tag{10.13}$$

$\mathbf{K}_T$ and $\mathbf{M}_T$ can be called the thermal stiffness (or conductance) matrix and thermal mass (or capacitance) matrix, respectively.

Suppose that the boundary S has four zones: $\mathrm{S} = \mathrm{S_I} + \mathrm{S_{II}} + \mathrm{S_{III}} + \mathrm{S_{IV}}$. On $\mathrm{S_I}$, the temperature is prescribed as $\mathrm{T_1}$, from which we conclude that $\delta\mathrm{T} = 0$. On $\mathrm{S_{II}}$, the heat flux is prescribed as $\mathbf{n}^{\mathbf{T}}\mathbf{q}_1$. On $\mathrm{S_{III}}$, the heat flux satisfies $\mathbf{n}^{\mathbf{T}}\mathbf{q} = \mathbf{n}^{\mathbf{T}}\mathbf{q}_1 - h_1(\mathrm{T} - \mathrm{T}_0)$, while on $\mathrm{S_{IV}}$, $\mathbf{n}^{\mathbf{T}}\mathbf{q} = \mathbf{n}^{\mathbf{T}}\mathbf{q}_1 - h_2\,d\,\mathrm{T}/dt$. The governing finite-element equation is now

$$[\mathbf{M}_T + \mathbf{M}_{TS}]\dot{\boldsymbol{\theta}}(t) + [\mathbf{K}_T + \mathbf{K}_{TS}]\boldsymbol{\theta}(t) = \mathbf{f}_T(t) \tag{10.14}$$

$$\mathbf{M}_{TS} = \int_{\mathrm{S_{IV}}} \boldsymbol{\Phi}_T^T\boldsymbol{\varphi}_T h_2\boldsymbol{\varphi}_T^T\boldsymbol{\Phi}_T dS, \qquad \mathbf{K}_{TS} = \int_{\mathrm{S_{III}}} \boldsymbol{\Phi}_T^{\mathbf{T}}\boldsymbol{\varphi}_T h_1\boldsymbol{\varphi}_T^{\mathbf{T}}\boldsymbol{\Phi}_T dS$$

$$\mathbf{f}_T(t) = \int_{\Omega} \boldsymbol{\Phi}_T^T\boldsymbol{\varphi}_T\mathbf{n}^T\mathbf{q}_1 dS, \qquad \Omega = \mathrm{S_{II}} + \mathrm{S_{III}} + \mathrm{S_{IV}}$$

10.3 ASSEMBLAGE AND IMPOSITION OF CONSTRAINTS

10.3.1 Rods

Consider the assemblage consisting of two rod elements, denoted as e and $e + 1$ [see Figure 10.3(a)]. There are three nodes, numbered n, $n + 1$, and $n + 2$. We first consider assemblage of the stiffness matrices, based on two principles: (a) the forces at the nodes are in equilibrium, and (b) the displacements at the nodes are continuous. Principle (a) implies that, in the absence of forces applied externally to the node, at node $n + 1$, the force of element $e + 1$ on element e is equal to and opposite the force of element e on element $e + 1$. It is helpful to carefully define global (assemblage

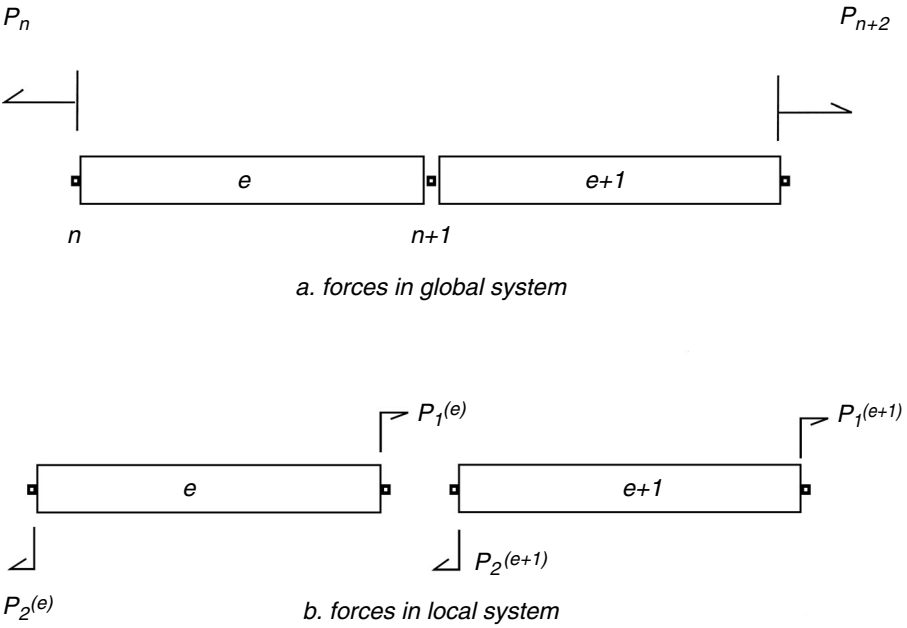

FIGURE 10.3 Assembly of rod elements.

level) and local (element level) systems of notation. The global system of forces is shown in (a), while the local system is shown in (b). At the center node,

$$P_1^{(e)} - P_2^{(e+1)} = 0 \tag{10.15}$$

since no external load is applied. Clearly, $P_2^{(e)} = P_n$ and $P_1^{(e+1)} = P_{n+2}$.

The elements satisfy

$$\begin{aligned} k^{(e)}\begin{bmatrix} 1 & -1 \\ -1 & 1 \end{bmatrix}\begin{pmatrix} u_n \\ u_{n+1} \end{pmatrix} &= \begin{pmatrix} -P_2^{(e)} \\ P_1^{(e)} \end{pmatrix} \\ k^{(e+1)}\begin{bmatrix} 1 & -1 \\ -1 & 1 \end{bmatrix}\begin{pmatrix} u_{n+1} \\ u_{n+2} \end{pmatrix} &= \begin{pmatrix} -P_2^{(e+1)} \\ P_1^{(e+1)} \end{pmatrix} \end{aligned} \tag{10.16}$$

and in this case, $k^{(e)} = k^{(e+1)} = \mathrm{E}A/L$. These relations can be written as four separate equations:

$$\begin{aligned} k^{(e)}u_n - k^{(e)}u_{n+1} &= -P_2^{(e)} && \text{(i)} \\ -k^{(e)}u_n + k^{(e)}u_{n+1} &= P_1^{(e)} && \text{(ii)} \\ k^{(e+1)}u_{n+1} - k^{(e+1)}u_{n+2} &= -P_2^{(e+1)} && \text{(iii)} \\ -k^{(e+1)}u_{n+1} + k^{(e+1)}u_{n+2} &= P_1^{(e+1)} && \text{(iv)} \end{aligned} \tag{10.17}$$

Add (ii) and (iii) and apply Equation 10.15 to obtain

$$\begin{aligned} k^{(e)}u_n - k^{(e)}u_{n+1} &= -P_2^{(e)} && \text{(i)} \\ -k^{(e)}u_n + [k^{(e)} + k^{(e+1)}]u_{n+1} - k^{(e+1)}u_{n+2} &= 0 && \text{(ii + iii)} \\ -k^{(e+1)}u_{n+1} - k^{(e+1)}u_{n+2} &= P_1^{(e+1)} && \text{(iv)} \end{aligned} \tag{10.18}$$

and in matrix form

$$\begin{bmatrix} k^{(e)} & -k^{(e)} & 0 \\ -k^{(e)} & k^{(e)} + k^{(e+1)} & -k^{(e+1)} \\ 0 & -k^{(e+1)} & k^{(e+1)} \end{bmatrix} \begin{pmatrix} u_n \\ u_{n+1} \\ u_{n+2} \end{pmatrix} = \begin{pmatrix} -P_n \\ 0 \\ P_{n+1} \end{pmatrix} \tag{10.19}$$

The assembled stiffness matrix shown in Equation 10.19 can be visualized as an overlay of two element stiffness matrices, referred to global indices, in which there is an intersection of the overlay. The intersection contains the sum of the lowest entry on the right side of the upper matrix and the highest entry on the left side of the lowest matrix. The overlay structure is depicted in Figure 10.4.

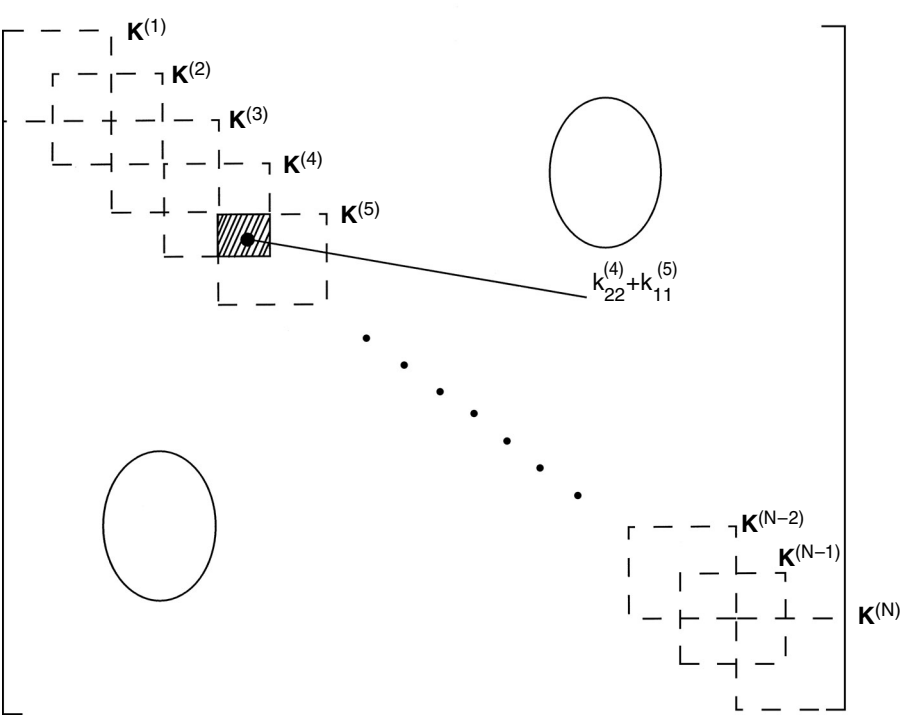

FIGURE 10.4 Assembled beam stiffness matrix.

Now, the equations of the individual elements are written in the global system as

$$\mathbf{K}^{(\mathbf{e})} \to \tilde{\mathbf{K}}^{(\mathbf{e})}, \quad \mathbf{K}^{(\mathbf{e}+1)} \to \tilde{\mathbf{K}}^{(\mathbf{e}+1)}$$

$$\tilde{\mathbf{K}}^{(\mathbf{e})} = k^{(e)}\begin{bmatrix} 1 & -1 & 0 \\ -1 & 1 & 0 \\ 0 & 0 & 0 \end{bmatrix}, \quad \tilde{\mathbf{K}}^{(\mathbf{e}+1)} = k^{(e+1)}\begin{bmatrix} 0 & 0 & 0 \\ 0 & 1 & -1 \\ 0 & -1 & 1 \end{bmatrix}. \tag{10.20}$$

The global stiffness matrix (the assembled stiffness matrix $\mathbf{K}^{(\mathbf{g})}$ of the two-element member) is the direct sum of the element stiffness matrices: $\mathbf{K}^{(\mathbf{g})} = \tilde{\mathbf{K}}^{(\mathbf{e})} + \tilde{\mathbf{K}}^{(\mathbf{e}+1)}$.

Generally, $\mathbf{K}^{(\mathbf{g})} = \sum_{\mathbf{e}} \tilde{\mathbf{K}}^{(\mathbf{e})}$. In this notation, the strain energy in the two elements can be written in the form

$$\begin{aligned} \mathbf{V}^{(\mathbf{e})} &= \frac{1}{2}\boldsymbol{\gamma}^{(\mathbf{e})\mathbf{T}}\tilde{\mathbf{K}}^{(\mathbf{e})}\boldsymbol{\gamma}^{(\mathbf{e})} \\ \mathbf{V}^{(\mathbf{e}+1)} &= \frac{1}{2}\boldsymbol{\gamma}^{(\mathbf{e})\mathbf{T}}\tilde{\mathbf{K}}^{(\mathbf{e}+1)}\boldsymbol{\gamma}^{(\mathbf{e})} \\ \boldsymbol{\gamma}^{(\mathbf{e})\mathbf{T}} &= (u_n \quad u_{n+1} \quad u_{n+2}). \end{aligned} \tag{10.21}$$

The total strain energy of the two elements is $\frac{1}{2}\boldsymbol{\gamma}^{\mathbf{T}}\mathbf{K}^{(\mathbf{g})}\boldsymbol{\gamma}$.

Finally, notice that $\mathbf{K}^{(\mathbf{g})}$ is singular: the sum of the rows is the zero vector, as is the sum of the columns. In this form, an attempt to solve the system will give rise to "rigid-body motion." To illustrate this reasoning, suppose, for simplicity's sake, that $k^{(e)} = k^{(e+1)}$, in which case equilibrium requires that $P_n = P_{n+2}$. If computations were performed with perfect accuracy, the equation would pose no difficulty. However, in performing computations, errors arise. For example, P_n is computed as $\hat{P}_n = P_n + \varepsilon_n$ and $\hat{P}_{n+1} = P_{n+1} + \varepsilon_{n+1}$, $P_{n+1} = P_n = P$. Computationally, there is now an unbalanced force, $\varepsilon_{n+1} - \varepsilon_n$. In the absence of mass, this, in principle, implies infinite accelerations. In the finite-element method, the problem of rigid-body motion can be detected if the output exhibits large deformation.

The problem is easily suppressed using **constraints**. In particular, symmetry implies that $u_{n+1} = 0$. Recalling Equation 10.19, we now have

$$\frac{EA}{L}\begin{bmatrix} 1 & -1 & 0 \\ -1 & 2 & -1 \\ 0 & -1 & 1 \end{bmatrix}\begin{pmatrix} u_n \\ 0 \\ u_{n+2} \end{pmatrix} = \begin{pmatrix} -P_n \\ R \\ P_{n+1} \end{pmatrix}, \tag{10.22}$$

in which R is a reaction force that arises to enforce physical symmetry in the presence of numerically generated asymmetry. The equation corresponding to the second equation is useless in predicting the unknowns u_n and u_{n+2} since it introduces the

new unknown R. The first and third equations are now rewritten as

$$\frac{EA}{L}\begin{bmatrix}1 & 0\\ 0 & 1\end{bmatrix}\begin{pmatrix}u_n\\ u_{n+1}\end{pmatrix}=\begin{pmatrix}-P+\varepsilon_n\\ P+\varepsilon_{n+1}\end{pmatrix}, \tag{10.23}$$

with the solution

$$u_n=[-P+\varepsilon_n]\Big/\frac{EA}{L}, \qquad u_{n+2}=[P+\varepsilon_{n+1}]\Big/\frac{EA}{L}. \tag{10.24}$$

To preserve symmetry, it is necessary for $u_n + u_{n+1} = 0$. However, the sum is computed as

$$u_n+u_{n+1}=\frac{\varepsilon_n+\varepsilon_{n+1}}{\left(\frac{EA}{L}\right)}. \tag{10.25}$$

The reaction force is given by $R=-[\varepsilon_n+\varepsilon_{n+1}]$, and, in this case, it can be considered as a measure of computational error.

Note that Equation 10.23 can be obtained from Equation 10.22 by simply "striking out" the second row of the matrices and vectors and the second column of the matrix.

The same assembly arguments apply to the inertial forces as to the elastic forces. Omitting the details, the kinetic energies T of the two elements are

$$T=\frac{1}{2}\dot{\boldsymbol{\gamma}}^{(\mathbf{e})\mathbf{T}}[\tilde{\mathbf{M}}^{(\mathbf{e})}+\tilde{\mathbf{M}}^{(\mathbf{e}+1)}]\dot{\boldsymbol{\gamma}}^{(\mathbf{e})} \tag{10.26}$$

$$\tilde{\mathbf{M}}^{(\mathbf{e})}=m^{(\mathbf{e})}\begin{bmatrix}1 & 1/2\\ 1/2 & 1\end{bmatrix}$$

$$m^{(\mathbf{e})}=\left[\frac{1}{3}\rho Al\right]^{(\mathbf{e})}$$

$$\dot{\boldsymbol{\gamma}}^{(\mathbf{e})\mathbf{T}}=\{\dot{u}_e \quad \dot{u}_{e+1} \quad \dot{u}_{e+2}\}$$

10.3.2 Beams

A similar argument applies for beams. The potential energy and stiffness matrix of the e^{th} element can be written as

$$V^{(\mathbf{e})}=\frac{1}{2}\boldsymbol{\gamma}_b^{\mathrm{T}}\mathbf{K}^{(\mathbf{e})}\boldsymbol{\gamma}_b$$

$$\mathbf{K}^{(\mathbf{e})}=\begin{bmatrix}\mathbf{K}_{\mathbf{11}}^{(\mathbf{e})} & \mathbf{K}_{\mathbf{12}}^{(\mathbf{e})}\\ \mathbf{K}_{\mathbf{21}}^{(\mathbf{e})\mathbf{T}} & \mathbf{K}_{\mathbf{22}}^{(\mathbf{e})}\end{bmatrix} \tag{10.27}$$

$$\boldsymbol{\gamma}_b^{\mathbf{T}}=\{w_e-w_e' \,|\, w_{e+1}-w_{e+1}'\}$$

In a two-element beam model analogous to the previous rod model, $V^{(g)} = V^{(e)} + V^{(e+1)}$, implying that

$$\mathbf{K}^{(g)} = \begin{bmatrix} \mathbf{K}_{11}^{(e)} & \mathbf{K}_{12}^{(e)} & \mathbf{0} \\ \mathbf{K}_{21}^{(e)T} & \mathbf{K}_{22}^{(e)} + \mathbf{K}_{11}^{(e+1)} & \mathbf{K}_{12}^{(e+1)} \\ \mathbf{0} & \mathbf{K}_{21}^{(e+1)T} & \mathbf{K}_{22}^{(e+1)} \end{bmatrix}. \tag{10.28}$$

Generally, in a global coordinate system, $\mathbf{K}^{(g)} = \sum_e \mathbf{K}^{(e)}$.

10.3.3 Two-Dimensional Elements

We next consider assembly in 2-D. Consider the model depicted in Figure 10.5 consisting of four rectangular elements, denoted as element e, $e + 1$, $e + 2$, and $e + 3$. The nodes are also numbered in the global system. Locally, the nodes in an element are numbered in a counterclockwise fashion. Suppose there is one degree of freedom per node (e.g., x-displacement) and one corresponding force.

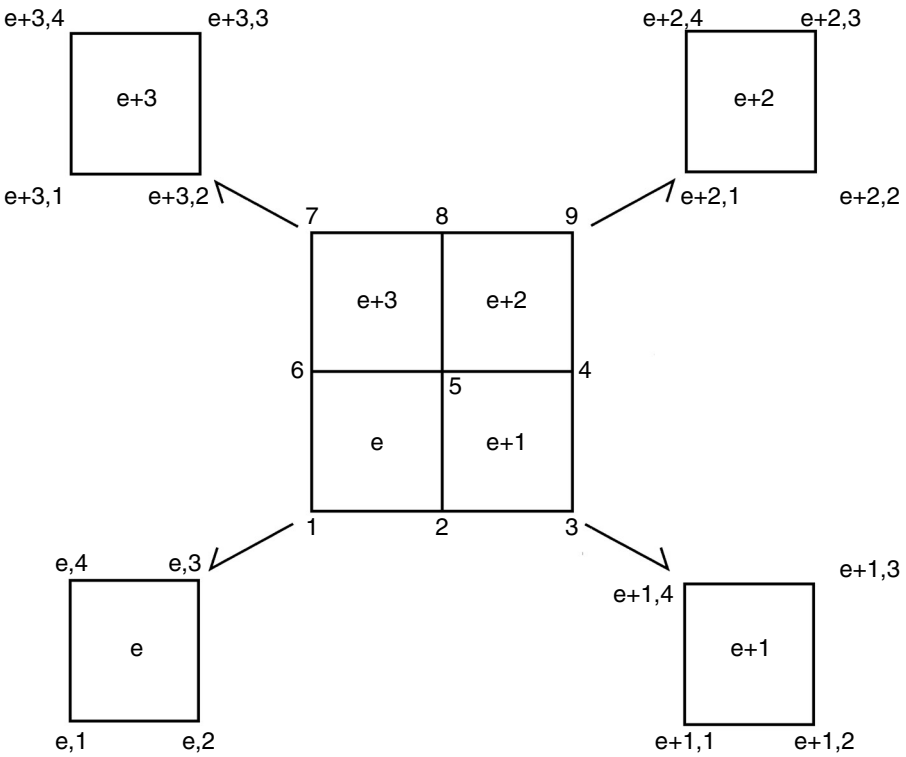

FIGURE 10.5 2-D assembly process.

In the local systems, the force on the center node induces displacements according to

$$\begin{aligned}
f_{e,3} &= k_{3,1}^{(e)}u_{e,1} + k_{3,2}^{(e)}u_{e,2} + k_{3,3}^{(e)}u_{e,3} + k_{3,4}^{(e)}u_{e,4} \\
f_{e+1,4} &= k_{4,1}^{(e+1)}u_{e+1,1} + k_{4,2}^{(e+1)}u_{e+1,2} + k_{4,3}^{(e+1)}u_{e+1,3} + k_{4,4}^{(e+1)}u_{e+1,4} \\
f_{e+2,1} &= k_{1,1}^{(e+2)}u_{e+2,1} + k_{1,2}^{(e+2)}u_{e+2,2} + k_{1,3}^{(e+2)}u_{e+2,3} + k_{1,4}^{(e+2)}u_{e+2,4} \\
f_{e+3,2} &= k_{2,1}^{(e+3)}u_{e+3,1} + k_{2,2}^{(e+3)}u_{e+3,2} + k_{2,3}^{(e+3)}u_{e+3,3} + k_{2,4}^{(e+3)}u_{e+3,4}
\end{aligned} \tag{10.29}$$

Globally,

$$\begin{aligned}
&u_{e,1} \to u_1 \qquad u_{e,2} \to u_2 \qquad u_{e,3} \to u_5 \qquad u_{e,4} \to u_6 \\
&u_{e+1,1} \to u_2 \qquad u_{e+1,2} \to u_3 \qquad u_{e+1,3} \to u_4 \qquad u_{e+1,4} \to u_5 \\
&u_{e+2,1} \to u_5 \qquad u_{e+2,2} \to u_4 \qquad u_{e+2,3} \to u_9 \qquad u_{e+2,4} \to u_8 \\
&u_{e+3,1} \to u_6 \qquad u_{e+3,2} \to u_5 \qquad u_{e+3,3} \to u_8 \qquad u_{e+3,4} \to u_7
\end{aligned} \tag{10.30}$$

Adding the forces of the elements on the center node gives

$$\begin{aligned}
f_5 = \; & k_{3,1}^{(e)}u_1 + \left[k_{3,2}^{(e)} + k_{4,1}^{(e+1)}\right]u_2 + k_{4,2}^{(e+1)}u_3 + \left[k_{4,3}^{(e+1)} + k_{1,2}^{(e+2)}\right]u_4 \\
& + \left[k_{3,3}^{(e)} + k_{4,4}^{(e+1)} + k_{1,1}^{(e+2)} + k_{2,2}^{(e+3)}\right]u_5 + \left[k_{3,4}^{(e)} + k_{2,1}^{(e+3)}\right]u_6 \\
& + k_{2,4}^{(e+3)}u_7 + \left[k_{1,4}^{(e+2)} + k_{2,3}^{(e+3)}\right]u_8 + k_{1,3}^{(e+2)}u_9
\end{aligned} \tag{10.31}$$

Taking advantage of the symmetry of the stiffness matrix, this implies that the fifth row of the stiffness matrix is

$$\begin{aligned}
\boldsymbol{\kappa}_5^{\mathbf{T}} = \Big\{ & k_{3,1}^{(e)} \quad \left[k_{3,2}^{(e)} + k_{4,1}^{(e+1)}\right] \quad k_{4,2}^{(e+1)} \quad \left[k_{4,3}^{(e+1)} + k_{1,2}^{(e+2)}\right] \\
& \left[k_{3,3}^{(e)} + k_{4,4}^{(e+1)} + k_{1,1}^{(e+2)} + k_{2,2}^{(e+3)}\right] \ldots \textit{symmetry} \ldots \Big\}
\end{aligned} \tag{10.32}$$

Finally, for later use, we consider damping, which generates a stress proportional to the strain rate. In linear problems, it leads to a vector-matrix equation of the form

$$\mathbf{M}\ddot{\boldsymbol{\gamma}} + \mathbf{D}\dot{\boldsymbol{\gamma}} + \mathbf{K}\boldsymbol{\gamma} = \mathbf{f}(t). \tag{10.33}$$

At the element level, the counterpart of the kinetic energy and the strain energy is the Rayleigh Damping Function, $\mathrm{D}^{(\mathbf{e})}$, given by $\mathrm{D}^{(\mathbf{e})} = \frac{1}{2}\dot{\boldsymbol{\gamma}}^{(\mathbf{e})\mathbf{T}}\mathbf{D}^{(\mathbf{e})}\dot{\boldsymbol{\gamma}}^{(\mathbf{e})}$, and the consistent damping force on the e^{th} element is

$$\mathbf{f}_d^{(\mathbf{e})}(t) = \frac{\partial}{\partial \dot{\boldsymbol{\gamma}}}\mathrm{D}^{(\mathbf{e})} = \mathbf{D}^{(\mathbf{e})}\dot{\boldsymbol{\gamma}}^{(\mathbf{e})}. \tag{10.34}$$

The Rayleigh Damping Function is additive over the elements. Accordingly, if $\hat{\mathbf{D}}^{(\mathbf{e})}$ is the damping matrix of the e^{th} element referred to the global system, the assembled damping matrix is given by

$$\mathbf{D}^{(\mathbf{g})} = \sum_{\mathbf{e}} \hat{\mathbf{D}}^{(\mathbf{e})}. \tag{10.35}$$

It should be evident that the global stiffness, mass, and damping matrices have the same bandwidth; the force on one given node depends on the displacements (velocities and accelerations) of the nodes of the elements connected at the given node, thus determining the bandwidth.

10.3 EXERCISES

1. The equation of static equilibrium in the presence of body forces, such as gravity, is expressed by

$$\frac{\partial S_{ij}}{\partial X_j} = -b_i.$$

Without the body forces, the dynamic Principle of Virtual Work is derived as

$$\int \delta E_{ij} S_{ij} dV + \int \delta u_i \rho \frac{\partial^2 u_i}{\partial t^2} dV = \int \delta u_i \tau_i dS.$$

How should the second equation be modified to include body forces?

2. Consider a one-dimensional system described by a sixth-order differential equation:

$$Q\frac{d^6 q}{dx^6} = 0, \qquad Q \text{ a constant.}$$

Consider an element from x_e to x_{e+1}. Using the natural coordinate $\xi = -1$ when $x = x_{e'} = +1$ when $x = x_{e+1}$, for an interpolation model with the minimum order that is meaningful, obtain expressions for $\boldsymbol{\varphi}(\xi)$, $\boldsymbol{\Phi}$, and $\boldsymbol{\gamma}$, serving to express $\mathbf{q}$ as

$$\mathbf{q}(\xi) = \boldsymbol{\varphi}^{\mathbf{T}}(\xi)\boldsymbol{\Phi}\boldsymbol{\gamma}.$$

3. Write down the assembled mass and stiffness matrices of the following three-element configuration (using rod elements). The elastic modulus is E, the mass density is ρ, and the cross-sectional area is A.

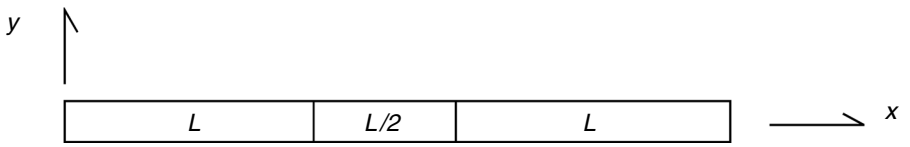

4. Assemble the stiffness coefficients associated with node *n*, shown in the following figure, assuming plane-stress elements. The modulus is E, and the Poisson's ratio is ν. $\mathbf{K}^{(1)}$, $\mathbf{K}^{(2)}$, and $\mathbf{K}^{(3)}$ denote the stiffness matrices of the elements.

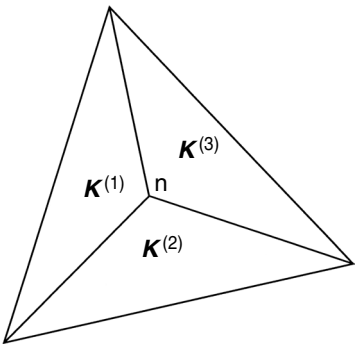

5. Suppose that a rod satisfies $\delta\Psi = 0$, in which Ψ is given by

$$\Psi = \int_0^L \frac{1}{2}\left(\frac{du}{dx}\right)^2 dx - \frac{Pu(L)}{\mathrm{E}}.$$

Use the interpolation model

$$u(x) = \{1 \quad x\}\mathbf{\Phi}\begin{pmatrix} u(x_e,t) \\ u(x_{e+1},t) \end{pmatrix}.$$

For an element $x_e < x < x_{e+1}$, find the matrix $\mathbf{K}_e$ such that

$$\mathbf{K}_e\begin{pmatrix} u(x_e,t) \\ u(x_{e+1},t) \end{pmatrix} = \begin{pmatrix} f_e \\ f_{e+1} \end{pmatrix}.$$

6. Redo this derivation for $\mathbf{K}_e$ in the previous exercise, using the natural coordinate ξ, whereby $\xi = ax + b$, in which a and b are such that $-1 = ax_e + b$, $+1 = ax_{e+1} + b$.
7. Next, regard the nodal-displacement vector as a function of t. Find the matrix $\mathbf{M}_e$ such that

$$\mathbf{M}_e\begin{pmatrix} u(x_e,t) \\ u(x_{e+1},t) \end{pmatrix}^{\bullet\bullet} + \mathbf{K}_e\begin{pmatrix} u(x_e,t) \\ u(x_{e+1},t) \end{pmatrix} = \begin{pmatrix} f_e \\ f_{e+1} \end{pmatrix},$$

in which ρ is the mass density. Derive $\mathbf{M}_e$ using both physical and natural coordinates.

8. Show that, for the rod under gravity, a two-element model gives the exact answer at $x = 1$, as well as a much better approximation to the exact displacement distribution.

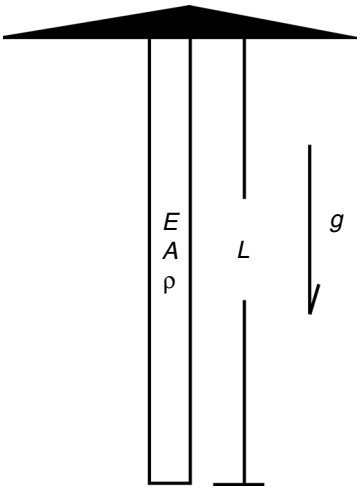

9. Apply the method of the previous exercise to consider a stepped rod, as shown in the figure, with each segment modeled as one element. Is the displacement at $x = 2L$ still exact?

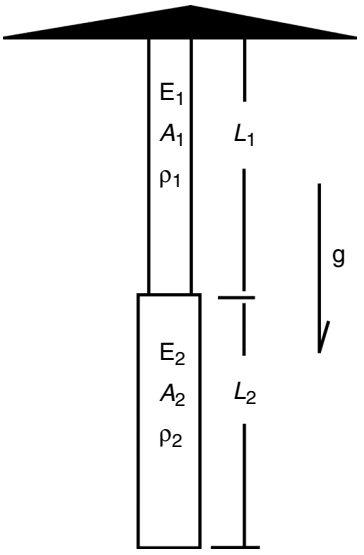

11 Solution Methods for Linear Problems

11.1 NUMERICAL METHODS IN FEA

11.1.1 Solving the Finite-Element Equations: Static Problems

Consider the numerical solution of the linear system $\mathbf{K}\boldsymbol{\gamma} = \mathbf{f}$, in which $\mathbf{K}$ is the positive-definite and symmetric stiffness matrix. In many problems, it has a large dimension, but is also banded. The matrix can be "triangularized": $\mathbf{K} = \mathbf{L}\mathbf{L}^{\mathrm{T}}$, in which $\mathbf{L}$ is a lower triangular, nonsingular matrix (zeroes in all entries above the diagonal). We can introduce $\mathbf{z} = \mathbf{L}^{\mathrm{T}}\boldsymbol{\gamma}$ and obtain $\mathbf{z}$ by solving $\mathbf{L}\mathbf{z} = \mathbf{f}$. Next, $\boldsymbol{\gamma}$ can be computed by solving $\mathbf{L}^{\mathrm{T}}\boldsymbol{\gamma} = \mathbf{z}$. Now $\mathbf{L}\mathbf{z} = \mathbf{f}$ can be conveniently solved by forward substitution. In particular, $\mathbf{L}\mathbf{z} = \mathbf{f}$ can be expanded as

$$\begin{bmatrix} l_{11} & 0 & . & . & . & 0 \\ l_{21} & l_{22} & . & . & . & . \\ l_{31} & l_{32} & l_{33} & . & . & . \\ . & . & . & . & . & . \\ . & . & . & . & . & 0 \\ l_{n1} & l_{n2} & . & . & . & l_{nn} \end{bmatrix} \begin{Bmatrix} z_1 \\ z_2 \\ z_3 \\ . \\ . \\ z_n \end{Bmatrix} = \begin{Bmatrix} f_1 \\ f_2 \\ f_3 \\ . \\ . \\ f_n \end{Bmatrix}. \tag{11.1}$$

Assuming that the diagonal entries are not too small, this equation can be solved, starting from the upper-left entry, using simple arithmetic: $z_1 = f_1/l_{11}$, $z_2 = [f_2 - l_{21}z_1]/l_{22}$, $z_3 = [f_3 - l_{31}z_1 - l_{32}z_2]/l_{33}$,... .

Next, the equation $\mathbf{L}^{\mathrm{T}}\boldsymbol{\gamma} = \mathbf{z}$ can be solved using backward substitution. The equation is expanded as

$$\begin{bmatrix} l_{11} & l_{12} & . & . & . & l_{1n} \\ 0 & l_{22} & . & . & . & . \\ 0 & 0 & . & . & . & . \\ . & . & . & l_{n-2,n-2} & l_{n-2,n-1} & l_{n-2,n} \\ . & . & . & 0 & l_{n-1,n-1} & l_{n-1,n} \\ 0 & 0 & . & 0 & 0 & l_{nn} \end{bmatrix} \begin{Bmatrix} \gamma_1 \\ \gamma_2 \\ \gamma_3 \\ . \\ . \\ \gamma_n \end{Bmatrix} = \begin{Bmatrix} f_1 \\ . \\ . \\ f_{n-2} \\ f_{n-1} \\ f_n \end{Bmatrix}. \tag{11.2}$$

Starting from the lower-right entry, solution can be achieved using simple arithmetic as $\gamma_n = f_n/l_{nn}$,

$$\gamma_{n-1} = [f_{n-1} - l_{n-1,1}\gamma_n]/l_{n-1,n-1},\ \gamma_{n-2} = [f_{n-2} - l_{n-2,n}\gamma_n - l_{n-2,n-1}\gamma_{n-1}]/l_{n-2,n-2}, \ldots .$$

In both procedures, only one unknown is encountered in each step (row).

11.1.2 Matrix Triangularization and Solution of Linear Systems

We next consider how to triangularize $\mathbf{K}$. Suppose that the upper-left $(j-1)\times(j-1)$ block $\mathbf{K}_{j-1}$ has been triangularized: $\mathbf{K}_{j-1} = \mathbf{L}_{j-1}\mathbf{L}_{j-1}^{\mathbf{T}}$. In determining whether the $j \times j$ block $\mathbf{K}_j$ can be triangularized, we consider

$$\mathbf{K}_j = \begin{bmatrix} \mathbf{K}_{j-1} & \mathbf{k}_j \\ \mathbf{k}_j^{\mathbf{T}} & \mathbf{k}_{jj} \end{bmatrix} = \begin{bmatrix} \mathbf{L}_{j-1} & \mathbf{0} \\ \boldsymbol{\lambda}_j^{\mathbf{T}} & l_{jj} \end{bmatrix} \begin{bmatrix} \mathbf{L}_{j-1}^{\mathbf{T}} & \boldsymbol{\lambda}_j \\ \mathbf{0}^{\mathbf{T}} & l_{jj} \end{bmatrix}, \tag{11.3}$$

in which $\mathbf{k}_j$ is a $(j-1)\times 1$ array of the first $j-1$ entries of the j^{th} column of $\mathbf{K}_j$. Simple manipulation suffices to furnish $\mathbf{k}_j$ and l_{jj}.

$$\begin{aligned} \mathbf{k}_j &= \mathbf{L}_{j-1}\boldsymbol{\lambda}_j \\ l_{jj} &= \sqrt{k_{jj} - \boldsymbol{\lambda}_j^{\mathbf{T}}\boldsymbol{\lambda}_j} \end{aligned} \tag{11.4}$$

Note that $\boldsymbol{\lambda}_j$ can be conveniently computed using forward substitution. Also, note that $l_{jj} = \sqrt{k_{jj} - \mathbf{k}_j^{\mathbf{T}}\mathbf{K}_{j-1}^{-\mathbf{1}}\mathbf{k}_j}$. The fact that $\mathbf{K}_j > 0$ implies that l_{jj} is real. Obviously, the triangularization process proceeds to the $(j+1)^{st}$ block and on to the complete stiffness matrix.

As an example, consider

$$\mathbf{A_3} = \begin{bmatrix} 1 & \frac{1}{2} & \frac{1}{3} \\ \frac{1}{2} & \frac{1}{3} & \frac{1}{4} \\ \frac{1}{3} & \frac{1}{4} & \frac{1}{5} \end{bmatrix}. \tag{11.5}$$

Clearly, $\mathbf{L_1} = \mathbf{L_1^T} \to 1$. For the second block,

$$\begin{bmatrix} 1 & 0 \\ \lambda_2 & l_{22} \end{bmatrix} \begin{bmatrix} 1 & \lambda_2 \\ 0 & l_{22} \end{bmatrix} = \begin{bmatrix} 1 & \frac{1}{2} \\ \frac{1}{2} & \frac{1}{3} \end{bmatrix}, \tag{11.6}$$

from which $\lambda_2 = 1/2$ and $l_{22} = \sqrt{1/3 - (1/2)^2} = 1/\sqrt{12}$. Now

$$\mathbf{L}_2 = \begin{bmatrix} 1 & 0 \\ 1/2 & 1/\sqrt{12} \end{bmatrix}. \tag{11.7}$$

We now proceed to the full matrix:

$$\begin{bmatrix} 1 & \frac{1}{2} & \frac{1}{3} \\ \frac{1}{2} & \frac{1}{3} & \frac{1}{4} \\ \frac{1}{3} & \frac{1}{4} & \frac{1}{5} \end{bmatrix} = \mathbf{L}_3\mathbf{L}_3^{\mathbf{T}}$$

$$= \begin{bmatrix} 1 & 0 & 0 \\ \frac{1}{2} & 1/\sqrt{12} & 0 \\ l_{31} & l_{32} & l_{33} \end{bmatrix} \begin{bmatrix} 1 & \frac{1}{2} & l_{31} \\ 0 & 1/\sqrt{12} & l_{32} \\ 0 & 0 & l_{33} \end{bmatrix}$$

$$= \begin{bmatrix} 1 & \frac{1}{2} & l_{31} \\ \frac{1}{2} & \frac{1}{3} & l_{31}/2 + l_{32}/\sqrt{12} \\ l_{31} & l_{31}/2 + l_{32}/\sqrt{12} & l_{31}^2 + l_{32}^2 + l_{33}^2 \end{bmatrix} \tag{11.8}$$

We conclude that $l_{31} = 1/3$, $l_{32} = 1/\sqrt{12}$, $l_{33}^2 = 1/5 - 1/9 - 1/12 = \frac{1}{180}$.

11.1.3 Triangularization of Asymmetric Matrices

Asymmetric stiffness matrices arise in a number of finite-element problems, including problems with unsteady rotation and thermomechanical coupling. If the matrix is still nonsingular, it can be decomposed into the product of a lower-triangular and an upper-triangular matrix:

$$\mathbf{K} = \mathbf{L}\mathbf{U}. \tag{11.9}$$

Now, the j^{th} block of the stiffness matrix admits the decomposition

$$\mathbf{K}_j = \begin{bmatrix} \mathbf{K}_{j-1} & \mathbf{k}_{1j} \\ \mathbf{k}_{2j}^{\mathbf{T}} & k_{jj} \end{bmatrix} = \begin{bmatrix} \mathbf{L}_{j-1} & \mathbf{0} \\ \boldsymbol{\lambda}_j^{\mathbf{T}} & l_{jj} \end{bmatrix} \begin{bmatrix} \mathbf{U}_{j-1} & \boldsymbol{u}_j \\ \mathbf{0}^{\mathbf{T}} & u_{jj} \end{bmatrix}$$

$$= \begin{bmatrix} \mathbf{L}_{j-1}\mathbf{U}_{j-1} & \mathbf{L}_{j-1}\boldsymbol{u}_j \\ \boldsymbol{\lambda}_j^{\mathbf{T}}\mathbf{U}_{j-1} & \boldsymbol{\lambda}_j^{\mathbf{T}}\boldsymbol{u}_j + u_{jj}l_{jj} \end{bmatrix} \tag{11.10}$$

in which it is assumed that the $(j-1)^{th}$ block has been decomposed in the previous step. Now, $\boldsymbol{u}_j$ is obtained by forward substitution using $\mathbf{L}_{j-1}\boldsymbol{u}_i = \mathbf{k}_{1i}$, and $\boldsymbol{\lambda}_i$ can be obtained by forward substitution using $\mathbf{U}_{j-1}^{\mathbf{T}}\boldsymbol{\lambda}_j = \mathbf{k}_{2j}$. Finally, $\boldsymbol{u}_{jj}l_{jj} = k_{jj} - \boldsymbol{\lambda}_j^{\mathbf{T}}\boldsymbol{u}_j$, for

which purpose u_{jj} can be arbitrarily set to unity. An equation of the form $\mathbf{Kx} = \mathbf{f}$ can now be solved by forward substitution applied to $\mathbf{Lz} = \mathbf{f}$, followed by backward substitution applied to $\mathbf{Ux} = \mathbf{z}$.

11.2 TIME INTEGRATION: STABILITY AND ACCURACY

Much insight can be gained from considering the model equation:

$$\frac{dy}{dt} = -\lambda y, \tag{11.11}$$

in which λ is complex. If $Re(\lambda) > 0$, for the initial value $y(0) = y_0$, $y(t) = y_0\ exp(-\lambda t)$, then clearly $y(t) \to 0$. The system is called asymptotically stable in this case.

We now consider whether numerical-integration schemes to integrate Equation 11.11 have stability properties corresponding to asymptotic stability. For this purpose, we apply the trapezoidal rule, the properties of which will be discussed in a subsequent section. Consider time steps of duration h, and suppose that the solution has been calculated through the n^{th} time step, and we seek to compute the solution at the $(n + 1)^{st}$ time step. The trapezoidal rule is given by

$$\frac{dy}{dt} \approx \frac{y_{n+1} - y_n}{h}, \qquad -\lambda y \approx -\frac{\lambda}{2}[y_{n+1} + y_n]. \tag{11.12}$$

Consequently,

$$\begin{aligned} y_{n+1} &= \frac{1 - \lambda h/2}{1 + \lambda h/2} y_n \\ &= \left[\frac{1 - \lambda h/2}{1 + \lambda h/2}\right]^n y_0 \end{aligned} \tag{11.13}$$

Clearly, $y_{n+1} \to 0$ if $\left|\frac{1 - \lambda h/2}{1 + \lambda h/2}\right| < 1$, and $y_{n+1} \to \infty$ if $\left|\frac{1 - \lambda h/2}{1 + \lambda h/2}\right| > 1$, in which $|\cdot|$ implies the magnitude. If the first inequality is satisfied, the numerical method is called *A-stable* (see Dahlquist and Bjork, 1974). We next write $\lambda = \lambda_r + i\lambda_i$, and now A-stability requires that

$$\frac{\left(1 - \frac{\lambda_r h}{2}\right)^2 + \left(\frac{\lambda_i h}{2}\right)^2}{\left(1 + \frac{\lambda_r h}{2}\right)^2 + \left(\frac{\lambda_i h}{2}\right)^2} < 1. \tag{11.14}$$

A-stability implies that $\lambda_r > 0$, which is precisely the condition for asymptotic stability.

Consider the matrix-vector system arising in the finite-element method:

$$\mathbf{M}\ddot{\boldsymbol{\gamma}} + \mathbf{D}\dot{\boldsymbol{\gamma}} + \mathbf{K}\boldsymbol{\gamma} = \mathbf{0}, \quad \boldsymbol{\gamma}(0) = \boldsymbol{\gamma}_0, \quad \dot{\boldsymbol{\gamma}}(0) = \dot{\boldsymbol{\gamma}}_0, \tag{11.15}$$

in which **M**, **D**, and **K** are positive-definite. Elementary manipulation serves to derive that

$$\frac{d}{dt}\left[\frac{1}{2}\dot{\boldsymbol{\gamma}}^{\mathrm{T}}\mathbf{M}\dot{\boldsymbol{\gamma}}+\frac{1}{2}\boldsymbol{\gamma}^{\mathrm{T}}\mathbf{K}\boldsymbol{\gamma}\right]=-\dot{\boldsymbol{\gamma}}^{\mathrm{T}}\mathbf{D}\dot{\boldsymbol{\gamma}}<\mathbf{0}. \tag{11.16}$$

It follows that $\dot{\boldsymbol{\gamma}}\to\mathbf{0}$ and $\boldsymbol{\gamma}\to\mathbf{0}$. We conclude that the system is asymptotically stable.

Introducing the vector $\mathbf{p}=\dot{\boldsymbol{\gamma}}$, the n-dimensional, second-order system is written in *state form* as the $(2n)$-dimensional, first-order system of ordinary differential equations:

$$\begin{bmatrix}\mathbf{M} & \mathbf{0}\\ \mathbf{0} & \mathbf{I}\end{bmatrix}\begin{pmatrix}\mathbf{p}\\ \boldsymbol{\gamma}\end{pmatrix}^{\bullet}+\begin{bmatrix}\mathbf{D} & \mathbf{K}\\ -\mathbf{I} & \mathbf{0}\end{bmatrix}\begin{pmatrix}\mathbf{p}\\ \boldsymbol{\gamma}\end{pmatrix}=\begin{pmatrix}\mathbf{f}\\ \mathbf{0}\end{pmatrix}. \tag{11.17}$$

We next apply the trapezoidal rule to the system:

$$\begin{bmatrix}\mathbf{M} & \mathbf{0}\\ \mathbf{0} & \mathbf{I}\end{bmatrix}\begin{pmatrix}\frac{1}{h}(\mathbf{p}_{n+1}-\mathbf{p}_n)\\ \frac{1}{h}(\boldsymbol{\gamma}_{n+1}-\boldsymbol{\gamma}_n)\end{pmatrix}+\begin{bmatrix}\mathbf{D} & \mathbf{K}\\ -\mathbf{I} & \mathbf{0}\end{bmatrix}\begin{pmatrix}\frac{1}{2}(\mathbf{p}_{n+1}+\mathbf{p}_n)\\ \frac{1}{2}(\boldsymbol{\gamma}_{n+1}+\boldsymbol{\gamma}_n)\end{pmatrix}=\begin{pmatrix}\frac{1}{2}(\mathbf{f}_{n+1}+\mathbf{f}_n)\\ \mathbf{0}\end{pmatrix}. \tag{11.18}$$

From the equation in the lower row, $\mathbf{p}_{n+1}=\frac{2}{h}[\boldsymbol{\gamma}_{n+1}-\boldsymbol{\gamma}_n]-\mathbf{p}_n$. Eliminating $\mathbf{p}_{n+1}$ in the upper row furnishes a formula underlying the classical Newmark method:

$$\begin{aligned}\mathbf{K}_{\mathbf{D}}\boldsymbol{\gamma}_{n+1}&=\mathbf{r}_{n+1},\qquad \mathbf{K}_{\mathbf{D}}=\left[\mathbf{M}+\frac{h}{2}\mathbf{D}+\frac{h^2}{4}\mathbf{K}\right]\\ \mathbf{r}_{n+1}&=\left[\mathbf{M}+\frac{h}{2}\mathbf{D}-\frac{h^2}{4}\mathbf{K}\right]y_n+\left[\mathbf{M}+\frac{h}{2}\mathbf{D}\right]\frac{h}{2}\mathbf{p}_n+\frac{h^2}{4}(\mathbf{f}_{n+1}+\mathbf{f}_n)\end{aligned} \tag{11.19}$$

and $\mathbf{K}_{\mathbf{D}}$ can be called the dynamic stiffness matrix. Equation 11.19 can be solved by triangularization of $\mathbf{K}_{\mathbf{D}}$, followed by forward and backward substitution.

11.3 NEWMARK'S METHOD

To fix the important notions, consider the model equation

$$\frac{dy}{dx}=f(y). \tag{11.20}$$

Suppose this equation is modeled as

$$\alpha y_{n+1}+\beta y_n+h[\gamma f_{n+1}+\delta f_n]=0. \tag{11.21}$$

We now use the Taylor series to express y_{n+1} and f_{n+1} in terms of y_n and f_n. Noting that $y_n' = f_n$ and $y_n'' = f_n'$, we obtain

$$0 = \alpha[y_n + y_n'h + y_n''h^2/2] + \beta y_n + h\gamma[y_n' + y_n''h] + h\delta y_n'. \tag{11.22}$$

For exact agreement through h^2, the coefficients must satisfy

$$\alpha + \beta = 0 \qquad \alpha + \gamma + \delta = 0 \qquad \alpha/2 + \gamma = 0. \tag{11.23}$$

We also introduce the convenient normalization $\gamma + \delta = 1$. Simple manipulation serves to derive that $\alpha = -1$, $\beta = 1$, $\gamma = 1/2$, $\delta = 1/2$, thus furnishing

$$\frac{y_{n+1} - y_n}{h} = \frac{1}{2}[f(y_{n+1}) + f(y_n)], \tag{11.24}$$

which can be recognized as the trapezoidal rule.

The trapezoidal rule is unique and optimal in having the following three characteristics:

It is a "one-step method" using only the values at the beginning of the current time step.
It is second-order-accurate; it agrees exactly with the Taylor series through h^2.
Applied to $dy/dt + \lambda y = 0$, with initial condition $y(0) = y_0$, it is A-stable whenever a system described by the equation is asymptotically stable.

11.4 INTEGRAL EVALUATION BY GAUSSIAN QUADRATURE

There are many integrations in the finite-element method, the accuracy and efficiency of which is critical. Fortunately, a method that is optimal in an important sense, called Gaussian quadrature, has long been known. It is based on converting physical coordinates to natural coordinates. Consider $\int_a^b f(x)dx$. Let $\xi = \frac{1}{b-a}[2x - (a+b)]$. Clearly, ξ maps the interval $[a, b]$ into the interval $[-1,1]$. The integral now becomes $\frac{1}{b-a}\int_{-1}^{1} f(\xi)d\xi$. Now consider the power series

$$f(\xi) = \alpha_0 + \alpha_1\xi + \alpha_2\xi^2 + \alpha_3\xi^3 + \alpha_4\xi^4 + \alpha_5\xi^5 + \cdots, \tag{11.25}$$

from which

$$\int_{-1}^{1} f(\xi)d\xi = 2\alpha_1 + 0 + \frac{2}{3}\alpha_3 + 0 + \frac{2}{5}\alpha_5 + 0 + \cdots. \tag{11.26}$$

The advantages illustrated for integration on a symmetric interval demonstrate that, with n function evaluations, an integral can be evaluated exactly through $(2n-1)^{st}$ order.

Consider the first $2n-1$ terms in a power-series representation for a function:

$$g(\xi) = \alpha_1 + \alpha_2\xi + \cdots + \alpha_{2n}\xi^{2n-1}. \tag{11.27}$$

Assume that n integration (Gauss) points ξ_i and n weights are used as follows:

$$\int_{-1}^{1} g(\xi)d\xi = \sum_{i=1}^{n} g(\xi_i)w_i = \alpha_1\sum_{i=1}^{n} w_i + \alpha_2\sum_{i=1}^{n} w_i\alpha_i + \cdots + \alpha_{2n}\sum_{i=1}^{n} w_i\xi_i^{2n-1}. \tag{11.28}$$

Comparison with Equation 11.26 implies that

$$\sum_{i=1}^{n} w_i = 1,\ \sum_{i=1}^{n} w_i\xi = 0,\ \sum_{i=1}^{n} w_i\xi_i^2 = 2/3,\ \ldots,\ \sum_{i=1}^{n} w_i\xi_i^{2n-2} = \frac{2}{2n-1},\ \sum_{i=1}^{n} w_i\xi_i^{2n-1} = 0. \tag{11.29}$$

It is necessary to solve for n integration points, ξ_i, and n weights, w_i. These are universal quantities. To integrate a given function, $g(\xi)$, exactly through ξ^{2n-i}, it is necessary to perform n function evaluations, namely to compute $g(\xi_i)$.

As an example, we seek two Gauss points and two weights. For $n = 2$,

$$\begin{aligned} w_1 + w_2 &= 2 \quad \text{(i)}, & w_1\xi_1 + w_2\xi_2 &= 0 \quad \text{(ii)} \\ w_1\xi_1^2 + w_2\xi_2^2 &= \frac{2}{3} \quad \text{(iii)}, & w_1\xi_1^3 + w_2\xi_2^3 &= 0 \quad \text{(iv)} \end{aligned} \tag{11.30}$$

From (ii) and (iv), $w_1\xi_1[\xi_1^2 - \xi_2^2] = 0$, leading to $\xi_2 = -\xi_1$. From (i) and (iii), it follows that $-\xi_2 = \xi_1 = 1/\sqrt{3}$. The normalization $w_1 = 1$ implies that $w_2 = 1$.

11.5 MODAL ANALYSIS BY FEA

11.5.1 Modal Decomposition

In the absence of damping, the finite-element equation for a linear mechanical system, which is unforced but has nonzero initial values, is described by

$$\mathbf{M}\ddot{\boldsymbol{\gamma}} + \mathbf{K}\boldsymbol{\gamma} = \mathbf{0}, \quad \boldsymbol{\gamma}(0) = \boldsymbol{\gamma}_0, \quad \dot{\boldsymbol{\gamma}}(0) = \dot{\boldsymbol{\gamma}}_0. \tag{11.31}$$

Assume a solution of the form $\boldsymbol{\gamma} = \hat{\boldsymbol{\gamma}}\, exp(\lambda t)$, which furnishes upon substitution

$$[\mathbf{K} + \lambda^2\mathbf{M}]\hat{\boldsymbol{\gamma}} = \mathbf{0}. \tag{11.32}$$

The j^{th} eigenvalue, λ_j, is obtained by solving $\det(\mathbf{K} + \lambda_j^2\mathbf{M}) = 0$, and a corresponding eigenvector vector, $\boldsymbol{\gamma}_j$, can also be computed (see Sample Problem 2).

For the sake of generality, suppose that λ_j and $\boldsymbol{\gamma}_j$ are complex. Let $\boldsymbol{\gamma}_j^{\mathbf{H}}$ denote the complex conjugate (Hermitian) transpose of $\boldsymbol{\gamma}_j$. Now, λ_j^2 satisfies

$$\lambda_j^2 = -\frac{\boldsymbol{\gamma}_j^{\mathbf{H}}\mathbf{K}\boldsymbol{\gamma}_j}{\boldsymbol{\gamma}_j^{\mathbf{H}}\mathbf{M}\boldsymbol{\gamma}_j}.$$

Since **M** and **K** are real and positive-definite, it follows that λ_j is pure imaginary: $\lambda_j = i\omega_j$. Without loss of generality, we can take $\boldsymbol{\gamma}_j$ to be real and orthonormal.

Sample Problem 1

As an example, consider

$$\mathbf{M} = \begin{bmatrix} 1 & 0 \\ 0 & 1 \end{bmatrix} \qquad \mathbf{K} = \begin{bmatrix} k_{11} & k_{12} \\ k_{12} & k_{22} \end{bmatrix}. \tag{11.33}$$

Now $\det[\mathbf{K} + \lambda^2\mathbf{I}] = 0$ reduces to

$$(\lambda^2)^2 + [k_{11} + k_{22}]\lambda^2 + [k_{11}k_{22} + k_{12}^2] = 0, \tag{11.34}$$

with the roots

$$\begin{aligned} \lambda_{+,-}^2 &= \frac{1}{2}\left[-[k_{11} + k_{22}] \pm \sqrt{[k_{11} + k_{22}]^2 - 4[k_{11}k_{22} + k_{12}^2]}\right] \\ &= \frac{1}{2}\left[-[k_{11} + k_{22}] \pm \sqrt{[k_{11} - k_{22}]^2 - 4k_{12}^2}\right] \end{aligned} \tag{11.35}$$

so that both λ_+^2 and λ_-^2 are negative (since k_{11} and k_{22} are positive).

We now consider eigenvectors. The eigenvalue equations for the i^{th} and j^{th} eigenvectors are written as

$$[\mathbf{K} + \omega_j^2\mathbf{M}]\mathbf{g}_j = \mathbf{0} \qquad [\mathbf{K} + \omega_k^2\mathbf{M}]\mathbf{g}_k = \mathbf{0} \tag{11.36}$$

It is easily seen that the eigenvectors have arbitrary magnitudes, and for convenience, we assume that they have unit magnitude $\boldsymbol{\gamma}_j^{\mathbf{T}}\boldsymbol{\gamma}_j = 1$. Simple manipulation furnishes that

$$\boldsymbol{\gamma}_k^{\mathbf{T}}\mathbf{K}\boldsymbol{\gamma}_j - \boldsymbol{\gamma}_j^{\mathbf{T}}\mathbf{K}\boldsymbol{\gamma}_k - [\omega_j^2\boldsymbol{\gamma}_k^{\mathbf{T}}\mathbf{M}\boldsymbol{\gamma}_j - \omega_k^2\boldsymbol{\gamma}_j^{\mathbf{T}}\mathbf{M}\boldsymbol{\gamma}_k] = 0. \tag{11.37}$$

Symmetry of **K** and **M** implies that

$$\boldsymbol{\gamma}_k^{\mathrm{T}}\mathbf{K}\boldsymbol{\gamma}_j - \boldsymbol{\gamma}_j^{\mathrm{T}}\mathbf{K}\boldsymbol{\gamma}_k = 0, \quad [\omega_j^2\boldsymbol{\gamma}_k^{\mathrm{T}}\mathbf{M}\boldsymbol{\gamma}_j - \omega_k^2\boldsymbol{\gamma}_j^{\mathrm{T}}\mathbf{M}\boldsymbol{\gamma}_k] = (\omega_j^2 - \omega_k^2)\boldsymbol{\gamma}_k^{\mathrm{T}}\mathbf{M}\boldsymbol{\gamma}_j = 0. \tag{11.38}$$

Assuming for convenience that the eigenvalues are all distinct, it follows that

$$\boldsymbol{\gamma}_j^{\mathrm{T}}\mathbf{M}\boldsymbol{\gamma}_k = 0, \quad \boldsymbol{\gamma}_j^{\mathrm{T}}\mathbf{K}\boldsymbol{\gamma}_k = 0, \quad j \neq k. \tag{11.39}$$

The eigenvectors are thus said to be orthogonal with respect to **M** and **K**. The quantities $\mu_j = \boldsymbol{\gamma}_j^{\mathrm{T}}\mathbf{M}\boldsymbol{\gamma}_j$ and $\kappa_j = \boldsymbol{\gamma}_j^{\mathrm{T}}\mathbf{K}\boldsymbol{\gamma}_j$ are called the (j^{th}) modal mass and (j^{th}) modal stiffness.

Sample Problem 2

Consider

$$\begin{bmatrix} 2 & 0 \\ 0 & 1 \end{bmatrix}\begin{pmatrix} \gamma_1 \\ \gamma_2 \end{pmatrix}^{\bullet\bullet} + \frac{k}{m}\begin{bmatrix} 2 & -1 \\ -1 & 1 \end{bmatrix}\begin{pmatrix} \gamma_1 \\ \gamma_2 \end{pmatrix} = \begin{pmatrix} 0 \\ 0 \end{pmatrix}. \tag{11.40}$$

Let $\zeta^2 = \omega_j^2/\omega_0^2$, $\omega_0^2 = k/m$. For the determinant to vanish, $1 - \zeta_{\pm}^2 = \pm 1/\sqrt{2}$. Using $1 - \zeta_+^2 = 1/\sqrt{2}$, the first eigenvector satisfies

$$\begin{bmatrix} \sqrt{2} & -1 \\ -1 & 1/\sqrt{2} \end{bmatrix}\begin{pmatrix} \gamma_1^{(1)} \\ \gamma_2^{(1)} \end{pmatrix} = \begin{pmatrix} 0 \\ 0 \end{pmatrix}, \qquad \left[\gamma_1^{(1)}\right]^2 + \left[\gamma_2^{(1)}\right]^2 = 1, \tag{11.41}$$

implying that $\gamma_1^{(1)} = 1/\sqrt{3}$, $\gamma_2^{(1)} = \sqrt{2}/\sqrt{3}$. The corresponding procedures for the second eigenvalue furnish that $\gamma_1^{(2)} = 1/\sqrt{3}$, $\gamma_2^{(2)} = -\sqrt{2}/\sqrt{3}$. It is readily verified that

$$\begin{aligned} &\boldsymbol{\gamma}^{(2)^{\mathrm{T}}}\mathbf{M}\boldsymbol{\gamma}^{(1)} = \boldsymbol{\gamma}^{(1)^{\mathrm{T}}}\mathbf{M}\boldsymbol{\gamma}^{(2)} = 0, \quad \mu_1 = 4/3, \qquad \mu_2 = 4/3, \\ &\boldsymbol{\gamma}^{(2)^{\mathrm{T}}}\mathbf{K}\boldsymbol{\gamma}^{(1)} = \boldsymbol{\gamma}^{(1)^{\mathrm{T}}}\mathbf{K}\boldsymbol{\gamma}^{(2)} = 0, \quad \kappa_1 = \frac{4}{3}[1 - 1/\sqrt{2}], \quad \kappa_2 = \frac{4}{3}[1 + 1/\sqrt{2}] \end{aligned} \tag{11.42}$$

The modal matrix **X** is now defined as

$$\mathbf{X} = [\boldsymbol{\gamma}_1 \quad \boldsymbol{\gamma}_2 \quad \boldsymbol{\gamma}_3 \quad \cdots \quad \boldsymbol{\gamma}_n]. \tag{11.43}$$

Since the jk^{th} entries of $\mathbf{X^T MX}$ and $\mathbf{X^T KX}$ are $\boldsymbol{\gamma}_j^{\mathbf{T}}\mathbf{M}\boldsymbol{\gamma}_k$ and $\boldsymbol{\gamma}_j^{\mathbf{T}}\mathbf{K}\boldsymbol{\gamma}_k$, respectively, it follows that

$$\mathbf{X^T MX} = \begin{bmatrix} \mu_1 & 0 & . & . & . \\ 0 & \mu_2 & . & . & . \\ . & . & . & . & . \\ . & . & . & . & . \\ . & . & . & . & \mu_n \end{bmatrix} \quad \mathbf{X^T KX} = \begin{bmatrix} \kappa_1 & 0 & . & . & . \\ 0 & \kappa_2 & . & . & . \\ . & . & . & . & . \\ . & . & . & . & . \\ . & . & . & . & \kappa_n \end{bmatrix}. \tag{11.44}$$

The modal matrix is said to be orthogonal with respect to **M** and **K**, but it is not purely orthogonal since $\mathbf{X}^{-1} \neq \mathbf{X}^{\mathbf{T}}$.

The governing equation is now rewritten as

$$\mathbf{X^T MX}\ddot{\boldsymbol{\xi}} + \mathbf{X^T KX}\boldsymbol{\xi} = \mathbf{g}, \quad \boldsymbol{\xi} = \mathbf{X}^{-1}\boldsymbol{\gamma}, \quad \mathbf{g} = \mathbf{X^T f}, \tag{11.45}$$

implying the uncoupled modes

$$\mu_j\ddot{\xi}_j + \kappa_j\xi_j = g_j(t). \tag{11.46}$$

Suppose that $g_j(t) = g_{j0} \sin(\omega t)$. Neglecting transients, the steady-state solution for the j^{th} mode is

$$\xi_j = \frac{g_{j0}}{\kappa_j - \omega^2\mu_j}\sin(\omega t). \tag{11.47}$$

It is evident that if $\omega^2 \sim \omega_j^2 = \kappa_j/\mu_j$ (resonance), the response amplitude for the j^{th} mode is much greater than for the other modes, so that the structural motion under this excitation frequency illustrates the mode. For this reason, the modes can easily be animated.

11.5.2 Computation of Eigenvectors and Eigenvalues

Consider $\mathbf{K}\boldsymbol{\gamma}_j = \omega_j^2\mathbf{M}\boldsymbol{\gamma}_j$, with $\boldsymbol{\gamma}_j^{\mathbf{T}}\boldsymbol{\gamma}_j = 1$. Many methods have been proposed to compute the eigenvalues and eigenvectors of a large system. Here, we describe a method that is easy to visualize, which we call the *hypercircle* method. The vectors $\mathbf{K}\boldsymbol{\gamma}_j$ and $\mathbf{M}\boldsymbol{\gamma}_j$ must be parallel to each other. Furthermore, the vectors $\mathbf{K}\gamma_j/\sqrt{\gamma_j^{\mathbf{T}}\mathbf{K}^2\gamma_j}$ and $\mathbf{M}\gamma_j/\sqrt{\gamma_j^{\mathbf{T}}\mathbf{M}^2\gamma_j}$ must terminate at the same point in a hypersphere in *n*-dimensional space. Suppose that $\boldsymbol{\gamma}_j^{(\nu)}$ is the ν^{th} iterate and that the two vectors

do not coincide in direction. Another iterate can be attained by an interval-halving method:

$$\mathbf{M}\hat{\boldsymbol{\gamma}}_j^{(\nu+1)} = \frac{1}{2}\left[\frac{\mathbf{M}\boldsymbol{\gamma}_j^{(\nu)}}{\sqrt{\boldsymbol{\gamma}_j^{(\nu)\mathrm{T}}\mathbf{M}^2\boldsymbol{\gamma}_j^{(\nu)}}} + \frac{\mathbf{K}\boldsymbol{\gamma}_j^{(\nu)}}{\sqrt{\boldsymbol{\gamma}_j^{(\nu)\mathrm{T}}\mathbf{K}^2\boldsymbol{\gamma}_j^{(\nu)}}}\right], \quad \boldsymbol{\gamma}_j^{(\nu+1)} = \hat{\boldsymbol{\gamma}}_j^{(\nu+1)} \Big/ \sqrt{\hat{\boldsymbol{\gamma}}_j^{(\nu+1)\mathrm{T}}\mathbf{M}^2\hat{\boldsymbol{\gamma}}_j^{(\nu+1)}}\,. \tag{11.48}$$

Alternatively, note that

$$C(\boldsymbol{\gamma}_j) = \frac{\boldsymbol{\gamma}_j^{\mathrm{T}}\mathbf{K}}{\sqrt{\boldsymbol{\gamma}_j^{\mathrm{T}}\mathbf{K}^2\boldsymbol{\gamma}_j}} \frac{\mathbf{M}\boldsymbol{\gamma}_j}{\sqrt{\boldsymbol{\gamma}_j^{\mathrm{T}}\mathbf{M}^2\boldsymbol{\gamma}_j}} \tag{11.49}$$

is the cosine of the angle between two unit vectors, and as such it assumes the maximum value of unity when the vectors coincide. A search can be executed on the hypersphere in the vicinity of the current point, seeking the path along which $C(\boldsymbol{\gamma}_j)$ increases until the maximum is attained.

Once the eigenvector $\boldsymbol{\gamma}_j$ is found, the corresponding eigenvalue is found from $\omega_j^2 = (\boldsymbol{\gamma}_j^{\mathrm{T}}\mathbf{K}\boldsymbol{\gamma}_j)/(\boldsymbol{\gamma}_j^{\mathrm{T}}\mathbf{M}\boldsymbol{\gamma}_j)$. Now, an efficient scheme is needed to "deflate" the system so that ω_1^2,and $\boldsymbol{\gamma}_1$ no longer are part of the eigenstructure in order to ensure that the solution scheme does not converge to values that have already been calculated.

Given $\boldsymbol{\gamma}_1$ and ω_1^2, we can construct a vector $\mathbf{p}_2$ that is $\mathbf{M}$-orthogonal to $\boldsymbol{\gamma}_1$ by using an intermediate vector $\hat{\mathbf{p}}_2$: $\mathbf{p}_2 = \hat{\mathbf{p}}_2 - \boldsymbol{\gamma}_1^{\mathrm{T}}\mathbf{M}\hat{\mathbf{p}}_2\boldsymbol{\gamma}_1$. Clearly, $\boldsymbol{\gamma}_1^{\mathrm{T}}\mathbf{M}\mathbf{p}_2 = \boldsymbol{\gamma}_1^{\mathrm{T}}\mathbf{M}\hat{\mathbf{p}}_2 - \boldsymbol{\gamma}_1^{\mathrm{T}}\mathbf{M}\hat{\mathbf{p}}_2\boldsymbol{\gamma}_1^{\mathrm{T}}\mathbf{M}\boldsymbol{\gamma}_1 = 0$ assuming $\mu_1 = 1$. However, $\mathbf{p}_2$ is also clearly orthogonal to $\mathbf{K}\boldsymbol{\gamma}_1$ since it is collinear with $\mathbf{M}\boldsymbol{\gamma}_1$. A similar procedure leads to vectors $\mathbf{p}_j$, which are orthogonal to each other and to $\mathbf{M}\boldsymbol{\gamma}_1$ and $\mathbf{K}\boldsymbol{\gamma}_1$. For example, with $\mathbf{p}_2$ set to unit magnitude, $\mathbf{p}_3 = \hat{\mathbf{p}}_3 - \mathbf{p}_2^{\mathrm{T}}\hat{\mathbf{p}}_3\mathbf{p}_2 - \boldsymbol{\gamma}_1^{\mathrm{T}}\mathbf{M}\hat{\mathbf{p}}_3\boldsymbol{\gamma}_1$. Now, $\mathbf{p}_2^{\mathrm{T}}\mathbf{p}_3 = 0$ and $\boldsymbol{\gamma}_1^{\mathrm{T}}\mathbf{M}\hat{\mathbf{p}}_3 = 0$.

Introduce the matrix $\mathbf{X}_1$ as follows: $\mathbf{X}_1 = [\boldsymbol{\gamma}_1 \quad \mathbf{p}_2 \quad \mathbf{p}_3 \quad \cdots \quad \mathbf{p}_n]$. For the k^{th} eigenvalue, we can write

$$\left[\mathbf{X}_1^{\mathrm{T}}\mathbf{K}\mathbf{X}_1 - \boldsymbol{\omega}_k^2\mathbf{X}_1^{\mathrm{T}}\mathbf{M}\mathbf{X}_1\right]\mathbf{X}_1^{-1}\boldsymbol{\gamma}_k = \mathbf{0}, \tag{11.50}$$

which decomposes to

$$\left[\begin{bmatrix}\omega_1^2 & \mathbf{0}\\ \mathbf{0}^{\mathrm{T}} & \tilde{\mathbf{K}}_{n-1}\end{bmatrix} - \omega_k^2\begin{bmatrix}1 & \mathbf{0}\\ \mathbf{0}^{\mathrm{T}} & \tilde{\mathbf{M}}_{n-1}\end{bmatrix}\right]\begin{pmatrix}0\\ \boldsymbol{\eta}_{n-1}\end{pmatrix} = \begin{pmatrix}0\\ \mathbf{0}\end{pmatrix}. \tag{11.51}$$

This implies the "deflated" eigenvalue problem

$$[\tilde{\mathbf{K}}_{n-1} - \omega_k\tilde{\mathbf{M}}_{n-1}]\boldsymbol{\eta}_{n-1} = \mathbf{0}. \tag{11.52}$$

The eigenvalues of the deflated system are also eigenvalues of the original system. The eigenvector $\boldsymbol{\eta}_{n-1}$ can be used to compute the eigenvectors of the original system

using transformations involving the matrix $\mathbf{X_1}$. The eigenvalues and eigenvectors of the deflated system can be computed by, for example, the hypercircle method described previously.

11.6 EXERCISES

1. Verify that the triangular factors $\mathbf{L}_3$ and $\mathbf{L}_3^{\mathrm{T}}$ for $\mathbf{A_3}$ in Equation 11.5 are correct.
2. Using $\mathbf{A_3}$ in Equation 11.5, use forward substitution followed by backward substitution to solve

$$\mathbf{A}_3\boldsymbol{\gamma} = \begin{pmatrix} 1 \\ 1 \\ 1 \end{pmatrix}.$$

3. Triangularize the matrix

$$\mathbf{K} = \begin{bmatrix} 36 & 30 & 18 \\ 30 & 41 & 23 \\ 18 & 23 & 14 \end{bmatrix}.$$

4. For the model equation $dy/dx = f(y)$, develop a *two-step* numerical-integration model:

$$(\alpha y_{n+1} + \beta y_n + \gamma y_{n-1}) + h[\delta f(y_{n+1}) + \varepsilon f(y_n) + \zeta f(y_{n-1})] = 0.$$

   What is the order of the integration method (highest power in h with exact agreement with the Taylor series)?
5. Find the integration (Gauss) points and weights for $n = 3$.
6. In the damped linear-mechanical system

$$\mathbf{M}\ddot{\boldsymbol{\gamma}} + \mathbf{D}\dot{\boldsymbol{\gamma}} + \mathbf{K}\boldsymbol{\gamma} = \mathbf{f}(t),$$

   suppose that $\boldsymbol{\gamma}(t) = \boldsymbol{\gamma}_n$ at the n^{th} time step. Derive $\mathbf{K_D}$ and $\mathbf{r}_{n+1}$ such that $\boldsymbol{\gamma}$ at the $(n + 1)^{st}$ time step satisfies

$$\mathbf{K_D}\boldsymbol{\gamma}_{n+1} = \mathbf{r}_{n+1}.$$

7. For the linear system

$$\begin{bmatrix} 36 & 30 & 24 \\ 30 & 41 & 32 \\ 24 & 32 & 27 \end{bmatrix} \begin{pmatrix} \gamma_1 \\ \gamma_2 \\ \gamma_3 \end{pmatrix} = \begin{pmatrix} 1 \\ 2 \\ 3 \end{pmatrix}$$

   triangularize the matrix and solve for γ_1, γ_2, γ_3.

8. (a) Find the modal masses μ_1, μ_2 and the modal stiffnesses κ_1 and κ_2 of the system

$$3\begin{bmatrix}1 & 0\\ 0 & 2\end{bmatrix}\begin{pmatrix}\ddot{\gamma}_1\\ \gamma_2\end{pmatrix}+27\begin{bmatrix}1 & -1\\ -1 & 2\end{bmatrix}\begin{pmatrix}\gamma_1\\ \gamma_2\end{pmatrix}=\begin{pmatrix}10\\ 20\end{pmatrix}\sin(10t).$$

   (b) Determine the steady-state response of the system (i.e., particular solution to the equation).

9. Triangularize

$$\begin{bmatrix}2\mu A/L & 0 & -A\\ 0 & 4\mu AL/Y^2 & -2\mu A/L\\ A & 2\mu A/L & 0\end{bmatrix}.$$

10. Put the following equations in state form, apply the trapezoidal rule, and triangularize the ensuing dynamic stiffness matrix:

$$\mathbf{M}\ddot{\boldsymbol{\gamma}}+\mathbf{K}\boldsymbol{\gamma}-\boldsymbol{\Sigma}\boldsymbol{\pi}=\mathbf{f},\qquad \boldsymbol{\Sigma}^{\mathrm{T}}\boldsymbol{\gamma}=\mathbf{0}.$$

12 Rotating and Unrestrained Elastic Bodies

12.1 FINITE ELEMENTS IN ROTATION

We first consider rotation about a fixed axis. The coordinate system is embedded in the fixed point and rotates. The undeformed position vector, $\mathbf{X}'$ in the rotated system is related to its counterpart, $\mathbf{X}$, in the unrotated system by $\mathbf{X}' = \mathbf{Q}(t)\mathbf{X}$. The counterpart for the deformed position is $\mathbf{x}' = \mathbf{Q}(t)\mathbf{x}$. The displacement also satisfies $\mathbf{u}' = \mathbf{Q}(t)\mathbf{u}$. The rotation is represented by the "axial" vector, $\boldsymbol{\omega}$, satisfying $\boldsymbol{\omega} \times (*) = \dot{\mathbf{Q}}(t)\mathbf{Q}^{\mathbf{T}}(t)(*)$. (Recall that $\dot{\mathbf{Q}}(t)\mathbf{Q}^{\mathbf{T}}(t)$ is antisymmetric). The time derivatives in rotating coordinates satisfy

$$\begin{aligned} \frac{d\mathbf{u}'}{dt} &= \frac{\partial \mathbf{u}'}{\partial t} + \boldsymbol{\omega} \times \mathbf{u}' \\ \frac{d^2\mathbf{u}'}{dt^2} &= \frac{\partial^2 \mathbf{u}'}{\partial t^2} + 2\boldsymbol{\omega} \times \mathbf{u}' + \boldsymbol{\omega} \times \boldsymbol{\omega} \times \mathbf{u} + \boldsymbol{\alpha} \times \mathbf{u} \end{aligned} \tag{12.1}$$

where $\boldsymbol{\alpha} = \frac{\partial \boldsymbol{\omega}}{\partial t}$ and $\frac{\partial(.)}{\partial t}$ imply differentiation with the coordinate system instantaneously fixed. The rightmost four terms in (12.1) are called the translational, Coriolis, centrifugal, and angular accelerations, respectively.

Applied to the Principle of Virtual Work, the inertial term becomes $\int \delta \mathbf{u}'^{\mathbf{T}} \rho \frac{d^2}{dt^2} [\mathbf{u}' + \mathbf{X}'] dV$. Assuming that $\mathbf{u}' = \boldsymbol{\varphi}^{\mathbf{T}}(\mathbf{X}')\boldsymbol{\Phi}\boldsymbol{\gamma}(t)$,

$$\int \delta \mathbf{u}'^{\mathbf{T}} \rho \frac{d^2\mathbf{u}'}{dt^2} dV = \delta \boldsymbol{\gamma}^{\mathbf{T}} \left[\mathbf{M} \frac{d^2\boldsymbol{\gamma}}{dt^2} + \mathbf{G}_1 \frac{d\boldsymbol{\gamma}}{dt} + (\mathbf{G}_2 + \mathbf{A})\boldsymbol{\gamma} \right] \tag{12.2}$$

$$\mathbf{M} = \boldsymbol{\Phi}^{\mathbf{T}} \int \rho \boldsymbol{\varphi} \boldsymbol{\varphi}^{\mathbf{T}} d\mathrm{V} \boldsymbol{\Phi}, \qquad \mathbf{G}_1 = \boldsymbol{\Phi}^{\mathbf{T}} \int \rho \boldsymbol{\varphi} \boldsymbol{\Omega} \boldsymbol{\varphi}^{\mathbf{T}} d\mathrm{V} \boldsymbol{\Phi},$$

$$\mathbf{G}_2 = \boldsymbol{\Phi}^{\mathbf{T}} \int \rho \boldsymbol{\varphi} \boldsymbol{\Omega}^2 \boldsymbol{\varphi}^{\mathbf{T}} d\mathrm{V} \boldsymbol{\Phi}, \qquad \mathbf{A} = \boldsymbol{\Phi}^{\mathbf{T}} \int \rho \boldsymbol{\varphi} \boldsymbol{A} \boldsymbol{\varphi}^{\mathbf{T}} d\mathrm{V} \boldsymbol{\Phi}.$$

The matrix $\mathbf{M}$ is the conventional positive-definite and symmetric mass matrix; the Coriolis matrix $\mathbf{G}_1$ is antisymmetric; the centrifugal matrix $\mathbf{G}_2$ is negative-definite; and the angular acceleration matrix $\mathbf{A}$ is antisymmetric. Also, $\boldsymbol{\Omega} = \dot{\mathbf{Q}}\mathbf{Q}^T, \boldsymbol{A} = \dot{\boldsymbol{\Omega}}$.

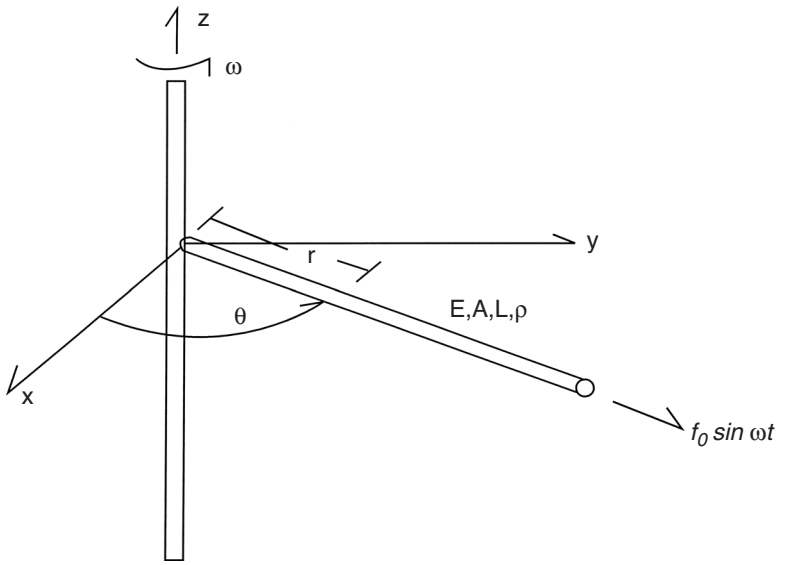

FIGURE 12.1 Elastic rod on rotating rigid shaft.

There is also a rigid-body force term:

$$\int \delta \mathbf{u}'^T \rho \frac{d^2}{dt^2} \mathbf{X}' d\mathrm{V} = -\delta \boldsymbol{\gamma}^T \mathbf{f}_{rot}, \qquad \mathbf{f}_{rot} = \boldsymbol{\Phi}^T \int \rho \boldsymbol{\varphi} [\boldsymbol{\Omega}^2 + \mathbf{A}] \mathbf{X}' d\mathrm{V}. \tag{12.3}$$

The governing equation is now

$$\mathbf{M} \frac{d^2 \boldsymbol{\gamma}}{dt^2} + \mathbf{G}_1 \frac{d\boldsymbol{\gamma}}{dt} + [\mathbf{K} + \mathbf{G}_2 + \mathbf{A}] \boldsymbol{\gamma} = \mathbf{f} - \mathbf{f}_{rot}. \tag{12.4}$$

Consider a rod attached to a thin shaft rotating steadily at angular velocity ω (see Figure 12.1), with $f_0 = 0$.

If r is the undeformed position along the shaft, the governing equation is

$$\mathbf{E}A \frac{d^2 u}{dr^2} = -\omega^2 [r + u]. \tag{12.5}$$

Assuming a one-element model with $u(r,t) = ru(L,t)/L$, we obtain

$$\left[\frac{EA}{L} - \frac{\rho \omega^2 AL}{3} \right] u(L,t) = -\rho \omega^2 A \int_0^L \frac{r}{L} r dr$$

$$= -\frac{\rho \omega^2 AL^2}{3} \tag{12.6}$$

Clearly, $u(L, t)$ becomes unbounded if ω becomes equal to the natural frequency $\omega = \sqrt{\frac{EA}{3}} \Big/ \sqrt{\frac{\rho AL}{3}}$, in which case, ω is called a critical speed.

12.2 FINITE-ELEMENT ANALYSIS FOR UNCONSTRAINED ELASTIC BODIES

Consider the response of an elastic body that has no fixed points, as in spacecraft. It is assumed that the tractions are prescribed on the undeformed surface. The response is referred to the "body axes" corresponding to axes embedded in the corresponding rigid body, for example, the principal axes of the moment of inertia tensor. The position vector $\mathbf{r}$ of a point in the body can be decomposed as follows:

$$\mathbf{r} = \mathbf{r}_c + \boldsymbol{\xi} + \mathbf{u}\,, \tag{12.7}$$

in which $\mathbf{r}_c$ is the position vector to the center of mass; $\boldsymbol{\xi}$ is the relative position-vector from the center of the mass to the undeformed position of the current point, referred to rotating axes; and $\mathbf{u}$ is the displacement from the undeformed to the deformed position in the rotating system (see Figure 12.2).

The balance of linear momentum becomes

$$\frac{\partial S_{ij}}{\partial \xi_j} = \rho[\ddot{r}_{ci} + \ddot{\xi}_i + \ddot{u}_i]. \tag{12.8}$$

Recall that $\dot{\boldsymbol{\xi}} = \boldsymbol{\omega} \times \boldsymbol{\xi}$, and the corresponding variational relation is $\delta\boldsymbol{\xi} = \delta\mathbf{u} \times \boldsymbol{\xi}$, $\omega = \dot{\boldsymbol{\theta}}$. It follows that $\delta\mathbf{r} = \delta\mathbf{r}_c + \delta\dot{\boldsymbol{\theta}} \times (\boldsymbol{\xi} + \mathbf{u}) + \delta\mathbf{u}'$, in which $\delta\mathbf{u}'$ is the variation of $\mathbf{u}$ with the axes instantaneously held fixed. The quantities $\mathbf{r}_c$, $\boldsymbol{\theta}$, and $\mathbf{u}'$ can be varied independently since there is no constraint relating them. For $\delta\mathbf{r}_c$, we have

$$\int \delta r_{ci} \left[\frac{\partial S_{ij}}{\partial \xi_j} - \rho[\ddot{r}_{ci} + \ddot{\xi}_i + \ddot{u}_i] \right] dV = 0. \tag{12.9}$$

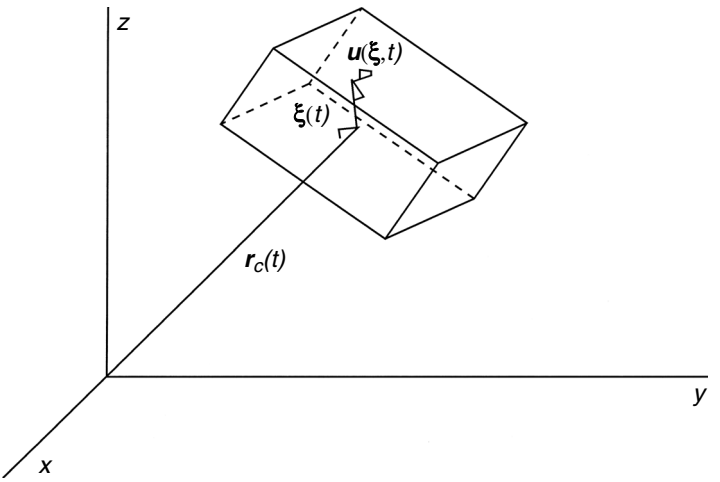

FIGURE 12.2 3-D unconstrained 3-D element.

Now $\int \delta r_{ci} \rho \ddot{\xi}_i dV = \delta r_{ci} \int \rho \ddot{\xi}_i dV = 0$ by virtue of the definition of the center of mass. Next $\int \delta r_{ci} \rho \ddot{u}_i dV = 0$ on the assumption, for which a strong argument can be made, that deformation does not affect the position of the center of mass. Then, $\int \delta r_{ci} \rho \ddot{r}_{ci} dV = \delta r_{ci} \ddot{r}_{ci} \int \rho dV = \delta r_{ci} m \ddot{r}_{ci}$. Finally,

$$\begin{aligned}\int \delta r_{ci} \frac{\partial S_{ij}}{\partial \xi_j} dV &= \delta r_{ci} \int \frac{\partial S_{ij}}{\partial \xi_j} dV \\ &= \delta r_{ci} \int S_{ij} n_j dS \\ &= \delta r_{ci} \int \tau_i dS \\ &= \delta r_{ci} P_i \end{aligned} \tag{12.10}$$

Consequently $\mathbf{P} = m\ddot{\mathbf{r}}_c$, as expected.

Consider the variation with respect to $\boldsymbol{\xi}$: $\delta\boldsymbol{\xi} = \delta\boldsymbol{\theta} \times \boldsymbol{\xi}$

$$\int \delta \xi_i \left[\frac{\partial S_{ij}}{\partial \xi_j} - \rho[\ddot{r}_{ci} + \ddot{\xi}_i + \ddot{u}_i] \right] dV = 0. \tag{12.11}$$

First,

$$\int \delta \xi_i \rho \ddot{r}_{ci} dV = \ddot{r}_{ci} \int \delta \xi_i \rho dV, \tag{12.12}$$

and $\delta[\int \rho \xi_i dV] = 0$. Recall that $\dot{\boldsymbol{\xi}} = \boldsymbol{\omega} \times \boldsymbol{\xi}$ and the corresponding variational relation is $\delta\boldsymbol{\xi} = \delta\boldsymbol{\theta} \times \boldsymbol{\xi}$, $\omega = \dot{\boldsymbol{\theta}}$. Now,

$$\int \delta \xi_i \rho \ddot{u}_i d\mathrm{V} = \int [\delta\boldsymbol{\theta} \times \boldsymbol{\xi}]_i \rho \ddot{u}_i dV = \delta\boldsymbol{\theta}^T \int \boldsymbol{\xi} \times \rho \ddot{\mathbf{u}} dV. \tag{12.13}$$

It is common to assume that $\int \boldsymbol{\xi} \times \mathbf{u} \rho dV = 0$, which also implies that $\int \boldsymbol{\xi} \times \rho \ddot{u}_i dV = 0$. This assumption implies that the body axes in the deformed configuration are not affected by deformation and are obtained by rotating the undeformed axes according to rigid-body relations.

Next, consider $\delta\xi_i$:

$$\begin{aligned}\int \delta \xi_i \rho \ddot{\xi}_i dV &= \delta\boldsymbol{\theta}^{\mathrm{T}} \int \rho \boldsymbol{\xi} \times [\boldsymbol{\omega} \times \boldsymbol{\omega} \times \boldsymbol{\xi} + \boldsymbol{\alpha} \times \boldsymbol{\xi}] \rho dV \\ &= \delta\boldsymbol{\theta}^{\mathrm{T}} \left[-\int \rho[\boldsymbol{\omega} \times \boldsymbol{\xi} \times \boldsymbol{\xi} \times \boldsymbol{\omega} + \boldsymbol{\xi} \times \boldsymbol{\xi} \times \boldsymbol{\alpha}] \rho dV \right] \\ &= \delta\boldsymbol{\theta}^{\mathrm{T}} [\boldsymbol{\omega} \times \mathbf{J}\boldsymbol{\omega} + \mathbf{J}\boldsymbol{\alpha}] \end{aligned} \tag{12.14}$$

in which $\mathbf{J} = -\int \boldsymbol{\rho} 3^2 dV$, and $3(.) = \boldsymbol{\xi} \times (.)$. Clearly, as the matrix corresponding to a vector product, 3 is antisymmetric. We determined in an earlier discussion that 3^2 is negative-definite, thus, the moment-of-inertia tensor $\mathbf{J}$ is positive-definite. Finally,

$$\int \delta\xi_i \frac{\partial S_{ij}}{\partial \xi_j} dV = \int \frac{\partial}{\partial \xi_j}(\delta\xi_i S_{ij}) dV - \int \left[\delta \frac{\partial \xi_i}{\partial \xi_j}\right] S_{ij} dV$$

$$= \int (\delta\xi_i S_{ij} n_i) dS$$

$$= \int \delta\xi_i t_i dS$$

$$= \delta\boldsymbol{\theta}^T \mathbf{m}, \qquad \mathbf{m} = \int \boldsymbol{\xi} \times \mathbf{t}\, dS \tag{12.15}$$

The vector-valued quantity $\mathbf{m}$ is recognized as the moment of the tractions referred to the center of mass. We thus obtain the Euler equation of a rigid body as

$$\mathbf{m} = \boldsymbol{\omega} \times \mathbf{J}\boldsymbol{\omega} + \mathbf{J}\boldsymbol{\alpha}\,. \tag{12.16}$$

Equations 12.10 and 12.16 can be solved separately from the finite-element equation for the displacements, to be presented next, to determine the origin and orientation of the "body axes."

Now consider the variation $\delta\mathbf{u}'$:

$$\int \delta u_i' \left[\frac{\partial \sigma_{ij}}{\partial \xi_j} - \rho[\ddot{r}_{ci} + \ddot{\xi}_i + \ddot{u}_i]\right] dV = 0. \tag{12.17}$$

First, note that $\int \delta u_i' \rho dV \ddot{r}_{ci} = 0$ since $\int \delta u_i' \rho dV = 0$. The remaining terms are exactly the same as for a body with a fixed point, and consequently it reduces to

$$\mathbf{M}\frac{d^2\boldsymbol{\gamma}}{dt^2} + \mathbf{G}_1 \frac{d\boldsymbol{\gamma}}{dt} + [\mathbf{K} + \mathbf{G}_2 + \mathbf{A}]\boldsymbol{\gamma} = \mathbf{f} - \mathbf{f}_{rot} \tag{12.18}$$

$$\mathbf{G}_1 = \boldsymbol{\Phi}^{\mathbf{T}} \int \rho \boldsymbol{\varphi} \boldsymbol{\Omega} \boldsymbol{\varphi}^T dV \boldsymbol{\Phi}, \qquad \mathbf{G}_2 = \boldsymbol{\Phi}^T \int \rho \boldsymbol{\varphi} \boldsymbol{\Omega}^2 \boldsymbol{\varphi}^T dV \boldsymbol{\Phi},$$

$$\mathbf{A} = \boldsymbol{\Phi}^{\mathbf{T}} \int \rho \boldsymbol{\varphi} \boldsymbol{A} \boldsymbol{\varphi}^T dV \boldsymbol{\Phi}, \qquad \mathbf{f}_{rot} = \boldsymbol{\Phi}^T \int \rho \boldsymbol{\varphi} [\boldsymbol{\Omega}^2 + \boldsymbol{A}] \mathbf{X}' dV$$

12.3 EXERCISES

1. Consider a one-element model for a steadily rotating rod (see Figure 12.1) to which is applied an oscillatory force, as shown. Find the steady-state solution.
2. Find the exact solution for $u(r)$ in Exercise 1. Does it agree with the one-element solution? Try two elements. Is the solution better? By how much?

3. Prove that the inertia tensor **J** is positive-definite.
   Find **J** for the brick "element" with density ρ.

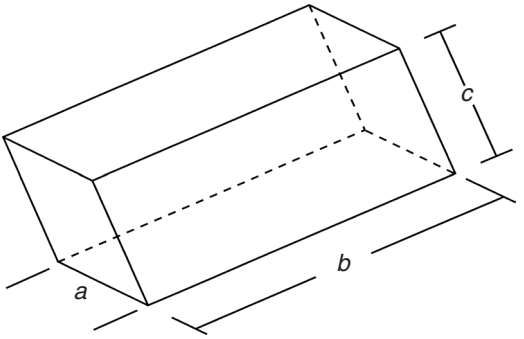

4. Write down the proof that for an unrestrained elastic body,

$$\text{if } \int \rho \boldsymbol{u} dV = 0 \text{ and } \int \rho \boldsymbol{\xi} \times \boldsymbol{u} dV = 0,$$

   then

$$\mathbf{F} = m\ddot{\mathbf{r}}_0 \qquad \mathbf{M} = \mathbf{J}\boldsymbol{\alpha} + \boldsymbol{\omega} \times \mathbf{J}\boldsymbol{\omega}.$$

5. Consider a thin *beam column* that is rotating unsteadily around a shaft. Its thin (local z) direction points in the direction of the motion, giving rise to Coriolis effects in bending. Derive the ensuing one-element model. Note that this situation couples extension and bending.

13 Thermal, Thermoelastic, and Incompressible Media

13.1 TRANSIENT CONDUCTIVE-HEAT TRANSFER

13.1.1 FINITE-ELEMENT EQUATION

The governing equation for conductive-heat transfer without heat sources, assuming an isotropic medium, is

$$k\nabla^2 \mathrm{T} = \rho c_e \dot{\mathrm{T}}. \tag{13.1}$$

With the interpolation model $\mathrm{T(t)} - \mathrm{T}_0 = \boldsymbol{\varphi}_{\mathrm{T}}^{\mathrm{T}}(\mathrm{x})\boldsymbol{\Phi}_{\mathrm{T}}\boldsymbol{\theta}(\mathrm{t})$ and $\nabla \mathrm{T} = \boldsymbol{\beta}_T^T \boldsymbol{\Phi}_T \boldsymbol{\theta}(t)$, the finite-element equation assumes the form

$$\begin{aligned} &\mathbf{K}_{\mathrm{T}}\boldsymbol{\theta} + \mathbf{M}_T\dot{\boldsymbol{\theta}} = -\mathbf{q}(t) \\ &\mathbf{K}_{\mathrm{T}} = \int \boldsymbol{\Phi}_T^T \boldsymbol{\beta}_T k \boldsymbol{\beta}_T^T \boldsymbol{\Phi}_T dV, \quad \mathbf{M}_T = \int \boldsymbol{\Phi}_T^T \boldsymbol{\varphi}_T \rho c_e \boldsymbol{\varphi}_{T_T}^{\mathrm{T}} \boldsymbol{\Phi}_T^T dV \end{aligned} \tag{13.2}$$

This equation is parabolic (first-order in the time rates), and implies that the temperature changes occur immediately at all points in the domain, but at smaller initial rates away from where the heat is added. This contrasts with the hyperbolic (second-order time rates) solid-mechanics equations, in which information propagates into the medium as finite velocity waves, and in which oscillatory response occurs in response to a perturbation.

13.1.2 DIRECT INTEGRATION BY THE TRAPEZOIDAL RULE

Equation 13.1 is already in state form since it is first-order, and the trapezoidal rule can be applied directly:

$$\mathbf{M}_T \frac{\boldsymbol{\theta}_{n+1} - \boldsymbol{\theta}_n}{h} + \mathbf{K}_T \frac{\boldsymbol{\theta}_{n+1} + \boldsymbol{\theta}_n}{2} = -\frac{\mathbf{q}_{n+1} + \mathbf{q}_n}{2}, \tag{13.3}$$

from which

$$\mathbf{K}_{DT}\boldsymbol{\theta}_{n+1} = \mathbf{r}_{n+1} \tag{13.4}$$

$$\mathbf{K}_{DT} = \mathbf{M}_T + \frac{h}{2}\mathbf{K}_T \qquad \mathbf{r}_{n+1} = \mathbf{M}_T\boldsymbol{\theta}_n - \frac{h}{2}\mathbf{K}_T\boldsymbol{\theta}_n - \frac{h}{2}(\mathbf{q}_{n+1} + \mathbf{q}_n)$$

For the assumed conditions, the dynamic thermal stiffness matrix is positive-definite, and for the current time step, the equation can be solved in the same manner as in the static counterpart, namely forward substitution followed by backward substitution.

13.1.3 Modal Analysis

Modes are not of much interest in thermal problems since the modes are not oscillatory or useful to visualize. However, the equation can still be decomposed into independent single degree of freedom systems. First, we note that the thermal system is asymptotically stable. In particular, suppose the inhomogeneous term vanishes and that $\boldsymbol{\theta}$ at $t = 0$ does not vanish. Multiplying the equation by $\boldsymbol{\theta}^{\mathbf{T}}$ and elementary manipulation furnishes that

$$\frac{d}{dt}\left(\frac{\boldsymbol{\theta}^{\mathbf{T}}\mathbf{M}_T\boldsymbol{\theta}}{2}\right) = -\boldsymbol{\theta}^{\mathbf{T}}\mathbf{K}_T\boldsymbol{\theta} < 0. \tag{13.5}$$

Clearly, the product $\boldsymbol{\theta}^{\mathbf{T}}\mathbf{M}_T\boldsymbol{\theta}$ decreases continuously. However, it only vanishes if $\boldsymbol{\theta}$ vanishes.

To examine the modes, assume a solution of the form $\boldsymbol{\theta}(t) = \boldsymbol{\theta}_{0j}\exp(\lambda_j t)$. The eigenvectors $\boldsymbol{\theta}_{0j}$ satisfy

$$\boldsymbol{\theta}_{0j}^{\mathbf{T}}\mathbf{M}_T\boldsymbol{\theta}_{0k} = \begin{cases} \mu_{Tj} & j = k \\ 0 & j \neq k \end{cases}, \quad \boldsymbol{\theta}_{0j}^{\mathbf{T}}\mathbf{K}_T\boldsymbol{\theta}_{0k} = \begin{cases} \kappa_{Tj} & j = k \\ 0 & j \neq k \end{cases} \tag{13.6}$$

and we call μ_{Tj} and κ_{Tj} the j^{th} modal thermal mass and j^{th} modal thermal stiffness, respectively. We can also form the modal matrix $\boldsymbol{\Theta} = [\boldsymbol{\theta}_{01} \ \ldots \ \boldsymbol{\theta}_{0n}]$, and again

$$\boldsymbol{\Theta}^{\mathbf{T}}\mathbf{M}_T\boldsymbol{\Theta} = \begin{bmatrix} \mu_{Tj} & 0 & . & . & 0 \\ 0 & \mu_{Tj} & . & . & . \\ . & . & . & . & . \\ . & . & . & . & . \\ 0 & . & . & . & . \end{bmatrix}, \quad \boldsymbol{\Theta}^{\mathbf{T}}\mathbf{K}_T\boldsymbol{\Theta} = \begin{bmatrix} \kappa_{Tj} & 0 & . & . & 0 \\ 0 & \kappa_{Tj} & . & . & . \\ . & . & . & . & . \\ . & . & . & . & . \\ 0 & . & . & . & . \end{bmatrix}. \tag{13.7}$$

Let $\boldsymbol{\xi} = \boldsymbol{\Theta}^{-1}\boldsymbol{\theta}$ and $g(t) = \boldsymbol{\Theta}^{\mathbf{T}}\mathbf{q}(t)$. Pre- and postmultiplying Equation 13.2 with $\boldsymbol{\Theta}^{\mathbf{T}}$ and $\boldsymbol{\Theta}$, respectively, furnishes the decoupled equation

$$\mu_{Tj}\dot{\xi}_j + \kappa_{Tj}\xi_j = g_j. \tag{13.8}$$

Suppose, for convenience, that g_j is a constant. Then, the general solution is of the form

$$\xi_j = \xi_{j0} \exp\left(-\frac{\kappa_{Tj}}{\mu_{Tj}} t\right) + \int_0^t \exp\left(-\frac{\kappa_{Tj}}{\mu_{Tj}}(t-T)\right) g_j \, d\tau, \tag{13.9}$$

illustrating the monotonically decreasing nature of the response. Now there are n uncoupled single degrees of freedom.

13.2 COUPLED LINEAR THERMOELASTICITY

13.2.1 Finite-Element Equation

The classical theory of coupled thermoelasticity accommodates the fact that the thermal and mechanical fields interact. For isotropic materials, assuming that temperature only affects the volume of an element, the stress-strain relation is

$$S_{ij} = 2\mu E_{ij} + \lambda(E_{kk} - \alpha(\mathrm{T} - \mathrm{T}_0))\delta_{ij}, \tag{13.10}$$

in which α denotes the volumetric thermal-expansion coefficient. The equilibrium equation is repeated as $\frac{\partial S_{ij}}{\partial x_j} = \rho \ddot{u}_i$. The Principle of Virtual Work implies that

$$\int \delta E_{ij}[2\mu E_{ij} + \lambda E_{kk}\delta_{ij}]\, dV_o + \int \delta u_i \rho \ddot{u}_i \, dV_o - \alpha\lambda \int \delta E_{ij}(\mathrm{T} - \mathrm{T}_0)\delta_{ij} \, dV_o = \int \delta u_j t_j \, dS_o. \tag{13.11}$$

Now consider the interpolation models

$$\boldsymbol{u} = \boldsymbol{N}^{\mathbf{T}}(\mathbf{x})\boldsymbol{\gamma}(t), \quad \mathrm{E}_{ij} \to \boldsymbol{E} = \boldsymbol{B}^{\boldsymbol{T}}(\mathbf{x})\boldsymbol{\gamma}(t), \quad \mathrm{T} - \mathrm{T}_0 = \mathbf{v}^{\boldsymbol{T}}(\mathbf{x})\boldsymbol{\theta}(t), \quad \nabla\mathrm{T} = \boldsymbol{B}_T^T(\mathbf{x})\boldsymbol{\theta}(t), \tag{13.12}$$

in which $\boldsymbol{E}$ is the strain written as a column vector in conventional finite-element notation. The usual procedures furnish the finite-element equation

$$\mathbf{M}\ddot{\boldsymbol{\gamma}}(t) + \mathbf{K}\boldsymbol{\gamma}(t) - \boldsymbol{\Sigma}\boldsymbol{\theta}(t) = \mathbf{f}(t), \qquad \Sigma = \alpha\lambda \int \boldsymbol{B}\boldsymbol{v}^{\boldsymbol{T}} dV_o. \tag{13.13}$$

The quantity $\boldsymbol{\Sigma}$ is the *thermomechanical stiffness matrix*. If there are n_m displacement degrees of freedom and n_t thermal degrees of freedom, the quantities appearing in the equation are

$$\mathbf{M},\ \mathbf{K}: n_m \times n_m, \qquad \boldsymbol{\gamma}(t),\ \mathbf{f}(t): n_m \times 1, \qquad \boldsymbol{\Sigma}: n_m \times n_t, \qquad \boldsymbol{\theta}(t): n_t \times 1.$$

We next address the thermal field. The energy-balance equation (from Equation 7.35), including mechanical effects, is given by

$$k\nabla^2 \mathrm{T} = \rho c_e \dot{\mathrm{T}} + \alpha\lambda \mathrm{T}_0 tr(\dot{\boldsymbol{E}}). \tag{13.14}$$

Application of the usual variational methods imply that

$$\mathbf{K}_T\boldsymbol{\theta}(t) + \mathbf{M}_T\dot{\boldsymbol{\theta}}(t) + \mathrm{T}_0\boldsymbol{\Sigma}^T\dot{\boldsymbol{\gamma}}(t) = -\mathbf{q}, \qquad \mathbf{q} = \int \boldsymbol{\nu}\mathbf{n}\cdot\mathbf{q}\,dS. \tag{13.15}$$

Case 1:

Suppose that T is constant. At the global level, $\boldsymbol{\theta}(t) = -\mathrm{T}_0\mathbf{K}_T^{-1}\boldsymbol{\Sigma}^{\mathrm{T}}\dot{\boldsymbol{\gamma}}(t) + \mathrm{T}_0\mathbf{K}_T^{-1}\mathbf{q}$. Thus, the thermal field is eliminated at the global level, giving the new governing equation as

$$\mathbf{M}\ddot{\boldsymbol{\gamma}}(t) + \mathrm{T}_0\boldsymbol{\Sigma}\mathbf{K}_T^{-1}\boldsymbol{\Sigma}^{\mathrm{T}}\dot{\boldsymbol{\gamma}}(t) + \mathbf{K}\boldsymbol{\gamma}(t) = \mathbf{f}(t). \tag{13.16}$$

Conductive-heat transfer is analogous to damping. The mechanical system is now asymptotically stable rather than asymptotically marginally stable.

We next put the global equations in *state form*:

$$\mathbf{Q}_1\dot{\mathbf{z}} + \mathbf{Q}_2\mathbf{z} = \mathbf{f} \tag{13.17}$$

$$\mathbf{Q}_1 = \begin{bmatrix} \mathbf{M} & \mathbf{0} & \mathbf{0} \\ \mathbf{0} & \mathbf{K} & \mathbf{0} \\ \mathbf{0} & \mathbf{0} & \mathbf{M}_{\mathrm{T}}/\mathrm{T}_0 \end{bmatrix} \qquad \mathbf{z} = \begin{pmatrix} \dot{\boldsymbol{\gamma}} \\ \boldsymbol{\gamma} \\ \boldsymbol{\theta} \end{pmatrix}$$

$$\mathbf{Q}_2 = \begin{bmatrix} \mathbf{0} & \mathbf{K} & -\boldsymbol{\Sigma} \\ -\mathbf{K} & \mathbf{0} & \mathbf{0} \\ \boldsymbol{\Sigma}^{\mathbf{T}} & \mathbf{0} & \mathbf{K}_{\mathrm{T}}/\mathrm{T}_0 \end{bmatrix} \qquad \mathbf{f} = \begin{pmatrix} \mathbf{f} \\ \mathbf{0} \\ -\mathbf{q}/\mathrm{T}_0 \end{pmatrix}$$

Clearly, Equation 13.17 can be integrated numerically using the trapezoidal rule:

$$\left[\mathbf{Q}_1 + \frac{h}{2}\mathbf{Q}_2\right]\mathbf{z}_{n+1} = \left[\mathbf{Q}_1 - \frac{h}{2}\mathbf{Q}_2\right]\mathbf{z}_n + \frac{h}{2}[\mathbf{f}_{n+1} + \mathbf{f}_n]. \tag{13.18}$$

Now, consider asymptotic stability, for which purpose it is sufficient to take $\mathbf{f} = \mathbf{0}$, $\mathbf{z}(0) = \mathbf{z}_0$. Upon premultiplying Equation 13.17 by $\mathbf{z}^{\mathrm{T}}$, we obtain

$$\begin{aligned}\frac{d}{dt}\left(\frac{1}{2}\mathbf{z}^{\mathrm{T}}\mathbf{Q}_1\mathbf{z}\right) &= -\mathbf{z}^{\mathrm{T}}\mathbf{Q}_2\mathbf{z} \\ &= -\mathbf{z}^{\mathrm{T}}\frac{1}{2}\left[\mathbf{Q}_2 + \mathbf{Q}_2^{\mathrm{T}}\right]\mathbf{z} \\ &= -\boldsymbol{\theta}^{\mathrm{T}}\mathbf{K}_T\boldsymbol{\theta} \end{aligned} \tag{13.19}$$

and $\mathbf{z}$ must be real. Assuming that $\boldsymbol{\theta} \neq \mathbf{0}$, it follows that $\mathbf{z} \downarrow \mathbf{0}$, and hence the system is asymptotically stable.

13.2.2 Thermoelasticity in a Rod

Consider a rod that is built into a large, rigid, nonconducting temperature reservoir at $x = 0$. The force, f_0, and heat flux, $-q_0$, are prescribed at $x = L$. A single element models the rod. Now,

$$u(x,t) = x\gamma(t)/L, \quad E(x,t) = \gamma(t)/L, \quad \mathrm{T} - \mathrm{T}_0 = x\theta(t)/L, \quad \frac{d\mathrm{T}}{dx} = \theta(t)/L. \tag{13.20}$$

The thermoelastic stiffness matrix becomes $\boldsymbol{\Sigma} = \alpha\lambda\int \boldsymbol{B}\boldsymbol{v}^{\mathrm{T}}dV \rightarrow \Sigma = \alpha\lambda A/2$. The governing equations are now

$$\begin{aligned}\frac{\rho AL}{3}\ddot{\gamma} + \frac{\mathrm{E}A}{L}\gamma - \frac{1}{2}\alpha\lambda A\theta &= \mathrm{f}_0 \\ \frac{1}{\mathrm{T}_0}\frac{\rho c_e AL}{3}\dot{\theta} + \frac{1}{\mathrm{T}_0}\frac{kA}{L}\theta + \frac{1}{2}\alpha\lambda A\dot{\gamma} &= -\mathrm{q}_0 \end{aligned} \tag{13.21}$$

13.3 COMPRESSIBLE ELASTIC MEDIA

For a compressible elastic material, the isotropic stress S_{kk} and the dilatational strain E_{kk} are related by $S_{\mathrm{kk}} = 3\kappa E_{\mathrm{kk}}$, in which the bulk modulus κ satisfies $\kappa = \mathrm{E}/[3(1-2\nu)]$. Clearly, as $\nu \rightarrow 1/2$, the pressure, $p = -S_{\mathrm{kk}}/3$, needed to attain a finite compressive volume strain ($E_{\mathrm{kk}} < 0$) becomes infinite. At the limit $\nu = 1/2$, the material is said to satisfy the internal constraint of incompressibility.

Consider the case of plane strain, in which $E_{zz} = 0$. The tangent modulus matrix $\boldsymbol{D}$ is readily found from

$$\begin{pmatrix} S_{xx} \\ S_{yy} \\ S_{zz} \end{pmatrix} = \frac{\mathrm{E}}{(1+\nu)(1-2\nu)}\begin{bmatrix} 1-\nu^2 & -\nu(1+\nu) & 0 \\ -\nu(1+\nu) & 1-\nu^2 & 0 \\ 0 & 0 & 1-2\nu \end{bmatrix}\begin{pmatrix} E_{xx} \\ E_{yy} \\ E_{zz} \end{pmatrix}. \tag{13.22}$$

Clearly, $\boldsymbol{D}$ becomes unbounded as $\nu \to 1/2$. Furthermore, suppose that for a material to be nearly incompressible, ν is estimated as .495, while the correct value is .49. It might be supposed that the estimated value is a good approximation for the correct value. However, for the correct value, $(1 - 2\nu)^{-1} = 50$. For the estimated value, $(1 - 2\nu)^{-1} = 100$, implying 100 percent error!

13.4 INCOMPRESSIBLE ELASTIC MEDIA

In an incompressible material, a pressure field arises that serves to enforce the constraint. Since the trace of the strains vanishes everywhere, the strains are not sufficient to determine the stresses. However, the strains together with the pressure are sufficient. In FEA, a general interpolation model is used at the outset for the displacement field. The Principle of Virtual Work is now expressed in terms of the displacements and pressure, and an adjoining equation is introduced to enforce the constraint *a posteriori*. The pressure can be shown to serve as a Lagrange multiplier, and the displacement vector and the pressure are varied independently.

In incompressible materials, to preserve finite stresses, we suppose that the second Lame coefficient satisfies $\lambda \to \infty$ as $tr(\boldsymbol{E}) \to 0$ in such a way that the product is an indeterminate quantity denoted by p:

$$\lambda tr(\boldsymbol{E}) \to -p. \tag{13.23}$$

The Lame form of the constitutive relations becomes

$$S_{ij} = 2\mu E_{ij} - p\delta_{ij}, \tag{13.24}$$

together with the incompressibility constraint $E_{ij}\delta_{ij} = 0$. There now are two independent principal strains and the pressure with which to determine the three principal stresses.

In a compressible elastic material, the strain-energy function w satisfies $S_{ij} = \frac{\partial w}{\partial E_{ij}}$, and the domain term in the Principle of Virtual Work can be rewritten as $\int \delta E_{ij} S_{ij} dV = \int \delta w dV$. The elastic-strain energy is given by $w = \mu E_{ij} E_{ij} + \frac{\lambda}{2} E_{kk}^2$. For reasons explained shortly, we introduce the augmented strain-energy function

$$w' = \mu E_{ij} E_{ij} - pE_{kk} \tag{13.25}$$

and assume the variational principle

$$\int \delta w' dV_o + \int \delta \boldsymbol{u}^T \rho_o \ddot{\boldsymbol{u}}\, dV_o = \int \delta \boldsymbol{u}^T \boldsymbol{\tau} dS_o. \tag{13.26}$$

Now, considering $\boldsymbol{u}$ and p to vary independently, the integrand of the first term becomes $\delta w' = \delta E_{ij}[2\mu E_{ij} - p\delta_{ij}] - \delta p E_{kk}$, furnishing two variational relations:

$$\int \delta E_{ij} S_{ij}\, dV_o + \int \delta u^T \rho_o \ddot{u}\, dV_o = \int \delta \boldsymbol{u}^T \boldsymbol{\tau} dS_o \qquad \text{(a)}$$
$$\int \delta p E_{kk} dV_0 = 0 \qquad \text{(b)} \tag{13.27}$$

The first relation is recognized as the Principle of Virtual Work, and the second equation serves to enforce the internal constraint of incompressibility.

We now introduce the interpolation models:

$$\boldsymbol{u} = \boldsymbol{N}^T(\boldsymbol{x})\boldsymbol{g}(t) \qquad \mathbf{e} = \boldsymbol{B}^T(\boldsymbol{x})\boldsymbol{g}(t)$$
$$E_{kk} = \boldsymbol{b}^T(x)\boldsymbol{g}(t) \qquad p(\boldsymbol{x}) = \boldsymbol{x}^T(\boldsymbol{x})\boldsymbol{p}(t) \tag{13.28}$$

Substitution serves to derive that

$$\mathbf{M}\ddot{\boldsymbol{\gamma}}(t) + \mathbf{K}\boldsymbol{\gamma}(t) - \boldsymbol{\Sigma}\boldsymbol{\pi}(t) = \mathbf{f}$$
$$\boldsymbol{\Sigma} = \int \boldsymbol{b}\boldsymbol{\xi}^{\mathbf{T}} dV_o, \quad \boldsymbol{\Sigma}^{\mathbf{T}}\boldsymbol{\gamma}(t) = \mathbf{0} \tag{13.29}$$

Assuming that these equations apply at the global level, use of *state form* furnishes

$$\begin{bmatrix} \mathbf{M} & \mathbf{0} & \mathbf{0} \\ \mathbf{0} & \mathbf{K} & \mathbf{0} \\ \mathbf{0}^{\mathbf{T}} & \mathbf{0}^{\mathbf{T}} & \mathbf{0} \end{bmatrix} \frac{d}{dt} \begin{pmatrix} \dot{\boldsymbol{\gamma}}(t) \\ \dot{\boldsymbol{\gamma}}(t) \\ \boldsymbol{\pi}(t) \end{pmatrix} + \begin{bmatrix} \mathbf{0} & \mathbf{K} & -\boldsymbol{\Sigma} \\ -\mathbf{K} & \mathbf{0} & \mathbf{0} \\ \boldsymbol{\Sigma}^{\mathbf{T}} & \mathbf{0}^{\mathbf{T}} & \mathbf{0} \end{bmatrix} \begin{pmatrix} \dot{\boldsymbol{\gamma}}(t) \\ \boldsymbol{\gamma}(t) \\ \boldsymbol{\pi}(t) \end{pmatrix} = \begin{pmatrix} \mathbf{f}(t) \\ \mathbf{0} \\ \mathbf{0} \end{pmatrix}. \tag{13.30}$$

The second matrix is antisymmetric. Furthermore, the system exhibits marginal asymptotic stability; namely, if $\mathbf{f}(t) = \mathbf{0}$ while $\dot{\boldsymbol{\gamma}}(0)$, $\boldsymbol{\gamma}(0)$, and $\boldsymbol{\pi}(0)$ do not all vanish, then

$$\frac{d}{dt}\left[\frac{1}{2} (\dot{\boldsymbol{\gamma}}^{\mathbf{T}}(t) \quad \boldsymbol{\gamma}^{\mathbf{T}}(t) \quad \boldsymbol{\pi}^{\mathbf{T}}(t)) \begin{bmatrix} \mathbf{M} & \mathbf{0} & \mathbf{0} \\ \mathbf{0} & \mathbf{K} & \mathbf{0} \\ \mathbf{0}^{\mathbf{T}} & \mathbf{0}^{\mathbf{T}} & \mathbf{0} \end{bmatrix} \begin{pmatrix} \dot{\boldsymbol{\gamma}}(t) \\ \boldsymbol{\gamma}(t) \\ \boldsymbol{\pi}(t) \end{pmatrix} \right] = 0 \tag{13.31}$$

13.5 EXERCISES

1. Find the exact solution for a circular rod of length L, radius r, mass density ρ, specific heat c_e, conductivity k, and cross-sectional area $A = \pi r^2$. The initial temperature is T_0, and the rod is built into a large wall at fixed temperature T_0 (see figure below). However, at time $t = 0$, the temperature T_1 is imposed at $x = L$. Compare the exact solution to the one- and two-element solutions. Note that for a one-element model,

$$\frac{kA}{L}\theta(L,t) + \frac{\rho c_e AL}{3}\dot{\theta}(L,t) = -q(L).$$

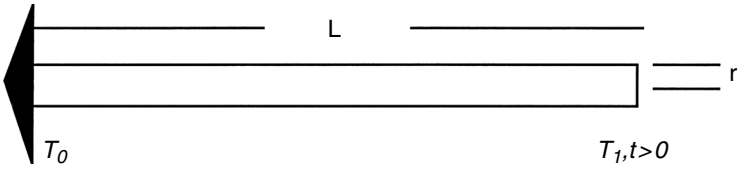

2. State the equations of a thermoelastic rod, and put the equations for the thermoelastic behavior of a rod in state form.
3. Put the following equations in state form, apply the trapezoidal rule, and triangularize the ensuing dynamic stiffness matrix, assuming that the triangular factors of **M** and **K** are known.

$$\mathbf{M}\ddot{\boldsymbol{\gamma}} + \mathbf{K}\boldsymbol{\gamma} - \boldsymbol{\Sigma}\boldsymbol{\pi} = \mathbf{f}, \qquad \boldsymbol{\Sigma}^{\mathrm{T}}\boldsymbol{\gamma} = \mathbf{0}.$$

4. In an element of an incompressible square rod of cross-sectional area A, it is necessary to consider the displacements v and w. Suppose the length is L, the lateral dimension is Y, and the interpolation models are linear for the displacements (u linear in x, with v,w linear in y) and constant for the pressure. Show that the finite-element equation assumes the form

$$\begin{bmatrix} 2\mu A/L & 0 & -A \\ 0 & 4\mu AL/Y^2 & -2AL/Y \\ A & 2AL/Y & 0 \end{bmatrix} \begin{pmatrix} u(L) \\ v(Y) \\ p \end{pmatrix} = \begin{pmatrix} f \\ 0 \\ 0 \end{pmatrix}$$

and that this implies that $3\mu\frac{u(L)}{L} = f$ (which can also be shown by an *a priori* argument).

14 Torsion and Buckling

14.1 TORSION OF PRISMATIC BARS

Figure 14.1 illustrates a member experiencing torsion. The member in this case is cylindrical with length L and radius r_0. The base is fixed, and a torque is applied at the top surface, which causes the member to twist. The twist at height z is θ(z), and at height L, it is θ_0.

Ordinarily, in the finite-element problems so far considered, the displacement is the basic unknown. It is approximated by an interpolation model, from which an approximation for the strain tensor is obtained. Then, an approximation for the stress tensor is obtained using the stress-strain relations. The nodal displacements are solved by an equilibrium principle, in the form of the Principle of Virtual Work. In the current problem, an alternative path is followed in which stresses or, more precisely, a stress potential, is the unknown. The strains are determined from the stresses. However, for arbitrary stresses satisfying equilibrium, the strain field may not be compatible. The compatibility condition (see Chapter 4) is enforced, furnishing

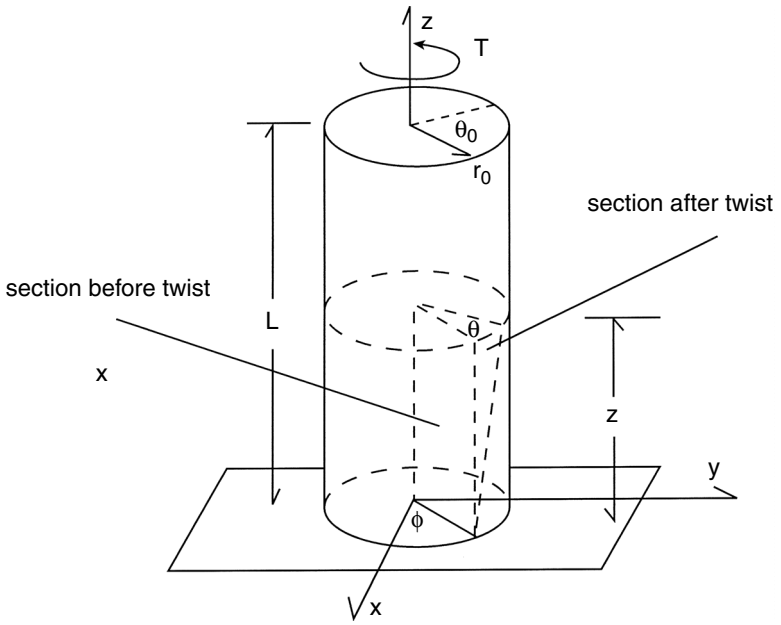

FIGURE 14.1 Twist of a prismatic rod.

a partial differential equation known as the Poisson Equation. A variational argument is applied to furnish a finite-element expression for the torsional constant of the section.

For the member before twist, consider points X and Y at angle ϕ and at radial position r. Clearly, $X = r\cos\phi$ and $Y = r\sin\phi$. Twist induces a rotation through angle $\theta(z)$, but it does not affect the radial position. Now, $x = r\cos(\phi + \theta)$, $y = r\sin(\phi + \theta)$. Use of double-angle formulae furnishes the displacements, and restriction to small angles θ furnishes, to first order,

$$u = -Y\theta, \qquad v = X\theta. \tag{14.1}$$

It is also assumed that torsion does not increase the length of the member, which is attained by requiring that axial displacement w only depends on X and Y. The quantity $w(X, Y)$ is called the *warping function*.

It is readily verified that all strains vanish except E_{xz} and E_{yz}, for which

$$E_{xz} = \frac{1}{2}\left[\frac{\partial w}{\partial x} - y\frac{\partial \theta}{\partial z}\right], \qquad E_{yz} = \frac{1}{2}\left[\frac{\partial w}{\partial y} + x\frac{\partial \theta}{\partial z}\right]. \tag{14.2}$$

Equilibrium requires that

$$\frac{\partial S_{xz}}{\partial x} + \frac{\partial S_{yz}}{\partial y} = 0. \tag{14.3}$$

The equilibrium relation can be identically satisfied by a potential function ψ for which

$$S_{xz} = \frac{\partial \psi}{\partial y}, \qquad S_{yz} = -\frac{\partial \psi}{\partial x}. \tag{14.4}$$

We must satisfy the compatibility condition to ensure that the strain field arises from a displacement field that is unique to within a rigid-body translation and rotation. (Compatibility is automatically satisfied if the displacements are considered the unknowns and are approximated by a continuous interpolation model. Here, the stresses are the unknowns.) From the stress-strain relation,

$$E_{xz} = \frac{1}{2\mu}S_{xz} = \frac{1}{2\mu}\frac{\partial \psi}{\partial y}, \qquad E_{yz} = \frac{1}{2\mu}S_{yz} = -\frac{1}{2\mu}\frac{\partial \psi}{\partial x}. \tag{14.5}$$

Compatibility (integrability) now requires that $\frac{\partial^2 w}{\partial x \partial y} = \frac{\partial^2 w}{\partial y \partial x}$, furnishing

$$-\frac{\partial}{\partial y}\left[\frac{1}{2\mu}\frac{\partial \psi}{\partial y} + \frac{1}{2}y\frac{d\theta}{dz}\right] + \frac{\partial}{\partial x}\left[-\frac{1}{2\mu}\frac{\partial \psi}{\partial x} - \frac{1}{2}x\frac{d\theta}{dz}\right] = 0, \tag{14.6}$$

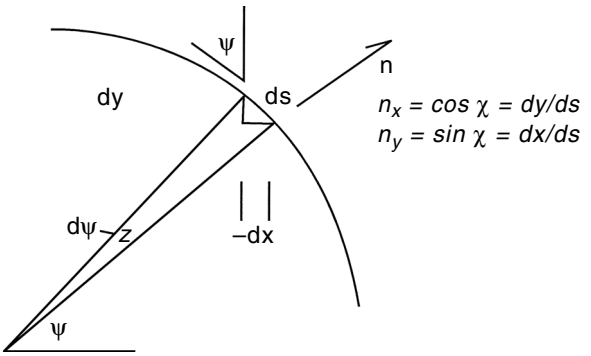

FIGURE 14.2 Illustration of geometric relation.

which in turn furnishes Poisson's Equation for the potential function ψ:

$$\frac{\partial^2 \psi}{\partial x^2} + \frac{\partial^2 \psi}{\partial y^2} = -2\mu \frac{d\theta}{dz}. \tag{14.7}$$

For boundary conditions, assume that the lateral boundaries of the member are unloaded. The stress-traction relation already implies that $\tau_x = 0$ and $\tau_y = 0$ on the lateral boundary S. For traction τ_z to vanish, we require that

$$\tau_z = n_x S_{xz} + n_y S_{yz} = 0 \quad on \quad S. \tag{14.8}$$

Upon examining Figure 14.2, it can be seen that $n_x = dy/ds$ and $n_y = -dx/ds$, in which s is the arc length along the boundary at z. Consequently,

$$\begin{aligned} \tau_z &= \frac{dy}{ds} S_{xz} - \frac{dx}{ds} S_{yz} \\ &= \frac{dy}{ds}\frac{\partial \psi}{\partial y} + \frac{dx}{ds}\frac{\partial \psi}{\partial x} \\ &= \frac{d\psi}{ds} \end{aligned} \tag{14.9}$$

Now, on S, $\frac{d\psi}{ds} = 0$, and therefore ψ is a constant, which can, in general, be taken as zero.

We next consider the total torque on the member. Figure 14.3 depicts the cross section at z. The torque on the element at x and y is given by

$$\begin{aligned} dT &= xS_{yz}dxdy - yS_{xz}dxdy \\ &= \left[-x\frac{d\psi}{dx} - y\frac{d\psi}{dy}\right]dxdy \end{aligned} \tag{14.10}$$

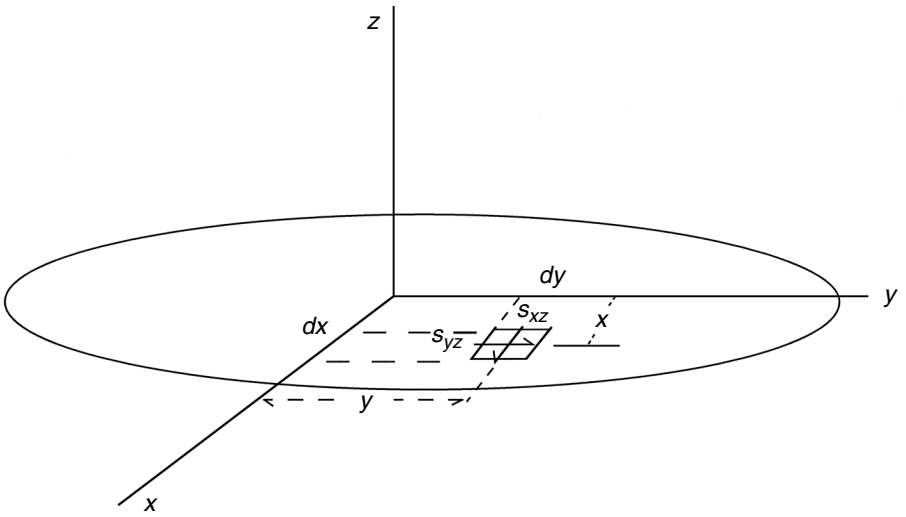

FIGURE 14.3 Evaluation of twisting moment.

Integration furnishes

$$T = -\int\left[x\frac{d\psi}{dx} + y\frac{d\psi}{dy}\right]dxdy$$

$$= -\int\left[\left[\frac{d(x\psi)}{dx} + \frac{d(y\psi)}{dy}\right] - \psi\left[\frac{dx}{dx} + \frac{dy}{dy}\right]\right]dxdy$$

$$= -\int\nabla\cdot\begin{pmatrix} x\psi \\ y\psi \end{pmatrix}dxdy + 2\int\psi\, dxdy \tag{14.11}$$

Application of the divergence theorem to the first term leads to $\int\psi[xn_x + yn_y]ds$, which vanishes since ψ vanishes on S. Finally,

$$T = 2\int\psi\, dxdy. \tag{14.12}$$

We apply variational methods to the Poisson Equation, considering the stress-potential function ψ to be the unknown. Now,

$$\int\delta\psi[\nabla\cdot\nabla\psi + 2\mu\theta']dxdy = 0. \tag{14.13}$$

Integration by parts, use of the divergence theorem, and imposition of the "constraint" $\psi = 0$ on S furnishes

$$\int (\nabla \delta\psi) \cdot \nabla \psi \, dxdy = \int \delta\psi 2\mu\theta' \, dxdy. \tag{14.14}$$

The integrals are evaluated over a set of small elements. In the e^{th} element, approximate ψ as $\nu_T^{\mathbf{T}}(x,y)\boldsymbol{\psi}_e\boldsymbol{\eta}_e$, in which ν_T is a vector with dimension (number of rows) equal to the number of nodal values of ψ. The gradient $\nabla\psi$ has a corresponding interpolation model $\nabla\psi = \boldsymbol{\beta}_T^{\mathbf{T}}(x,y)\boldsymbol{\psi}_e\boldsymbol{\eta}_e$, in which $\boldsymbol{\beta}_T$ is a matrix. The finite-element counterpart of the Poisson Equation at the element level is written as

$$\begin{aligned} \mathbf{K}_T^{(e)}\boldsymbol{\eta}_e &= 2\mu\theta' \mathbf{f}_T^{(e)} \\ \mathbf{K}_T^{(e)} &= \boldsymbol{\psi}_e^{\mathbf{T}} \int \boldsymbol{\beta}_T \boldsymbol{\beta}_T^{\mathbf{T}} \, dxdy \boldsymbol{\psi}_e \\ \mathbf{f}_T^{(e)} &= \boldsymbol{\psi}_e^{\mathbf{T}} \int \nu_T(x,y) dxdy \end{aligned} \tag{14.15}$$

and the stiffness matrix should be nonsingular, since the constraint $\psi = 0$ on S has already been used. It follows that, globally, $\boldsymbol{\eta}_{\mathbf{g}} = 2\mu\theta' \mathbf{K}_T^{(\mathbf{g})^{-1}} \mathbf{f}_T^{(\mathbf{g})}$. The torque satisfies

$$\begin{aligned} T &= \int 2\psi \, dxdy \\ &= 2\boldsymbol{\eta}_{\mathbf{g}}^{\mathbf{T}} \mathbf{f}_T^{(\mathbf{g})} \\ &= 4\mu\theta' \mathbf{f}_T^{(\mathbf{g})^{\mathbf{T}}} \mathbf{K}_T^{(\mathbf{g})^{-1}} \mathbf{f}_T^{(\mathbf{g})} \end{aligned} \tag{14.16}$$

In the theory of torsion, it is common to introduce the torsional constant *J,* for which $T = 2\mu J\theta'$. It follows that $J = 2\mathbf{f}_T^{(g)^T} \mathbf{K}_T^{(g)^{-1}} \mathbf{f}_T^{(g)}$.

14.2 BUCKLING OF BEAMS AND PLATES

14.2.1 Euler Buckling of Beam Columns

14.2.1.1 Static Buckling

Under in-plane compressive loads, the resistance of a thin member (beam or plate) can be reduced progressively, culminating in *buckling*. There are two equilibrium states that the member potentially can sustain: compression only, or compression with bending. The member will "snap" to the second state if it involves less "potential energy" than the first state. The notions explaining buckling are addressed in detail in subsequent chapters. For now, we will focus on beams and plates, using classical equations in which, by retaining lowest-order corrections for geometric nonlinearity, in-plane compressive forces appear.

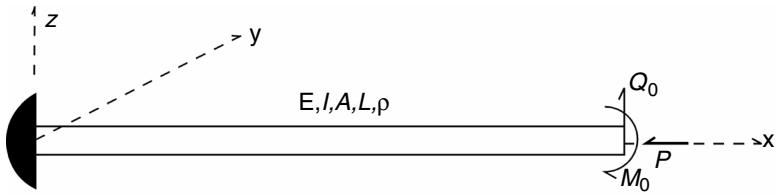

FIGURE 14.4 Euler buckling of a beam column.

For the beam shown in Figure 14.4, the classical Euler buckling equation is

$$EIw^{iv} + Pw'' + \rho A\ddot{w} = 0, \tag{14.17}$$

and P is the axial compressive force. The interpolation model for $w(x)$ is recalled as $w(x) = \boldsymbol{\varphi}^{\mathbf{T}}(x)\boldsymbol{\Phi}\boldsymbol{\gamma}$. Following the usual variational procedures (integration by parts) furnishes

$$\int \delta w \rho A \ddot{w}\, dx \rightarrow \delta\boldsymbol{\gamma}^{\mathbf{T}}\mathbf{M}\ddot{\boldsymbol{\gamma}}, \qquad \mathbf{M} = \boldsymbol{\Phi}^{\mathbf{T}} \int \boldsymbol{\varphi}(x)\rho A \boldsymbol{\varphi}^{\mathbf{T}}(x) dV \boldsymbol{\Phi} \tag{14.18}$$

$$\int \delta w[EIw^{iv} + Pw'']dx = \int \delta w'' EIw'' dx - \int \delta w' Pw' dx$$
$$-[(\delta w)(-Pw' - EIw''')]_0^L - [(-\delta w')(-EIw'')]_0^L$$

At $x = 0$, both δw and $-\delta w'$ vanish, while the shear force V and the bending moment M are identified as $V = -EIw'''$ and $M = -EIw''$. The "effective shear force" Q is defined as $Q = -Pw' - EIw'''$.

For the specific case illustrated in Figure 14.3, for a one-element model, we can use the interpolation formula

$$w(x) = (x^2 \quad x^3)\begin{bmatrix} L^2 & L^3 \\ -2L & -3L^2 \end{bmatrix}^{-1} \boldsymbol{\gamma}(t), \qquad \boldsymbol{\gamma}(t) = \begin{pmatrix} w(L) \\ -w'(L) \end{pmatrix}. \tag{14.19}$$

The mass matrix is shown, after some algebra, to be

$$\mathbf{M} = \rho AL\mathbf{K}_0, \qquad \mathbf{K}_0 = \begin{bmatrix} \frac{13}{35} & \frac{11}{210}L \\ \frac{11}{210}L & \frac{1}{105}L^2 \end{bmatrix}. \tag{14.20}$$

Similarly,

$$\int \delta w' P w' dx = \delta \boldsymbol{\gamma}^T \frac{P}{L} \mathbf{K}_1 \boldsymbol{\gamma}, \qquad \mathbf{K}_1 = \begin{bmatrix} \frac{6}{5} & \frac{1}{10} L \\ \frac{1}{10} L & \frac{2}{15} L^2 \end{bmatrix}$$
$$\int \delta w'' \mathrm{E}I w'' dx = \delta \boldsymbol{\gamma}^T \frac{\mathrm{E}I}{L^3} \mathbf{K}_2 \boldsymbol{\gamma}, \qquad \mathbf{K}_2 = \begin{bmatrix} 12 & 6L \\ 6L & 4L^2 \end{bmatrix} \tag{14.21}$$

The governing equation is written in finite-element form as

$$\left[\frac{\mathrm{E}I}{L^3} \mathbf{K}_2 - \frac{P}{L} \mathbf{K}_1 \right] \boldsymbol{\gamma} + \rho A L \mathbf{K}_0 \ddot{\boldsymbol{\gamma}} = \mathbf{f}, \qquad \mathbf{f} = \begin{pmatrix} Q_0 \\ M_0 \end{pmatrix}. \tag{14.22}$$

In a static problem, $\ddot{\boldsymbol{\gamma}} = \mathbf{0}$, the solution has the form

$$\boldsymbol{\gamma} = \frac{\mathrm{cof}\left(\boldsymbol{K}_2 - \frac{PL^2}{\mathrm{E}I} \boldsymbol{K}_1 \right)}{\det\left(\boldsymbol{K}_2 - \frac{PL^2}{\mathrm{E}I} \boldsymbol{K}_1 \right)} \boldsymbol{f}, \tag{14.23}$$

in which cof denotes the cofactor, and $\boldsymbol{\gamma} \to \infty$ for values of $\frac{PL^2}{\mathrm{E}I}$ which render $\det(\mathbf{K}_2 - \frac{PL^2}{\mathrm{E}I} \mathbf{K}_1) = 0$.

14.2.1.2 Dynamic Buckling

In a dynamic problem, it may be of interest to determine the effect of P on the resonance frequency. Suppose that $\mathbf{f}(t) = \mathbf{f}_0 \, exp(i\omega t)$, in which $\mathbf{f}_0$ is a known vector. The displacement function satisfies $\boldsymbol{\gamma}(t) = \boldsymbol{\gamma}_0 \, exp(i\omega t)$, in which the amplitude vector $\boldsymbol{\gamma}_0$ satisfies

$$\left[\frac{\mathrm{E}I}{L^3} \mathbf{K}_2 - \frac{P}{L} \mathbf{K}_1 - \omega^2 \rho A L \mathbf{K}_0 \right] \boldsymbol{\gamma}_0 = \mathbf{f}_0. \tag{14.24}$$

Resonance occurs at a frequency ω_0, for which

$$\det\left[\frac{\mathrm{E}I}{L^3} \mathbf{K}_2 - \frac{P}{L} \mathbf{K}_1 - \omega_0^2 \rho A L \mathbf{K}_0 \right] = 0. \tag{14.25}$$

Clearly, ω_0^2 is an eigenvalue of the matrix $\frac{1}{\rho \mathrm{AL}} \mathbf{K}_0^{-1/2} [\frac{EI}{L^3} \mathbf{K}_2 - \frac{P}{L} \mathbf{K}_1] \mathbf{K}_0^{-1/2}$. The resonance frequency ω_0^2 is reduced by the presence of P and vanishes precisely at the critical value of P.

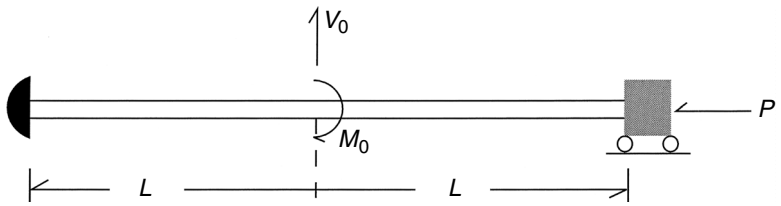

FIGURE 14.5 Buckling of a clamped-clamped beam.

14.2.1.3 Sample Problem: Interpretation of Buckling Modes

Consider static buckling of a clamped-clamped beam, as shown in Figure 14.5.

This configuration can be replaced with two beams of length L, for which the right beam experiences shear force V_1 and bending moment M_1, while the left beam experiences shear force $V_0 - V_1$ and bending moment $M_0 - M_1$. The beam on the right is governed by

$$\int \delta w' P w' dx = \delta \boldsymbol{\gamma}^T \frac{P}{L} \mathbf{K}_1 \boldsymbol{\gamma}, \qquad \mathbf{K}_1 = \begin{bmatrix} \frac{6}{5} & \frac{1}{10}L \\ \frac{1}{10}L & \frac{2}{15}L^2 \end{bmatrix}$$
$$\int \delta w'' \mathrm{E}I w'' dx = \delta \boldsymbol{\gamma}^T \frac{\mathrm{E}I}{L^3} \mathbf{K}_2 \boldsymbol{\gamma}, \qquad \mathbf{K}_2 = \begin{bmatrix} 12 & 6L \\ 6L & 4L^2 \end{bmatrix} \tag{14.26}$$

The governing equation is written in finite-element form as

$$\left(\frac{\mathrm{E}I}{L^3} \begin{bmatrix} 12 & 6L \\ 6L & 4L^2 \end{bmatrix} - \frac{P}{L} \begin{bmatrix} \frac{6}{5} & \frac{1}{10}L \\ \frac{1}{10}L & \frac{2}{15}L^2 \end{bmatrix} \right) \boldsymbol{\gamma} = \mathbf{f} \tag{14.27}$$

$$\mathbf{f} = \begin{pmatrix} V_1 \\ M_1 \end{pmatrix}, \qquad \boldsymbol{\gamma} = \begin{pmatrix} w(L) \\ -w'(L) \end{pmatrix}$$

Consider the symmetric case in which $M_0 = 0$, with the implication that $w'(L) = 0$. The equation reduces to

$$\left[12 \frac{\mathrm{E}I}{L^3} - \frac{6}{5} \frac{P}{L} \right] w(L) = V_1, \tag{14.28}$$

from which we obtain the critical buckling load given by $P_1 = 10\mathrm{E}I/L^2$.

Next, consider the antisymmetric case in which $V_0 = 0$ and $w(L) = 0$. The counterpart of Equation 14.28 is now

$$\left[4\frac{\mathrm{E}I}{L} - \frac{2}{15}PL\right](-w'(L)) = M_1, \tag{14.29}$$

and $P_2 = 30\mathrm{E}I/L^2$.

If neither the constraint of symmetry nor axisymmetry is applicable, there are two critical buckling loads, to be obtained in Exercise 2 as $27.8\frac{EI}{L^2}$ and $8.9\frac{EI}{L^2}$. These values are close enough to the symmetric and antisymmetric cases to suggest an interpretation of the two buckling loads as corresponding to the two "pure" buckling modes.

Compare the obtained values with the exact solution, assuming static conditions. Consider the symmetric case. Let $w(x) = w_c(x) + w_p(x)$, in which $w_c(x)$ is the characteristic solution and $w_p(x)$ is the particular solution reflecting the perturbation. From the Euler buckling equation demonstrated in Equation 14.17, $w_c(x)$ has a general solution of the form $w_c(x) = \alpha + \beta x + \gamma\cos\kappa x + \delta\sin\kappa x$, in which $\kappa = \sqrt{PL^2/\mathrm{E}I}$. Now, $w = -w' = 0$ at $x = 0$, $-w'(L) = 0$, and $\mathrm{E}Iw'''(L) = V_1$, expressed as the conditions

$$\begin{aligned}
1\alpha + 0\beta + 1\gamma + 0\delta &= -w_p(0)\\
0\alpha + 1\beta + 0\gamma + \kappa\delta &= -w_p'(0)\\
0\alpha + L\beta - \gamma\kappa\sin\kappa L + \delta\kappa\cos\kappa L &= -w_p'(L)\\
0\alpha + 0\beta + \gamma\kappa^3\sin\kappa L - \delta\kappa^3\cos\kappa L &= -EIw_p'''(L) + V_1
\end{aligned} \tag{14.30}$$

or otherwise stated

$$\mathbf{Bz} = \begin{pmatrix} -w_p(0)\\ -w_p'(0)\\ -w_p'(L)\\ -\mathrm{E}Iw_p'''(L) + V_1 \end{pmatrix}, \quad \mathbf{B} = \begin{bmatrix} 1 & 0 & 1 & 0\\ 0 & 1 & 0 & \kappa\\ 0 & L & -\kappa\sin\kappa L & \kappa\cos\kappa L\\ 0 & 0 & \kappa^3\sin\kappa L & -\kappa^3\cos\kappa L \end{bmatrix}, \quad \mathbf{z} = \begin{pmatrix} \alpha\\ \beta\\ \gamma\\ \delta \end{pmatrix} \tag{14.31}$$

For the solution to "blow up," it is necessary for the matrix **B** to be singular, which it is if the corresponding homogeneous problem has a solution. Accordingly, we seek conditions under which there exists a nonvanishing vector **z**, for which $\mathbf{Bz} = 0$. Direct elimination of α and β furnishes $\alpha = -\gamma$ and $\beta = -\kappa\delta$. The remaining coefficients must satisfy

$$\begin{bmatrix} -\sin\kappa L & \cos\kappa L - \kappa L\\ \sin\kappa L & \cos\kappa L \end{bmatrix}\begin{pmatrix}\gamma\\ \delta\end{pmatrix} = \begin{pmatrix}0\\ 0\end{pmatrix}. \tag{14.32}$$

A nonvanishing solution is possible only if the determinant vanishes, which reduces to $\sin \kappa L = 0$. This equation has many solutions for κL, including $\kappa L = 0$. The lowest nontrivial solution is $\kappa L = \pi$, from which $P_{crit} = \pi^2 EI/L^2 = 9.87\ EI/L^2$. Clearly, the symmetric solution in the previous two-element model ($P_{crit} = 10\ EI/L^2$) gives an accurate result.

For the antisymmetric case, the corresponding result is that $\tan \kappa L = \kappa L$. The lowest meaningful root of this equation is $\kappa L = 4.49$ (see Brush and Almroth, 1975), giving $P_{crit} = 20.19\ EI/L^2$. Clearly, the axisymmetric part of the two-element model is not as accurate, unlike the symmetric part. This issue is addressed further in the subsequent exercises.

Up to this point, it has been implicitly assumed that the beam column is initially perfectly straight. This assumption can lead to overestimates of the critical buckling load. Consider a known initial distribution $w_0(x)$. The governing equation is

$$\frac{d^2}{dx^2}\mathrm{E}I\frac{d^2}{dx^2}(w - w_0) + P\frac{d^2}{dx^2}(w - w_0) = 0, \tag{14.33}$$

or equivalently,

$$\frac{d^2}{dx^2}\mathrm{E}I\frac{d^2}{dx^2}w + P\frac{d^2}{dx^2}w = \frac{d^2}{dx^2}\mathrm{E}I\frac{d^2}{dx^2}w_0 + P\frac{d^2}{dx^2}w_0. \tag{14.34}$$

The crookedness is modeled as a perturbation. Similarly, if the cross-sectional properties of the beam column exhibit a small amount of variation, for example, $\mathrm{E}I(x) = EI_0[1 + \vartheta \sin(\pi x/L)]$, the imperfection can also be modeled as a perturbation.

14.2.2 Euler Buckling of Plates

The governing equation for a plate element subject to in-plane loads is

$$\frac{\mathrm{E}h^2}{12(1-\nu^2)}\nabla^4 w + P_x\frac{\partial^2 w}{\partial x^2} + P_y\frac{\partial^2 w}{\partial y^2} + P_{xy}\frac{\partial^2 w}{\partial x \partial y} = 0 \tag{14.35}$$

(see Wang 1953), in which the loads are illustrated as shown in Figure 14.6. The usual

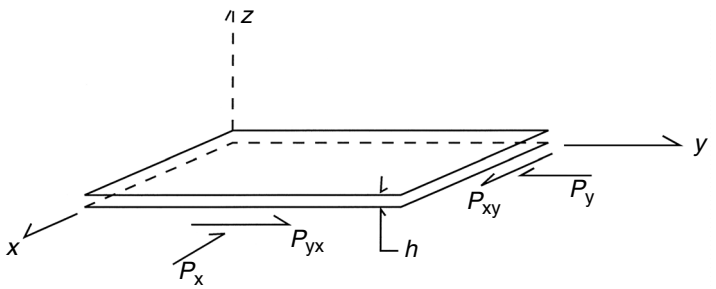

FIGURE 14.6 Plate element with in-plane compressive loads.

variational methods furnish, with some effort,

$$\int \delta w \nabla^4 w \, dA = \int \delta w (\mathbf{n} \cdot \nabla) \nabla^2 w \, dS - \int \delta \nabla w \cdot (\mathbf{n}\mathbf{P} \cdot \nabla) \nabla w \, dS + \int tr(\delta \mathbf{W}\mathbf{W}) dA, \tag{14.36}$$

in which $\mathbf{W} = \nabla\nabla^{\mathbf{T}} w$ (a matrix!). In addition,

$$\int \delta w \left[P_x \frac{\partial^2 w}{\partial x^2} + P_y \frac{\partial^2 w}{\partial y^2} + P_{xy} \frac{\partial^2 w}{\partial x \partial y} \right] dA = \int dw (n_x \quad n_y) \mathbf{p} \, dS$$

$$- \int \{\delta w_x \quad \delta w_y\} \mathbf{P} \begin{pmatrix} w_x \\ w_y \end{pmatrix} dA, \tag{14.37}$$

$$\mathbf{p} = \begin{pmatrix} \left[P_x \frac{\partial w}{\partial x} + \frac{1}{2} P_{xy} \frac{\partial w}{\partial y} \right] \\ \left[\frac{1}{2} P_{xy} \frac{\partial w}{\partial x} + P_y \frac{\partial w}{\partial y} \right] \end{pmatrix}, \qquad \mathbf{P} = \begin{bmatrix} P_x & \frac{1}{2} P_{xy} \\ \frac{1}{2} P_{xy} & P_y \end{bmatrix}$$

For simplicity's sake, assume that $w(x, y) = \boldsymbol{\varphi}_{b2}^{\mathbf{T}} \boldsymbol{\Phi}_{b2} \boldsymbol{\gamma}_{b2}$ from which we can obtain the form

$$\nabla w = \begin{pmatrix} w_x \\ w_y \end{pmatrix} = \boldsymbol{\beta}_{1b2}^{\mathbf{T}} \boldsymbol{\Phi}_{b2} \boldsymbol{\gamma}_{b2}, \qquad VEC(\mathbf{W}) = \boldsymbol{\beta}_{2b2}^{\mathbf{T}} \boldsymbol{\Phi}_{b2} \boldsymbol{\gamma}_{b2}. \tag{14.38}$$

We also assume that the secondary variables $(\mathbf{n} \cdot \nabla)\nabla^2 w$, $(\mathbf{n} \cdot \nabla)\nabla w$, and also $\begin{pmatrix} [P_x \frac{\partial w}{\partial x} + \frac{1}{2} P_{xy} \frac{\partial w}{\partial y}] \\ [\frac{1}{2} P_{xy} \frac{\partial w}{\partial x} + P_y \frac{\partial w}{\partial y}] \end{pmatrix}$ are prescribed on S.

These conditions serve to obtain

$$[\mathbf{K}_{b21} - \mathbf{K}_{b22}] \boldsymbol{\gamma}_{b2} = \mathbf{f} \tag{14.39}$$

$$\mathbf{K}_{\mathrm{b21}} = \frac{\mathrm{E}h^2}{12(1-\nu^2)} \boldsymbol{\Phi}_{\mathrm{b2}}^{\mathbf{T}} \int \boldsymbol{\beta}_{2\mathrm{b2}} \boldsymbol{\beta}_{2\mathrm{b2}}^{\mathbf{T}} \mathrm{d}A \boldsymbol{\Phi}_{\mathrm{b2}}$$

$$\mathbf{K}_{\mathrm{b22}} = \boldsymbol{\Phi}_{\mathrm{b2}}^{\mathbf{T}} \int \boldsymbol{\beta}_{1\mathrm{b2}} \mathbf{P} \boldsymbol{\beta}_{1\mathrm{b2}}^{\mathbf{T}} \mathrm{d}V \boldsymbol{\Phi}_{\mathrm{b2}}$$

and $\mathbf{f}$ reflects the quantities prescribed on S.

As illustrated in Figure 14.7, we now consider a three-dimensional loading space in which P_x, P_y, and P_{xy} correspond to the axes, and seek to determine a surface in the space of critical values at which buckling occurs. In this space, a straight line

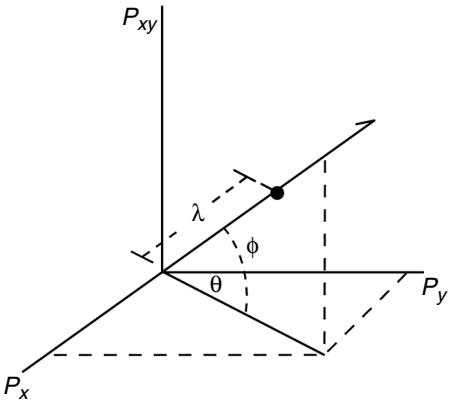

FIGURE 14.7 Loading space for plate buckling.

emanating from the origin represents a *proportional loading* path. Let the load intensity, λ, denote the distance to a given point on this line. By analogy with spherical coordinates, there exist two angles, θ and ϕ, such that

$$P_x = \lambda \cos\theta \cos\phi, \quad P_y = \lambda \sin\theta \cos\phi, \quad P_{xy} = \lambda \sin\phi \tag{14.40}$$

Now,

$$\begin{aligned} \mathbf{K}_{b22} &= \lambda \hat{\mathbf{K}}_{b22}(\theta, \varphi) \\ \hat{\mathbf{K}}_{b22}(\theta, \varphi) &= \mathbf{\Phi}_{b2}^{\mathbf{T}} \int \boldsymbol{\beta}_{1b2} \hat{\mathbf{P}}(\theta, \varphi) \boldsymbol{\beta}_{1b2}^{\mathbf{T}} dV \mathbf{\Phi}_{b2} \\ \hat{\mathbf{P}}(\theta, \phi) &= \begin{bmatrix} \cos\theta \cos\varphi & \sin\varphi \\ \sin\varphi & \sin\theta \cos\varphi \end{bmatrix} \end{aligned} \tag{14.41}$$

For each pair (θ, ϕ), buckling occurs at a critical load intensity, $\lambda_{crit}(\theta, \phi)$, satisfying

$$\det[\mathbf{K}_{b21} - \lambda_{crit}(\theta, \phi) \hat{\mathbf{K}}_{b22}] = 0. \tag{14.42}$$

A surface of critical load intensities, $\lambda_{crit}(\theta, \phi)$, can be drawn in the loading space shown in Figure 14.7 by evaluating $\lambda_{crit}(\theta, \phi)$ over all values of (θ, ϕ) and discarding values that are negative.

14.3 EXERCISES

1. Consider the triangular member shown to be modeled as one finite element. Assume that

$$\psi(x,y) = (1 \quad x \quad y)\begin{bmatrix} 1 & x_1 & y_1 \\ 1 & x_2 & y_2 \\ 1 & x_3 & y_3 \end{bmatrix}^{-1}\begin{pmatrix} \psi_1 \\ \psi_2 \\ \psi_3 \end{pmatrix}.$$

Find $\mathbf{K_T}$, $\mathbf{f_T}$, and the torsional constant $\mathbf{T}$.

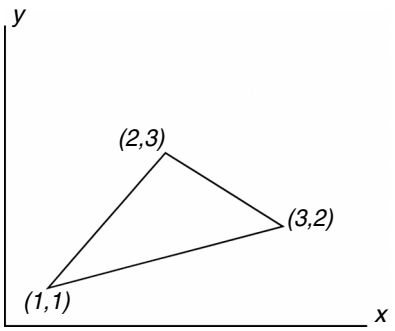

Triangular shaft cross section.

2. Find the torsional constant for a unit square cross section using two triangular elements.
3. Derive the matrices $\mathbf{K}_0$, $\mathbf{K}_1$, and $\mathbf{K}_2$ in Equations 14.20 and 14.21.
4. Compute the two critical values in Equation 14.23.
5. Use the four-element model shown in Figure 14.5, and determine how much improvement, if any, occurs in the symmetric and antisymmetric cases.
6. Consider a two-element model and a four-element model of the simple-simple case shown in the following figure. Compare P_{crit} in the symmetric and antisymmetric cases with exact values.

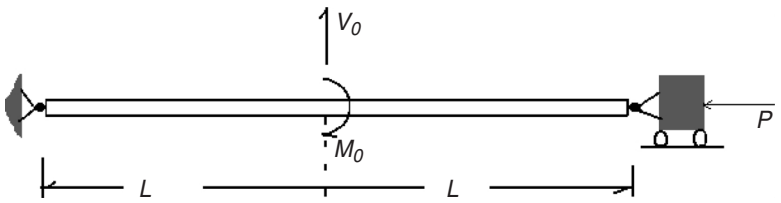

7. Consider a cantilevered beam with a compressive load P, as shown in the following figure. The equation is

$$\mathrm{E}I\frac{d^4w}{dx^4}+P\frac{d^2w}{dx^2}=0.$$

The primary variables at $x = L$ are $w(L)$ and $-w'(L)$, and

$$\int_0^L \delta w''\mathrm{E}Iw''dx=\delta\boldsymbol{\gamma}^{\mathrm{T}}\frac{\mathrm{E}I}{L^3}\begin{bmatrix}12 & 6L\\ 6L & 4L^2\end{bmatrix}\boldsymbol{\gamma},\quad \int_0^{\mathrm{L}} \delta w'Pw'dx=\delta\boldsymbol{\gamma}^{\mathrm{T}}\frac{P}{L}\begin{bmatrix}12 & 6L\\ 6L & 4L^2\end{bmatrix}\boldsymbol{\gamma}.$$

Find the critical buckling load(s).

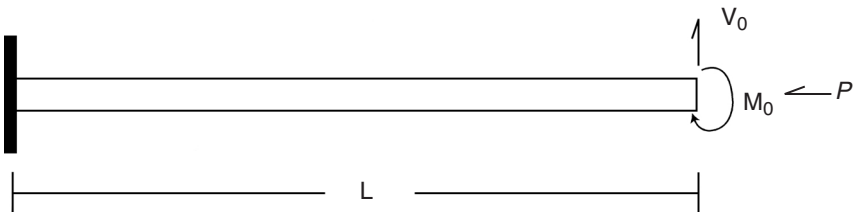

15 Introduction to Contact Problems

15.1 INTRODUCTION: THE GAP

In many practical problems, the information required to develop a finite-element model, for example, the geometry of a member and the properties of its constituent materials, can be determined with little uncertainty or ambiguity. However, often the loads experienced by the member are not so clear. This is especially true if loads are transmitted to the member along an interface with a second member. This class of problems is called contact problems, and they are arguably the most common boundary conditions encountered in practical problems. The finite-element community has devoted, and continues to devote, a great deal of effort to this complex problem, leading to gap and interface elements for contact. Here, we introduce gap elements.

First, consider the three-spring configuration in Figure 15.1. All springs are of stiffness k. Springs A and C extend from the top plate, called the *contactor*, to the bottom plate, called the *target*. The bottom of spring B is initially remote from the target by a gap g. The exact stiffness of this configuration is

$$k_c = \begin{cases} 2k & \delta < g \\ 3k & \delta \geq g. \end{cases} \tag{15.1}$$

From the viewpoint of the finite-element method, Figure 15.1 poses the following difficulty. If a node is set at the lowest point on spring B and at the point directly

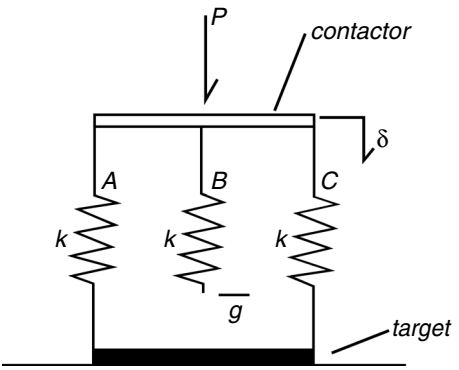

FIGURE 15.1 Simple contact problem.

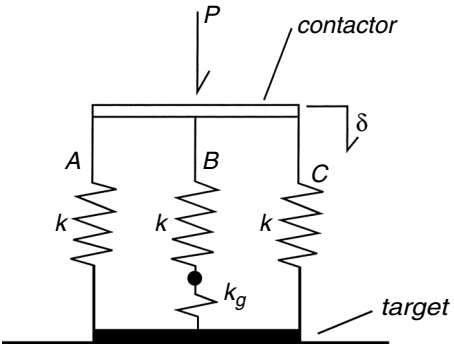

FIGURE 15.2 Spring representing contact element.

below it on the target, these nodes are not initially connected, but are later connected in the physical problem. Furthermore, it is necessary to satisfy the *nonpenetration constraint* whereby the middle spring does not move through the target. If the nodes are considered unconnected in the finite-element model, there is nothing to enforce the nonpenetration constraint. If, however, the nodes are considered connected, the stiffness is artificially high.

This difficulty is overcome in an approximate sense by a bilinear contact element. In particular, we introduce a new spring, k_g, as shown in Figure 15.2.

The stiffness of the middle spring (B in series with the contact spring) is now denoted as k_m, and

$$k_m = \left[\frac{1}{k} + \frac{1}{k_g}\right]^{-1}. \tag{15.2}$$

It is desirable for the middle spring to be soft when the gap is open ($g > \delta$) and to be stiff when the gap is closed ($g \le \delta$):

$$k_g = \begin{cases} k/100 & g > \delta \\ 100k & g \le \delta. \end{cases} \tag{15.3}$$

Elementary algebra serves to demonstrate that

$$k_c \approx \begin{cases} 2k + 0.01k & g > \delta \\ 2k + 0.99k & g \le \delta. \end{cases} \tag{15.4}$$

Consequently, the model with the contact is too stiff by 0.5% when the gap is open, and too soft by 0.33% when the gap is closed (contact). One conclusion that can be drawn from this example is that the stiffness of the gap element should be related to the stiffnesses of the contactor and target in the vicinity of the contact point.

15.2 POINT-TO-POINT CONTACT

Generally, it is not known what points will come into contact, and there is no guarantee that target nodes will come into contact with foundation nodes. The gap elements can be used to account for the unknown contact area, as follows. Figure 15.3 shows a contactor and a target, on which are indicated candidate contact areas, dS_c and dS_t, containing nodes c1, c2,…..,cn, t1, t2,…..,tn. The candidate contact areas must contain all points for which there is a possibility of establishing contact.

The gap (i.e., the distance in the undeformed configuration) from the i^{th} node of the contactor to the j^{th} node of the target is denoted by g_{ij}. (For the purpose of this discussion, the gap is constant, i.e., not updated.) In point-to-point contact, the i^{th} node on the contactor is connected to each node of the target by a spring with a bilinear stiffness. (Clearly, this element may miss the edge of the contact zone when it does not occur at a node.) It follows that each node of the target is connected by a spring to each of the nodes on the contactor. The angle between the spring and the normal at the contactor node is α_{ij}, while the angle between the spring and the normal to the target is α_{ji}. Under load, the i^{th} contactor node experiences displacement u_{ij} in the direction of the j^{th} target node, and the j^{th} target node experiences displacement u_{ji}. For example, the spring connecting the i^{th} contactor node with the j^{th} target node has stiffness k_{ij}, given by

$$k_{ij} = \begin{cases} k_{ijlower} & \delta_{ij} < g_{ij} \\ k_{ijupper} & \delta_{ij} \geq g_{ij}, \end{cases} \tag{15.5}$$

in which $\delta_{ij} = u_{ij} + u_{ji}$ is the relative displacement. The force in the spring connecting the i^{th} contactor node and j^{th} target node is $f_{ij} = k_{ij}(g_{ij})\delta_{ij}$. The total normal force experienced by the i^{th} contactor node is $f_i = \sum_j f_{ij} \cos(\alpha_{ij})$.

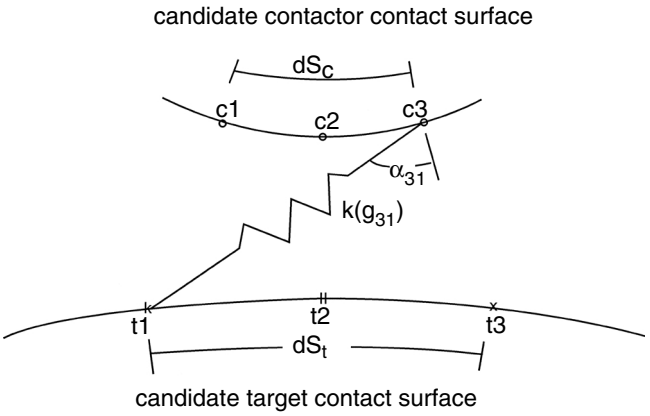

FIGURE 15.3 Point-to-point contact.

As an example of how the spring stiffness might depend upon the gap, consider the function

$$k_{ij}(g_{ij}-\delta_{ij}) = k_0\left[\varepsilon+(1-2\varepsilon)\frac{2}{\pi}\tan^{-1}\left(\frac{\alpha}{2}\left[\sqrt{(g_{ij}-\delta_{ij}-\gamma)^2}-(g_{ij}-\delta_{ij}-\gamma)\right]\right)\right], \tag{15.6}$$

where γ, α, and ε are positive parameters selected as follows. When $g_{ij}-\delta_{ij}-\gamma>0$, k_{ij} attains the lower-shelf value, $k_0\varepsilon$, and we assume that $\varepsilon \ll 1$. If $g_{ij}-\delta_{ij}-\gamma<0$, k_{ij} approaches the upper-shelf value, $k_0\,(1-\varepsilon)$. We choose γ to be a small value to attain a narrow transition range from the lower- to the upper-shelf values. In the range $0<g_{ij}-\delta_{ij}<\gamma$, there is a rapid but continuous transition from the lower-shelf (soft) value to the upper-shelf (stiff) value. If we now choose α such that $\alpha\gamma=1$, k_{ij} becomes $k_0/2$, when the gap closes ($g_{ij}=\delta_{ij}$). The spring characteristic is illustrated in Figure 15.4.

The total normal force on a contactor node is the sum of the individual contact-element forces, namely

$$f_{tj}=\sum_{i}^{N_c}k_{ij}(g_{ij}-\delta_{ij})\delta_{ij}\cos(\alpha_{ij}). \tag{15.7}$$

Clearly, significant forces are exerted only by the contact elements that are "closed."

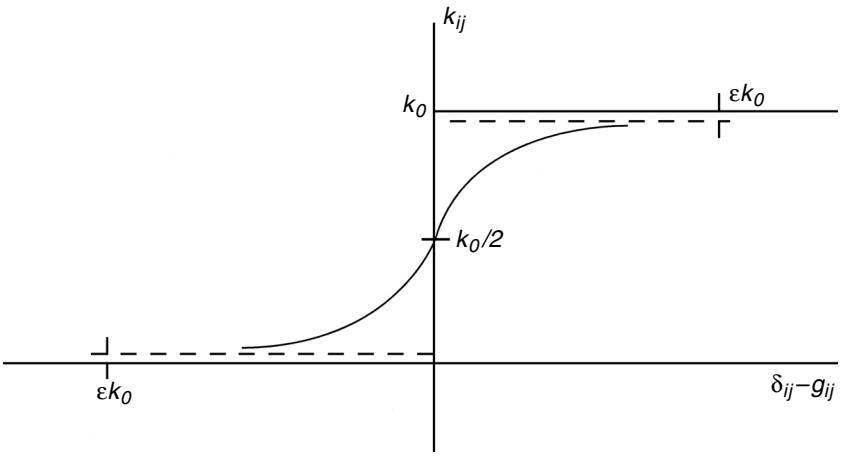

FIGURE 15.4 Illustration of a gap-stiffness function.

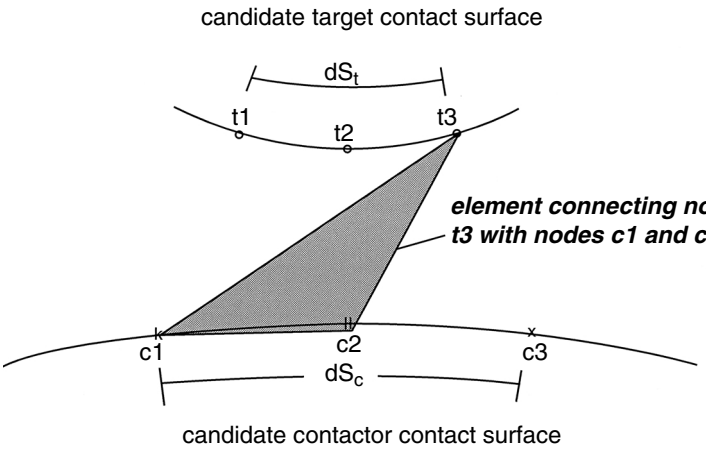

FIGURE 15.5 Element for point-to-surface contact.

15.3 POINT-TO-SURFACE CONTACT

We now briefly consider point-to-surface contact, illustrated in Figure 15.5 using a triangular element. Here, target node t3 is connected via a triangular element to contactor nodes c1 and c2. The stiffness matrix of the element is written as $k([g_1 - \delta_1], [g_2 - \delta_2])\,\hat{\mathbf{K}}$, in which $g_1 - \delta_1$ is the gap between nodes t1 and c1, and $\hat{\mathbf{K}}$ is the geometric part of the stiffness matrix of a triangular elastic element. The stiffness matrix of the element can be made a function of both gaps. Total force normal to the target node is the sum of the forces exerted by the contact elements on the candidate contactor nodes.

In some finite-element codes, the foregoing scheme is used to approximate the tangential force in the case of friction. Namely, an "elastic-friction" force is assumed in which the tangential tractions are assumed proportional to the normal traction through a friction coefficient. This model does not appear to consider sliding and can be considered a bonded contact. Advanced models address sliding contact and incorporate friction laws not based on the Coulomb model.

15.4 EXERCISES

1. Consider a finite-element model for a set of springs, illustrated in the following figure. A load moves the plate on the left toward the fixed plate on the right.
   What is the load-deflection curve of the configuration?
   For a finite-element model, an additional bilinear spring is supplied, as shown. What is the load-deflection curve of the finite-element model?
   Identify a k_g value for which the load-deflection behavior of the finite-element model is close to the actual configuration.
   Why is the new spring needed in the finite-element model?

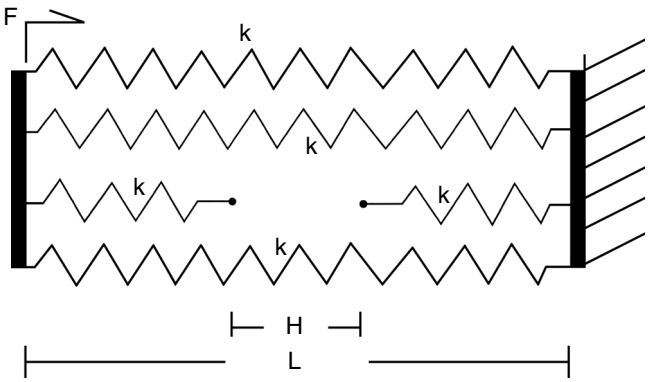

2. Suppose a contact element is added in the previous problem, in which the stiffness (spring rate) satisfies

$$k(g_{ij}-\delta_{ij})$$
$$= k_0\left[\varepsilon+(1-2\varepsilon)\frac{2}{\pi}\tan^{-1}\left(\frac{\alpha}{2}\left[\left|\sqrt{(g_{ij}-\delta_{ij}-\gamma)^2}-(g_{ij}-\delta_{ij}-\gamma)\right|\right]\right)\right].$$

Suppose $\alpha\gamma = 1$, $k_L = k/100$, and $k_u = 100k$. Compute the stiffness k for the configuration as a function of the deflection δ.

16 Introduction to Nonlinear FEA

16.1 OVERVIEW

The previous section addressed finite-element methods for linear problems. Applications that linear methods serve to analyze include structures under mild loads, disks and rotors spinning at modest angular velocities, and heated plates. However, a large number of problems are nonlinear. Plasticity is a nonlinear materials theory suited for metals in metal forming, vehicle crash, and ballistics applications. In problems with high levels of heat input, mechanical properties, such as the elastic modulus, and thermal properties, such as the coefficient of specific heat, can be strongly temperature-dependent. Rubber seals and gaskets commonly experience strains exceeding 50%. Soft biological tissues typically are modeled as rubberlike. Many problems involve variable contact, for example, meshing gear teeth. Heat conducted across electrical contacts can be strongly dependent on normal pressures. Fortunately, much of the linear finite-element method can be adapted to nonlinear problems, as explained in this chapter. The next chapter focuses on isothermal problems. The extension to thermomechanical problems will be presented in a subsequent chapter.

16.2 TYPES OF NONLINEARITY

There are three major types of nonlinearity in thermomechanical boundary-value problems: *material nonlinearity, geometric nonlinearity*, and *boundary-condition nonlinearity.* Nonlinearities can also be present if the formulation is referred to deformed coordinates, possibly introducing stress fluxes and converted coordinates.

Material nonlinearity can occur through nonlinear dependence of the stress on the strain or temperature, including temperature dependence of the tangent modulus tensor. Metals undergoing plastic flow exhibit nonlinear material behavior.

Geometric nonlinearity occurs because of large deformation, especially in problems referred to undeformed coordinates. Rubber components typically exhibit large deformation and require nonlinear kinematic descriptions. In this situation, a strain measure needs to be chosen, as does the stress conjugate to it. Boundary-condition nonlinearity occurs because of nonlinear supports on the boundary and contact. An example of a nonlinear support is a rubber pad placed under a machine to absorb vibrations.

For finite-element methods for nonlinear problems, the loads or time steps are applied in increments. Then, incremental variational principles, together with interpolation models, furnish algebraic (static) or ordinary differential equations (dynamic)

in terms of vector-valued incremental displacements or incremental temperatures. For mechanical systems, a typical equation is

$$\mathbf{K}(\boldsymbol{\gamma})\Delta\boldsymbol{\gamma} + \mathbf{M}(\boldsymbol{\gamma})\Delta\ddot{\boldsymbol{\gamma}} = \Delta\mathbf{f}, \tag{16.1}$$

in which $\Delta\boldsymbol{\gamma}$ is the *incremental displacement vector*, $\Delta\mathbf{f}$ is the *incremental force vector*, $\mathbf{K}(\boldsymbol{\gamma})$ is the *tangent stiffness matrix*, and $\mathbf{M}(\boldsymbol{\gamma})$ is the *tangent mass matrix*. It will be seen that this type of equation is a realization of the optimal Newton iteration method for nonlinear equations.

16.3 COMBINED INCREMENTAL AND ITERATIVE METHODS: A SIMPLE EXAMPLE

Consider a one-dimensional rod of nonlinear material under small deformation in which the elastic modulus is a function of strain: $\mathrm{E} = \mathrm{E}_0(1 + \alpha\varepsilon)$, $\varepsilon = E_{11}$. Under static loading, the equilibrium equation is

$$\frac{A\mathrm{E}_0}{L}\left(1 + \alpha\frac{\gamma}{L}\right)\gamma = P\,. \tag{16.2}$$

Suppose the load is applied in increments, $\Delta_j P$, and that the load at the n^{th} load step is P_n. Suppose further that the solution γ_n is known at the n^{th} load. We now consider the steps necessary to determine the solution γ_{n+1} for P_{n+1}. We introduce the increment $\Delta_n\gamma = \gamma_{n+1} - \gamma_n$. Subtracting Equation 16.2 at the n^{th} step from the equation at the $(n+1)^{st}$ step, the incremental equilibrium equation for the n^{th} increment is now

$$\frac{A\mathrm{E}_0}{L}\left(1 + 2\alpha\frac{\gamma_{n+1} + \Delta_n\gamma}{L}\right)\Delta_n\gamma = \Delta_n P\,. \tag{16.3}$$

This equation is quadratic in the increments. In fact, geometric nonlinearity generally leads to a quadratic function of increments. The error of neglecting the nonlinearity may be small if the load increment is sufficiently small. However, we will retain the nonlinear term for the sake of illustrating the use of iterative procedures. In particular, the previous equation can be written with obvious identifications in the form

$$g(x) = \beta x + \zeta x^2 - \eta = 0. \tag{16.4}$$

Newton iteration (discussed in Chapter 3) furnishes the optimal iteration scheme for the ν^{th} iterate:

$$x^{\nu+1} = x^{\nu} - \frac{[\beta x^{\nu} + \zeta x^{\nu 2} - \eta]}{\beta + 2\zeta x^{\nu}}, \quad x^0 = \eta/\beta. \tag{16.5}$$

Sample Problem 1

The efficiency of this scheme is addressed as follows. Consider $\zeta = 1$, $\beta = 12$, and $\eta = 1$. The correct solution is $x = 0.0828$. Starting with the initial value $x = 0$, the first two iterates are, approximately, $\frac{1}{12} = 0.833$, and $\frac{1}{12}(1 - \frac{1}{144}) = 0.0828$. This illustrates the rapid *quadratic* convergence of Newton iteration.

16.4 FINITE STRETCHING OF A RUBBER ROD UNDER GRAVITY: A SIMPLE EXAMPLE

Figure 16.1 shows a rubber rod under gravity. It is assumed to attain finite strain. The rod is also assumed to experience uniaxial tension. The figure refers to the undeformed configuration, with the element occupying the interval (X_e, X_{e+1}). Its length is l_e, its cross-sectional area is A_e, and its mass density is ρ. It is composed of rubber and is stretched axially by the loads P_e and P_{e+1}. Prior to stretching, a given material particle is located at X. After deformation, it is located at $x(X)$, and the displacement $u(X)$ is given by $u(X) = x(X) - X$.

16.4.1 Nonlinear Strain-Displacement Relations

The element is assumed short enough that a satisfactory approximation for the displacement $u(X)$ is provided by the linear interpolation model

$$\begin{aligned} u(X) &= u_e + (X - X_e)(u_{e+1} - u_e)/l_e \\ &= \mathbf{N}^{\mathbf{T}}\mathbf{a}_e, \qquad \mathbf{N}^{\mathbf{T}} = \frac{1}{l_e}\{x_e - x \quad x - x_e\}, \end{aligned} \tag{16.6}$$

in which $\mathbf{a}_e^{\mathbf{T}} = \{u_e \quad u_{e+1}\}$. Now, $u(X_e) = u_e$ and $u(X_{e+1}) = u_{e+1}$ are viewed as the unknowns to be determined using the finite-element method. The Lagrangian strain

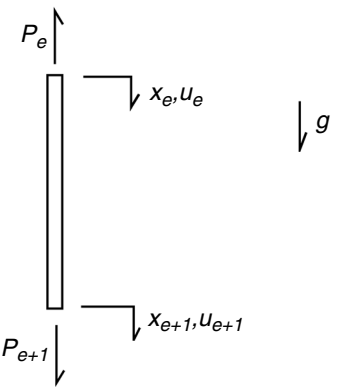

FIGURE 16.1 Rubber rod under load.

$E = E_{xx}$ is given by

$$E = \frac{\partial u}{\partial x} + \frac{1}{2}\left(\frac{\partial u}{\partial x}\right)^2$$

$$= \frac{u_{e+1} - u_e}{l_e} + \frac{1}{2}\left(\frac{u_{e+1} - u_e}{l_e}\right)^2$$

$$= \frac{1}{l_e}\{-1 \quad 1\}\mathbf{a}_e + \frac{1}{2}\mathbf{a}_e^{\mathbf{T}}\frac{1}{l_e^2}\begin{bmatrix} 1 & -1 \\ -1 & 1 \end{bmatrix}\mathbf{a}_e. \tag{16.7}$$

Note that

$$dE = \mathbf{B}^{\mathbf{T}} d\mathbf{a}_e, \qquad \mathbf{B} = \mathbf{B}_L + \mathbf{B}_{NL}\mathbf{a}_e \tag{16.8}$$

$$\mathbf{B}_L = \frac{1}{l_e}\begin{Bmatrix} -1 \\ 1 \end{Bmatrix} \qquad \mathbf{B}_{NL} = \frac{1}{l_e^2}\begin{bmatrix} 1 & -1 \\ -1 & 1 \end{bmatrix}.$$

The vector $\mathbf{B}_L$ and the matrix $\mathbf{B}_{NL}$ are the *strain-displacement matrices*.

The following sections illustrate two different approaches to formulating a finite-element model for the rubber rod. One is based on satisfying the incompressibility constraint *a priori*. The second is based on satisfying the constraint *a posteriori*, which is typical of finite-element code practice. In addition, we also include a slight variant involving a near-incompressibility constraint in an *a posteriori* manner.

16.4.2 Stress and Tangent Modulus Relations

The Neohookean strain-energy density function, w, accommodating incompressibility, is expressed in terms of the eigenvalues c_1, c_2, and c_3 of $\mathbf{C} = 2E + \mathbf{I}$, as follows:

$$w = \frac{D}{2}(c_1 + c_2 + c_3 - 3), \quad \text{subject to } c_1 c_2 c_3 - 1 = 0\,, \tag{16.9}$$

in which D is the (small-strain) elastic modulus. We can show, with some effort, that under uniaxial tension, $c_2 = c_3$.

We first enforce the incompressibility constraint *a priori* by using the substitution

$$c_2 = c_3 = \frac{1}{\sqrt{c_1}}. \tag{16.10}$$

After elementary manipulations,

$$w = \frac{D}{2}[2E + 1 + 2/(2E+1)^{-1/2} - 3]\,. \tag{16.11}$$

The (2nd Piola-Kirchhoff) stress, S, defined in Chapter 5, is now obtained as

$$S = \frac{\partial w}{\partial E}$$
$$= \frac{1}{3} D[1-(2E+1)^{-3/2}]. \tag{16.12}$$

The tangent modulus, D, is also required:

$$D_T = \frac{\partial S}{\partial E}$$
$$= D(2E+1)^{-5/2}. \tag{16.13}$$

If the strain E is small compared to unity, D_T reduces to D.

We next satisfy the incompressibility constraint *a posteriori*. An augmented strain-energy function w^* is introduced by

$$w^* = \frac{D}{2}[c_1 + c_2 + c_3 - 3] - \frac{p}{2}(c_1 c_2 c_3 - 1), \tag{16.14}$$

in which the Lagrange multiplier, p, is the (true) hydrostatic pressure. The augmented energy is stationary with respect to p as well as c_1, c_2, and c_3, from which it follows that $c_1c_2c_3 - 1 = 0$ (incompressibility).

The stresses satisfy

$$S_1 = \frac{\partial w^*}{\partial E_1} = 2\frac{\partial w^*}{\partial c_1} = \frac{D}{2} - \frac{p}{2}\frac{c_1c_2c_3}{c_1}$$
$$S_2 = \frac{\partial w^*}{\partial E_2} = 2\frac{\partial w^*}{\partial c_2} = \frac{D}{2} - \frac{p}{2}\frac{c_1c_2c_3}{c_2} = 0 \tag{16.15}$$
$$S_3 = \frac{\partial w^*}{\partial E_3} = 2\frac{\partial w^*}{\partial c_3} = \frac{D}{2} - \frac{p}{2}\frac{c_1c_2c_3}{c_3} = 0.$$

It is readily shown that $c_2 = c_3$. Enforcement of the stationary condition for p ($c_1c_2c_3 - 1 = 0$), with $S_2 = 0$, now furnishes that $p = D/\sqrt{c_1}$. It follows that $S_1 = D[1 - c_1^{-3/2}]/2$, in agreement with Equation 16.12.

16.4.3 Incremental Equilibrium Relation

The Principle of Virtual Work states the condition for static equilibrium as

$$\int_{X_e}^{X_{e+1}} \mathbf{B} S_e A dX - \mathbf{P}^e - \left[\rho g \int_{X_e}^{X_{e+1}} \mathbf{N}^{\mathbf{T}} A dX\right] \mathbf{a}_e = \mathbf{0}, \quad \mathbf{P}^e = \begin{pmatrix} P_e^e \\ P_{e+1}^e \end{pmatrix}, \tag{16.16}$$

in which the third term represents the weight of the element, while P_e represents the forces from the adjacent elements. In an incremental formulation, we can replace the loads and displacements by their differential forms. In particular,

$$\begin{aligned} d\mathbf{P}^e &= \int_{X_e}^{X_{e+1}} \mathbf{B}\, dS A_e dX + \int_{X_e}^{X_{e+1}} d\,\mathbf{B} S A_e dX \\ &= \mathbf{K}_e d\mathbf{a}_e \\ &= \{\mathbf{K}_{1e} + \mathbf{K}_{2e} + \mathbf{K}_{3e} + \mathbf{K}_{4e}\} d\mathbf{a}_e \end{aligned} \tag{16.17}$$

in which

$$\begin{aligned} \mathbf{K}_{1e} &= A_e \int_{X_e}^{X_{e+1}} \mathbf{B}_L D_T \mathbf{B}_L^{\mathrm{T}} dX \\ &= \frac{\overline{D}_T A_e}{l_e} \begin{bmatrix} 1 & -1 \\ -1 & 1 \end{bmatrix} \end{aligned} \tag{16.18a}$$

$$\begin{aligned} \mathbf{K}_{2e} &= A_e \int_{X_e}^{X_{e+1}} D_T \left(\mathbf{B}_L \mathbf{a}_e^{\mathrm{T}} \mathbf{B}_{NL} + \mathbf{B}_{NL} \mathbf{a}_e \mathbf{B}_L^{\mathrm{T}} \right) dX \\ &= \frac{\overline{D}_T A_e}{l_e} 2 \frac{[u_{e+1} - u_e]}{l_e} \begin{bmatrix} 1 & -1 \\ -1 & 1 \end{bmatrix} \end{aligned} \tag{16.18b}$$

$$\begin{aligned} \mathbf{K}_{3e} &= A_e \int_{X_e}^{X_{e+1}} \mathbf{B}_{NL} \mathbf{a}_e \mathbf{a}_e^{\mathrm{T}} \mathbf{B}_{NL}^{\mathrm{T}} dX \\ &= \frac{\overline{D}_T A_e}{l_e} \left(\frac{u_{e+1} - u_e}{l_e} \right)^2 \begin{bmatrix} 1 & -1 \\ -1 & 1 \end{bmatrix} \end{aligned} \tag{16.18c}$$

$$\begin{aligned} \mathbf{K}_{4e} &= A_e \int_{X_e}^{X_{e+1}} \mathbf{B}_L S dX \\ &= \frac{\overline{S} A_e}{l_e} \begin{bmatrix} 1 & -1 \\ -1 & 1 \end{bmatrix} \end{aligned} \tag{16.18d}$$

and

$$\overline{D}_T = \frac{1}{l_e} \int_{X_e}^{X_{e+1}} D_T dX, \qquad \overline{S} = \frac{1}{l_e} \int_{X_e}^{X_{e+1}} S dX. \tag{16.19}$$

Combining Equations 16.18 and 16.19 produces the simple relation

$$\mathbf{K}_e = \kappa \begin{bmatrix} 1 & -1 \\ -1 & 1 \end{bmatrix}, \quad \kappa = \frac{\overline{D}_T A_e}{l_e} \left\{ 1 + 2\frac{u_{e+1} - u_e}{l_e} + \left(\frac{u_{e+1} - u_e}{l_e} \right)^2 \right\} + \frac{\overline{S} A_e}{l_e}. \quad (16.20)$$

Suppose $(u_{e+1} - u_e)/l_e$ is small compared to unity, with the consequence that E is also small compared to unity. It follows in this case that $\overline{D}_T \approx D$, $\overline{S} \approx S$. As a result, $\mathbf{K}_e$ reduces to the stiffness matrix for a rod element of linearly elastic material experiencing small strain:

$$\mathbf{K}_e = \frac{\mathrm{E} A_e}{l_e} \begin{bmatrix} 1 & -1 \\ -1 & 1 \end{bmatrix}. \quad (16.21)$$

Several special cases illuminate additional aspects of finite-element modeling.

Sample Problem 1: Single Element Built in at One End

Figure 16.2 depicts a single-element model of a rod that is built in at $X = 0$: $X_e = X_0 = 0$. At the opposite end, $X_{e+1} = X_1 = 1$. The rod is submitted to the load P. The displacement at $X = 0$ is subject to the constraint $u(0) = u_0 = 0$, so that Equation 16.20 becomes

$$\kappa \begin{bmatrix} 1 & -1 \\ -1 & 1 \end{bmatrix} \begin{pmatrix} 0 \\ du_1 \end{pmatrix} = \begin{pmatrix} -dP_r \\ dP \end{pmatrix}, \quad (16.22)$$

in which dP_r is an incremental reaction force that is not known *a priori* (of course, from equilibrium, $dP_r = dP$). For the only unknown reaction, this last equation "condenses" to

$$k du_1 = dP. \quad (16.23)$$

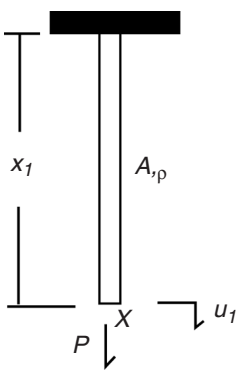

FIGURE 16.2 Rubber rod element under load: built in at top.

For later use, the current shape function degenerates to the expression $\mathbf{N} \rightarrow N = X/X_1$.

The (Lagrangian) strain is given by

$$E(u_1) = \frac{u_1}{X_1} + \frac{1}{2}\left(\frac{u_1}{X_1}\right)^2, \tag{16.24}$$

and the strain-displacement matrices reduce to

$$\mathbf{B} \rightarrow B = \frac{1}{X_1} + \frac{u_1}{X_1^2}. \tag{16.25}$$

The (2^{nd} Piola-Kirchhoff) stress S is now a function of u_1:

$$S(u_1) = \frac{1}{3} D \left[1 - \left[2\left\{ \frac{u_1}{X_1} + \frac{1}{2}\left(\frac{u_1}{X_1}\right)^2 \right\} - 1 \right]^{-\frac{3}{2}} \right]. \tag{16.26}$$

16.4.4 Numerical Solution by Newton Iteration

Equation 16.22 can be solved by Newton iteration, sometimes called "load balancing," the reason for which is explained shortly. We introduce the "residual" function $\phi(u_1) = 0$ as follows. The Principle of Virtual Work implies that if gravity is considered in Figure 16.2,

$$\begin{aligned}
\phi(u_1) &= \int_0^{X_1} BSA\, dX - P - \left[\rho g \int_0^{X_1} \mathbf{N}^{\mathbf{T}} A\, dX \right] \mathbf{a}_e \\
&= \left[\frac{1}{l_e} + \frac{u_1}{l_e^2} \right] A X_1 \left(\frac{1}{3} D \left[1 - \left[2\left\{ \frac{u_1}{X_1} + \frac{1}{2}\left(\frac{u_1}{X_1}\right)^2 \right\} - 1 \right]^{-\frac{3}{2}} \right] \right) - P - \rho g A \frac{X_1}{2} u_1 \\
&= 0.
\end{aligned} \tag{16.27}$$

when u_1 is the solution. Consider an iteration process in which the j^{th} iterate u_1^j has been determined. Newton iteration determines the next iterate, u_1^{j+1}, using

$$\begin{aligned}
\kappa\left(u_1^j\right) \Delta_j u_1 &= -\phi\left(u_1^j\right) \\
u_1^{j+1} &= u_1^j + \Delta_j u_1.
\end{aligned} \tag{16.28}$$

Convergence of this scheme to the correct value u_1 is usually rapid, provided that the initial iterate u_1^0 is sufficiently close to u_1. A satisfactory initial iterate is

often obtained using an incremental procedure. Suppose that the solution has been obtained at previous load steps. A starting iterate for the current load step is obtained by extrapolating from the previous solutions. As an example, suppose the solution is known at the load $P = k\Delta P$, in which ΔP is a load increment. The load is now incremented to produce $P = (k + 1)\Delta P$, and the solution $u_{1,k+1}$ at this load is determined using Newton iteration. It is frequently satisfactory to start the iteration using $u^0_{1,k+1} = u_1$. This numerical procedure is illustrated more extensively at the end of this chapter.

Sample Problem 2: Assembled Stiffness Matrix for a Two-Element Model

Assemblage procedures are used to combine the element-equilibrium relations to obtain the global equilibrium relation for an assemblage of elements. For elements 'e' and '$e + 1$', the element-equilibrium relations are expanded as

$$\begin{aligned} k^e_{11}du_e + k^e_{12}du_{e+1} &= dP^e_e \qquad \text{(i)} \\ k^e_{21}du_e + k^e_{22}du_{e+1} &= dP^e_{e+1} \qquad \text{(ii)} \\ k^{e+1}_{11}du_{e+1} + k^{e+1}_{12}du_{e+2} &= dP^{e+1}_{e+1} \qquad \text{(iii)} \\ k^{e+1}_{21}du_{e+1} + k^{e+1}_{22}du_{e+2} &= dP^{e+1}_{e+2} \qquad \text{(iv).} \end{aligned} \tag{16.29}$$

The superscript indicates the element index, and the subscript indicates the node index. If no external force is applied at x_{e+1}, the interelement force balance is expressed as

$$dP^e_{e+1} + dP^{e+1}_{e+1} = 0. \tag{16.30}$$

Adding Equation 16.29(ii) and Equation 16.29(iii) furnishes

$$k^e_{21}du_e + \left(k^e_{22} + k^{e+1}_{11}\right)du_{e+1} + k^{e+1}_{12}du_{e+2} = 0\,. \tag{16.31}$$

Equations 16.29, 16.30, and 16.31 are expressed in matrix form as

$$\begin{bmatrix} k^e_{11} & k^e_{12} & 0 \\ k^e_{21} & k^e_{22} + k^{e+1}_{11} & k^{e+1}_{12} \\ 0 & k^{e+1}_{21} & k^{e+1}_{22} \end{bmatrix} \begin{Bmatrix} du_e \\ du_{e+1} \\ du_{e+2} \end{Bmatrix} = \begin{Bmatrix} dP^e_e \\ 0 \\ dP^{e+1}_{e+2} \end{Bmatrix}. \tag{16.32}$$

Equation 16.32 illustrates that the (incremental) global stiffness matrix is formed by "overlaying" $\mathbf{K}_e$ and $\mathbf{K}_{e+1}$, with the entries added in the intersection.

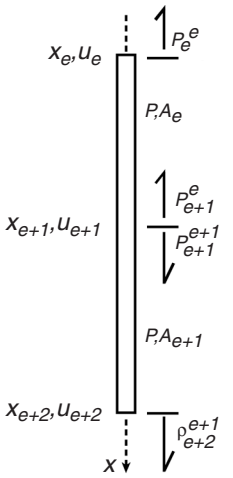

FIGURE 16.3 Two rubber rods under load.

Sample Problem 3: Two Identical Elements under Gravity under Equal End-Loads

If $\mathbf{K}_e = \mathbf{K}_{e+1}$ and $dP_e^e = -dP_{e+1}^{e+1} = -dP$, overlaying the element matrices leads to the global (two-element) relation

$$\kappa \begin{bmatrix} 1 & -1 & 0 \\ -1 & 2 & -1 \\ 0 & -1 & 1 \end{bmatrix} \begin{pmatrix} du_1 \\ du_2 \\ du_3 \end{pmatrix} = \begin{pmatrix} -dP \\ 0 \\ dP \end{pmatrix}. \tag{16.33}$$

Note that Equation 16.33 has *no solution* since the global stiffness matrix has no inverse: the second row is the negative of the sum of the first and last rows. This suggests that, due to numerical errors in the load increments, the condition for static equilibrium is not satisfied numerically, and therefore that the body is predicted to accelerate indefinitely (undergo rigid-body motion). However, we also know that the configuration under incremental loads is symmetric, implying a constraint $du_2 = 0$. This constraint permits "condensation," that is, reducing Equation 16.33 to a system with two unknowns by eliminating rows and columns associated with the middle incremental displacement:

$$\kappa \begin{bmatrix} 1 & -1 \\ -1 & 1 \end{bmatrix} \begin{pmatrix} du_1 \\ du_3 \end{pmatrix} = \begin{pmatrix} -dP \\ dP \end{pmatrix}. \tag{16.34}$$

The condensed matrix is now proportional to the identity matrix, and the system has a solution. In general, stiffness matrices can easily be singular or nearly singular

(with a large condition number) unless constraints are used to suppress "rigid-body modes."

16.5 ILLUSTRATION OF NEWTON ITERATION

Unfortunately, since elastomers or metals experiencing plasticity are typically quite compliant, it is common to encounter convergence problems, for which there are four major approaches:

1. Increasing stiffness, such as by introducing additional constraints if available
2. Reducing load-step sizes and reforming the stiffness matrix after each iteration
3. Switching to displacement control rather than load control
4. Using an arc-length method (described in Chapter 3)

For an equation of the form

$$\psi(x) = 0, \tag{16.35}$$

Newton iteration seeks a solution through an iterative process given by

$$x_{j+1} = x_j - \left[\frac{d\psi(x_j)}{dx}\right]^{-1} \psi(x_j)\,. \tag{16.36}$$

Clearly, using two sequential iterates,

$$\begin{aligned} x_{j+1} - x_j &= x_j - x_{j-1} - \left[\frac{d\psi(x_j)}{dx}\right]^{-1} \psi(x_j) - \left[\frac{d\psi(x_{j-1})}{dx}\right]^{-1} \psi(x_{j-1}) \\ &= x_j - x_{j-1} - \left[\left[\frac{d\psi(x^*)}{dx} + \frac{d^2\psi(x^*)}{dx^2}(x_j - x^*)\right]^{-1}\right. \\ &\quad \times \left[\psi(x^*) + \frac{d\psi(x^*)}{dx}(x_j - x^*)\right] - \left[\frac{d\psi(x^*)}{dx} + \frac{d^2\psi(x^*)}{dx^2}(x_{j-1} - x^*)\right]^{-1} \\ &\quad \left.\times \left[\psi(x^*) + \frac{d\psi(x^*)}{dx}(x_{j-1} - x^*)\right]\right] + \cdots \\ &= \left(1 - \left(\frac{d\psi(x^*)}{dx}\right)^{-1} \frac{d\psi(x^*)}{dx}\right)(x_j - x_{j-1}) + O([x_j - x_{j-1}]^2) \end{aligned} \tag{16.37}$$

for some x^* between x_j and x_{j-1}.

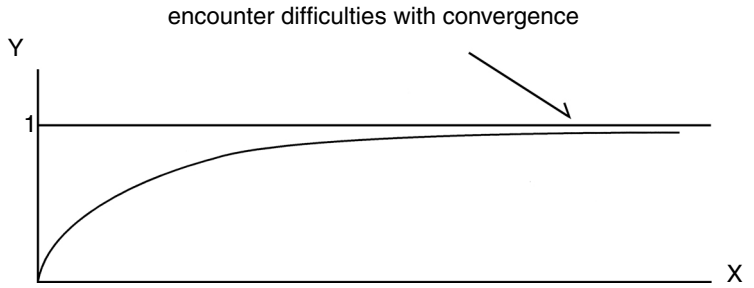

FIGURE 16.4 Illustration of the inverse tangent function.

16.5.1 Example

The performance of Newton iteration procedure is illustrated using a simple example showing convergence problems. Consider

$$\varphi(x) = \frac{2}{\pi}\tan^{-1}(x) - y = 0. \tag{16.38}$$

The goal is to find the solution of x as y is incremented in the range (0,1). Clearly, x approaches infinity as y approaches unity, so that the goal is to generate the $x(y)$ relationship accurately as close as possible to $y = 1$. The curve appears as shown in Figure 16.4. As y is incremented by small amounts just below unity, the differences in x due to the increment are large, so that the solution value is far from the initial iterate.

Suppose that y is incremented such that the n^{th} value of y is

$$y_n = n\Delta y. \tag{16.39}$$

To obtain the solution of the $(n + 1)^{st}$ step, the Newton iteration procedure generates the $(\nu + 1)^{st}$ iterate from the ν^{th} iterate, as follows:

$$x_{n+1}^{\nu+1} = x_{n+1}^{\nu} - \left[\frac{d\phi\left(x_{n+1}^{\nu}\right)}{dx}\right]^{-1} \phi\left(x_{n+1}^{\nu}\right), \tag{16.40}$$

in which x_{n+1}^{ν} is the ν^{th} iterate for the solution x_{n+1}.

Of course, a starting iterate, x_{n+1}^{0}, is needed. An attractive candidate is x_{n+1}. However, this may not be good enough when convergence difficulties appear.

Newton iteration was implemented for this example in a simple problem using increments of 0.001. A stopping criterion of 10 iterations was used. Convergence was found to fail near y = 0.999.

16.6 EXERCISES

1. Doing the algebra, make judicious choices of starting iterates, and develop the first few iterates for the roots of the equations

$$x^2 + 3x + 2 = 0$$

$$x^2 - 1 = 0$$

$$(x-1)^2 = 0$$

2. Write a simple program implementing Newton iteration, and apply it to the examples in Exercise 1.
3. Using Example 5.1, write a simple program using Newton iteration to compute $X(Y)$ using increments $\Delta y = 0.001$. Set the stopping criterion as the first of: (a) 10 iterates or (b) an absolute difference of less than 0.001 in the successive values of x. Note the value of x at which convergence fails, and compare the values of x with accurate values available from the formulae and tables in Abramawitz and Stegun (1997).

17 Incremental Principle of Virtual Work

17.1 INCREMENTAL KINEMATICS

Recall that the displacement vector $\mathbf{u}(\mathbf{X})$ is assumed to admit a satisfactory approximation at the element level in the form $\mathbf{u}(\mathbf{X}) = \boldsymbol{\varphi}^{\mathbf{T}}(\mathbf{X})\boldsymbol{\Phi}\boldsymbol{\gamma}(t)$. Also recall that the deformation-gradient tensor is given by $\mathbf{F} = \frac{\partial x}{\partial \mathbf{x}}$. Suppose that the body under study is subjected to a load vector, $\mathbf{P}$, which is applied incrementally via load increments, $\Delta_j\mathbf{P}$. The load at the n^{th} load step is denoted as $\mathbf{P}_n$. The solution, $\mathbf{P}_n$, is known, and the solution of the increments of the displacements is sought. Let $\Delta_n\mathbf{u} = \mathbf{u}_{n+1} - \mathbf{u}_n$, so that $\Delta_n\mathbf{u} = \boldsymbol{\varphi}^{\mathbf{T}}(\mathbf{X})\boldsymbol{\Phi}\Delta_n\boldsymbol{\gamma}$. By suitably arranging the derivatives of $\Delta_n\mathbf{u}$ with respect to $\mathbf{X}$, a matrix, $\boldsymbol{M}(\mathbf{X})$, can easily be determined for which $VEC(\Delta_n\mathbf{F}) = \boldsymbol{M}(\mathbf{X})\Delta_n\boldsymbol{\gamma}$.

We next consider the Lagrangian strain, $\boldsymbol{E}(\mathbf{X}) = \frac{1}{2}(\mathbf{F}^{\mathbf{T}}\mathbf{F} - \mathbf{I})$. Using Kronecker Product algebra from Chapter 2, we readily find that, to first order in increments,

$$\begin{aligned}
\Delta_n\mathbf{e} &= VEC(\Delta_n\boldsymbol{E}) \\
&= VEC\left(\frac{1}{2}[\mathbf{F}^{\mathbf{T}}\Delta_n\mathbf{F} + \Delta_n\mathbf{F}^{T}\mathbf{F}]\right) \\
&= \frac{1}{2}[\mathbf{I}\otimes\mathbf{F}^{\mathbf{T}} + \mathbf{F}^{\mathbf{T}}\otimes\mathbf{IU}]VEC(\Delta_n\mathbf{F}) \\
&= \mathbf{G}\Delta_n\mathbf{g}, \qquad \mathbf{G}^{\mathbf{T}} = \frac{1}{2}[\mathbf{I}\otimes\mathbf{F}^{\mathbf{T}} + \mathbf{F}^{\mathbf{T}}\otimes\mathbf{IU}]\boldsymbol{M}(\mathbf{X})\Delta_n\mathbf{g}.
\end{aligned} \tag{17.1}$$

This form shows the advantages of Kronecker Product notation. Namely, it enables moving the incremental displacement vector to the end of the expression outside of domain integrals, which we will encounter subsequently.

Alternatively, for the current configuration, a suitable strain measure is the Eulerian strain, $\boldsymbol{\mathfrak{Z}} = \frac{1}{2}(\mathbf{I} - \mathbf{F}^{-\mathbf{T}}\mathbf{F}^{-\mathbf{1}})$, which refers to deformed coordinates. Note that since $\Delta_n(\mathbf{FF}^{-\mathbf{1}}) = \mathbf{0}$, $\Delta_n\mathbf{F}^{-\mathbf{1}} = -\mathbf{F}^{-\mathbf{1}}\Delta_n\mathbf{F}\mathbf{F}^{-\mathbf{1}}$. Similarly, $\Delta_n\mathbf{F}^{-\mathbf{T}} = -\mathbf{F}^{-\mathbf{T}}\Delta_n\mathbf{F}^{\mathbf{T}}\mathbf{F}^{-\mathbf{T}}$. Simple manipulation furnishes that

$$VEC(\Delta_n\boldsymbol{\mathfrak{Z}}) = \frac{1}{2}[\mathbf{F}^{-T}\mathbf{F}^{-1}\otimes\mathbf{F}^{-T}\mathbf{U} + \mathbf{F}^{-1}\otimes\mathbf{F}^{-\mathbf{T}}\mathbf{F}^{-\mathbf{1}}]\mathbf{M}\Delta_n\mathbf{g}. \tag{17.2}$$

There also are geometric changes for which an incremental representation is useful. For example, since the Jacobian $J = \det(\mathbf{F})$ satisfies $dJ = Jtr(\mathbf{F}^{-1}d\mathbf{F})$, we obtain

the approximate formula

$$\begin{aligned}\Delta J &= Jtr(\mathbf{F}^{-1}\Delta_n\mathbf{F}) \\ &= JVEC^{\mathbf{T}}(\mathbf{F}^{-1^T})VEC(\Delta_n\mathbf{F}) \\ &= VEC^{\mathbf{T}}(\mathbf{F}^{-T})J\boldsymbol{M}\Delta_n\boldsymbol{\gamma}.\end{aligned} \tag{17.3}$$

Also of interest are

$$\begin{aligned}\frac{d[\mathbf{n}\,dS]}{dt} &= [tr(\mathbf{D})\mathbf{I} - \mathbf{L}^T]\mathbf{n}\,dS \\ \frac{d\mathbf{n}}{dt} &= [(\mathbf{n}^T\mathbf{D}\mathbf{n})\mathbf{I} - \mathbf{L}^T]\mathbf{n} \\ \frac{d}{dt}dS &= [tr(\mathbf{D}) - \mathbf{n}^T\mathbf{D}\mathbf{n}]dS\end{aligned} \tag{17.4}$$

Using Equation 17.4, we obtain the incremental forms

$$\begin{aligned}\boldsymbol{\Delta}_n[\mathbf{n}dS] &= dS[\mathbf{n}VEC^T(\mathbf{F}^{-T}) - \mathbf{n}^T \otimes \mathbf{F}^{-T}\mathbf{U}]\boldsymbol{M}\boldsymbol{\Delta}_n\boldsymbol{\gamma} \\ \Delta_n\mathbf{n} &= [\mathbf{n}(\mathbf{n}^T\mathbf{F}^{-T}) \otimes \mathbf{n}^T - \mathbf{n}^T \otimes \mathbf{F}^{-T}\mathbf{U}]\boldsymbol{M}\Delta_n\boldsymbol{\gamma} \\ \Delta_n dS &= dS[\mathbf{n}VEC^T(\mathbf{F}^{-T}) - \mathbf{n}(\mathbf{n}^T\mathbf{F}^{-T}) \otimes \mathbf{n}^T]\boldsymbol{M}\Delta_n\boldsymbol{\gamma}.\end{aligned} \tag{17.5}$$

17.2 INCREMENTAL STRESSES

For the purposes of deriving an incremental variational principle, we shall see that the incremental 1st Piola-Kirchhoff stress, $\Delta_n\overline{\boldsymbol{S}}$, is the starting point. However, to formulate mechanical properties, the objective increment of the Cauchy stress, $\mathring{\Delta}_n\boldsymbol{T}$, is the starting point. Furthermore, in the resulting variational statement, which we called the *Incremental Principle of Virtual Work*, we find that the quantity that appears is the increment of the 2nd Piola-Kirchhoff stress, $\Delta_n\boldsymbol{S}$.

From Chapter 5, we learned that $\overline{\boldsymbol{S}} = \boldsymbol{S}\mathbf{F}^{\mathbf{T}}$, from which, to first order,

$$\Delta_n\overline{\boldsymbol{S}} = \Delta_n\boldsymbol{S}\mathbf{F}^T + \boldsymbol{S}\Delta_n\mathbf{F}^T. \tag{17.6}$$

For the Cauchy stress, the increment must take into account the rotation of the underlying coordinate system and thereby be objective. We recall the objective Truesdell stress flux, $\partial\mathring{\boldsymbol{T}}/\partial t$, introduced in Chapter 5:

$$\partial\mathring{\boldsymbol{T}}/\partial t = \partial\boldsymbol{T}/\partial t + \boldsymbol{T}tr(\mathbf{D}) - \mathbf{L}\boldsymbol{T} - \boldsymbol{T}\mathbf{L}^T. \tag{17.7}$$

Among the possible stress fluxes, it is unique in that it is proportional to the rate of the 2nd Piola-Kirchhoff stress, namely

$$\partial \boldsymbol{S}/\partial t = J\mathbf{F}^{-1}\partial \overset{\circ}{\boldsymbol{T}}/\partial t\mathbf{F}^{-T}. \tag{17.8}$$

An objective Truesdell stress increment is readily obtained as

$$VEC(\overset{\circ}{\Delta}_n \boldsymbol{T}) = \frac{1}{J}\mathbf{F}^T \otimes \mathbf{F}VEC(\Delta_n \boldsymbol{S}). \tag{17.9}$$

Furthermore, once $VEC(\overset{\circ}{\Delta}_n \boldsymbol{T})$ has been determined, the (nonobjective) increment of the Cauchy stress can be computed using

$$\overset{\circ}{\Delta}_n \boldsymbol{T} = \Delta_n \boldsymbol{T} + \boldsymbol{T}tr(\Delta_n \mathbf{F}\mathbf{F}^{-1}) - \Delta_n \mathbf{F}\mathbf{F}^{-1}\boldsymbol{T} - \boldsymbol{T}\mathbf{F}^{-T}\Delta_n \mathbf{F}^T, \tag{17.10}$$

from which

$$VEC(\Delta_n \boldsymbol{T}) = VEC(\overset{\circ}{\Delta}_n \boldsymbol{T}) + [\boldsymbol{T}VEC^T(\mathbf{F}^{-T}) - (\boldsymbol{T}\mathbf{F}^{-T}) \otimes \mathbf{I} - \mathbf{I} \otimes (\boldsymbol{T}\mathbf{F}^{-T})]\boldsymbol{M}\Delta_n \boldsymbol{\gamma}. \tag{17.11}$$

17.3 INCREMENTAL EQUILIBRIUM EQUATION

We now express the incremental equation of nonlinear solid mechanics (assuming that there is no net rigid-body motion). In the deformed (Eulerian) configuration, equilibrium at t_n requires

$$\int \boldsymbol{T}^T \mathbf{n}\, dS = \int \rho \ddot{\mathbf{u}}\, dV. \tag{17.12}$$

Referred to the undeformed (Lagrangian) configuration, this equation becomes

$$\int \overline{\boldsymbol{S}}^T \mathbf{n}_0 dS_0 = \int \rho_0 \ddot{\mathbf{u}}\, dV_0, \tag{17.13}$$

in which, as indicated before, $\overline{\boldsymbol{S}}$ is the 1st Piola-Kirchhoff stress, S denotes the surface (boundary) in the deformed configuration, and $\mathbf{n}_0$ is the surface normal vector in the undeformed configuration. Suppose the solution for $\overline{\boldsymbol{S}}$ is known as $\overline{\boldsymbol{S}}_n$ at time t_n and is sought at t_{n+1}. We introduce the increment $\Delta_n \overline{\boldsymbol{S}}$ to denote $\overline{\boldsymbol{S}}_{n+1} - \overline{\boldsymbol{S}}_n$. A similar definition is introduced for the increment of the displacements. Now, equilibrium applied to $\overline{\boldsymbol{S}}_{n+1}$ and $\overline{\boldsymbol{S}}_n$ implies

$$\int \Delta_n \overline{\boldsymbol{S}}^T \mathbf{n}_0\, dS_0 = \int \rho_0 \Delta_n \ddot{\mathbf{u}}\, dV_0. \tag{17.14}$$

Application of the divergence theorem furnishes the differential equation

$$\nabla^T \Delta_n \bar{\boldsymbol{S}}^T = \rho_0 \Delta_n \ddot{\mathbf{u}}^T. \tag{17.15}$$

17.4 INCREMENTAL PRINCIPLE OF VIRTUAL WORK

To derive a variational principle for the current formulation, the quantity to be varied is the incremental displacement vector since it is now the unknown. Following Chapter 5,

Equation 17.15 is multiplied by $(\delta\Delta_n \mathbf{u})^{\mathrm{T}}$.
Integration is performed over the domain.
The Gauss divergence theorem is invoked once.
Terms appearing on the boundary are identified as primary and secondary variables.
Boundary conditions and constraints are applied.

The reasoning process is similar to that in the derivation of the Principle of Virtual Work in finite deformation in which **u** is the unknown, and furnishes

$$\int tr(\delta\Delta_n \boldsymbol{E}^{\mathbf{T}} \Delta_n \boldsymbol{S}) dV_0 + \int \delta\Delta_n \mathbf{F}\boldsymbol{S}\Delta_n \mathbf{F}^{\mathbf{T}} dV_0 + \int \delta\Delta_n \mathbf{u}^T \rho_0 \Delta_n \ddot{\mathbf{u}}\, dV_0 = \int \delta\Delta_n \mathbf{u}^T \Delta_n \boldsymbol{\tau}_0 dS_0, \tag{17.16}$$

in which $\boldsymbol{\tau}_0$ is the traction experienced by dS_0. The fourth term describes the virtual external work of the incremental tractions. The first term describes the virtual internal work of the incremental stresses. The third term describes the virtual internal work of the incremental inertial forces. The second term has no counterpart in the previously formulated Principle of Virtual Work in Chapter 5, and arises because of geometric nonlinearity. We simply call it the geometric stiffness integral. Due to the importance of this relation, Equation 17.16 is derived in detail in the equations that follow. It is convenient to perform the derivation using tensor-indicial notation:

$$\int \delta\Delta_n u_i \frac{\partial}{\partial X_j}(\Delta_n \bar{S}_{ij}) dV_0 = \int \frac{\partial}{\partial X_j}[\delta\Delta_n u_i (\Delta_n \bar{S}_{ij})] dV_0 - \int \frac{\partial}{\partial X_j}[\delta\Delta_n u_i] \Delta_n \bar{S}_{ij} dV_0$$

$$= \int \delta\Delta_n u_i \rho_0 \Delta_n \ddot{u}_i dV_0. \tag{17.17}$$

The first term on the right is converted using the divergence theorem to

$$\int \frac{\partial}{\partial X_j}[\delta\Delta_n u_i (\Delta_n \bar{S}_{ij})] dV_0 = \int \delta\Delta_n u_i (n_j \Delta_n \bar{S}_{ij}) dS_0$$

$$= \int \delta\Delta_n u_i \tau_{0j}\, dS_0 \tag{17.18}$$

which is recognized as the fourth term in Equation 17.16.

To first-order in increments, the second term on the right is written, using tensor notation, as

$$\int \frac{\partial}{\partial X_j}[\delta\Delta_n u_i]\Delta_n \bar{S}_{ij} dV_0 = \int tr(\delta\Delta_n \mathbf{F}\Delta_n \bar{\boldsymbol{S}}) dV_0$$

$$= \int tr(\delta\Delta_n \mathbf{F}[\Delta_n \boldsymbol{S}\mathbf{F}^T + \boldsymbol{S}\Delta_n \mathbf{F}^T]) dV_0$$

$$= \int tr(\mathbf{F}^T\delta\Delta_n \mathbf{F}\Delta_n \boldsymbol{S}) dV_0 + \int tr(\delta\Delta_n \mathbf{F}\boldsymbol{S}\Delta_n \mathbf{F}^T) dV_0 \qquad (17.19)$$

The second term is recognized as the second term in Equation 17.16.

The first term now becomes

$$\int tr(\mathbf{F}^T\delta\Delta_n \mathbf{F}\Delta_n \mathrm{S}) dV_0 = \int tr\left(\frac{1}{2}[\mathbf{F}^T\delta\Delta_n \mathbf{F} + \delta\Delta_n \mathbf{F}^T\mathbf{F}]\Delta_n \mathrm{S}\right) dV_0$$

$$= \int tr(\delta\Delta_n \mathrm{E}^T\Delta_n \mathrm{S}) dV_0 \qquad (17.20)$$

which is recognized as the first term in Equation 17.16.

17.5 INCREMENTAL FINITE-ELEMENT EQUATION

For present purposes, let us suppose constitutive relations in the form

$$\Delta_n \boldsymbol{S} = \boldsymbol{D}(\boldsymbol{X}, \gamma_n)\Delta_n \boldsymbol{E}, \qquad (17.21)$$

in which $\boldsymbol{D}(\boldsymbol{X}, \gamma)$ is the *fourth-order tangent modulus tensor.* It is rewritten as

$$\Delta_n \boldsymbol{s} = \boldsymbol{\chi}(\boldsymbol{X}, \gamma_n)\Delta_n \mathbf{e} \qquad (17.22)$$

$$\boldsymbol{s} = VEC(\boldsymbol{S}), \quad \boldsymbol{e} = VEC(\boldsymbol{E}), \quad \chi = TEN22(\boldsymbol{D}).$$

Also for present purposes, we assume that $\Delta\boldsymbol{\tau}_0$ is prescribed on the boundary S_0, a common but frequently unrealistic assumption that is addressed in a subsequent section.

In *VEC* notation, and using the interpolation models, Equation 17.16 becomes

$$\delta\Delta_n \boldsymbol{\gamma}^{\mathbf{T}}[(\mathbf{K}_T + \mathbf{K}_G)\Delta_n \boldsymbol{\gamma} + \mathbf{M}\Delta_n \ddot{\boldsymbol{\gamma}} - \Delta_n \mathbf{f}] = 0 \qquad (17.23)$$

$$\boldsymbol{K}_T = \int \boldsymbol{M}^T \mathbf{G}\boldsymbol{\chi}\mathbf{G}^T \boldsymbol{M}\, dV_0 \qquad \boldsymbol{K}_G = \int \boldsymbol{M}^T \boldsymbol{S} \otimes \boldsymbol{I}\boldsymbol{M}\, dV_0$$

$$\boldsymbol{M} = \int \rho_0 \boldsymbol{\Phi}^T \boldsymbol{\varphi}\boldsymbol{\varphi}^T \boldsymbol{\Phi} dV_0 \qquad \Delta_n \boldsymbol{f} = \int \rho_0 \boldsymbol{\Phi}^T \boldsymbol{\varphi}\Delta\boldsymbol{\tau}_0 dS_0$$

$\mathbf{K}_T$ is now called the tangent modulus matrix, $\mathbf{K}_G$ is the geometric stiffness matrix, $\mathbf{M}$ is the (incremental) mass matrix, and $\Delta_n\mathbf{f}$ is the incremental force vector.

17.6 INCREMENTAL CONTRIBUTIONS FROM NONLINEAR BOUNDARY CONDITIONS

Again, let I_i denote the principal invariants of $\mathbf{C}$, and let $\mathbf{i} = VEC(\mathbf{I})$, $c_2 = VEC(\mathbf{C}^2)$, $\mathbf{n}_i^{\mathbf{T}} = \partial I_i/\partial \mathbf{c}$, and $\mathbf{A}_i = \partial \mathbf{n}_i/\partial \mathbf{c}$. Recall from Chapter 2 that

$$\begin{aligned} &\boldsymbol{n}_1 = \boldsymbol{i} \qquad \boldsymbol{n}_2 = I_1\boldsymbol{i} - \boldsymbol{c} \qquad \mathbf{n}_3 = I_2\mathbf{i} - I_1\boldsymbol{c} + \boldsymbol{c}_2 \qquad \mathbf{I}_9 = \mathbf{I}\otimes\mathbf{I} \\ &\boldsymbol{A}_1 = \mathbf{0} \qquad \boldsymbol{A}_2 = \boldsymbol{i}\boldsymbol{i}^T - \boldsymbol{I}_9 \qquad \mathbf{A}_3 = \mathbf{I}\otimes\mathbf{C} + \mathbf{C}\otimes\mathbf{I} - (\mathbf{i}\mathbf{c}^T + \mathbf{c}\mathbf{i}^T) + I_1(\mathbf{i}\mathbf{i}^T - \mathbf{I}_9). \end{aligned} \tag{17.24}$$

Equation 17.23 is complete if increments of tractions are prescribed on the undeformed surface S_0. We now consider the more complex situation in which $\boldsymbol{\tau}$ is referred to the deformed surface S, on which they are prescribed functions of $\mathbf{u}$. From Chandrasekharaiah and Debnath (1994), conversion is obtained using

$$\begin{aligned} &\boldsymbol{\tau}\, dS = \boldsymbol{\tau}_0\, dS_0 \qquad \mathbf{n}^T\mathbf{q}\, dS = \mathbf{n}_0^T\mathbf{q}_0\, dS_0 \\ &dS = \mu dS_0 \qquad \mu = J\sqrt{\mathbf{n}_0^T\mathbf{C}^{-1}\mathbf{n}_0} = \sqrt{\mathbf{n}_0^T\otimes\mathbf{n}_0^T\mathbf{n}_3} \end{aligned} \tag{17.25}$$

and from Nicholson and Lin (1997b)

$$\Delta\mu \approx d\mu = \mathbf{m}^{\mathbf{T}} d\mathbf{c} \approx \mathbf{m}^{\mathbf{T}}\Delta\mathbf{c}, \qquad \mathbf{m}^{\mathbf{T}} = \mathbf{n}_0^{\mathbf{T}}\otimes\mathbf{n}_0^{\mathbf{T}}\mathbf{A}_3/2\mu. \tag{17.26}$$

Suppose that $\Delta\boldsymbol{\tau}$ is expressed on S as follows:

$$\Delta\boldsymbol{\tau} = \Delta\underline{\boldsymbol{\tau}} - \mathbf{A}_M^T\Delta\mathbf{u}. \tag{17.27}$$

Here, $d\underline{\boldsymbol{\tau}}$ is prescribed, while $\mathbf{A}_M$ is a known function of $\mathbf{u}$. Also, S_0 is the undeformed counterpart of S. These relations are capable of modeling boundary conditions, such as support by a nonlinear elastic foundation.

From the fact that $\boldsymbol{\tau}\, dS = \boldsymbol{\tau}_0\, dS_0 = \mu\boldsymbol{\tau}_0\, dS$, we conclude that $\boldsymbol{\tau} = \mu\boldsymbol{\tau}_0$. It follows that

$$\begin{aligned} \Delta\boldsymbol{\tau}_0 &= \frac{1}{\mu}\Delta\boldsymbol{\tau} - \frac{\boldsymbol{\tau}}{\mu^2}\Delta\mu \\ &= \frac{1}{\mu}(\Delta\underline{\boldsymbol{\tau}} - \mathbf{A}_M^T\Delta\boldsymbol{u}) - \frac{\boldsymbol{\tau}}{\mu^2}\mathbf{m}^T\Delta\boldsymbol{c} \end{aligned} \tag{17.28}$$

From the Incremental Principle of Virtual Work, the rhs term is written as

$$\int \delta\Delta\boldsymbol{u}^T \Delta\boldsymbol{\tau}_0 dS_0 = \int \delta\Delta\boldsymbol{u}^T \left[\frac{1}{\mu}(\Delta\underline{\boldsymbol{\tau}} - \boldsymbol{A}_M^T \Delta\boldsymbol{u}) - \frac{\boldsymbol{\tau}}{\mu^2}\mathbf{m}^T \Delta\boldsymbol{c} \right] dS_0. \tag{17.29}$$

Recalling the interpolation models for the increments, we obtain an incremental force vector plus two boundary contribution to the stiffness terms. In particular,

$$\int \delta\Delta\boldsymbol{u}^T \Delta\boldsymbol{\tau}_0 dS_0 = \delta\Delta\boldsymbol{\gamma}^T \Delta\boldsymbol{f} - \delta\Delta\boldsymbol{\gamma}^T [\boldsymbol{K}_{BF} + \boldsymbol{K}_{BN}]\Delta\boldsymbol{\gamma} \tag{17.30}$$

$$\Delta\mathbf{f} = \int \frac{1}{\mu}\Delta\underline{\boldsymbol{\tau}}\, dS_0, \quad \mathbf{K}_{BF} = \int \mathbf{N}\mathbf{A}_M^T \mathbf{N}^T dS_0, \quad \mathbf{K}_{BN} = \int \frac{\boldsymbol{\tau}}{\mu^2}\mathbf{m}^T \mathbf{G}\, dS_0$$

The first boundary contribution is from the nonlinear elastic foundation coupling the traction and displacement increments on the boundary. The second arises from geometric nonlinearity when the traction increment is prescribed on the current configuration.

17.7 EFFECT OF VARIABLE CONTACT

In many, if not most, "real-world" problems, loads are transmitted to the member of interest via contact with other members, for example, gear teeth. The extent of the contact zone is an unknown to be determined as part of the solution process. Solution of contact problems, introduced in Chapter 15, is a difficult problem that has absorbed the attention of many investigators. Some algorithms are suited primarily for linear kinematics. Here, a development is given for one particular formulation, which is mostly of interest for explicitly addressing the effect of large deformation.

Figure 17.1 shows a contactor moving into contact with a foundation that is assumed to be rigid. We seek to follow the development of the contact area and the tractions arising throughout it. From Chapter 15, we recall that corresponding to a point $\mathbf{x}$ on the contactor surface there is a target point $\mathbf{y}(\mathbf{x})$ on the foundation to which the normal $\mathbf{n}(\mathbf{x})$ at $\mathbf{x}$ points. As the contactor starts to deform, $\mathbf{n}(\mathbf{x})$ rotates and points toward a new value, $\mathbf{y}(\mathbf{x})$. As the point $\mathbf{x}$ approaches contact, the point $\mathbf{y}(\mathbf{x})$ approaches the foundation point, which comes into contact with the contactor point at $\mathbf{x}$.

We define a gap function, g, using $\mathbf{y}(\mathbf{x}) = \mathbf{x} + g\mathbf{n}$. Let $\mathbf{m}$ be the surface normal-vector to the target at $\mathbf{y}(\mathbf{x})$. Let S_c be the candidate contact surface on the contactor, whose undeformed counterpart is S_{0c}. There also is a candidate contact surface S_f on the foundation.

We limit our attention to bonded contact, in which particles coming into contact with each other remain in contact. Algorithms for sliding contact with and without friction are available. For simplicity's sake, we also assume that shear tractions, in

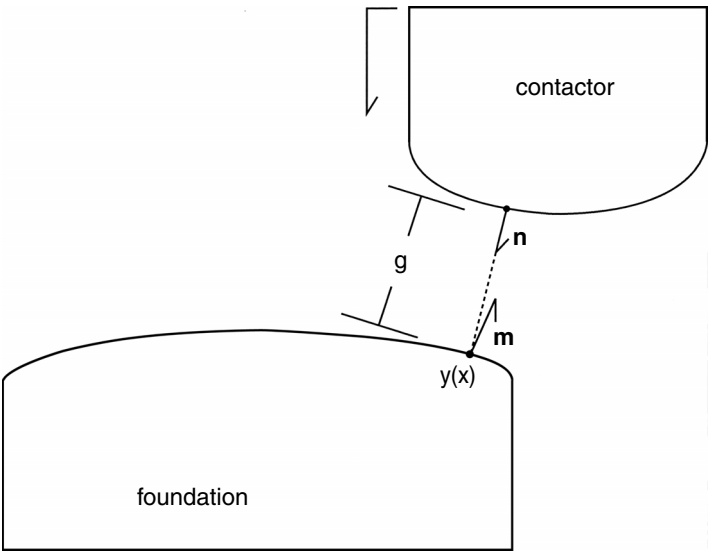

FIGURE 17.1 Contact.

the osculating plane of point of interest, are negligible. Suppose that the interface can be represented by an elastic foundation satisfying the incremental relation

$$\Delta\tau_n = -k(g)\Delta u_n. \tag{17.31}$$

Here, $\tau_n = \mathbf{n}^T\tau$ and $u_n = \mathbf{n}^T\mathbf{u}$ are the normal components of the traction and displacement vectors. Since the only traction to consider is the normal traction (to the contactor surface), the transverse components of $\Delta\mathbf{u}$ are not needed (do not result from work). Also, $k(g)$ is a nonlinear stiffness function given in terms of the gap by, for example,

$$k(g) = \frac{k_H}{\pi}\left[\frac{\pi}{2} - arctan(\alpha_k g - \varepsilon_r)\right] + k_L, \qquad k_H/k_L >> 1. \tag{17.32}$$

As in Chapter 15, when g is positive, the gap is open and k approaches k_L, which should be chosen as a small number, theoretically zero. When g becomes negative, the gap is closed and k approaches k_H, which should be chosen as a large number, theoretically infinity to prevent penetration of the rigid body).

Under the assumption that only the normal traction on the contactor surface is important, it follows that $\boldsymbol{\tau} = \tau_n\mathbf{n}$, from which

$$\Delta\boldsymbol{\tau} = \Delta\tau_n\boldsymbol{n} + \tau_n\Delta\boldsymbol{n}. \tag{17.33}$$

The contact model contributes the matrix $\mathbf{K}_c$ to the stiffness matrix as follows (see Nicholson and Lin, 1997b):

$$\int \delta\Delta\mathbf{u}^T \Delta\boldsymbol{\tau}\mu \, dS_0 = \int \delta\Delta u_n{}^T \Delta\tau_n \mu \, dS_0$$

$$= -\delta\Delta\boldsymbol{\gamma}^T \mathbf{K}_c \Delta\boldsymbol{\gamma} \tag{17.34}$$

$$\mathbf{K}_c = -2\int \mathbf{N}\mathbf{n}\tau_n \mathbf{m}^T \boldsymbol{\beta}^T dS_{c0} + \int k_c(g)\mathbf{N}\mathbf{n}\mathbf{n}^T\mathbf{N}^T \mu \, dS_{c0} + \int \mathbf{N}\tau_n \mu \mathbf{h}^T dS_{c0}.$$

To update the gap, use the following relations proved in Nicholson and Lin (1997-b). The differential vector, $d\mathbf{y}$, is tangent to the foundation surface, hence, $\mathbf{m}^\mathbf{T} d\mathbf{y} = 0$. It follows that

$$0 = \mathbf{m}^\mathbf{T} d\mathbf{u} + g\mathbf{m}^\mathbf{T} d\mathbf{n} + \mathbf{m}^\mathbf{T}\mathbf{n}\, dg$$

$$\Delta g = -\frac{\mathbf{m}^\mathbf{T}\Delta\mathbf{u} + g\mathbf{m}^\mathbf{T}\Delta\mathbf{n}}{\mathbf{m}^\mathbf{T}\mathbf{n}}. \tag{17.35}$$

Using Equation 17.5, we may derive, with some effort, that

$$\Delta g = \boldsymbol{\Gamma}^\mathbf{T}\Delta\boldsymbol{\gamma}, \quad \boldsymbol{\Gamma}^\mathbf{T} = -\frac{\mathbf{m}^\mathbf{T}\mathbf{N} + g\mathbf{h}^\mathbf{T}}{\mathbf{m}^\mathbf{T}\mathbf{n}}, \quad \mathbf{h}^\mathbf{T} = [\mathbf{n}[(\mathbf{n}^\mathbf{T}\mathbf{F}^{-\mathbf{T}}) \otimes \mathbf{n}^\mathbf{T}] - \mathbf{n}^\mathbf{T} \otimes \mathbf{F}^{-\mathbf{T}}]\mathbf{M}^\mathbf{T}. \tag{17.36}$$

17.8 INTERPRETATION AS NEWTON ITERATION

The (nonincremental) Principle of Virtual Work can be restated in the undeformed configuration as

$$\int tr(\delta\mathbf{E}\mathbf{S}) dV_o + \int \delta\mathbf{u}^T \rho\ddot{\mathbf{u}} \, dV_o = \int \delta\mathbf{u}^T \boldsymbol{\tau} \, dS_o. \tag{17.37}$$

We assume for convenience that $\boldsymbol{\tau}$ is prescribed on S_o. The interpolation model satisfies the form

$$\delta\mathbf{e} = \left[\mathbf{B}_L^T + \mathbf{B}_{NL}^T(\boldsymbol{\gamma})\right]\delta\boldsymbol{\gamma}$$

$$\mathbf{B}_L^T = \frac{1}{2}(\mathbf{I}\otimes\mathbf{I} + \mathbf{I}\otimes\mathbf{I}\mathbf{U})\mathbf{M}(\mathbf{X})$$

$$\mathbf{B}_{NL}^T = \frac{1}{2}\left(\mathbf{I}\otimes\mathbf{F}_u^T + \mathbf{F}_u\otimes\mathbf{I}\mathbf{U}\right)\mathbf{M}(\mathbf{X}) \tag{17.38}$$

$$\mathbf{F}_u = \frac{\partial\mathbf{u}}{\partial\mathbf{X}}.$$

Clearly, $\mathbf{F}_u$ and $\mathbf{B}_{NL}$ are linear in $\boldsymbol{\gamma}$.

Upon cancellation of the variation $\delta\boldsymbol{\gamma}^T$, an algebraic equation is obtained as

$$\boldsymbol{\Phi}(\boldsymbol{\gamma},\mathbf{f}) = \int [(\mathbf{B}_L + \mathbf{B}_{NL}(\boldsymbol{\gamma})]\mathbf{s}\, dV_o + \int \mathbf{N}^T \rho \ddot{\mathbf{u}}\, dV_o, \quad \mathbf{f} = \int \mathbf{N}^T \boldsymbol{\tau}_o dS_o. \tag{17.39}$$

At the load step, Newton iteration is expressed as

$$\boldsymbol{\gamma}_{n+1}^{(v+1)} = \boldsymbol{\gamma}_{n+1}^{(v)} - \mathbf{J}^{-1}\boldsymbol{\Phi}\left(\boldsymbol{\gamma}_{n+1}^{(v)}, \mathbf{f}_{n+1}\right), \qquad \mathbf{J} = \left[\frac{\partial \boldsymbol{\Phi}}{\partial \gamma}\left(\boldsymbol{\gamma}_{n+1}^{(v)}, \mathbf{f}_{n+1}\right)\right]^{-1} \tag{17.40}$$

or as a linear system

$$\begin{aligned} \mathbf{J}\left(\boldsymbol{\gamma}_{n+1}^{(v+1)} - \boldsymbol{\gamma}_{n+1}^{(v)}\right) &= \boldsymbol{\Phi}\left(\boldsymbol{\gamma}_{n+1}^{(v)}, \mathbf{f}_{n+1}\right), \\ \boldsymbol{\gamma}_{n+1}^{(v+1)} &= \boldsymbol{\gamma}_{n+1}^{(v)} + \left[\boldsymbol{\gamma}_{n+1}^{(v+1)} - \boldsymbol{\gamma}_{n+1}^{(v)}\right]. \end{aligned} \tag{17.41}$$

If the load increments are small enough, the starting iterate can be estimated as the solution from the n^{th} load step. Also, a stopping (convergence) criterion is needed to determine when the effort to generate additional iterates is not rewarded by increased accuracy.

Careful examination of the relations from this and the incremental formulations uncovers that

$$\mathbf{J} = \mathbf{K}_T + \mathbf{K}_G, \tag{17.42}$$

so that the incremental stiffness matrix is the same as the Jacobian matrix in Newton iteration. This, of course, is a satisfying result. The Jacobian matrix can be calculated by conventional finite-element procedures at the element level followed by conventional assembly procedures. If the incremental equation is only solved once at each load increment, the solution can be viewed as the first iterate in a Newton iteration scheme. The one-time incremental solution can potentially be improved by additional iterations, as shown in Equation 17.41, but at the cost of computing the "residual" Φ at each load step.

17.9 BUCKLING

Finite-element equations based on classical buckling equations for beams and plates were addressed in Chapter 14. In the classical equations, geometrically nonlinear terms appear through a linear correction term, thereby furnishing linear equations. Here, in the absence of inertia and nonlinearity in the boundary conditions, we briefly present a general viewpoint based on the incremental equilibrium equation

$$(\mathbf{K}_T + \mathbf{K}_G)\Delta\boldsymbol{\gamma}_{n+1} = \Delta\mathbf{f}_{n+1}. \tag{17.43}$$

This solution predicts a large incremental displacement if the stiffness matrix $\mathbf{K}_T + \mathbf{K}_G$ is ill-conditioned or outright singular. Of course, in elastic media, $\mathbf{K}_T$ is positive-definite. However, in the presence of in-plane compression, $\mathbf{K}_G$ may have a negative eigenvalue whose magnitude is comparable to the smallest positive eigenvalue of $\mathbf{K}_T$. To see this recall that

$$\mathbf{K}_T = \int \boldsymbol{M}^T \mathbf{G} \boldsymbol{\chi} \mathbf{G}^T \boldsymbol{M}\, dV_0 \qquad \mathbf{K}_G = \int \boldsymbol{M}^T \mathrm{S} \otimes \mathbf{I} \boldsymbol{M}\, dV_0. \tag{17.44}$$

We suppose that the element in question is thin in a local z (out-of-plane direction). This suggests the assumption of plane stress. Now, in plate-and-shell theory, it is necessary to add a transverse shear stress on the element boundaries to allow the element to support transverse loads. We assume that the transverse shear stresses only appear in the incremental force term and the tangent stiffness term, and that the geometric stiffness term strictly satisfies the plane-stress assumption. It follows that if the z-direction is out of the plane, in the geometric stiffness term,

$$\mathbf{S} \otimes \mathbf{I} \rightarrow \begin{bmatrix} S_{11}\mathbf{I} & S_{12}\mathbf{I} & 0\mathbf{I} \\ S_{12}\mathbf{I} & S_{22}\mathbf{I} & 0\mathbf{I} \\ 0\mathbf{I} & 0\mathbf{I} & 0\mathbf{I} \end{bmatrix}. \tag{17.45}$$

In classical buckling, it is assumed that loads applied proportionately induce proportionate in-plane stresses. Thus, for a given load path, only one parameter, the length of the straight line the stress point traverses in the space of in-plane stresses, arises in the eigenvalue problem for the critical buckling load. In nonlinear problems, there is no assurance that the stress point follows a straight line. Instead, if λ denotes the distance along the line followed by the load point in proportional loading, the stresses become numerical functions of λ.

As a simple alternative to the general case, we consider buckling of a single element and suppose that the stresses appearing in Equation 17.46 are applied in a compressive sense along the faces of the element in a proportional manner whereby

$$\boldsymbol{S} \otimes \boldsymbol{I} \rightarrow \lambda \begin{bmatrix} (-\hat{S}_{11})\mathbf{I} & (-\hat{S}_{12})\mathbf{I} & 0\mathbf{I} \\ (-\hat{S}_{12})\mathbf{I} & (-\hat{S}_{22})\mathbf{I} & 0\mathbf{I} \\ 0\mathbf{I} & 0\mathbf{I} & 0\mathbf{I} \end{bmatrix}, \tag{17.46}$$

in which the circumflex implies a reference value along the stress path at which $\lambda = 1$, and the negative signs on the stresses are present since buckling is associated with compressive stresses. At the element level, the equation now becomes

$$(\mathbf{K}_T - \lambda \hat{\mathbf{K}}_G) \Delta \boldsymbol{\gamma}_{n+1} = \Delta \mathbf{f}_{n+1}. \tag{17.47}$$

At a given load increment, the critical buckling load for the current path, as a function of two angles determining the path in the stress space illustrated in Chapter 14, is obtained by computing the λ value rendering $(\mathbf{K}_T - \lambda\hat{\mathbf{K}}_G)$ singular.

17.10 EXERCISES

1. Assuming linear interpolation models for u,v in a plane triangular membrane element with vertices (0,0),(1,0),(0,1), obtain the matrix M, G, $\mathbf{B}_{\mathrm{L}}$, and $\mathbf{B}_{\mathrm{NL.}}$
2. Repeat Exercise 1 with linear interpolation models for u, v, and w in a tetrahedral element with vertices (0,0,0),(1,0,0),(0,1,0),(0,0,1).

18 Tangent-Modulus Tensors for Thermomechanical Response of Elastomers

18.1 INTRODUCTION

Within an element, the finite-element method makes use of interpolation models for the displacement vector $\mathbf{u}(\mathbf{X}, t)$ and temperature $\mathrm{T}(\boldsymbol{X}, t)$ (and pressure $p = -\,trace(\boldsymbol{\tau})/3$ in incompressible or near-incompressible materials):

$$\mathbf{u}(\boldsymbol{X},t) = \mathbf{N}^{\boldsymbol{T}}(\boldsymbol{X})\gamma(t), \quad \mathrm{T}(\boldsymbol{X},t) - \mathrm{T}_0 = \nu^{\boldsymbol{T}}(\boldsymbol{X})\theta(t), \quad p = \xi^{\boldsymbol{T}}(\boldsymbol{X})\psi(t), \tag{18.1}$$

in which T_0 is the temperature in the reference configuration, assumed constant. Here, $\mathbf{N}$, ν, and $\boldsymbol{\xi}$ are shape functions and $\boldsymbol{\gamma}$, $\boldsymbol{\theta}$, and $\boldsymbol{\psi}$ are vectors of nodal values. Application of the strain-displacement relations and their thermal analogs furnishes

$$\begin{aligned} &\mathbf{f}_1 = VEC(\mathbf{F}-\mathbf{I}) = \boldsymbol{M}_1\boldsymbol{g} = \mathbf{U}^{\mathrm{T}}\boldsymbol{M}_2\boldsymbol{g}, \quad \mathbf{f}_2 = VEC(\mathbf{F}^{\mathrm{T}}-\mathbf{I}) = \boldsymbol{M}_2\boldsymbol{g}, \quad \delta\mathbf{e} = \boldsymbol{b}^{\mathrm{T}}\delta\boldsymbol{g}, \\ &\boldsymbol{b} = \boldsymbol{M}_2\mathbf{G}, \quad \mathbf{G}^{\mathrm{T}} = \frac{1}{2}(\mathbf{F}^{\mathrm{T}}\otimes\mathbf{I} + \mathbf{I}\otimes\mathbf{F}^{\mathrm{T}}\mathbf{U}), \quad \nabla\mathrm{T} = \boldsymbol{b}_T^{\mathrm{T}}\boldsymbol{q} \end{aligned} \tag{18.2}$$

in which $\mathbf{U}$ is a 9×9 universal permutation tensor such that $VEC(\boldsymbol{A}^T) = \mathbf{U}VEC(\boldsymbol{A})$, and $\mathbf{e} = VEC(\boldsymbol{E})$ is the Lagrangian strain vector. Also, ∇ is the gradient operator referred to the deformed configuration. The matrix $\boldsymbol{\beta}$ and the vector $\boldsymbol{\beta}_T$ are typically expressed in terms of isoparametric coordinates.

18.2 COMPRESSIBLE ELASTOMERS

The Helmholtz potential was introduced in Chapter 7 and shown to underlie the relations of classical coupled thermoelasticity. The thermohyperelastic properties of compressible elastomers are also derived from the Helmholtz free-energy density ϕ (per unit mass), which is a function of T and $\boldsymbol{E}$. Under isothermal conditions it is conventional to introduce the strain energy density $w(\boldsymbol{E}) = \rho_0\phi(\mathrm{T}, \boldsymbol{E})$ (T constant), in which ρ_0 is the density in the undeformed configuration. Typically, the elastomer is assumed to be isotropic, in which case ϕ can be expressed as a function of T, I_1, I_2, and I_3. Alternatively, it may be expressed as a function of T and the stretch ratios λ_1, λ_2, and λ_3.

With ϕ known as a function of T, I_1, I_2, and I_3, the entropy density η per unit mass and the specific heat c_e at constant strain are obtained as

$$c_e = \mathrm{T}\frac{\partial \eta}{\partial \mathrm{T}}\bigg|_E \qquad \eta = -\frac{\partial \phi}{\partial \mathrm{T}}. \tag{18.3}$$

The 2nd Piola-Kirchhoff stress, $\boldsymbol{s} = VEC(\boldsymbol{S})$, is obtained from

$$\mathbf{s}^T = \rho_0 \frac{\partial \phi}{\partial \boldsymbol{e}}\bigg|_T = 2\sum_i \rho_0 \phi_i \mathbf{n}_i, \qquad \phi_i = \frac{\partial \phi}{\partial I_i}. \tag{18.4}$$

Also of importance is the (isothermal) tangent-modulus matrix

$$\boldsymbol{D}_T = \frac{\partial \boldsymbol{s}}{\partial \boldsymbol{e}}\bigg|_{\mathrm{T}} = 4\sum_i \sum_j \rho_0 \phi_{ij} \mathbf{n}_i \mathbf{n}_j^T + 4\sum_i \rho_0 \phi_i \boldsymbol{A}_i, \qquad \phi_{ij} = \frac{\partial^2 \phi}{\partial I_i \partial I_j}. \tag{18.5}$$

An expression for $\boldsymbol{D}_T$ has been derived by Nicholson and Lin (1997c) for compressible, incompressible, and near-incompressible elastomers described by strain-energy functions (Helmholtz free-energy functions) and based on the use of stretch ratios (singular values of **F**) rather than invariants.

18.3 INCOMPRESSIBLE AND NEAR-INCOMPRESSIBLE ELASTOMERS

When the temperature T is held constant, elastomers often satisfy the constraint of incompressibility or near-incompressibility. The constraint is accommodated by augmenting ϕ with terms involving a new parameter similar to a Lagrange multiplier. Typically, this new parameter is related to the pressure p. The thermohyperelastic properties of incompressible and near-incompressible elastomers can be derived from the augmented Helmholtz free energy, which is a function of $\boldsymbol{E}$, **T**, and p. The constraint introduces additional terms into the governing finite-element equations and requires an interpolation model for p.

If the elastomer is incompressible at a constant temperature, the augmented Helmholtz function, ϕ, can be written as

$$\phi = \phi_d(J_1, J_2, \mathrm{T}) - \lambda \xi(J, \mathrm{T})/\rho_0, \qquad J_1 = I_1/I_3^{1/3}, \qquad J_2 = I_2/I_3^{2/3}, \tag{18.6}$$

where ξ is a material function satisfying the constraint $\xi(J, T) = 0$ and $J = I_3^{1/2} = \det(\mathbf{F})$. It is easily shown that ϕ_d depends on the deviatoric Lagrangian strain $\boldsymbol{E}_d$, due to the introduction of the deviatoric invariants J_2 and J_3. The Lagrange multiplier λ is, in fact, the (true) pressure p:

$$p = -trace(\boldsymbol{T})/3 = \frac{\partial \xi}{\partial J}\bigg|_{\mathrm{T}}. \tag{18.7}$$

For an elastomer that is near-incompressible at a constant temperature, ϕ can be written as

$$\rho_0\phi = \rho_0\phi_d(J_1, J_2, \mathrm{T}) - p\xi(J, \mathrm{T}) - p^2/2\kappa, \tag{18.8}$$

in which κ_0 is a constant. The near-incompressibility constraint is expressed by $\partial\phi/\partial p = 0$, which implies

$$p = -\kappa\xi(J, \mathrm{T}). \tag{18.9}$$

The bulk modulus κ is given by

$$\kappa = -\left.\frac{\partial p}{\partial J}\right|_{\mathrm{T}} = \kappa_0 \left.\frac{\partial \xi}{\partial J}\right|_{\mathrm{T}}. \tag{18.10}$$

Chen et al. (1997) presented sufficient conditions under which near-incompressible models reduce to the incompressible case as $\kappa \to \infty$. Nicholson and Lin (1996) formulated the relations

$$\xi(J, \mathrm{T}) = f^3(\mathrm{T})J - 1, \quad \phi_d = \phi_1(J_1, J_2) + \phi_2(\mathrm{T}), \quad \phi_2(\mathrm{T}) = c_e\mathrm{T}(1 - ln(\mathrm{T}/\mathrm{T}_0)), \tag{18.11}$$

with the consequence that

$$p = -\kappa_0(f^3(\mathrm{T})J - 1), \qquad \kappa = f^3(\mathrm{T})\kappa_0. \tag{18.12}$$

Equation 18.12 provides a linear pressure-volume relation in which thermomechanical effects are confined to thermal expansion expressed using a constant-volume coefficient α. If the constraint is assumed to be satisfied *a priori*, the Helmholtz free energy is recovered as

$$\phi(I_1, I_2, I_3) = \phi_d(J_1, J_2, \mathrm{T}) + \kappa_0(f^3(\mathrm{T}) - 1)^2/2\rho_0. \tag{18.13}$$

Alternatively, the latter term results from retaining the lowest nonvanishing term in a Taylor-series representation of ϕ about $f^3(\mathrm{T})J - 1$.

Given Equation 18.13, the entropy now includes a term involving p:

$$\eta = -\frac{\partial \phi_d}{\partial \mathrm{T}} + \pi\alpha f^4(\mathrm{T})/\rho_0, \qquad \pi = p/f^3(\mathrm{T}). \tag{18.14}$$

The stress and the tangent-modulus matrices are correspondingly modified:

$$\begin{aligned} \mathbf{s}^T &= \rho_0 \left.\frac{\partial \phi_d}{\partial \mathbf{e}}\right|_{\mathrm{T},\pi} - \pi f^3(\mathrm{T})\mathbf{n}_3^T/J \\ \boldsymbol{D}_{\mathrm{TP}} &= \left.\frac{\partial \mathbf{s}}{\partial \mathbf{e}}\right|_{\mathrm{T},\pi} = \rho_0\left(\frac{\partial}{\partial \mathbf{e}}\right)^{\mathrm{T}} \frac{\partial \phi_{\mathrm{d}}}{\partial \mathbf{e}} - \pi f^3(\mathrm{T})\left[2\mathbf{A}_3/J - \mathbf{n}_3\mathbf{n}_3^{\mathrm{T}}/J^3\right] \end{aligned} \tag{18.15}$$

18.3.1 Specific Expressions for the Helmholtz Potential

There are two broad approaches to the formulation of Helmholtz potential:

To express ϕ as a function of I_1, I_2, and I_3, and T (and p)
To express ϕ as a function of the principal stretches λ_1, λ_2, and λ_3, and T (and p).

The latter approach is thought to possess the convenient feature of allowing direct use of test data, for example, from uniaxial tension. We will now examine several cases.

18.3.1.1 Invariant-Based Incompressible Models: Isothermal Problems

The strain-energy function depends only on I_1, I_2, and incompressibility is expressed by the constraint $I_3 = 1$, assumed to be satisfied *a priori*. In this category, the most widely used models include the Neo-Hookean material:

$$\phi = C_1(I_1 - 3), \quad I_3 = 1 \tag{18.16}$$

and the (two-term) Mooney-Rivlin material:

$$\phi = C_1(I_1 - 3) + C_2(I_2 - 3), \quad I_3 = 1, \tag{18.17}$$

in which C_1 and C_2 are material constants. Most finite-element codes with hyperelastic elements support the Mooney-Rivlin model. In principle, Mooney-Rivlin coefficients C_1 and C_2 can be determined independently by "fitting" suitable load-deflection curves, for example, uniaxial tension. Values for several different rubber compounds are listed in Nicholson and Nelson (1990).

18.3.1.2 Invariant-Based Models for Compressible Elastomers under Isothermal Conditions

Two widely studied strain-energy functions are due to Blatz and Ko (1962). Let G_0 be the shear modulus and v_0 the Poisson's ratio, referred to the undeformed configuration. The two models are:

$$\begin{aligned}
\rho_0\phi_1 &= \frac{1}{2}G_0\left(I_1 + \frac{1-2v_0}{v_0}I_3 - I_3^{\frac{v_0}{1-2v_0}} - \frac{1+v_0}{v_0}\right) \\
\rho_0\phi_2 &= \frac{1}{2}G_0\left(\frac{I_2}{I_3} + 2I_3 - 5\right)
\end{aligned} \tag{18.18}$$

Let w denote the Helmholtz free energy evaluated at a constant temperature, in which case it is the strain energy. We note a general expression for w which is implemented

in several commercial finite-element codes (e.g., ANSYS, 2000):

$$w(J_1, J_2, J) = \sum_i \sum_j C_{ij}(J_1 - 3)^i (J_2 - 3)^j + \sum_k (J_r - 1)^k / D_k, \quad J_r = J/(1 + E_{th}), \tag{18.19}$$

in which E_{th} is called the thermal expansion strain, while C_{ij} and D_k are material constants. Several codes also provide software for estimating the model coefficients from user-supplied data.

Several authors have attempted to uncouple the response into isochoric (incompressible) and volumetric parts even in the compressible range, giving rise to functions of the form $\phi = \phi_1(J_1, J_2) + \phi_2(J)$. A number of proposed forms for ϕ_2 are discussed in Holzappel (1996).

18.3.1.3 Thermomechanical Behavior under Nonisothermal Conditions

Now we come to the accommodation of coupled thermomechanical effects. Simple extensions of, for example, the Mooney-Rivlin material have been proposed by Dillon (1962), Nicholson and Nelson (1990), and Nicholson (1995) for compressible elastomers, and in Nicholson and Lin (1996) for incompressible and near-incompressible elastomers. From the latter,

$$\rho_0 \phi = C_1(J_1 - 2) + C_2(J_2 - 3) + \rho_0 c_e \mathrm{T}(1 - ln(\mathrm{T}/\mathrm{T}_o) - \kappa(f^3(\mathrm{T})J - 1)\pi - \pi^2/2\kappa, \tag{18.20}$$

in which $\pi = p/f^3(\mathrm{T})$. As previously mentioned, a model similar to Nicholson and Lin (1996) has been proposed by Holzappel and Simo (1996) for compressible elastomers described using stretch ratios.

18.4 STRETCH RATIO-BASED MODELS: ISOTHERMAL CONDITIONS

For compressible elastomers, Valanis and Landel (1967) proposed a strain-energy function based on the decomposition

$$\phi(\lambda_1, \lambda_2, \lambda_3, \mathrm{T}) = \phi(\lambda_1, \mathrm{T}) + \phi(\lambda_2, \mathrm{T}) + \phi(\lambda_3, \mathrm{T}), \quad \mathrm{T}\ \textit{fixed}. \tag{18.21}$$

Ogden (1986) has proposed the form

$$\rho_0 \phi(\lambda, \mathrm{T}) = \sum_1^N \mu_p(\lambda^{\alpha p} - 1), \quad \mathrm{T}\ \textit{fixed}. \tag{18.22}$$

In principle, in incompressible isotropic elastomers, stretch ratio-based models have the advantage of permitting direct use of "archival" data from single-stress tests, for example, uniaxial tension.

We now illustrate the application of Kronecker Product algebra to thermohyperelastic materials under isothermal conditions and accommodate thermal effects. From Nicholson and Lin (1997c), we invoke the expression for the differential of a tensor-valued isotropic function of a tensor. Namely, let **A** denote a nonsingular n × n tensor with distinct eigenvalues, and let **F(A)** be a tensor-valued isotropic function of **A**, admitting representation as a convergent polynomial:

$$\mathbf{F}(\mathbf{A}) = \sum_{0}^{\infty} \phi_j \mathbf{A}^j. \tag{18.23}$$

Here, ϕ_j are constants. A compact expression for the differential $d\mathbf{F}(\mathbf{A})$ is presented using Kronecker Product notation.

The reader is referred to Nicholson and Lin (1997c) for the derivation of the following expression. With $\mathbf{f} = VEC(\mathbf{F})$ and $\mathbf{a} = VEC(\mathbf{A})$,

$$\begin{aligned} d\boldsymbol{f}(\boldsymbol{a}) &= \frac{1}{2}\boldsymbol{F'^T} \oplus \boldsymbol{F'} d\boldsymbol{a} + \mathrm{W} d\boldsymbol{\omega} \\ \mathbf{F}'(\mathbf{A}) &= \sum_{0}^{\infty} j\phi_j \mathbf{A}^{j-1} \qquad \frac{d\mathbf{F}}{d\mathbf{A}} = ITEN22\left(\frac{d\mathbf{f}}{d\mathbf{a}}\right) \\ \mathbf{W} &= -(\boldsymbol{F} - \boldsymbol{AF'}/2)^T \ominus (\boldsymbol{F} - \boldsymbol{AF'}/2) + \frac{1}{2}(\boldsymbol{A}^T \otimes \boldsymbol{F'} - \boldsymbol{F'^T} \otimes \boldsymbol{A}) \end{aligned} \tag{18.24}$$

Also, $d\boldsymbol{\omega} = VEC(d\boldsymbol{\Omega})$, in which $d\boldsymbol{\Omega}$ is an antisymmetric tensor representing the rate of rotation of the principal directions. The critical step is to determine a matrix **J** such that $\mathbf{W}d\boldsymbol{\omega} = -\mathbf{J}d\mathbf{a}$. It is shown in Dahlquist and Bjork that $\mathbf{J} = -[\mathbf{A}^T \ominus \mathbf{A}]^{-1}\mathbf{W}$, in which $[\mathbf{A}^T \ominus \mathbf{A}]^I$ is the Morse-Penrose inverse [(Dahlquist and Bjork(1974)]. Thus,

$$\mathrm{d}\mathbf{f}/\mathrm{d}\mathbf{a} = \mathbf{F'}^T \oplus \mathbf{F'}/2 - [\mathbf{A}^T \ominus \mathbf{A}]'\mathbf{W}. \tag{18.25}$$

We now apply the tensor derivative to elastomers modeled using stretch ratios, especially in the model presented by Ogden (1986). In particular, a strain-energy function, *w*, was proposed, which, for compressible elastomers and isothermal response, is equivalent to the form

$$w = tr\left(\sum_i \xi_i [\mathbf{C}^{\zeta_i} - \boldsymbol{I}]\right), \tag{18.26}$$

in which c_i are the eigenvalues of **C**, and ξ_i, ζ_i are material properties. The tangent-modulus tensor $\boldsymbol{\chi}$ appearing in Chapter 17 for the incremental form of the Principle

of Virtual Work is obtained as

$$\boldsymbol{\chi} = 4\sum_i \zeta_i \xi_i (\zeta_i - 1)\mathbf{C}^{\zeta_{i-2}} \oplus \mathbf{C}^{\zeta_{i-2}}/2 + 4\sum_i \zeta_i \xi_i [\mathbf{A}^T \ominus \mathbf{A}]' \mathbf{W}_i \tag{18.27}$$

$$\mathbf{W}_i = -\frac{3-\zeta_i}{2}\mathbf{C}^{\zeta_i} \otimes \mathbf{C}^{\zeta_i} + \frac{\zeta_i - 1}{2}[\mathbf{C}^{\zeta_i - 2} \otimes \mathbf{C} - \mathbf{C} \otimes \mathbf{C}^{\zeta_i - 2}]. \tag{18.28}$$

18.5 EXTENSION TO THERMOHYPERELASTIC MATERIALS

Equations 18.27 and 18.28 can be extended to thermohyperelastic behavior as follows, based on Nicholson and Lin (1996). The body initially experiences temperature T_0 uniformly. It is assumed that temperature effects occur primarily as thermal expansion, that volume changes are small, and that volume changes depend linearly on temperature. Thus, materials of present interest can be described as mechanically nonlinear but thermally linear.

Due to the role of thermal expansion, it is desirable to uncouple dilatational and deviatoric effects as much as possible. To this end, we introduce the deviatoric Cauchy-Green strain $\hat{\mathbf{C}} = \mathbf{C}/I_3^{1/3}$ in which I_3 is the third principal invariant of $\mathbf{C}$. Now, modifying w and expanding it in $J - 1$, $(J = I_3^{1/2})$ and retaining lowest-order terms gives

$$w = tr\left(\sum_i \xi_i [\hat{\mathbf{C}}^{\zeta_i} - \mathbf{I}]\right) + \frac{1}{2}\kappa (J-1)^2, \tag{18.29}$$

in which κ is the bulk modulus. The expression for $\boldsymbol{\chi}$ in Equation 18.27 is affected by these modifications.

To accommodate thermal effects, it is necessary to recognize that w is simply the Helmholtz free-energy density $\rho_o \phi$ under isothermal conditions, in which ρ_o is the mass density in the undeformed configuration. It is assumed that $\phi = 0$ in the undeformed configuration. As for invariant-based models, we can obtain a function ϕ with three terms: a purely mechanical term ϕ_M, a purely thermal term ϕ_T, and a mixed term ϕ_{TM}. Now, with entropy, η, ϕ satisfies the relations

$$\boldsymbol{s}^T = \rho_o \frac{\partial \varphi}{\partial \mathbf{e}|_{\mathrm{T}}} \qquad \eta = -\frac{\partial \varphi}{\partial \mathrm{T}|_{\mathrm{e}}}. \tag{18.30}$$

Following conventional practice, the specific heat at constant strain, $c_e = \mathrm{T}\partial\eta/\partial \mathrm{T}\,|_{\mathrm{e}}$, is assumed to be constant, from which we obtain

$$\phi_T = c_e \mathrm{T}[ln(\mathrm{T}/\mathrm{T}_0) + 1]. \tag{18.31}$$

On the assumption that thermal effects in shear (i.e., deviatoric effects) can be

neglected relative to thermal effects in dilatation, the purely mechanical effect is equated with the deviatoric term in Equation 18.29:

$$\phi_M = tr\left(\sum_i \xi_i[\hat{\mathbf{C}}^{\zeta_i} - I]\right). \tag{18.32}$$

Of greatest interest is ϕ_{TM}. The development of Nicholson and Lin (1996) furnishes

$$\phi_{TM} = \frac{\kappa[\beta^3(\mathrm{T})J - 1]^2}{2\rho} \qquad \beta(\mathrm{T}) = (1 + \alpha(\mathrm{T}/\mathrm{T}_0)/3)^{-1}. \tag{18.33}$$

The tangent-modulus tensor $\boldsymbol{\chi}' = \partial \boldsymbol{s}/\partial \boldsymbol{e}$ now has two parts: $\mathbf{X}_M + \mathbf{X}_{TM}$, in which $\mathbf{X}_M$ is recognized as $\boldsymbol{\chi}$, derived in Equation 18.29. Without providing the details, Kronecker Product algebra furnishes the following:

$$\boldsymbol{\chi}_{TM} = \frac{\kappa}{J\rho}\beta^3\left[\frac{\beta^3}{J^2}\mathbf{n}_3\mathbf{n}_3^{\mathrm{T}} + (\beta^3 J - 1)\left[\mathbf{A}_3 - \frac{\mathbf{n}_3\mathbf{n}_3^{\mathrm{T}}}{J^2}\right]\right]. \tag{18.34}$$

The foregoing discussion of stretch-based thermohyperelastic models has been limited to compressible elastomers. However, many elastomers used in applications, such as seals, are incompressible or near-incompressible. For such applications, as we have seen, an additional field variable is introduced, namely, the hydrostatic pressure (referred to deformed coordinates). It serves as a Lagrange multiplier enforcing the incompressibility and near-incompressibility constraints. Following the approach for invariant-based models, Equations 18.33 and 18.34 can be extended to incorporate the constraints of incompressibility and near-incompressibility.

The tangent-modulus tensor presented here only addresses the differential of stress with respect to strain. However, if coupled heat transfer (conduction and radiation) is considered, a general expression for the tangent-modulus tensor is required, expressing increments of stress and entropy in terms of increments of strain and temperature. A development accommodating heat transfer for invariant-based elastomers is given in Nicholson and Lin (1997a).

18.6 THERMOMECHANICS OF DAMPED ELASTOMERS

Thermoviscohyperelasticity is a topic central to important applications, such as rubber mounts in hot engines. The current section introduces a thermoviscohyperelastic constitutive model thought to be suitable for near-incompressible elastomers exhibiting modest levels of viscous damping following a Voigt model. Two potential functions are used to provide a systematic treatment of reversible and irreversible effects. One is the familiar Helmholtz free energy in terms of the strain and the temperature; it describes reversible, thermohyperelastic effects. The second potential function, based on the model of Ziegler and Wehrli (1987), models viscous

dissipation and arises directly from the entropy-production inequality. It provides a consistent thermodynamic framework for describing damping in terms of a *viscosity tensor* that depends on strain and temperature.

The formulation leads to a simple energy-balance equation, which is used to derive a rate-variational principle. Together with the Principle of Virtual Work, variational equations governing coupled thermal and mechanical effects are presented. Finite-element equations are derived from the thermal-equilibrium equation and from the Principle of Virtual Work. Several quantities, such as internal energy density, χ, have reversible and irreversible portions, indicated by the subscripts r and i: $\chi = \chi_{\mathrm{r}} + \chi_{\mathrm{i}}$. The thermodynamic formulation in the succeeding paragraphs is referred to undeformed coordinates.

There are several types of viscoelastic behaviors in elastomers, especially if they contain fillers such as carbon black. For example, under load, elastomers experience stress softening and compression set, which are long-term viscoelastic phenomena. Of interest here is the type of damping that is usually assumed in vibration isolation in which the stresses have an elastic and a viscous portion reminiscent of the classical Voigt model, and the viscous portion is proportional to strain rates. The time constants are small. This type of damping is viewed as arising in small motions superimposed on the large strains, which already reflect long-term viscoelastic effects.

18.6.1 Balance of Energy

The conventional equation for the balance of energy is expressed as

$$\begin{aligned}\rho_0\dot{\chi} &= \mathbf{s}^{\mathrm{T}}\dot{\mathbf{e}} - \nabla_0^{\mathrm{T}}\mathbf{q}_0 + \rho_0 h \\ &= \mathbf{s}_r^{\mathrm{T}}\dot{\mathbf{e}} + \mathbf{s}_i^{\mathrm{T}}\dot{\mathbf{e}} - \nabla_0^{\mathrm{T}}\mathbf{q}_0 + \rho_0 h\end{aligned} \tag{18.35}$$

where $\boldsymbol{s} = VEC(\boldsymbol{S})$ and $\boldsymbol{e} = VEC(\boldsymbol{E})$. Here, χ is the internal energy per unit mass, $\mathbf{q}_0$ is the heat-flux vector, ∇_0 is the divergence operator referred to undeformed coordinates, and h is the heat input per unit mass, for simplicity's sake, assumed independent of temperature. The state variables are thus **e** and T. The Helmholtz free energy, ϕ_r per unit mass, and the entropy, η per unit mass, are introduced using

$$\phi_r = \chi - \mathrm{T}\eta. \tag{18.36}$$

Now,

$$\nabla_0^T\mathbf{q}_0 - \rho_0 h = \mathbf{s}_{\mathrm{r}}^{\mathrm{T}}\dot{\mathbf{e}} + \mathbf{s}_{\mathrm{i}}^{\mathrm{T}}\dot{\mathbf{e}} - \rho_0\mathrm{T}\dot{\eta} - \rho_0\eta\dot{\mathrm{T}} - \rho_0\dot{\boldsymbol{\phi}}_r. \tag{18.37}$$

18.6.2 Entropy Production Inequality

The entropy-production inequality is stated as

$$\begin{aligned}\rho_0\mathrm{T}\dot{\eta} &\geq -\nabla_0^T\mathbf{q}_0 + \rho_0 h + \boldsymbol{q}_0^T\nabla\mathrm{T}/\mathrm{T} \\ &\geq \rho_0\dot{\phi}_r - \mathbf{s}_r^T\dot{\mathbf{e}} - \mathbf{s}_i^T\dot{\mathbf{e}} + \rho_0\mathrm{T}\dot{\eta} + \rho_0\eta\dot{\mathrm{T}} + \mathbf{q}_0^T\nabla\mathrm{T}/\mathrm{T}\end{aligned} \tag{18.38}$$

The Helmholtz potential is assumed to represent *reversible* thermohyperelastic effects. We decompose η into reversible and irreversible portions: $\eta = \eta_r + \eta_i$. Now, ϕ_r, η_r, and η_i are assumed to be differentiable functions of $\boldsymbol{E}$ and T. Furthermore, we suppose that $\eta_i = \eta_{i1} + \eta_{i2}$ and

$$\rho_0 \mathrm{T}\dot{\eta}_{i2} = \left[-\nabla_0^T \boldsymbol{q}_0 + \rho_0 h\right]_i. \tag{18.39}$$

This allows us to say that the viscous dissipation is "absorbed" as heat. We also suppose that reversible effects are "absorbed" as a portion of the heat input as follows:

$$\rho_0 \mathrm{T}\dot{\eta}_r = \left[-\nabla_0^T \boldsymbol{q}_0 + \rho_0 h\right]_r. \tag{18.40}$$

In addition, from conventional arguments,

$$\rho \partial \phi_r / \partial \mathbf{e} = \mathbf{s}_r^T \qquad \partial \phi_r / \partial \mathrm{T} = -\eta_r, \tag{18.41}$$

it follows that

$$\mathbf{s}_\mathrm{i}^\mathbf{T}\dot{\mathbf{e}} - \mathbf{q}_0^\mathbf{T}\nabla_0 \mathrm{T}/\mathrm{T} \geq -\rho_0 \eta_{i1}\dot{T}. \tag{18.42}$$

Inequality as shown in Equation 18.42 can be satisfied if $\rho_0 \eta_i \dot{\mathrm{T}} \geq 0$ and

$$\mathbf{s}_\mathrm{i}^\mathbf{T}\dot{\mathbf{e}} \geq 0 \quad \text{(a)} \qquad -\mathbf{q}_0^T \nabla \mathrm{T}/\mathrm{T} \geq 0 \quad \text{(b)}. \tag{18.43}$$

Inequality as shown in Equation 18.43b is conventionally assumed to express the fact that heat flows *irreversibly* from cold to hot zones. Inequality as shown in Equation 18.43a requires that viscous effects be dissipative.

18.6.3 Dissipation Potential

Following Ziegler and Wehrli (1987), the specific dissipation potential $\Psi(\boldsymbol{q}_0, \dot{\mathbf{e}}, \mathbf{e}, \mathrm{T}) = -\rho_0 \eta_i \dot{\mathrm{T}}$ is introduced, for which

$$\mathbf{s}_i^T = \rho_0 \Lambda_i \partial \Psi / \partial \dot{\mathbf{e}} \quad \text{(a)}. \qquad -\nabla_0^T \mathrm{T}/\mathrm{T} = \Lambda_t \rho_0 \partial \Psi / \partial \mathbf{q}_0. \quad \text{(b)}. \tag{18.44}$$

The function Ψ is selected such that Λ_i and Λ_t are positive scalars, in which case the inequalities in Equations 18.44a and 18.44b require that

$$(\partial \Psi / \partial \dot{\mathbf{e}})\,\dot{\mathbf{e}} \geq 0 \qquad (\partial \Psi / \partial \mathbf{q}_0)\mathbf{q}_0 \geq 0. \tag{18.45}$$

This can be interpreted as indicating the convexity of a dissipation surface in $(\dot{\mathbf{e}}, \boldsymbol{q}_0)$ space. Clearly, to state the constitutive relations, it is sufficient to specify ϕ_r and Ψ.

A simple illustration is now provided showing how the dissipation potential in Equation 18.45 provides a "framework" for describing dissipative effects. On the expectation that properties governing heat transfer are not affected by strain, we introduce the decomposition

$$\Psi = \Psi_i + \Psi_t \qquad \rho_0 \Psi_t = [\boldsymbol{q}_0^T \boldsymbol{q}_0]^{\frac{1}{2}} [\Lambda_t/2]. \tag{18.46}$$

Now, Ψ_t represents thermal effects, and we assume for simplicity's sake that Λ_t is a material constant. Inequality in Equation 18.46 implies that

$$-\nabla_0 \mathrm{T}/\mathrm{T} = \mathbf{q}_0/\Lambda_t. \tag{18.47}$$

This is essentially the conventional Fourier law of heat conduction, with Λ_t recognized as the thermal conductivity. As an elementary example of viscous dissipation, suppose that

$$\Psi_i = \mu(\mathrm{T}, J_1, J_2)\dot{\mathbf{e}}^{\mathbf{T}}\dot{\mathbf{e}}/2 \qquad \Delta_i = 1, \tag{18.48}$$

in which $\mu(\mathrm{T}, J_1, J_2)$ is the viscosity. Hence,

$$\mathbf{s}_i = \mu(\mathrm{T}, J_1, J_2)\dot{\mathbf{e}}, \tag{18.49}$$

and Equation 18.44a requires that μ be positive.

18.6.4 Thermal-Field Equation for Damped Elastomers

The energy-balance equations of thermohyperelasticity (i.e., the reversible response) are now reappearing in terms of a balance law among reversible portions of the stress, entropy, and internal energy. Equation 18.40 is repeated as

$$\rho_0 \dot{\phi}_r = \mathbf{s}_{\mathrm{r}}^{\mathbf{T}}\dot{\mathbf{e}} - \rho_0 \eta_r \dot{\mathrm{T}}. \tag{18.50}$$

The ensuing Maxwell relation is

$$\partial \boldsymbol{s}_r^T/\partial \mathrm{T} = -\rho_0 \partial \eta_r/\partial \mathbf{e}. \tag{18.51}$$

Conventional operations furnish the reversible part of the equation of thermal equilibrium (balance of energy):

$$[-\nabla_0^T \boldsymbol{q}_0 + \rho_0 h]_r = -\mathrm{T}(\partial \mathbf{s}_r^T/\partial \mathrm{T})\dot{\mathbf{e}} + \rho_0 c_e \dot{\mathrm{T}}, \qquad c_e = \mathrm{T}\partial \eta_r/\partial \mathrm{T}. \tag{18.52}$$

For the irreversible part, we recall the relations

$$-\left(\nabla_0^T \mathbf{q}_0 - \rho_0 h\right)_i = -\mathbf{s}_{\mathrm{i}}^{\mathbf{T}}\dot{\mathbf{e}} + \rho_0 c_i \dot{\mathrm{T}} \tag{18.53}$$

and

$$\rho_0 \mathrm{T}\dot{\eta}_{i2} = \rho_0 \mathrm{T}\frac{\partial \eta_{i2}}{\partial \mathbf{e}}\dot{\mathbf{e}} + \rho_0 \mathrm{T}\frac{\partial \eta_{i2}}{\partial \mathrm{T}}\dot{\mathrm{T}} \tag{18.54}$$

and

$$-\mathbf{s}_i^{\mathbf{T}} = \rho_0 \mathrm{T}\frac{\partial \eta_{i2}}{\partial \mathbf{e}}, \qquad c_i = \mathrm{T}\frac{\partial \eta_{i2}}{\partial \mathrm{T}}. \tag{18.55}$$

Upon adding the relations, we obtain the thermal-field equation

$$-\nabla_0^{\mathbf{T}}\mathbf{q}_0 + \rho_0 h = -\mathrm{T}\partial \mathbf{s}_r^{\mathbf{T}}/\partial \mathrm{T}\dot{\mathbf{e}} - \mathbf{s}_i^{\mathbf{T}}\dot{\mathbf{e}} + \rho_0(c_e + c_i)\dot{\mathrm{T}}. \tag{18.56}$$

It is easily seen that Equation 18.55 directly reduces to a well-known expression in classical linear thermoelasticity. In addition, under adiabatic conditions in which $-\nabla_0^{\mathbf{T}}\mathbf{q}_0 + \rho_0 h = 0$, most of the "viscous" work, $\mathbf{s}_i^{\mathbf{T}}\dot{\mathbf{e}}$, is "absorbed" as a temperature increase controlled by $\rho_0(c_e + c_i)$, while a smaller portion is "absorbed" into the elastic strain-energy field.

18.7 CONSTITUTIVE MODEL: POTENTIAL FUNCTIONS

18.7.1 Helmholtz Free-Energy Density

In the moderately damped, thermohyperelastic material, the elastic (reversible) stress is assumed to satisfy a *thermohyperelastic* constitutive relation suitable for near-incompressible elastomers. In particular,

$$\phi_r = \phi_{rm}(I_1, I_2, I_3) + \phi_{rt}(\mathrm{T}) + \phi_{rtm}(\mathrm{T}, I_3) + \phi_{ro}. \tag{18.57}$$

Here, ϕ_{rm} represents the purely mechanical response and can be identified as the conventional, isothermal, strain-energy density function associated, for example, with the Mooney-Rivlin model. Again, I_1, I_2, I_3 are the principal invariants of the (right) Cauchy-Green strain tensor. The formulation can easily be adapted to stretch ratio-based models, such as the Ogden (1986) model. The function $\phi_{rt}(\mathrm{T})$ represents the purely thermal portion of the Helmholtz free-energy density. Finally, $\phi_{rtm}(\mathrm{T}, I_3)$ represents thermomechanical effects, again based on the assumption that the primary coupling is through volumetric expansion. The quantity ϕ_{ro} represents the Helmholtz free energy in the reference state, and, for simplicity's sake, is assumed to vanish. The forms of ϕ_{rt} and ϕ_{rtm} are introduced in the current presentation:

$$\phi_{rt}(\mathrm{T}) = c_e \mathrm{T}[1 - ln(\mathrm{T}/\mathrm{T}_0)] \tag{18.58}$$

$$\phi_{rtm}(\mathrm{T}, I_3) = \frac{\kappa}{2\rho_0}[f^3(\mathrm{T})J - 1]^2 \tag{18.59}$$

$$J = I_3^{1/2} = \det(\boldsymbol{F}) \quad f(\mathrm{T}) = \left[1 + \frac{\alpha}{3}(\mathrm{T} - \mathrm{T}_0)\right]^{-1}$$

and α is the volumetric coefficient of thermal expansion. For the sake of illustration, for $\Phi_{rm}(I_1, I_2, I_3)$, we display the classical two-term Mooney-Rivlin model:

$$\phi_{rm}(I_1, I_2, I_3) = C_1(J_1 - 1) + C_2(J_2 - 1), \qquad I_3 = 1, \tag{18.60}$$

in which $J_1 = I_1/I_3^{1/3}$ and $J_2 = I_2/I_3^{2/3}$ are the "deviatoric invariants" of $\mathbf{C}$. The reversible stress is obtained as

$$\begin{gathered} \mathbf{s}_r = 2\phi_j \mathbf{n}_j \qquad \phi_j = \partial\phi_r/\partial I_j \\ \mathbf{n}_1 = \mathbf{i}, \quad \mathbf{i} = VEC(\mathbf{I}) \quad \mathbf{n}_1 = I_1\mathbf{i} - \mathbf{c}, \quad \mathbf{c} = VEC(\mathbf{C}) \quad \mathbf{n}_3 = I_3 VEC(\mathbf{C}^{-1}) \end{gathered} \tag{18.61}$$

18.7.2 Specific Dissipation Potential

Fourier's law of conduction is obtained from:

$$\rho\Psi_t = [\boldsymbol{q}_0^T \boldsymbol{q}_0]^{1/2}[k_t/2]. \tag{18.62}$$

The viscous stress $\mathbf{s}_i$ depends on the shear part of the strain rate as well as the temperature. However, since the elastomers of interest are nearly incompressible, to good approximation $\mathbf{s}_i$ can be taken as a function of the (total) Lagrangian strain rate.

The current framework admits several possible expressions for Ψ_i, of which an example was already given in Section 6.3. Here, taking a more general viewpoint, we seek expressions of the form $\Psi_i = \frac{1}{2}\dot{\mathbf{e}}^T \boldsymbol{D}_v(\mathbf{e}, \mathrm{T})\dot{\mathbf{e}}$, in which $\boldsymbol{D}_v$ is called the viscosity tensor; it is symmetric and positive-definite. (Of course, the correct expression is determined by experiments.) The simplest example was furnished in Section 18.6.3. As a second example, to ensure isotropy, suppose that Ψ_i is a function of $\dot{J}_1$ and $\dot{J}_2$: $\Psi_i(\dot{J}_1, \dot{J}_2)$, and note that

$$\dot{J}_1 = \mathbf{m}_1^T \dot{\boldsymbol{e}}, \quad \mathbf{m}_1^T = 2\left[\mathbf{i}^T - \frac{1}{3}\frac{I_1}{I_3}\mathbf{n}_3^T\right] \Big/ I_3^{1/3} \quad \dot{J}_2 = \mathbf{m}_2^T \dot{\boldsymbol{e}}, \quad \mathbf{m}_2^T = 2\left[\mathbf{n}_2^T - \frac{2}{3}\frac{I_2}{I_3}\mathbf{n}_3^T\right] \Big/ I_3^{2/3}. \tag{18.63}$$

For an expression reminiscent of the two-term Mooney-Rivlin strain-energy function, let us consider the specific form

$$\Psi_i = \mu_1(\mathrm{T})\left[C_{1v}\dot{J}_1^{\,2}/2 + C_{2v}\dot{J}_2^{\,2}\right], \tag{18.64}$$

in which C_{1v} and C_{2v} are positive material coefficients. We obtain the viscosity tensor,

$$\boldsymbol{D}_v = \mu(\mathrm{T})\left[C_{1v}\mathbf{m}_1\mathbf{m}_1^T + C_{2v}\mathbf{m}_2\mathbf{m}_2^T\right]. \tag{18.65}$$

Unfortunately, this tensor is only positive-semidefinite. As a second example, suppose that the dissipation potential is expressed in terms of the deformation rate

tensor **D**, in particular, $\Psi_i = \mu(\mathrm{T})tr(\mathbf{D}^2)/2$, which has the advantage in that the deformation rate tensor **D** is in the observed (current) configuration. With $\mathbf{d} = VEC(\mathbf{D})$,

$$\mathbf{d} = \mathbf{F}^{-T} \otimes \mathbf{F}^{-T}\dot{\mathbf{e}} \qquad \boldsymbol{D}_v = \mu(\mathrm{T})(2\boldsymbol{\varepsilon} + \boldsymbol{I})^{-1} \otimes (2\boldsymbol{\varepsilon} + \boldsymbol{I})^{-1}, \tag{18.66}$$

which is positive-definite.

18.8 VARIATIONAL PRINCIPLES

18.8.1 Mechanical Equilibrium

In this section, we present one of several possible formulations for the finite-element equations of interest, neglecting inertia. Application of variational methods to the mechanical field furnishes the Principle of Virtual Work in the form

$$\int tr(\delta \boldsymbol{E}\boldsymbol{S}_i)dV_0 = \int \delta \boldsymbol{u}^T \boldsymbol{\tau}_0 dS_0 - \int tr(\delta \boldsymbol{E}\boldsymbol{S}_r)dV_0, \tag{18.67}$$

in which $\boldsymbol{\tau}_0$ denotes the traction vector on the undeformed surface S_0. As illustrated in the examples in the previous section, we expect that the dissipation potential has the form $\Psi_i = \frac{1}{2}\dot{\mathbf{e}}^T \boldsymbol{D}_v(\mathbf{e}, \mathrm{T})\,\dot{\mathbf{e}}$, from which

$$\mathbf{s}_i = \boldsymbol{D}_v \dot{\mathbf{e}}, \tag{18.68}$$

in which $\boldsymbol{D}_v$ is again the viscosity tensor, and it will be taken as symmetric and positive-definite. (It is positive-definite since $\mathbf{s}_i^{\mathbf{T}}\dot{\mathbf{e}} \geq 0$ for all $\dot{\mathbf{e}}$.) Equation 18.67 is thus rewritten as

$$\int \delta \mathbf{e}^T \mathbf{D}_t \dot{\mathbf{e}} dV_0 = \int \delta \mathbf{u}^T \mathbf{t}_0 dS_0 - \int \delta \mathbf{e}^T \boldsymbol{s}_r dV_0. \tag{18.69}$$

18.8.2 Thermal Equilibrium

The equation for thermal equilibrium is rewritten as

$$\rho_0(\dot{\eta}_r + \dot{\eta}_{i2}) = \left[-\nabla_0^T \boldsymbol{q}_0 + \rho_0 h\right]/\mathrm{T}, \tag{18.70}$$

and note that it is in *rate form*, in contrast to the equation of mechanical equilibrium (see Equation 18.69). For the sake of a unified rate formulation, we first introduce the integrated form of this relation. The current value of $\eta_r + \eta_{i2}$, assuming that the initial values of the entropies vanish, is now given by

$$\rho_0(\eta_r + \eta_{i2}) = \int \left[\left[-\nabla_0^T \boldsymbol{q}_0 + \rho_0 h\right]/\mathrm{T}\right] dt. \tag{18.71}$$

The corresponding variational principle is stated as

$$\int \delta \mathrm{T} \rho_0 (\eta_r + \eta_{i2}) dV_0 = \int \delta \mathrm{T} \left(\int \left[\left[-\nabla_0^T \boldsymbol{q}_0 + \rho_0 h \right] / \mathrm{T} \right] dt \right) dV_0. \tag{18.72}$$

With some effort, a rate (incremental) variational principle can be obtained in the form

$$\int \delta \mathrm{T} \left[-\mathrm{T} \partial \mathbf{s}_r^T / \partial \mathrm{T} \dot{\mathbf{e}} - \mathbf{s}_\mathrm{i}^\mathbf{T} \dot{\mathbf{e}} + \rho_0 (c_e + c_i) \dot{\mathrm{T}} \right] / \mathrm{T} dV_0 = \int \delta \mathrm{T} \left[\left[-\nabla_0^T \mathbf{q}_0 + \rho_0 h \right] / \mathrm{T} \right] dV_0. \tag{18.73}$$

(The motivation behind writing Equations 18.71 and 18.72 is simply to establish how a rate principle is obtained in the thermal field as the counterpart of the rate (incremental) principle for the mechanical field.) Upon approximating T in the denominator by T_0 and letting k denote the thermal conductivity, we can obtain the thermal-equilibrium equation in the form

$$\begin{aligned} &\int \delta \mathrm{T} \left[-\partial \mathbf{s}_r^T / \partial \mathrm{T} \mathbf{e} - \mathbf{s}_\mathrm{i}^\mathbf{T} \dot{\mathbf{e}} - \rho_0 (\mathrm{c}_e + \mathrm{c}_i) \dot{\mathrm{T}} \right] / \mathrm{T}_0 dV_0 \\ &+ \int [k (\nabla_0 \delta \mathrm{T})^T \nabla_0 \delta \mathrm{T} / \mathrm{T}_0] dV_0 = \int \delta \mathrm{T} \rho_0 h / \mathrm{T}_0 dV_0 - \int \mathbf{n}^T (\delta \mathrm{T} \mathbf{q} / \mathrm{T}_0) dS_0 \end{aligned} \tag{18.74}$$

Using interpolation models for displacement and temperature, Equations 18.69 and 18.74 reduce directly into finite-element equations for the mechanical and thermal fields.

18.9 EXERCISES

1. Derive explicit forms of the stress and tangent-modulus tensors using the Helmoltz potential in Equation 18.20.
2. Derive the quantities $\mathbf{m}_1$ and $\mathbf{m}_2$ in Equation 18.63.
3. Verify Equation 18.58 by recovering c_e upon differentiating twice with respect to T.
4. Substitute the required interpolation models in Equations 18.69 and 18.74 to obtain an element-level finite-element equation for the mechanical and thermal fields.

19 Inelastic and Thermoinelastic Materials

19.1 PLASTICITY

Plasticity and thermoplasticity are topics central to the analysis of important applications, such as metal forming, ballistics, and welding. The main goal of this section is to present a model of plasticity and thermoplasticity, along with variational and finite-element statements, accommodating the challenging problems of finite strain and kinematic hardening.

19.1.1 KINEMATICS

Elastic and plastic deformation satisfies the additive decomposition

$$\mathbf{D} = \mathbf{D}_r + \mathbf{D}_i, \tag{19.1}$$

from which we can formally introduce strains:

$$\exists = \int \boldsymbol{D} dt \qquad \exists_r = \int \boldsymbol{D}_r dt \qquad \exists_i = \int \boldsymbol{D}_i dt. \tag{19.2}$$

The Lagrangian strain $\boldsymbol{E}$ satisfies the decomposition

$$\dot{\boldsymbol{E}} = \mathbf{F}^{\mathbf{T}}\mathbf{D}\mathbf{F} \qquad \boldsymbol{E}_r = \int \mathbf{F}^{\mathbf{T}}\mathbf{D}_{\mathbf{r}}\mathbf{F} dt \qquad \boldsymbol{E}_i = \int \mathbf{F}^{\mathbf{T}}\mathbf{D}_{\mathbf{i}}\mathbf{F} dt. \tag{19.3}$$

Typically, plastic strain is viewed as permanent strain. As illustrated in Figure 19.1, in a uniaxial tensile specimen, the stress, S_{11}, can be increased to the point A, and then unloaded along the path AB. The slope of the unloading portion is E, the same as that of the initial elastic portion. When the stress becomes equal to zero, there still is a residual strain, E_{i}, which is identified as the inelastic strain. However, if instead the stress was increased to point C, it would encounter reversed loading at point D, which reflects the fact that the elastic region need not include the zero-stress value.

19.1.2 PLASTICITY

We will present a constitutive equation for plasticity to illustrate how the tangent modulus is stated. The ideas leading to the equation will be presented subsequently in the section on thermoplasticity. With $\boldsymbol{\chi}_{\mathrm{e}} = ITEN22(\boldsymbol{D}_{\mathrm{e}})$ and $\boldsymbol{D}_{\mathrm{e}}$ denoting the

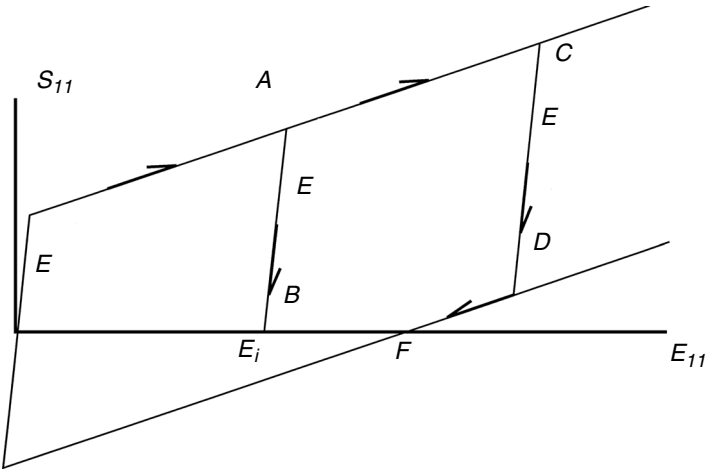

FIGURE 19.1 Illustration of inelastic strain.

tangent-modulus tensor relating the elastic-strain rate to the stress rate (assuming a linear relation), the constitutive equation of interest is

$$\dot{\mathbf{e}}_i = \mathbf{C}_i \dot{\mathbf{s}}, \quad \dot{\mathbf{e}}_\mathbf{e} = \mathbf{C}_e \dot{\mathbf{s}}, \quad \mathbf{C}_e = \boldsymbol{\chi}_e^{-1}, \quad \dot{\boldsymbol{k}} = \mathbf{K}\dot{\mathbf{e}}_i$$
$$\mathbf{C}_i = \left(\frac{\partial \boldsymbol{\Psi}_i}{\partial \boldsymbol{s}}\right)^T \frac{\partial \boldsymbol{\Psi}_i}{\partial \boldsymbol{s}} \Big/ H, \quad H = -\left[\left(\frac{\partial \boldsymbol{\Psi}_i}{\partial \boldsymbol{e}_i} + \frac{\partial \boldsymbol{\Psi}_i}{\partial \boldsymbol{k}} \boldsymbol{K}\right)\left(\frac{\partial \boldsymbol{\Psi}_i}{\partial \boldsymbol{s}}\right)^T\right]. \tag{19.4}$$

In Equation 19.4, $\boldsymbol{\Psi}_i$ is the yield function. $\boldsymbol{\Psi}_i = 0$ determines a closed convex surface in stress space called the yield surface. (We will see later that $\boldsymbol{\Psi}_i$ also serves as a [complementary] dissipation potential.) The stress point remains on the yield surface during plastic flow, and is moving toward its exterior. The plastic strain rate, expressed as a vector, is typically assumed to be normal to the yield surface at the stress point. If the stress point is interior to, or moving tangentially on, the yield surface, only elastic deformation occurs. On all interior paths, for example, due to unloading, the response is only elastic. Plastic deformation induces "hardening," corresponding to a nonvanishing value of $\mathbf{C}_i$. Finally, $\boldsymbol{k}$ is a history-parameter vector, introduced to represent dependence on the history of plastic strain, for example, through the amount of plastic work.

The yield surface is distorted and moved by plastic strain. In Figure 19.2(a), the conventional model of isotropic hardening is illustrated in which the yield surface expands as a result of plastic deformation. This model is unrealistic in predicting a growing elastic region. Reversed plastic loading is encountered at much higher stresses than isotropic hardening predicts. An alternative is kinematic hardening (see Figure 19.2[b]), in which the yield surface moves with the stress point. Within a few percentage points of plastic strain, the yield surface may cease to encircle the origin.

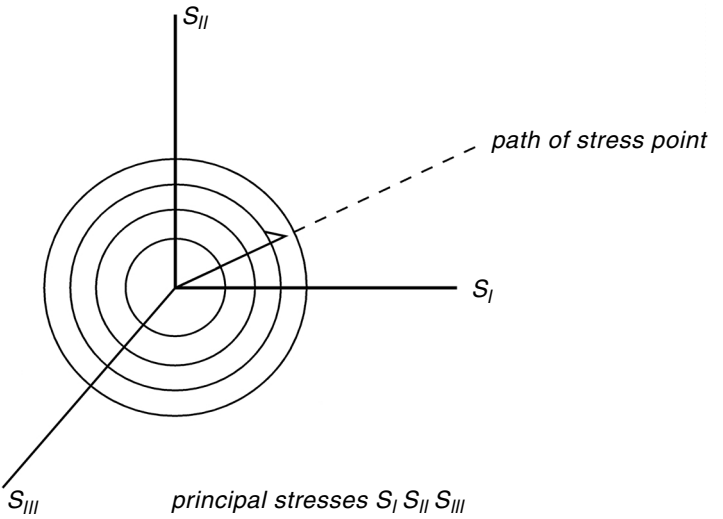

FIGURE 19.2(a) Illustration of yield-surface expansion under isotropic hardening.

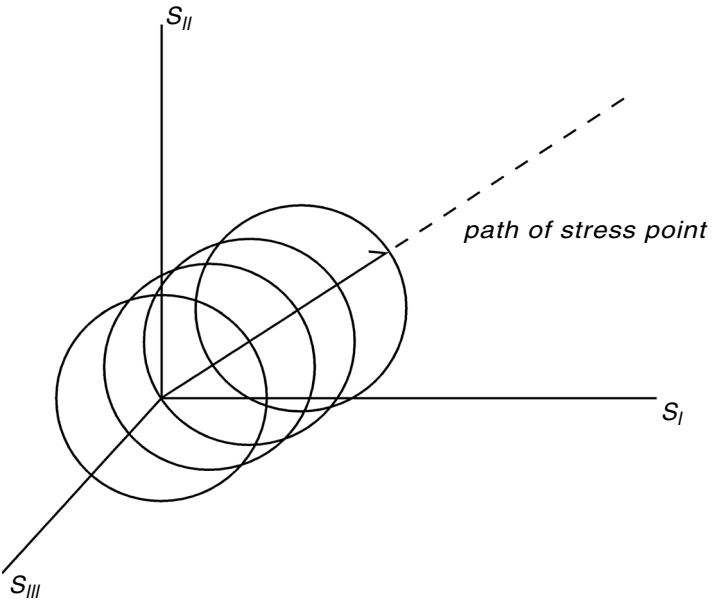

FIGURE 19.2(b) Illustration of yield-surface motion under kinematic hardening.

A reference point interior to the yield surface, sometimes called the back stress, must be identified to serve as the point at which the elastic strain vanishes. Combined isotropic and kinematic hardening are shown in Figure 19.2(c). However, the yield surface contracts, which is closer to actual observations (e.g., Ellyin [1997]).

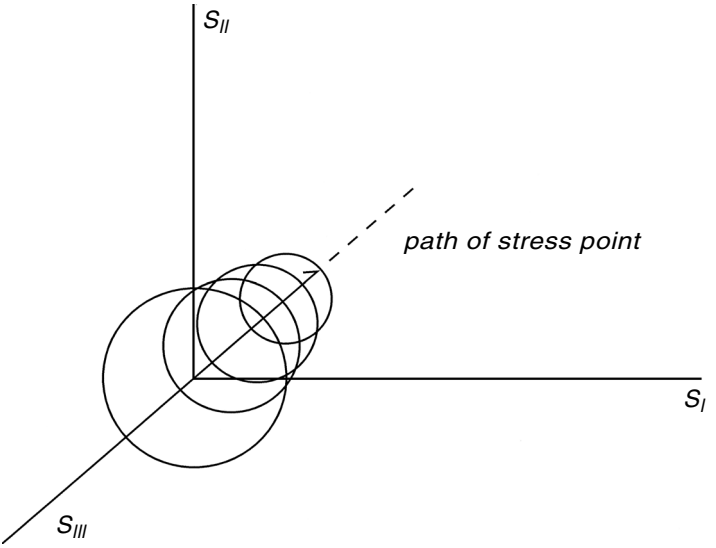

FIGURE 19.2(c) Illustration of combined kinematic and isotropic hardening.

The rate of movement must exceed the rate of contraction for the material to remain stable with a positive tangent modulus.

Combining the elastic and inelastic portions furnishes the tangent-modulus tensor:

$$\boldsymbol{\chi} = \left[\boldsymbol{\chi}_e^{-1} + \mathbf{C}_i\right]^{-1} = [\mathbf{I} + \boldsymbol{\chi}_e \mathbf{C}_i]^{-1} \boldsymbol{\chi}_e. \tag{19.5}$$

Suppose that in uniaxial tension, the elastic modulus is E_e and the inelastic modulus-relating stress and inelastic strain increments are E_i, and $E_i << E_e$. The total uniaxial modulus is then $\frac{E_i}{(1 + E_i / E_e)}$.

19.2 THERMOPLASTICITY

As in Chapter 18, two potential functions are introduced to provide a systematic way to describe irreversible and dissipative effects. The first is interpreted as the Helmholtz free-energy density, and the second is for dissipative effects. To accommodate kinematic hardening, we also assume an extension of the Green and Naghdi (G-N) (1965) formulation, in which the Helmholtz free energy decomposes into reversible and irreversible parts, with the irreversible part depending on the "plastic strain." Here, it also depends on the temperature and a workless *internal state variable*.

19.2.1 Balance of Energy

The conventional equation for energy balance is augmented using a vector-valued, workless internal variable, $\boldsymbol{\alpha}_0$, regarded as representing "microstructural rearrangements":

$$\rho_o \dot{\chi}_0 = \mathbf{s}^T \dot{\mathbf{e}}_r + \mathbf{s}^T \dot{\mathbf{e}}_i - \nabla_0^T \boldsymbol{q}_0 + \rho_o h + \boldsymbol{\beta}_0^T \dot{\boldsymbol{\alpha}}_0, \tag{19.6}$$

where χ_o is the internal energy per unit mass in the undeformed configuration and $\mathbf{s} = VEC(\boldsymbol{S})$, $\mathbf{e} = VEC(\boldsymbol{E})$, and $\boldsymbol{\beta}_0$ is the flux per unit mass associated with $\boldsymbol{\alpha}_0$. However, note that $\boldsymbol{\beta} = \mathbf{0}$, thus $\boldsymbol{\beta}_i = -\boldsymbol{\beta}_r$. Also, χ is the internal energy per unit mass, $\mathbf{q}_0$ is the heat-flux vector referred to undeformed coordinates, and h is the heat input per unit mass, for simplicity's sake, assumed independent of temperature. The state variables are $\boldsymbol{E}_r$, $\boldsymbol{E}_i$, T, and $\boldsymbol{\alpha}_0$.

The next few paragraphs will go over some of the same ground as for damped elastomers in Chapter 18, except for two major points. In that chapter, the stress was assumed to decompose into reversible and irreversible portions in the spirit of elementary Voigt models. In the current context, the strain shows the decomposition in the spirit of the classical Maxwell model. In addition, as seen in the following, it proves beneficial to introduce a workless internal variable to give the model the flexibility to accommodate phenomena such as kinematic hardening.

The Helmholtz free energy, ϕ, per unit mass and the entropy, η, per unit mass are introduced using

$$\phi = \chi - \mathrm{T}\eta. \tag{19.7}$$

Now,

$$\nabla_0^{\boldsymbol{T}}\boldsymbol{q}_0 - \rho_0 h = \mathbf{s}^T\dot{\mathbf{e}}_r + \mathbf{s}^T\dot{\mathbf{e}}_i - \rho_0\mathrm{T}\dot{\eta} - \rho_0\eta\dot{\mathrm{T}} - \rho_0\dot{\phi} + \boldsymbol{\beta}_0^{\boldsymbol{T}}\dot{\boldsymbol{\alpha}}_0. \tag{19.8}$$

19.2.2 Entropy-Production Inequality

The entropy now satisfies

$$\begin{aligned}\rho_0\mathrm{T}\dot{\eta} &\geq -\nabla_0^T\boldsymbol{q}_0 + \rho_0 h + \boldsymbol{q}_0^T\nabla\mathrm{T}/\mathrm{T} \\ &\geq \rho_0\dot{\phi} - \mathbf{s}^{\boldsymbol{T}}\dot{\mathbf{e}}_r - \mathbf{s}^{\boldsymbol{T}}\dot{\mathbf{e}}_i + \rho_0\mathrm{T}\dot{\eta} + \rho_0\eta\dot{\mathrm{T}} + \boldsymbol{q}_0^{\mathrm{T}}\nabla\mathrm{T}/\mathrm{T} - \boldsymbol{\beta}_0^{\boldsymbol{T}}\dot{\boldsymbol{\alpha}}_0.\end{aligned} \tag{19.9}$$

Viewing ϕ_r as a differentiable function of $\boldsymbol{e}_r$, T, and $\boldsymbol{\alpha}_0$, we conclude that

$$\partial\phi_r/\partial\mathbf{e}_r = \mathbf{s}^T \qquad \partial\phi_r/\partial\mathrm{T} = -\rho_0\eta_r \qquad \partial\phi_r/\partial\boldsymbol{\alpha}_0 = \boldsymbol{\beta}_{0r}^T. \tag{19.10}$$

Extending the G-N formulation, let $\mathbf{s}^{*T} = \rho_0\partial\phi_i/\partial\mathbf{e}_i$ and assume that $\eta_i = -\partial\phi_i/\partial\mathrm{T}$ and $\rho_0\partial\phi_i/\partial\boldsymbol{\alpha}_0 = \boldsymbol{\beta}_{0i}^T$. Now,

$$\mathbf{s}^{*T} = \rho_0\partial\phi_i/\partial\mathbf{e}_i \qquad \eta_i = -\partial\phi_i/\partial\mathrm{T} \qquad \rho_0\partial\phi_i/\partial\boldsymbol{\alpha}_0 = \boldsymbol{\beta}_{0i}^T. \tag{19.11}$$

The entropy-production inequality (see Equation 19.9) is now restated as

$$(\mathbf{s}^T - \mathbf{s}^{*T})\dot{\mathbf{e}}_i - \boldsymbol{q}_0^{\boldsymbol{T}}\nabla_0\mathrm{T}/\mathrm{T} \geq 0. \tag{19.12}$$

The inequality shown in Equation 19.12 can be satisfied if

$$(\mathbf{s}^T - \mathbf{s}^{*T})\dot{\mathbf{e}}_i \geq 0 \quad \text{(a)} \qquad -\boldsymbol{q}_0^T \nabla_0 \mathrm{T}/\mathrm{T} \geq 0 \quad \text{(b)}. \tag{19.13}$$

The first inequality involves a quantity, $\mathbf{s}^* = VEC(\boldsymbol{S}^*)$, with dimensions of stress. In the subsequent sections, $\mathbf{s}^*$ will be viewed as a reference stress, often called the back stress, which is interior to a yield surface and can be used to characterize the motion of the yield surface in stress space. In classical kinematic hardening in which the hyperspherical yield surface does not change size or shape but just moves, the reference stress is simply the geometric center. If kinematic hardening occurs, as stated before, the yield surface need not include the origin even with small amounts of plastic deformation. Thus, there is no reason to regard $\dot{\mathbf{e}}_r$ as vanishing at the origin. Instead, $\dot{\mathbf{e}}_r = \mathbf{0}$ is now associated with a moving-reference stress interior to the yield surface, identified here as the back stress $\mathbf{s}^*$.

19.2.3 Dissipation Potential

As in Chapter 18, we introduce a specific dissipation potential, Ψ_i, for which

$$\dot{\mathbf{e}}_i^T = \rho_0 \Lambda_i \, \partial \Psi_\mathbf{i} / \partial \mathfrak{s} \quad \text{(i)} \qquad -\nabla_0^T \mathrm{T}/\mathrm{T} = \Lambda_t \rho_0 \partial \Psi_\mathbf{i} / \partial \mathbf{q}_0 \quad \text{(ii)} \qquad \mathfrak{s} = \mathbf{s} - \mathbf{s}^* \quad \text{(iii)}, \tag{19.14a}$$

from which, with $\Lambda_i > 0$ and $\Lambda_t > 0$,

$$\rho_0 \Lambda_i (\partial \Psi / \partial \mathfrak{s})\, \mathfrak{s} + \rho_0 \Lambda_t (\partial \Psi / \partial \mathbf{q}_0)\mathbf{q}_0 > 0. \tag{19.14b}$$

On the expectation that properties governing heat transfer are not affected by strain, we introduce the decomposition into inelastic and thermal portions:

$$\Psi = \Psi_i + \Psi_t \qquad \rho_0 \Psi_t = \frac{\Lambda_t}{2} \sqrt{\mathbf{q}_0^T \mathbf{q}_0}, \tag{19.15a}$$

where Ψ_i represents mechanical effects and is identified in the subsequent sections. The thermal constitutive relation derived from the dissipation potential implies Fourier's law:

$$-\nabla_0 \mathrm{T}/\mathrm{T} = \mathbf{q}_0 / \Lambda_t. \tag{19.15b}$$

The inelastic portion is discussed in the following section.

19.3 THERMOINELASTIC TANGENT-MODULUS TENSOR

The elastic strain rate satisfies a *thermohypoelastic* constitutive relation:

$$\dot{\mathbf{e}}_r = \mathrm{C}_r(\mathbf{s} - \mathbf{s}^*)^{\bullet} + \boldsymbol{a}_r \dot{\mathrm{T}}. \tag{19.16}$$

$\mathbf{C}_r$ is a 9×9 second-order, elastic compliance tensor, and $\boldsymbol{a}_r$ is the 9×1 thermoelastic expansion vector, with both presumed to be known from measurements. Analogously, for rate-independent thermoplasticity, we seek tensors $\mathbf{C}_i$ and $\boldsymbol{a}_i$, depending on $\mathfrak{s}$, $\mathbf{e}_i$, and T such that

$$\dot{\mathbf{e}}_i = \mathbf{C}_i(\mathbf{s} - \mathbf{s}^*)^{\bullet} + \boldsymbol{a}_i \dot{\mathrm{T}} \tag{19.17a}$$

$$\dot{\mathbf{e}} = [\mathbf{C}_r + \mathbf{C}_i](\mathbf{s} - \mathbf{s}^*)^{\bullet} + (\boldsymbol{a}_r + \boldsymbol{a}_i)\dot{\mathrm{T}}. \tag{19.17b}$$

During thermoplastic deformation, the stress and temperature satisfy a thermoplastic *yield condition* of the form

$$\Pi_i(\mathfrak{s}, \mathbf{e}_i, \boldsymbol{k}, \mathrm{T}, \eta_{i2}) = 0, \tag{19.18}$$

and Π_i is called the *yield function*. Here, the vector $\boldsymbol{k}$ is introduced to represent the effect of the history of inelastic strain, $\dot{\mathbf{e}}_i$, such as work hardening. It is assumed to be given by a relation of the form

$$\dot{\boldsymbol{k}} = \boldsymbol{K}(\mathbf{e}_i, \boldsymbol{k}, \mathrm{T})\dot{\mathbf{e}}_i. \tag{19.19}$$

The "consistency condition" requires that $\dot{\Pi}_i = 0$ during thermoplastic flow, from which

$$\frac{d\Pi_i}{d\mathfrak{s}}\dot{\mathfrak{s}} + \frac{d\Pi_i}{d\mathbf{e}_i}\dot{\mathbf{e}}_i + \frac{d\Pi_i}{d\boldsymbol{k}}\dot{\boldsymbol{k}} + \frac{d\Pi_i}{d\,\mathrm{T}}\dot{\mathrm{T}} + \frac{d\Pi_i}{d\eta_{\mathrm{i}}}\dot{\eta}_i = 0. \tag{19.20}$$

We introduce a thermoplastic extension of the conventional associated flow rule, whereby the inelastic strain-rate vector is normal to the yield surface at the current stress point,

$$\dot{\mathbf{e}}_i = \Lambda_i \left(\frac{d\Pi_i}{d\mathfrak{s}} \right)^T \qquad \text{(a)} \qquad \dot{\eta}_{\mathrm{i}} = \Lambda_i \frac{d\Pi_i}{d\eta_{\mathrm{i}}} \qquad \text{(b)}. \tag{19.21}$$

Equation 19.14a suggests that *the yield function may be identified as the dissipation potential*: $\Pi_i = \rho_0 \Psi_i$. Standard manipulation furnishes

$$\dot{\mathbf{e}}_i = \mathrm{C}_i \dot{\mathfrak{e}} + \boldsymbol{a}_i \dot{\mathrm{T}} \qquad \dot{\eta}_{i2} = \boldsymbol{b}_i^T \dot{\mathfrak{e}} + \mathrm{c}_i \dot{\mathrm{T}}$$

$$\mathbf{C}_i = \left(\frac{\partial \Psi_i}{\partial \mathfrak{e}}\right)^T \frac{\partial \Psi_i}{\partial \mathfrak{e}} \Big/ H \qquad \boldsymbol{a}_i = \boldsymbol{b}_i = \left(\frac{\partial \Psi_i}{\partial \mathfrak{e}}\right)^T \frac{\partial \Psi_i}{\partial \mathrm{T}} \Big/ H \tag{19.22}$$

$$\mathrm{c}_i = \left(\frac{\partial \Psi_i}{\partial T}\right)^2 \Big/ H \qquad H = -\left[\left(\frac{\partial \Psi_i}{\partial \boldsymbol{e}_i} + \frac{\partial \Psi_i}{\partial \boldsymbol{k}} \boldsymbol{K}\right)\left(\frac{\partial \Psi_i}{\partial \mathfrak{e}}\right)^T + \frac{\partial \Psi_i}{\partial \eta_{i2}} \frac{\partial \Psi_i}{\partial \mathrm{T}}\right]$$

and H must be positive for Λ_i to be positive. Note that, in the current formulation, the dependence of the yield function on temperature accounts for c_i. The thermodynamic inequality shown in Equation 19.13a is now satisfied if $H > 0$.

Next, note that $\mathbf{s}^*$ depends on $\mathbf{e}_i$, T, and $\boldsymbol{\alpha}_0$ since $\mathbf{s}^{*T} = \rho_0 \partial \phi_i / \partial \mathbf{e}_i$. For simplicity's sake, we neglect dependence on $\boldsymbol{\alpha}_0$ and assume that a relation of the following form can be measured for $\mathbf{s}^*$:

$$\dot{\mathbf{s}}^* = \boldsymbol{\Gamma} \dot{\mathbf{e}}_i + \vartheta \dot{\mathrm{T}} \qquad \boldsymbol{\Gamma} = \frac{\partial}{\partial \mathbf{e}_i}\left(\frac{\partial}{\partial \mathbf{e}_i}\right)^T \Psi_{\mathrm{I}} \qquad \vartheta^T = \partial^2 \Psi_i / \partial \mathbf{e}_i \partial \mathrm{T}. \tag{19.23}$$

From Equations 19.16 and 19.17, the *thermoinelastic tangent-modulus tensor* and thermal thermomechanical vector are obtained as

$$\dot{\mathbf{e}} = \mathbf{C} \dot{\mathbf{s}} + \boldsymbol{a} \dot{\mathrm{T}} \tag{19.24a}$$

$$\begin{aligned} \mathbf{C} &= (\mathbf{C}_r + \mathbf{C}_i)[\mathbf{I} - (\mathbf{I} + \boldsymbol{\Gamma} \mathbf{C}_i)^{-1} \boldsymbol{\Gamma} \mathbf{C}_i] \\ \boldsymbol{a} &= [\boldsymbol{a}_r + \boldsymbol{a}_i + (\mathbf{C}_r + \mathbf{C}_i)\boldsymbol{\Gamma} \boldsymbol{a}_i - (\mathbf{C}_r + \mathbf{C}_i)(\mathbf{I} + \boldsymbol{\Gamma} \mathbf{C}_i)^{-1} \vartheta] \end{aligned} \tag{19.24b}$$

If appropriate, the foregoing formulation can be augmented to accommodate plastic incompressibility.

19.3.1 Example

We now provide a simple example using the Helmholtz free-energy density function and the dissipation-potential function to derive constitutive relations. The following expression involves a Von Mises yield function, linear kinematic hardening, linear work hardening, and linear thermal softening.

i. Helmholtz free-energy density:

$$\phi = \phi_r + \phi_t \qquad \rho_0\phi_t = k_3\mathbf{e}_i^T\mathbf{e}_i$$
$$\rho_0\phi_r = \mathbf{e}_r^T\mathbf{C}_r^{-1}\mathbf{e}_r/2 - \boldsymbol{a}^T\mathbf{C}_r^{-1}(\mathrm{T}-\mathrm{T}_0)\mathbf{e}_r + \rho_0 \mathrm{c}_r'\mathrm{T}(1-ln(\mathrm{T}/\mathrm{T}_0)) \tag{19.25}$$

in which c_r' is a known constant. From Equation 19.28,

$$\mathfrak{s} = \rho_0(\partial\phi_r/\partial\mathbf{e}_r)^{\mathrm{T}} = \mathbf{C}_r^{-1}[\mathbf{e}_r - \boldsymbol{a}_r(\mathrm{T}-\mathrm{T}_0)]. \tag{19.26}$$

Finally,

$$\mathrm{c}_r = -\mathrm{T}\frac{\partial^2\phi_r}{\partial\mathrm{T}^2} = \mathrm{c}' \tag{19.27}$$

ii. Dissipation potential:

$$\Psi = \Psi_i + \Psi_t \qquad \rho_0\Psi_t = \frac{\Lambda_t}{2}\sqrt{\mathbf{q}_0^T\mathbf{q}_0} \tag{19.28}$$

$$\Psi_i = \sqrt{\mathfrak{s}^T\mathfrak{s}} - [k_0 + k_1 k - k_2(\mathrm{T}-\mathrm{T}_0)] = 0 \qquad \dot{k} = \mathfrak{s}^T\,\dot{\mathbf{e}}_i \tag{19.29}$$

Straightforward manipulations serve to derive

$$H = k_1\sqrt{\mathfrak{s}^T\mathfrak{s}} = k_1[k_0 + k_1 k - k_2(\mathrm{T}-\mathrm{T}_0)] \tag{19.30}$$

$$\boldsymbol{C}_i = \frac{\mathfrak{s}\mathfrak{s}^T}{\mathfrak{s}^T\mathfrak{s}}\Big/H \qquad \mathrm{c}_i = k_2^2/H \qquad \boldsymbol{a}_i = \boldsymbol{b}_i = \frac{k_2\mathfrak{s}}{\sqrt{\mathfrak{s}^T\mathfrak{s}}}\Big/H \tag{19.31}$$

Consider a two-stage thermomechanical loading, as illustrated schematically in Figure 19.3. Let S_{I}, S_{II}, S_{III} denote the principal values of the 2nd Piola-Kirchhoff stress, and suppose that $S_{\mathrm{III}} = 0$. In the first stage, with the temperature held fixed at T_0, the stresses are applied proportionally well into the plastic range. The center of the yield surface moves along a line in the (S_1, S_2) plane, and the yield surface expands as it moves. In the second stage, suppose that the stresses S_1 and S_2 are fixed, but that the temperature increases to T_1 and then to T_2 and T_3. The plastic strain must increase, thus, the center of the yield surface moves. In addition, strain hardening tends to cause the yield surface to expand, while the increased temperature tends to make it contract. However, in this case, thermal softening must dominate strain hardening, and contraction must occur since the center of the yield surface must move further along the path shown even as the yield surface continues to "kiss" the fixed stresses S_{I} and S_{II}.

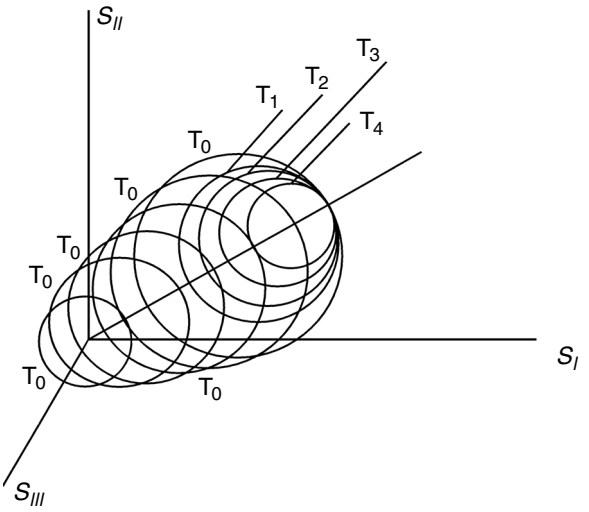

FIGURE 19.3 Effect of load and temperature on yield surface.

Unfortunately, accurate finite-element computations in plasticity and thermoplasticity often require close attention to the location of the front of the yielded zone. This front will occur within elements, essentially reducing the continuity order of the fields (discontinuity in strain gradients). Special procedures have been developed in some codes to address this difficulty.

The shrinkage of the yield surface with temperature provides an element of the explanation of the phenomenon of adiabatic shear banding, which is commonly encountered in some materials during impact or metal forming. In rapid processes, plastic work is mostly converted into heat and on into high temperatures. There is not enough time for the heat to flow away from the spot experiencing high deformation. However, the process is unstable while the stress level is maintained. Namely, as the material gets hotter, the rate of plastic work accelerates, thanks to the softening evident in Figure 19.3. The instability is manifested in small, periodically spaced bands, in the center of which the material is melted and resolidified, usually in a much more brittle form than before. These bands can nucleate brittle failure.

19.4 TANGENT-MODULUS TENSOR IN VISCOPLASTICITY

The thermodynamic discussion in the previous section applies to thermoinelastic deformation, for which the first example given concerned quasi-static plasticity and thermoplasticity. However, it is equally applicable when rate sensitivity is present, in which case viscoplasticity and thermoviscoplasticity are attractive models. An example

of a constitutive model, for example, following Perzyna (1971), is given in undeformed coordinates as

$$\mu_{\bar{\omega}}\dot{\boldsymbol{e}}_i = <1-\frac{k}{\Psi_{\mathbf{i}}}> \frac{\left(\dfrac{\partial \Psi_{\mathrm{i}}}{\partial \mathfrak{s}}\right)^T}{\sqrt{\dfrac{\partial \Psi_{\mathrm{i}}}{\partial \mathfrak{s}}\left(\dfrac{\partial \Psi_{\mathrm{i}}}{\partial \mathfrak{s}}\right)^T}}, \quad <1-\frac{k}{\Psi_{\mathrm{i}}}> = \begin{cases} 1-\dfrac{k}{\Psi_{\mathrm{i}}}, & \text{if} \quad 1-\dfrac{k}{\Psi_{\mathrm{i}}} \geq 0 \\ 0, & \text{otherwise,} \end{cases} \tag{19.32}$$

and $\Psi_{\mathbf{i}}(\mathfrak{s}, \mathbf{e}_i, \boldsymbol{k}, T, \eta_i)$ is a loading surface function. The elastic response is still considered linear in the form

$$\dot{\mathbf{e}}_r = \boldsymbol{\chi}_r^{-1}\dot{\mathbf{s}} + \boldsymbol{\alpha}_r\dot{\mathrm{T}}. \tag{19.33}$$

Recall from thermoplasticity that

$$\dot{\mathbf{s}}^* = \boldsymbol{\Gamma}\dot{\mathbf{e}}_i + \vartheta\dot{\mathrm{T}} \qquad \boldsymbol{\Gamma} = \frac{\partial}{\partial \mathbf{e}_i}\left(\frac{\partial}{\partial \mathbf{e}_i}\right)^T \Psi_i \qquad \vartheta^T = \partial^2\Psi_i/\partial \mathbf{e}_i \partial \mathrm{T}. \tag{19.34}$$

Corresponding to $\mathfrak{s}$, there is a reference stress $\mathbf{s}'$ and a corresponding vector $\mathfrak{s}' = \mathbf{s}' - \mathbf{s}^*$ such that $\Psi_i(\mathfrak{s}', \mathbf{e}_i, \boldsymbol{k}, \mathrm{T}, \eta_i) = k(\mathbf{e}_i, \boldsymbol{k}, \mathrm{T}, \eta_i)$ determines a quasi-static, reference-yield surface. The vectors $\mathfrak{s}$ and $\mathfrak{s}'$ have the same origin and direction, but the latter terminates at the reference surface, while the latter terminates outside the reference surface if inelastic flow is occurring. Interior to the surface, no inelastic flow occurs. If exterior to the surface, inelastic flow occurs at a rate dependent on the distance to the exterior of the reference surface. This situation is illustrated in Figure 19.4.

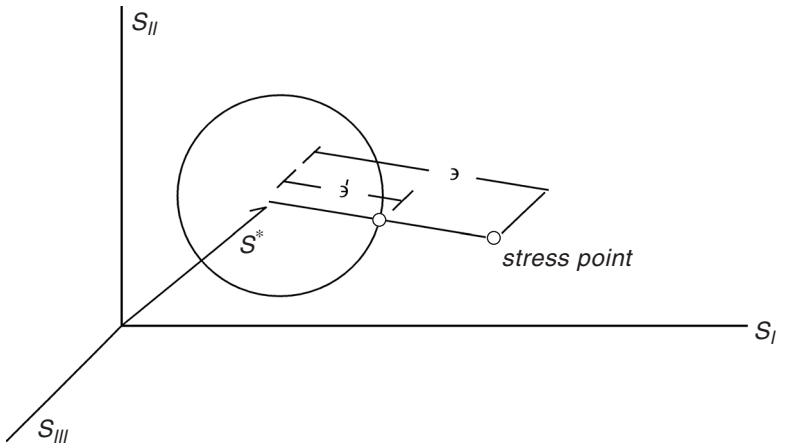

FIGURE 19.4 Illustration of reference surface in viscoplasticity.

It should be evident that viscoplasticity and thermoviscoplasticity can be formulated to accommodate phenomena such as kinematic hardening and thermal shrinkage of the reference-yield surface.

The tangent-modulus matrix now reduces to elastic relations, and viscoplastic effects can be treated as an initial force (after canceling the variation) since

$$\dot{\mathbf{s}} = \boldsymbol{\chi}_r \dot{\mathbf{e}} + \boldsymbol{\chi}_r \boldsymbol{\alpha}_r \dot{\mathrm{T}} - \left(\boldsymbol{\Gamma} - \frac{\boldsymbol{\chi}_r}{\mu_v} \right) < 1 - \frac{k}{\Psi_{\mathrm{i}}} > \frac{\left(\frac{\partial \Psi_{\mathrm{i}}}{\partial \mathfrak{s}} \right)^T}{\sqrt{\frac{\partial \Psi_{\mathrm{i}}}{\partial \mathfrak{s}} \left(\frac{\partial \Psi_{\mathrm{i}}}{\partial \mathfrak{s}} \right)^T}}. \tag{19.35}$$

In particular, the Incremental Principle of Virtual Work is now stated, to first order, as

$$\int \delta \Delta \mathbf{e}^T \boldsymbol{\chi}_r \Delta \mathbf{e} dV_o + \int \delta \Delta \mathbf{e}^T \boldsymbol{\chi}_r \boldsymbol{\alpha}_r \Delta \mathrm{T} dV_o + \int \delta \Delta \mathbf{u}^T \rho_o \Delta \ddot{\mathbf{u}} dV_o$$

$$= \int \delta \Delta \mathbf{u}^T \Delta \boldsymbol{\tau} \, dS_o + \int \delta \Delta \mathbf{e}^T \left(\boldsymbol{\Gamma} - \frac{\boldsymbol{\chi}_r}{\mu_v} \right) < 1 - \frac{k}{\Psi_{\mathrm{i}}} > \frac{\left(\frac{\partial \Psi_{\mathrm{i}}}{\partial \mathfrak{s}} \right)^T}{\sqrt{\frac{\partial \Psi_{\mathrm{i}}}{\partial \mathfrak{s}} \left(\frac{\partial \Psi_{\mathrm{i}}}{\partial \mathfrak{s}} \right)^T}} dV_o \tag{19.36}$$

19.5 CONTINUUM DAMAGE MECHANICS

Ductile fracture occurs by processes associated with the notion of damage. An internal-damage variable is introduced that accumulates with plastic deformation. It also manifests itself in reductions in properties, such as the experimental values of the elastic modulus and yield stress. When the damage level in a given element reaches a known or assumed critical value, the element is considered to have failed. It is then removed from the mesh (considered to be no longer supporting the load). The displacement and temperature fields are recalculated to reflect the element deletion.

There are two different schools of thought on the suitable notion of a damage parameter. One, associated with Gurson (1977), Tvergaard (1981), and Thomasson (1990), considers damage to occur by a specific mechanism occurring in a three-stage process: nucleation of voids, their subsequent growth, and their coalescence to form a macroscopic defect. The coalescence event is used as a criterion for element failure. The parameter used to measure damage is the void-volume fraction *f*. Models and criteria for the three processes have been formulated. For both nucleation and growth, evolution of *f* is governed by a constitutive equation of the form

$$\dot{f} = \Xi(f, \mathbf{e}_i, T), \tag{19.37}$$

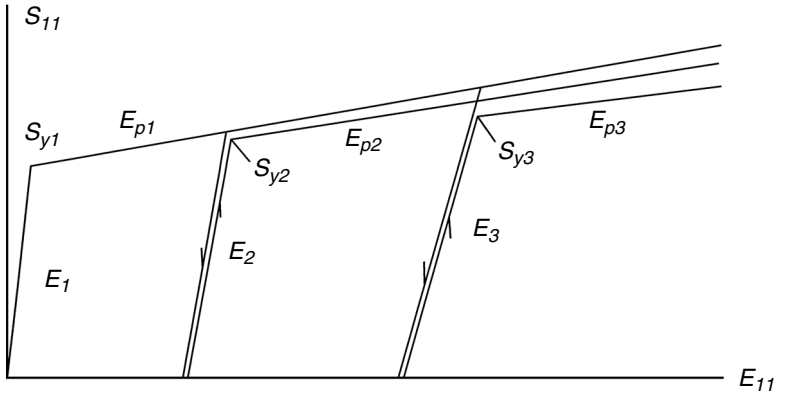

FIGURE 19.5 Illustration of effect of damage on elastic-plastic properties.

for which several specific forms have been proposed. To this point, a nominal stress is used in the sense that the reduced ability of material to support stress is not accommodated.

The second school of thought is more empirical in nature and is not dependent on a specific mechanism. It uses the parameter D, which is interpreted as the fraction of damaged area A_d to total area A_o that the stress (traction) acts on. Consider a uniaxial tensile specimen with damage, but experiencing elastic behavior. Suppose that damaged area A_d can no longer support a load (is damaged). For a given load P, the *true* stress at a point in the undamaged zone is $S = \frac{P}{A_o - A_D} = \frac{1}{1-D}\frac{P}{A_o} = \frac{1}{1-D}S'$. Here, S' is a nominal stress, but is also the measured stress. If E is the elastic modulus measured in an undamaged specimen, the modulus measured in the current specimen will be $E' = E(1 - D)$, demonstrating that damage is manifest in small changes in properties.

As an illustration of damage, suppose specimens are loaded into the plastic range, unloaded, and then loaded again. Without damage, the stress-strain curve should return to its original path. However, due to the damage, there are slight changes in the elastic slope, in the yield stress, and in the slope after yield (exaggerated in Figure 19.5).

From the standpoint of thermodynamics, damage is a dissipative internal variable. In reality, the amount of mechanical or thermal energy absorbed by damage is probably small, so that its role in the energy-balance equation can be neglected. At the risk of being slightly conservative, in dynamic (adiabatic) problems, the plastic work can be assumed to be completely converted into heat. Even so, for the sake of a consistent framework for treating dissipation, a dissipation potential, Ψ_d, can be introduced for damage, as has been done, for example, by Bonora (1997). The contribution to the irreversible entropy production can be introduced in the form $\mathcal{D}\dot{D} \geq 0$, in which $\mathcal{D}$ is the "force" associated with flux $\dot{D}$. Positive dissipation is assured if we assume

$$\mathcal{D} = \frac{\partial \Psi_d}{\partial \dot{D}}, \qquad \Psi_d = \frac{1}{2}\Lambda_d(\mathbf{e}_i, T, \boldsymbol{k})\dot{D}^2, \qquad \Lambda_d(\mathbf{e}_i, T, \boldsymbol{k}) > 0. \tag{19.38}$$

An example of a satisfactory function is $\Lambda_d(\mathbf{e}_i, \mathrm{T}, \boldsymbol{k}) = \Lambda_{do}\int(\boldsymbol{s} - \boldsymbol{s}^*)\,\dot{\mathbf{e}}_i\,dt$, Λ_{do} a positive constant, showing damage to depend on plastic work.

Specific examples of constitutive relations for damage are given, for example, in Bonora (1997).

At the current values of the damage parameter, the finite-element equations are solved for the nodal displacements, from which the inelastic strains can be computed. This information can then be used to update the damage-parameter values. Upon doing so, the damage-parameter values are compared to critical values. As stated previously, if the critical value is obtained, the element is deleted. The path of deleted elements can be viewed as a crack.

The code LS-DYNA Ver. 9.5, (2000) incorporates a material model that includes viscoplasticity and damage mechanics. It can easily be upgraded to include thermal effects, assuming that all viscoplastic work is turned into heat. Such a model has been shown to reproduce the location and path of a crack in a dynamically loaded welded structure (see Moraes [2002]).

19.6 EXERCISES

1. In isothermal plasticity, assuming the following yield function, find the uniaxial stress-strain curve:

$$\Psi_{\mathrm{i}} = \sqrt{(\mathbf{s} - k_1\mathbf{e}_i)^T(\mathbf{s} - k_1\mathbf{e}_i)} - \left(k_o + k_2 \int_0^t \sqrt{\dot{\mathbf{e}}_i^{\,T}\dot{\mathbf{e}}_i}\,dt\right).$$

   Assume small strain and that the plastic strain is incompressible: $tr(\boldsymbol{E}_i) = 0$.
2. Regard the expression in Exercise 1 as defining the reference-yield surface in viscoplasticity, with viscosity η_{v}. Find the stress-strain curve under uniaxial tension if a constant strain rate is imposed.

20 Advanced Numerical Methods

In nonlinear finite-element analysis, solutions are typically sought using Newton iteration, either in classical form or augmented as an arc-length method to bypass critical points in the load-deflection behavior. Here, two additional topics of interest are briefly presented.

20.1 ITERATIVE TRIANGULARIZATION OF PERTURBED MATRICES

20.1.1 INTRODUCTION

In solving large linear systems, it is often attractive to use Cholesky triangularization followed by forward and backward substitutions. In computational problems, such as in the nonlinear finite-element method, solutions are attained incrementally, with the stiffness matrix slightly modified whenever it is updated. The goal here is to introduce and demonstrate an iterative method of determining the changes in the triangular factors ensuing from modifying the stiffness matrix. A heuristic convergence argument is given, as well as a simple example indicating rapid convergence. Apparently, no efficient iterative method for matrix triangularization has previously been established.

The finite-element method often is applied to problems requiring solution of large linear systems of the form $\mathbf{K}_0\boldsymbol{\gamma}_0 = \mathbf{f}_0$, in which the stiffness matrix $\mathbf{K}_0$ is positive-definite, symmetric, and may be banded. As discussed in a previous chapter, an attractive method of solution is based on Cholesky decomposition (triangularization), in which $\mathbf{K}_0 = \mathbf{L}_0\,\mathbf{L}_0^{\mathbf{T}}$ and $\mathbf{L}_0$ is lower-triangular, and it is also banded if $\mathbf{K}_0$ is banded. The decomposition enables an efficient solution process consisting of forward substitution followed by backward substitution. Often, however, the stiffness matrix is updated during the solution process, leading to a slightly different (perturbed) matrix, $\mathbf{K} = \mathbf{K}_0 + \Delta\mathbf{K}$, in which $\Delta\mathbf{K}$ is small when compared to $\mathbf{K}_0$. For example, this situation may occur in modeling nonlinear problems using an updated Lagrangian scheme and load incrementation. Given the fact that triangular factors are available for $\mathbf{K}_0$, it would appear to be attractive to use an iteration scheme for the perturbed matrix $\mathbf{K}$, in which the initial iterate is $\mathbf{L}_0$. The iteration scheme should not involve solving intermediate linear systems except by using current triangular factors. A scheme is introduced in the following section and produces, in a simple example, good estimates within a few iterations.

The solution of perturbed linear systems has been the subject of many investigations. Schemes based on explicit matrix inversion include the Sherman-Morrison-Woodbury formulae (see Golub and Van Loan [1996]). An alternate method is to carry bothersome terms to the right side and iterate. For example, the perturbed linear

system can be written as

$$\mathbf{K}_0\Delta\boldsymbol{\gamma} = \Delta\mathbf{f} - \Delta\mathbf{K}\boldsymbol{\gamma}_0 - \Delta\mathbf{K}\Delta\boldsymbol{\gamma}, \tag{20.1}$$

and an iterative-solution procedure, assuming convergence, can be employed as

$$\mathbf{K}_0\Delta\boldsymbol{\gamma}^{(j+1)} = \Delta\mathbf{f} - \Delta\mathbf{K}\boldsymbol{\gamma}_0 - \Delta\mathbf{K}\Delta\boldsymbol{\gamma}^{(j)}. \tag{20.2}$$

Unfortunately, in a typical nonlinear problem involving incremental loading, especially in systems with decreasing stiffness, it will eventually be necessary to update the triangular factors frequently.

20.1.2 Notation and Background

A square matrix is said to be *lower-triangular* if all super-diagonal entries vanish. Similarly, a square matrix is said to be *upper-triangular* if all subdiagonal entries vanish. Consider a nonsingular real matrix **A**. It can be decomposed as

$$\mathbf{A} = \mathbf{A}_l + diag(\mathbf{A}) + \mathbf{A}_u, \tag{20.3}$$

in which $diag(\mathbf{A})$ consists of the diagonal entries of **A**, with zeroes elsewhere; $\mathbf{A}_l$ coincides with **A** below the diagonal with all other entries set to zero; and $\mathbf{A}_u$ coincides with **A** above the diagonal, with all other entries set to zero. For later use, we introduce the matrix functions:

$$lower(\mathbf{A}) = \mathbf{A}_l + \frac{1}{2}diag(\mathbf{A}), \quad upper(\mathbf{A}) = \mathbf{A}_u + \frac{1}{2}diag(\mathbf{A}). \tag{20.4}$$

Note that: (a) the product of two lower-triangular matrices is also lower-triangular, and (b) the inverse of a nonsingular, lower-triangular matrix is also lower-triangular. Likewise, the product of two upper-triangular matrices is upper-triangular, and the inverse of a nonsingular, upper-triangular matrix is upper-triangular. In proof of (a), let $\mathbf{L}^{(1)}$ and $\mathbf{L}^{(2)}$ be two $n \times n$ lower-triangular matrices. The ij^{th} entry of the product matrix is given by $\sum_{k=1,n} l^{(1)}_{ik} l^{(2)}_{kj}$. Since $\mathbf{L}^{(1)}$ is lower-triangular, $l^{(1)}_{ik}$ vanishes unless $k \le i$. Similarly, $l^{(2)}_{kj}$ vanishes unless $k \ge j$. Clearly, all entries of $\sum_{k=1,n} l^{(1)}_{ik} l^{(2)}_{kj}$ vanish unless $i \ge j$, which is to say that $\mathbf{L}^{(1)}\mathbf{L}^{(2)}$ is lower-triangular.

In proof of (b), let **A** denote the inverse of a lower-triangular matrix **L**. We multiply the j^{th} column of **A** by **L** and set it equal to the vector $\mathbf{e}_j$ ($\mathbf{e}_j^{\mathbf{T}} = \{0\ldots\ldots 1\ldots\ldots 0\}$ with unity in the j^{th} position): now,

$$\begin{aligned}
l_{11}a_{1j} &= 0 \\
l_{21}a_{1j} + l_{22}a_{2j} &= 0 \\
l_{31}a_{1j} + l_{32}a_{2j} + l_{33}a_{3j} &= 0 \\
&\vdots \\
l_{j1}a_{1j} + l_{j2}a_{2j} + l_{j3}a_{3j} + \cdots + l_{jj}a_{jj} &= 1
\end{aligned} \tag{20.5}$$

Forward substitution establishes that $a_{kj} = 0$, if $k < j$, and $a_{jj} = l_{jj}^{-1}$, thus, $\mathbf{A} = \mathbf{L}^{-1}$ is lower-triangular.

20.1.3 Iteration Scheme

Let $\mathbf{K}_0$ denote a symmetric, positive-definite matrix, for which the unique triangular factors are $\mathbf{L}_0$ and $\mathbf{L}_0^{\mathbf{T}}$. If $\mathbf{K}_0$ is banded, the maximum width of its rows (the bandwidth) equals $2b - 1$, in which b is the bandwidth of $\mathbf{L}_0$. The factors of the perturbed matrix $\mathbf{K}$ can be written as

$$[\mathbf{K}_0 + \Delta\mathbf{K}] = [\mathbf{L}_0 + \Delta\mathbf{L}][\mathbf{L}_0^{\mathbf{T}} + \Delta\mathbf{L}^{\mathbf{T}}]. \tag{20.6}$$

We can rewrite Equation 20.6 as

$$[\mathbf{I} + \mathbf{L}_0^{-1}\Delta\mathbf{L}][\mathbf{I} + \Delta\mathbf{L}^{\mathbf{T}}\mathbf{L}_0^{-\mathbf{T}}] = \mathbf{L}_0^{-1}[\mathbf{K}_0 + \Delta\mathbf{K}]\mathbf{L}_0^{-\mathbf{T}}, \tag{20.7}$$

from which

$$\mathbf{L}_0^{-1}\Delta\mathbf{L} + \Delta\mathbf{L}^{\mathbf{T}}\mathbf{L}_0^{-\mathbf{T}} = \mathbf{L}_0^{-1}\Delta\mathbf{K}\mathbf{L}_0^{-\mathbf{T}} - \mathbf{L}_0^{-1}\Delta\mathbf{L}\Delta\mathbf{L}^{\mathbf{T}}\mathbf{L}_0^{-\mathbf{T}}. \tag{20.8}$$

Note that $\mathbf{L}_0^{-1}\Delta\mathbf{L}$ is lower-triangular. It follows that

$$\Delta\mathbf{L} = \mathbf{L}_0 lower\left(\mathbf{L}_0^{-1}\Delta\mathbf{K}\mathbf{L}_0^{-\mathbf{T}} - \mathbf{L}_0^{-1}\Delta\mathbf{L}\Delta\mathbf{L}^{\mathbf{T}}\mathbf{L}_0^{-\mathbf{T}}\right). \tag{20.9}$$

The factor of 1/2 in the definition of the *lower* and *upper* matrix functions is motivated by the fact that the diagonal entries of $\mathbf{L}_0^{-1}\Delta\mathbf{L}$ and $\Delta\mathbf{L}^{\mathbf{T}}\mathbf{L}_0^{-\mathbf{T}}$ are the same.

Furthermore, for banded matrices, if $\Delta\mathbf{L}$ and $\mathbf{L}_0$ have the same semibandwidth, b, it follows that, for the correct value of $\Delta\mathbf{L}$, $\mathbf{L}_0^{-1}\Delta\mathbf{K}\mathbf{L}_0^{-\mathbf{T}} - \mathbf{L}_0^{-1}\Delta\mathbf{L}\Delta\mathbf{L}^{\mathbf{T}}\mathbf{L}_0^{-\mathbf{T}}$ is also banded, with a bandwidth no greater than b. Unfortunately, it is not yet clear how to take advantage of this behavior.

An iteration scheme based on Equation 20.9 is introduced as

$$\begin{aligned}\Delta\mathbf{L}^{(j+1)} &= \mathbf{L}_0 lower\left(\mathbf{L}_0^{-1}\Delta\mathbf{K}\mathbf{L}_0^{-\mathbf{T}} - \mathbf{L}_0^{-1}\Delta\mathbf{L}^{(j)}\Delta\mathbf{L}^{(j)\mathbf{T}}\mathbf{L}_0^{-\mathbf{T}}\right)\\ \Delta\mathbf{L}^{(1)} &= \mathbf{L}_0 lower\left(\mathbf{L}_0^{-1}\Delta\mathbf{K}\mathbf{L}_0^{-\mathbf{T}}\right)\end{aligned} \tag{20.10}$$

Explicit formation of the fully populated inverses $\mathbf{L}_0^{-1}$ and $\mathbf{L}_0^{-\mathbf{T}}$ can be avoided by using forward and backward substitution. In particular, $\mathbf{L}_0^{-1}\Delta\mathbf{K} = [\mathbf{L}_0^{-1}\Delta\mathbf{k}_1\ \mathbf{L}_0^{-1}\Delta\mathbf{k}_2 \ldots \mathbf{L}_0^{-1}\Delta\mathbf{k}_n]$, where $\Delta\mathbf{k}_1$ is the first column of $\Delta\mathbf{K}$. We can now solve for $\mathbf{b}_j = \mathbf{L}_0^{-1}\Delta\mathbf{k}_j$ by solving the system $\mathbf{L}_0\,\mathbf{b}_j = \Delta\mathbf{k}_j$.

20.1.4 Heuristic Convergence Argument

For an approximate convergence argument, we use the similar relation

$$\Delta\mathbf{A} = \Delta\mathbf{K} - 2\mathbf{A}^{-1}(\Delta\mathbf{A})_{\infty}(\Delta\mathbf{A}), \tag{20.11}$$

in which $(\Delta\mathbf{A})_\infty$ is the solution (converged iterate) for $\Delta\mathbf{A}$. Consider the iteration scheme

$$\Delta\mathbf{A}^{(j+1)} = \Delta\mathbf{K} - 2\mathbf{A}^{-1}(\Delta\mathbf{A})_\infty(\Delta\mathbf{A})^{(j)}. \tag{20.12}$$

Subtraction of two successive iterates and application of matrix-norm inequalities furnish

$$\Delta\mathbf{A}^{(j+2)} - \Delta\mathbf{A}^{(j+1)} = 2\mathbf{A}^{-1}\Delta\mathbf{A}_\infty[\Delta\mathbf{A}^{(j+1)} - \Delta\mathbf{A}^{(j)}]. \tag{20.13}$$

Convergence is assured in this example if $\sigma(\mathbf{A}^{-1}\Delta\,\mathrm{A}_\infty) < \frac{1}{2}$, in which σ denotes the spectral radius (see Dahlquist and Bjork [1974]). An approximate convergence criterion is obtained as

$$\max_j \left|\lambda_j(\Delta\mathbf{A}_\infty)\right| < \frac{1}{2}\min_k \left|\lambda_k(\mathbf{A})\right|, \tag{20.14}$$

in which $\lambda_j(\Delta\mathbf{A})$ denotes the j^{th} eigenvalue of the $n \times n$ matrix $\Delta\mathbf{A}$. Clearly, convergence is expected if the perturbation matrix has a sufficiently small norm. Applied to the current problem, we also expect convergence will occur if $max_j \mid \lambda_j(\Delta\mathbf{L}_\infty)\mid < \frac{1}{2} min_k \mid \lambda_k(\mathbf{L})\mid$.

20.1.5 Sample Problem

Let $\mathbf{L}_0$ and $\mathbf{K}_0$ be given by

$$\mathbf{L}_0 = \begin{bmatrix} a & 0 \\ b & c \end{bmatrix}, \qquad \mathbf{K}_0 = \begin{bmatrix} a^2 & ab \\ ab & b^2 + c^2 \end{bmatrix}. \tag{20.15}$$

Now suppose that the matrices are perturbed according to

$$\mathbf{L} = \begin{bmatrix} a & 0 \\ b & c+d \end{bmatrix}, \qquad \mathbf{K}_0 = \begin{bmatrix} a^2 & ab \\ ab & b^2 + (c+d)^2 \end{bmatrix} \tag{20.16}$$

so that

$$\Delta\mathbf{K} = \begin{bmatrix} 0 & 0 \\ 0 & d(2c+d) \end{bmatrix}. \tag{20.17}$$

We are interested in the case in which $d/c << 1$, for example, $d/c = 0.1$, ensuring that the perturbation is small. We also use the fact that

$$\mathbf{L}_0^{-1} = \frac{1}{ac}\begin{bmatrix} c & 0 \\ -b & a \end{bmatrix}. \tag{20.18}$$

The correct answer, which should emerge from the iteration scheme, is

$$\Delta\mathbf{L}_\infty = \begin{bmatrix} 0 & 0 \\ 0 & d \end{bmatrix}. \tag{20.19}$$

The initial iterate is found from straightforward manipulation as

$$\Delta\mathbf{L}^{(1)} = \begin{bmatrix} 0 & 0 \\ 0 & d\left(1+\frac{1}{2}\frac{d}{c}\right) \end{bmatrix}. \tag{20.20}$$

The ratio of the norms of the error is

$$\begin{aligned} error &= \frac{norm(\Delta\mathbf{L}^{(1)}) - norm(\Delta\mathbf{L}_\infty)}{norm(\Delta\mathbf{L}_\infty)} \\ &= \frac{d\left(1+\frac{1}{2}\frac{d}{c}\right) - d}{d} \\ &= 5\% \end{aligned} \tag{20.21}$$

Letting $\Delta = d(1+\frac{1}{2}\frac{d}{c})$, the second iterate is found, after straightforward manipulation, as

$$\begin{aligned} \Delta\mathbf{L}^{(2)} &= \begin{bmatrix} 0 & 0 \\ 0 & \Delta - \frac{1}{2}\frac{\Delta^2}{c} \end{bmatrix} \\ &= \begin{bmatrix} 0 & 0 \\ 0 & d\left(1-\frac{d^2}{c^2}-\frac{1}{8}\frac{d^3}{c^3}\right) \end{bmatrix} \end{aligned} \tag{20.22}$$

The relative error is now

$$\begin{aligned} error &= \frac{d^2}{c^2}\left[1+\frac{1}{8}\frac{d}{c}\right] \\ &= 0.01\left(1+\frac{1}{80}\right) \end{aligned} \tag{20.23}$$

Clearly, this is a significant improvement over the initial iterate.

20.2 OZAWA'S METHOD FOR INCOMPRESSIBLE MATERIALS

In this section, thermal and inertial effects are neglected and the traction is assumed to be prescribed on the undeformed exterior boundary. Using a two-field formulation for an incompressible elastomer leads to an incremental relation, in global form, as follows (see Nicholson, 1995):

$$\begin{bmatrix} \mathbf{K}_{\mathrm{MM}} & \mathbf{K}_{\mathrm{MP}} \\ -\mathbf{K}_{\mathrm{MP}}^{\mathrm{T}} & 0 \end{bmatrix} \begin{Bmatrix} d\boldsymbol{\gamma} \\ d\psi \end{Bmatrix} = \begin{Bmatrix} d\mathbf{f}_{\mathrm{M}} \\ \mathbf{0} \end{Bmatrix}. \tag{20.24}$$

If $\mathbf{K}_{\mathrm{MM}}$ is singular, it can be replaced with $\mathbf{K}'_{\mathrm{MM}} = \mathbf{K}_{\mathrm{MM}} + \chi \mathbf{K}_{\mathrm{MP}} \mathbf{K}_{\mathrm{MP}}^{\mathbf{T}}$, and χ can be chosen to render $\mathbf{K}'_{\mathrm{MM}}$ positive-definite (see Zienkiewicz, 1989).

The presence of zeroes on the diagonal poses computational difficulties, which have received considerable attention. Here, we discuss a modification of the Ozawa method discussed by Zienkiewicz and Taylor (1989). In particular, Equation 20.24 is replaced with the iteration scheme

$$\begin{bmatrix} \mathbf{K}'_{MM} & \mathbf{K}_{MP} \\ -\mathbf{K}_{MP}^{T} & \mathbf{I}/\rho_a \end{bmatrix} \begin{Bmatrix} d\boldsymbol{\gamma} \\ d\boldsymbol{\psi} \end{Bmatrix}^{j+1} = \begin{Bmatrix} d\mathbf{f}_M \\ d\boldsymbol{\psi}^j/\rho_a \end{Bmatrix}, \tag{20.25}$$

in which the superscript j denotes the j^{th} iterate and ρ_a is an acceleration parameter. This scheme converges rapidly for suitable choices of ρ_a.

If the assumed pressure fields are discontinuous at the element boundaries, this method can be used at the element level to eliminate pressure variables (see Hughes, 1987). In this event, the global equilibrium equation only involves displacement degrees-of-freedom.

For each iteration, it is necessary to solve a linear system. Computation can be expedited using a convenient version of the **LU** decomposition. Let $\mathbf{L}_1$ and $\mathbf{L}_2$ denote lower-triangular matrices arising in the following Cholesky decompositions:

$$\mathbf{K}'_{MM} = \mathbf{L}_1 \mathbf{L}_1^{\mathbf{T}} \qquad \mathbf{I}/\rho_a + \mathbf{K}_{MP}^{\mathbf{T}} \mathbf{L}_1 \mathbf{L}_1^{\mathbf{T}} \mathbf{K}_{MP} = \mathbf{L}_2 \mathbf{L}_2^{\mathbf{T}}. \tag{20.26}$$

Then, a triangularization is attained as

$$\begin{bmatrix} \mathbf{K}'_{MM} & \mathbf{K}_{MP} \\ -\mathbf{K}_{MP}^{T} & \mathbf{I}/\rho_a \end{bmatrix} = \begin{bmatrix} \mathbf{L}_1 & \mathbf{0} \\ -\mathbf{K}_{MP}^{T} \mathbf{L}_1^{-T} & \mathbf{L}_2 \end{bmatrix} \begin{bmatrix} \mathbf{L}_1^{T} & \mathbf{L}_1^{-1} \mathbf{K}_{MP} \\ \mathbf{0}^{T} & \mathbf{L}_2^{T} \end{bmatrix}. \tag{20.27}$$

Forward and backward substitution can now be exploited to solve the linear system arising in the incremental finite-element method.

20.3 EXERCISES

1. Examine the first two iterates for the matrices

$$\mathbf{K} = \begin{bmatrix} a & 0 & 0 \\ b & c & 0 \\ d & e & f \end{bmatrix} \begin{bmatrix} a & b & d \\ 0 & c & e \\ 0 & 0 & f \end{bmatrix} = \begin{bmatrix} a^2 & ab & ad \\ ab & b^2 + c^2 & bd + ce \\ ad & bd + ce & d^2 + e^2 + f^2 \end{bmatrix}$$

$$\mathbf{K} + \Delta\mathbf{K} = \begin{bmatrix} a & 0 & 0 \\ b & c & 0 \\ d & e + g & f \end{bmatrix} \begin{bmatrix} a & b & d \\ 0 & c & e + g \\ 0 & 0 & f \end{bmatrix}$$

$$= \begin{bmatrix} a^2 & ab & ad \\ ab & b^2 + c^2 & bd + c(e + g) \\ ad & bd + c(e + g) & d^2 + (e + g)^2 + f^2 \end{bmatrix}.$$

2. Verify that the product and inverse of lower-triangular matrices are lower-triangular using

$$\mathbf{L}_1 = \begin{bmatrix} a & 0 \\ b & c \end{bmatrix}, \quad \mathbf{L}_2 = \begin{bmatrix} d & 0 \\ e & f \end{bmatrix}.$$

3. Verify the triangularization scheme in the matrix

$$\mathbf{A} = \begin{bmatrix} 2 & -1 & 1 \\ -1 & 2 & -1 \\ -1 & 1 & 0 \end{bmatrix}.$$

Use the triangular factors to solve the equation

$$\mathbf{Ab} = \begin{Bmatrix} 2 \\ -1 \\ 1 \end{Bmatrix}.$$

Monographs and Texts

Abramawitz, M. and Stegun, I., Eds, *Handbook of Mathematical Functions, with Formulas, Graphs and Mathematical Tables*, Dover Publications, Inc., New York, 1997.

Belytschko, T., Liu, W.K., and Moran, B., *Nonlinear Finite Elements for Continua and Structures*, John Wiley and Sons, New York, 2000.

Bonet, J. and Wood, R., *Nonlinear Continuum Mechanics for Finite Element Analysis*, Cambridge University Press, Cambridge, 1997.

Brush, D. and Almroth, B., *Buckling of Bars, Plates and Shells*, McGraw-Hill Book Company, New York, 1975.

Callen, H.B., *Thermodynamics and an Introduction to Thermostatistics*, 2nd ed., John Wiley and Sons, New York, 1985.

Chandrasekharaiah, D. and Debnath, L., *Continuum Mechanics*, Academic Press, San Diego, 1994.

Chung, T.J., *Continuum Mechanics*, Prentice-Halls, Englewood Cliffs, NJ, 1988.

Dahlquist, G. and Bjork, A., *Numerical Methods*, Prentice-Hall, Englewood Cliffs, NJ, 1974.

Ellyin, F., *Fatigue Damage, Crack Growth and Life Prediction*, Chapman & Hall, FL, 1997.

Eringen, A.C., *Nonlinear Theory of Continuous Media*, McGraw-Hill, New York, 1962.

Ewing, G.M., *Calculus of Variations with Applications*, Dover Publications, Mineola, N.Y., 1985.

Gent, A.N., Ed, *Engineering with Rubber: How to Design Rubber Components*, Hanser, New York, 1992.

Golub, G. and Van Loan, C., *Matrix Computations*, Johns Hopkins University Press, Baltimore, MD, 1996.

Graham, A., *Kronecker Products and Matrix Calculus with Applications*, Ellis Horwood, Ltd., Chichester, 1981.

Hughes, T., *The Finite Element Method: Linear Static and Dynamic Analysis*, Dover Publishers Inc., New York, 2000.

Kleiber, M., *Incremental Finite Element Modeling in Non-Linear Solid Mechanics*, Ellis Horwood, Ltd., Chichester, 1989.

Oden, J.T., *Finite Elements of Nonlinear Continua*, McGraw-Hill Book Company, New York, 1972.

Schey, H.M., *DIV, GRAD, CURL and All That*, Norton, New York, 1973.

Thomason, P.F., *Ductile Fracture of Metals*, Pergamon Press, Oxford, 1990.

Wang, C-T., *Applied Elasticity*, The Maple Press Company, York, PA, 1953.

Zienkiewicz, O.C. and Taylor, R.L., *The Finite Element Method*. Volume 2, 4th ed, McGraw-Hill Book Company, London, 1989.

Articles and Other Sources

ANSYS User Manual, ver 6.0, Swanson Analysis Systems, 2000.

Blatz, P.J. and Ko, W.L., Application of finite elastic theory to the deformation of rubbery materials, *Trans. Soc. Rheol.*, 6, 223, 1962.

Bonora, N., A nonlinear CDM model for ductile failure, *Engineering Fracture Mechanics*, 58, 1/2, 11, 1997.

Chen, J., Wan, W., Wu, C.T., and Duan, W., On the perturbed Lagrangian formulation for nearly incompressible and incompressible hyperelasticity, *Comp. Methods Appl. Mech. Eng.*, 142, 335, 1997.

Dillon, O.W., A nonlinear thermoelasticity theory, *J. Mech. Phys. Solids*, 10, 123, 1962.

Green, A. and Naghdi, P., A general theory of an elastic-plastic continuum, *Arch. Rat. Mech. Anal.*, 18/19, 1965.

Gurson, A.L., Continuum theory of ductile rupture by void nucleation and growth, part 1: yield criteria and flow rules for porous ductile media, *J. Eng. Mat's Technol.*, 99, 2, 1977.

Holzappel, G., On large strain viscoelasticity: continuum applications and finite element applications to elastomeric structures, *Int. J. Numer. Meth. Eng.*, 39, 3903, 1996.

Holzappel, G. and Simo, J., Entropy elasticity of isotropic rubber-like solids at finite strain, *Comp. Methods Appl. Mech. Eng.*, 132, 17, 1996.

LS-DYNA, ver. 95, Livermore Software Technology Corporation, Livermore, CA, 2000.

Moraes, R. and Nicholson D.W., Local damage criterion for ductile fracture with application to welds under dynamic loads, in *Advances in Fracture and Damage Mechanics*, Guagliano, M. and Aliabadi, M.H., Eds., 2nd ed. Hoggar Press, Geneva, 277, 2002.

Nicholson, D.W. and Nelson, N., Finite element analysis in design with rubber (Rubber Reviews), *Rubber Chem. Tech.*, 63, 638, 1990.

Nicholson, D.W., Tangent modulus matrix for finite element analysis of hyperelastic materials, *Acta Mech.*, 112, 187, 1995.

Nicholson, D.W. and Lin, B., Theory of thermohyperelasticity for near-incompressible elastomers, *Acta Mech.*, 116, 15, 1996.

Nicholson, D.W. and Lin, B., Finite element method for thermomechanical response of near-incompressible elastomers, *Acta Mech.*, 124, 181, 1997a.

Nicholson, D.W. and Lin, B., Incremental finite element equations for thermomechanical of elastomers: effect of boundary conditions including contact, *Acta Mech.*, 128, 1–2, 81, 1997b.

Nicholson, D.W. and Lin, B., On the tangent modulus tensor in hyperelasticty, *Acta Mech.*, 131, 1997c.

Nicholson, D.W., Nelson, N., Lin, B., and Farinella, A., Finite element analysis of hyperelastic components, *Appl. Mech. Rev.*, 51, 5, 303, 1999.

Ogden, R.W., Recent advances in the phenomenological theory of rubber elasticity, *Rubber Chem. Tech.*, 59, 361, 1986.

Perzyna, P., Thermodynamic theory of viscoplasticity, *Adv. Appl. Mech.*, 11, 1971.

Valanis, K. and Landel, R.F., The strain energy function of a hyperelastic material in terms of the extension ratios, *J. Appl. Physics*, 38, 2997, 1967.

Tvergaard, V., Influence of voids on shear band instabilities under plane strain conditions, *Int. J. Fracture*, 17, 389–407, 1981.

Ziegler, H. and Wehrli, C., The derivation of constitutive relations from the free energy and the dissipation function, *Adv. Appl. Mech.*, 25, 187, 1987.